Caractérisation texturale et analyse par stéréocorrélation d'images de la déformation des fromages à pâte molle et de leurs simulants formulés

Mary Lynn Li Yuet Hee

INSTITUT NATIONAL POLYTECHNIQUE DE LORRAINE
École Nationale Supérieure d'Agronomie et des Industries Alimentaires
Laboratoire de Science et Génie Alimentaires

THÈSE

Présentée devant l'Institut National Polytechnique de Lorraine
Pour obtenir le grade de

Docteur de l'INPL

Spécialité : Procédés Biotechnologiques et Alimentaires

Caractérisation texturale et analyse par stéréocorrélation d'images de la déformation des fromages à pâte molle et de leurs simulants formulés

Textural characterization and digital image correlation analysis of the deformation of soft cheeses and their formulated simulants

Par

Mary Lynn LI YUET HEE

Soutenue publiquement le 16 Octobre 2007 devant la commission d'examen composée de:

Rapporteurs :
Mme Catherine Dacremont, Professeur, ENSBANA, Dijon
Mme Laurence Mioche, Professeur, INRA, Theix

Examinateurs :
Mme Nathalie Cayot, Professeur, ENESAD, Dijon
Mme Laurence Lambert, Maître assistante, GIP-InSIC, Saint-Dié-des-Vosges
M. Stéphane Desobry, Professeur, ENSAIA-INPL, Nancy
Mme Muriel Jacquot, Maître de conférences, ENSAIA-INPL, Nancy

Invité :
M. Joël Hardy, Professeur émérite, ENSAIA-INPL, Nancy

First and foremost I would like to thank Pr. Stéphane Desobry, Director of the Laboratoire de Science et Génie Alimentaires, for the opportunity he gave me to work in his laboratory in pursuit of my PhD and for supervising this research work.
His expert knowledge, intelligence, valuable advice and continued support played a key role in this work.

I also extend my gratitude to Dr. Muriel Jacquot and Pr. Joël Hardy for supervising this research. My sincere thanks are due to their trust, time commitment, advice and support.

I wish to thank Pr. Nathalie Cayot, Professor at ENESAD, Dijon, chairperson, Pr. Catherine Dacremont, Professor at ENSBANA, Dijon and Pr. Laurence Mioche, Professor at INRA Theix, reviewers, Dr. Laurence Lambert, assistant professor at GIP-InSIC, St. Dié, for serving on the examination committee.
I also wish to thank Dr. Laurence Lambert for collaboration and work done on digital image correlation and the Breuckmann scanning systems.

The lab was a great and entertaining work environment and my sincere thanks are therefore due to everybody in LSGA.

I am very much grateful to my brother, Terence and my parents for their wonderful support and unlimited faith in me.

LIST OF SYMBOLS AND ABBREVIATIONS

AU	Anson units
a	fitting parameter of mathematical equation (mm) relating *Z* to Y
b	fitting parameter of mathematical equation (mm^{-1}) relating *Z* to Y
cam	Camembert cheese
cou	Coulommiers cheese
DE	dextrose equivalent
E_1	elasticity modulus of first element of Maxwell model (kPa)
E_2	elasticity modulus of second element of Maxwell model (kPa)
E_3	elasticity modulus of third element of Maxwell model (kPa)
k_{z1}	coefficient of mathematical model relating elasticity modulus to Z_0
k_{z2}	coefficient of mathematical model relating firmness to Z_0
k_{b1}	coefficient of mathematical model relating elasticity modulus to *b*
k_{b2}	coefficient of mathematical model relating firmness to *b*
k_{a1}	coefficient of mathematical model relating elasticity modulus to *a*
k_{a2}	coefficient of mathematical model relating firmness to *a*
k_{a3}	coefficient of mathematical model relating relaxation time constant to *a*
r_1	relaxation time constant of first element of Maxwell model (s)
r_2	relaxation time constant of second element of Maxwell model (s)
r_3	relaxation time constant of third element of Maxwell model (s)
$X_{gelatin}$	actual gelatin content
$X_{maltodextrin}$	actual maltodextrin content
X_{starch}	actual starch content
X	distance across probe (mm)
Y	radial distance from probe (mm)
Z	displacement in *Z* direction/surface depression (mm)
Z_0	value to which the surface displacement will tend to when radial distance from probe is very large
3D	three-dimensional
α	stress (kPa)

ε	strain
t	time (s)
IUTM	Instron Universal Testing Machine

Publications

L. Li Yuet Hee, M. Jacquot, J. Hardy, S. Desobry. (2007). Formulating polymeric gels simulating soft cheeses texture. *Food hydrocolloids. In press*
(doi:10.1016/j.foodhyd.2007.05.002)

L. Li Yuet Hee, M. Jacquot, J. Hardy, S. Desobry. Gelatin and other main gels used as model food in texture studies. *Critical Review in Food Science and Nutrition. Submitted*

Communications

L. Li Yuet Hee, M. Jacquot, J. Hardy, S. Desobry. (2007). Use of 3D digital image analysis to determine textural properties of soft cheeses and their simulant. *IFT 2007*, Chicago, USA. Oral presentation

L. Li Yuet Hee, M. Jacquot, J. Hardy, S. Desobry. (2006). Synthetic gel simulating Coulommiers cheese. *IUFoST 13*, Nantes, France. Paper N°703. Poster

L. Li Yuet Hee, M. Jacquot, J. Hardy, S. Desobry. (2006). Formulation d'un gel polymérique simulant les propriétés texturales du fromage. *Séminaire annuel de l'Ecole Doctorale RP2E,* Nancy, France, avec acte. (ISBN 2-9518564-4). Poster

RÉSUMÉ EN FRANÇAIS

INTRODUCTION GÉNÉRALE

De nos jours, les emballages inviolables sont très répandus dans le domaine alimentaire. Néanmoins, il y a encore quelques produits qui restent accessibles aux consommateurs, notamment les fromages types Camembert et Coulommiers. Par ailleurs, les français ont pour habitude d'appuyer avec le doigt sur ces fromages pour choisir le degré de maturation et donc la texture qu'ils préfèrent. Il est probable toutefois que les consommateurs soient amenés à abandonner cette habitude. En effet, par souci d'hygiène et de sécurité, les entreprises agroalimentaires mettent en rayon des produits dans les emballages inviolables.
Comment alors permettre aux consommateurs, mais aussi aux industriels de suivre l'évolution de la texture du fromage au cours du stockage autrement qu'en ouvrant la boîte et d'appuyer sur le produit ?
La solution proposée dans ce travail de recherche est de créer un simulant du Camembert et du Coulommiers dont la texture évolue au cours du temps pour simuler les modifications texturales du fromage.
De plus, afin d'élargir le domaine d'applications de ce simulant, il est formulé à partir de mélange de gélatine et de polysaccharides. En effet, l'incorporation des constituants présents dans le fromage permettrait sans doute d'obtenir plus facilement un gel avec une texture proche de celle du fromage. Cependant, cela impliquerait que le simulant serait employé pour imiter les fromages seulement. Au contraire, un gel de gélatine et de polysaccharides pourrait simuler la texture de produits autres que le Camembert et le Coulommiers et cela en faisant varier la concentration des constituants du gel.

La texture des aliments peut être caractérisée par évaluation sensorielle ou mesure instrumentale. Or, les paramètres instrumentaux ne décrivent pas complètement la texture d'un aliment perçue par un juge d'évaluation sensorielle. Le deuxième objectif de ce travail était donc de proposer une nouvelle approche pour déterminer les mesures rhéologiques des aliments. La numérisation tridimensionnelle (mesure de champs de déplacement tridimensionnelle par stéréocorrélation d'images et mesure topométrique tridimensionnelle de Breuckmann) a donc été utilisée pour analyser la déformation des fromages et de leurs simulants. Les nouveaux paramètres obtenus par cette technique pourraient permettre

d'obtenir des modèles pouvant prédire, avec précision, des mesures sensorielles hédoniques à partir de paramètres instrumentaux.

Le matériel et les méthodes utilisés dans cette étude sont décrits dans le chapitre I.

Le chapitre II présente et discute les résultats obtenus. Ce chapitre est organisé en trois parties. Le but de cette première partie était de mettre au point un simulant du Camembert et du Coulommiers âgés de 10 jours. Une fois la composition et la concentration du simulant déterminées, ce gel est ensuite additionné d'enzyme afin de faire évoluer sa texture au cours du temps. Ceci, afin d'imiter la cinétique d'évolution de la texture du Camembert et du Coulommiers. Les résultats obtenus sont présentés dans la deuxième partie. La troisième et dernière partie du chapitre résultats et discussion expose l'intérêt de l'utilisation de la numérisation tridimensionnelle comme nouvel outil pour caractériser la texture d'un aliment.

MATÉRIEL ET METHODES

1. MATÉRIEL

1.1. Fromages à pâte molle

Camembert et Coulommiers

Des Coulommiers âgés d'un jour ont été fournis par La Fromagerie de Sorcy (Lactalis®) France et des Camembert Président® (Lactalis®) ont été achetés du commerce. La composition, le poids et la taille des fromages sont indiqués dans le tableau I.

Tableau I. Composition, poids et diamètre du Coulommiers et du Camembert

		Coulommiers	Camembert
Protéines	g/100	20,5	22,0
Glucides	g/100	_	_
Lipides	g/100	23	20
Matière grasse dans produit sans son humidité	g/100	52	45
Calcium	g/100	0,49	0,45
Poids	g	350	250
Diamètre	cm	~13	~11

1.2. Gels de gélatine et polysaccharides imitant la texture des fromages à pâte molle âgés de 10 jours

Des simulants sont créés afin d'imiter les propriétés texturales des fromages à pâte molle. Cinq simulants sont formulés à partir de mélange de gélatine de type A avec un degré Bloom de 260 (PB Gelatin France SA, Furdenheim, France) et des polysaccharides (Tableau II). Le guar (Sigma Chemical Co., Mo, USA), le karaya (Alland and Robert, Port-Mort, France), la xanthane (Systems Bio-Industries, Boulogne, France) ou un mélange de maltodextrine 19 DE (Roquette Frères, France) et d'amidon gélatinisé (Sigma Chemical Co., Mo, USA) sont ajoutés à la gélatine. Les gels formulés contiennent 0,02 % (p/p) d'azoture de sodium (Acros Organics, New Jersey, USA) afin d'éviter le développement de microorganismes.

Tableau II. Composition des cinq gels formulés

Gels	Composition (% p/p)
1	gélatine (6)
2	gélatine (6) - guar (1)
3	gélatine (6) - karaya (3)
4	gélatine (6) - xanthan (3)
5	gélatine (6) - maltodextrine (20) – amidon gélatinisé (3)

1.2.1. Gel de gélatine

La poudre de gélatine est mélangée à l'eau distillée qui a une température de 22±2 °C. La suspension est agitée rapidement avec une tige en verre et laissée au repos pendant environ 30 minutes. Cette suspension est ensuite portée à une température de 60 °C pendant 30 minutes sous agitation modérée, puis transvasée dans des récipients cylindriques de 11 cm de diamètre et de 3,5 cm de haut. Chaque récipient contient 300 g de suspension et la hauteur du gel obtenu est d'environ 3 cm. Les gels sont maintenus à 7±1 °C, recouverts d'un film de paraffine pendant 12 heures avant analyse.

1.2.2. Gel de gélatine-guar

La gomme de guar est ajoutée à l'eau distillée puis la suspension est portée à une température de 90 °C pendant 30 minutes. Une suspension de gélatine (préparée selon la procédure décrite plus haut) est ajoutée à la gomme de guar et le mélange est maintenu sous agitation magnétique pendant 30 minutes avant d'être transvasé dans des récipients cylindriques, recouverts d'un film de paraffine et maintenu à 7±1 °C pendant 12 heures avant analyse.

1.2.3. Gels de gélatine-karaya et gélatine-xanthane

Les gels de gélatin-karaya et de gélatin-xanthane sont réalisés selon le même mode de préparation. Après mélange de la poudre de karaya (ou de xanthane) avec de l'eau distillée, la suspension est maintenue à 7±1 °C pendant 12 heures pour permettre l'hydratation des

particules. Une suspension de gélatine (préparée selon la procédure décrite plus haut) est ajoutée au karaya (ou xanthane). Le mélange est ensuite porté à 60 °C pendant 15 minutes sous agitation modérée puis transvasé dans des récipients cylindriques recouverts d'un film de paraffine et maintenu à 7±1 °C pendant 12 heures avant analyse.

1.2.4. Gel de gélatine-maltodextrine-amidon

La poudre de maltodextrine est dispersée dans de l'eau distillée, puis la solution est portée à 90 °C pendant 30 minutes sous agitation magnétique. L'amidon est ensuite ajouté à de l'eau distillée et la suspension est portée à 90 °C jusqu'à l'obtention d'une solution gélatinisée. Les solutions de maltodextrine et d'amidon gélatinisé sont ajoutées à la suspension de gélatine et le mélange est transvasé dans des récipients cylindriques recouverts d'un film de paraffine et maintenu à 7±1 °C pendant 12 heures avant analyse.

1.3. Simulant de Coulommiers âgé de 10 jours

Le module d'optimisation du logiciel Expert-Design 6.0.6 trial software (Stat-Ease Inc., Minneapolis, MN, USA) permet de déterminer la concentration des composants d'un gel de gélatine-maltodextrine-amidon dont la texture est le plus proche possible de celle d'un Coulommiers âgé de 10 jours. Ce gel est obtenu à partir de 7,8% (p/p) gélatine, 20,2% (p/p) maltodextrine 19 DE et 2% (p/p) amidon gélatinisé.

Ce simulant est préparé en ajoutant de la maltodextrine dans de l'eau distillée et la solution est portée à 90 °C pendant 30 minutes sous agitation magnétique à 300 tours/min. L'amidon est ensuite ajouté à de l'eau distillée et la suspension est portée à 90 °C jusqu'à l'obtention d'une solution gélatinisée. Les solutions de maltodextrine et d'amidon gélatinisé sont ajoutées à la suspension de gélatine et le mélange est transvasé dans des récipients cylindriques recouverts d'un film de paraffine et maintenu à 7±1 °C pendant 12 heures avant analyse.
Ce simulant est soumis :

- aux tests de pénétrométrie et de relaxation afin d'étudier l'évolution de leurs propriétés texturales au cours du stockage et

- à l'analyse de la déformation par stéréocorrélation d'images et numérisation tridimensionnel de Breuckmann.

1.4. Simulant de Coulommiers additionné de Subtilisine Carlsberg (Alcalase®) et imitant la texture des fromages au cours de leur maturation

Des quantités croissantes d'enzyme Alcalase®, type FG (protease Subtilisin Carlsberg, Novo Nordisk, Denmark) sont additionnées au simulant de Coulommiers – 7,8% (p/p) gelatine, 20,2% (p/p) maltodextrine DE 19 et 2% (p/p) amidon gélatinisé – afin d'induire des modifications texturales qui évoluent au cours du temps. L'activité de l'Alcalase est de 2,4 unités Anson/g (UA/g). Le volume d'Alcalase® étant faible (inférieure à 10 µL), une solution diluée est préparée en ajoutant 1 mL d'enzyme à 10 mL d'eau distillée.

Quatre types de simulants de Coulommiers sont préparés : un gel sans enzyme, qui sera appelé gel standard et trois gels additionnés de 2, 4 et 10 µL d'Alcalase® correspondant respectivement à 0,006 ; 0,012 et 0,03 UA (soit un rapport d'enzyme/gélatine de 0,06 ; 0,12 et 0,30 µL/g respectivement).

Les simulants imitant le Coulommiers et contenant de l'Alcalase® sont obtenus à partir du mode préparatoire suivant. La maltodextrine est ajoutée à de l'eau distillée et la solution est portée à 90 °C pendant 30 minutes sous agitation à 300 rpm. L'Alcalase® est ensuite ajoutée à la solution de maltodextrine après refroidissement de cette dernière (température 30 °C), l'amidon est ajouté à de l'eau distillée et la suspension est portée à 90 °C jusqu'à l'obtention d'une solution gélatinisée. La maltodextrine et l'amidon gélatinisé sont ensuite rajoutés à une suspension de gélatine. Le mélange est ensuite transvasé dans des récipients cylindriques recouverts d'un film de paraffine et maintenu à 7±1 °C pendant 12 heures avant analyse.

Ces simulants sont soumis aux tests de pénétrométrie et de relaxation 1, 8, 43, 50 et 120 jours après leur préparation.

1.5. Simulant de Camembert âgé de 30 jours

Le module d'optimisation du logiciel Expert-Design 6.0.6 trial software (Stat-Ease Inc., Minneapolis, MN, USA) a permis de déterminer la concentration des composants d'un gel de gélatine-maltodextrine-amidon dont la texture est la plus proche possible de celle d'un Camembert âgé de 30 jours. Ce gel est obtenu à partir de 6,5% (p/p) gélatine, 21,5% (p/p) maltodextrine 19 DE et 2% (p/p) amidon gélatinisé. Le mode de préparation de ce simulant est le même que celui du simulant de Coulommiers âgés de 10 jours.
Ce simulant est soumis à l'analyse de la déformation par stéréocorrélation d'images et numérisation tridimensionnelle de Breuckmann.

2. MÉTHODES

2.1. Caractérisation des propriétés texturales par mesures instrumentales

Les propriétés texturales des fromages et de leurs simulants sont déterminées par mesures instrumentales à l'aide de la machine d'essai universelle (Llyod Instruments LRX). Les données sont acquises et traitées par le logiciel Nexygen Series 4.5 (Lloyd Instruments Ltd., Hants, UK). Les échantillons sont analysés à 7±1 °C. L'emballage des fromages est enlevé avant analyse. Les tests de pénétrométrie et de relaxation sont réalisés sur les échantillons avec six et trois répétitions pour les fromages et les simulants respectivement.

2.1.1. Test de pénétrométrie

2.1.1.1. Principe

Le test de pénétrométrie est couramment utilisé pour évaluer les propriétés texturales des aliments (deMan, 1969; Gregson *et al.*, 1999; Ross and Scanlon, 1999; Anand and Scanlon, 2002). Dans ce test, une sonde est insérée dans l'échantillon et la force nécessaire pour

atteindre une certaine profondeur de pénétration est mesurée. La valeur de la force constitue une mesure de la fermeté (Bourne, 2002).

2.1.1.2. Procédure

Durant le test de pénétrométrie, une sonde constituée par une tige métallique cylindrique d'un diamètre de 20 mm est insérée à une vitesse de 10 mm/min dans l'échantillon à 25 mm du bord de ce dernier jusqu'à une profondeur de 10 mm. Un capteur de force de 500 N est utilisé et les données sont enregistrées à une fréquence de 80 Hz.

2.1.1.3. Traitement des données

La valeur de la force est enregistrée pour une profondeur de pénétration fixée à 10 mm. Cette valeur correspond à la mesure de fermeté de l'échantillon et est obtenue à partir de la figure I.

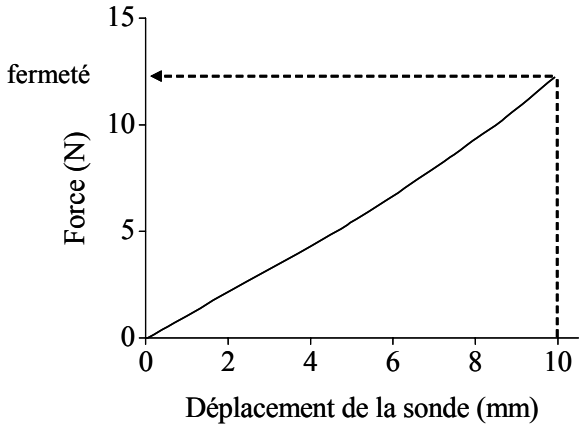

Figure I. Courbe de force-déplacement obtenue à partir d'un test de pénétrométrie réalisé sur le Coulommiers. La fermeté correspond à la force nécessaire pour insérer la sonde à une profondeur de pénétration de 10 mm.

2.1.2. Test de relaxation

2.1.2.1. Principe

Le comportement des matières viscoélastiques en relaxation est habituellement représenté par le corps de Maxwell généralisé constitué par l'association en parallèle de *n* modèles de

Maxwell, chacun d'entre eux étant caractérisé par un modèle d'élasticité E_i et un coefficient de viscosité η_i (figure II).

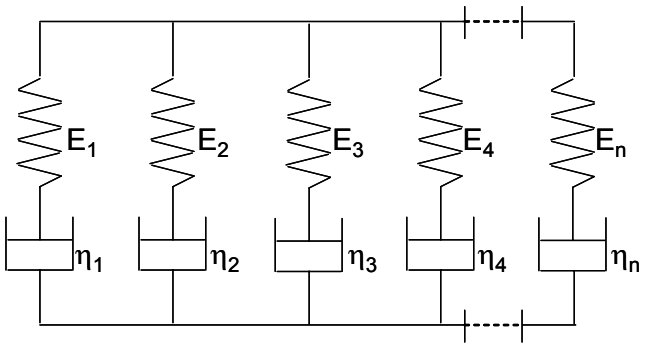

Figure II. Modèle de Maxwell généralisé

La réponse de ce modèle à une déformation appliquée instantanément peut être écrite selon équation I :

$$E(t) = \sum_{i=1}^{n} E_i \exp(-t/r_i) \qquad \text{(I)}$$

Dans l'équation I, *E(t)* est le module d'élasticité au temps *t*, défini comme la variation de la contrainte avec le temps quand une déformation égale à l'unité est soudainement imposée à la matière. Les coefficients r_i sont appelés temps de relaxation et représentent le temps nécessaire pour que la contrainte aux bornes de la *i*ème branche soit réduite dans le rapport 1/e.

2.1.2.2. Procédure

Le test de relaxation est réalisé en imposant 10% de déformation à l'échantillon à l'aide d'une sonde cylindrique de 20 mm de diamètre. La durée de la relaxation est limitée à 10 minutes et la vitesse d'application de la déformation est de 200 mm/min. La sonde est positionnée à 25 mm du bord de l'échantillon. Un capteur de force de 10 N est utilisé et les données sont enregistrées à une fréquence de 80 Hz.

2.1.2.3. Traitement des données

Les paramètres viscoélastiques, modules d'élasticité et temps de relaxation des fromages et des simulants sont obtenus en ajustant le modèle de Maxwell à la courbe expérimentale de relaxation (Figure XII). Les résultats sont exploités suivant l'analyse mathématique des résidus successifs (Mohsenin, 1986).

2.2. Plan de mélange

Un plan mélange à trois composants est utilisé pour déterminer la concentration de gélatine, maltodextrine et d'amidon du simulant qui aura une texture la proche possible de celle des fromages à pâte molle. Des expériences préliminaires ont permis de déterminer le domaine expérimental choisi (Tableau III).

Tableau III. Limites inférieures et supérieures des composants avec une quantité d'eau fixée à 70 % (p/p)

Composants	limite inférieure % (p/p)	limite supérieure % (p/p)
Gelatine	5	10
Maltodextrine	16	23
Amidon	2	4

Les gels ont une quantité d'eau fixée à 70 % (p/p). Les coefficients du model cubique de Scheffé sont estimés en utilisant un plan D-optimal. Une série de 15 expériences, dont trois points de répétition est réalisée afin de détecter un éventuel manque d'ajustement (Tableau IV).

Tableau IV. Expériences du plan de mélange

Essais	Gélatine (%p/p)	Maltodextrine (%p/p)	Amidon (%p/p)
1	7,5	20,5	2,0
2	8,8	18,8	2,5
3	7,5	19,5	3,0
4	10,0	16,0	4,0
5	5,0	23,0	2,0
6	10,0	16,0	4,0
7	10,0	18,0	2,0
8	10,0	18,0	2,0
9	8,8	17,7	3,5
10	5,0	22,0	3,0
11	5,0	21,0	4,0
12	6,3	20,7	3,0
13	10,0	16,7	3,3
14	5,0	23,0	2,0
15	6,7	19,3	4,0

Les modèles mathématiques sont ensuite validés grâce à quatre gels dont les compositions sont différentes de celles des autres gels formulés à partir du plan de mélange (Tableau V). Le logiciel Expert-Design 6.0.6 trial software (Stat-Ease Inc., Minneapolis, MN, USA) est utilisé pour réaliser le plan de mélange et traiter les données obtenues.

Tableau V. Composition de quatre gels utilisés pour valider les modèles mathématiques

Essais	Gélatine (%p/p)	Maltodextrine (%p/p)	Amidon (%p/p)
16	6,0	20,0	4,0
17	9,0	19,0	2,0
18	8,3	19,7	2,0
19	7,8	20,2	2,0

2.3. Mesure de champs de déplacement 3D par stéréocorrélation d'images

Le système de stréréocorrélation d'image est composé de deux caméras (QICAM Fast 1394 CCD caméra, équipé d'un objectif Nikon 35-70 mm f/2.8 AF-D) avec une ouverture de f/5.6 et un temps d'exposition de 47 ms. Les images sont acquises et traitées avec les logiciels Vic-Snap® (version 3.0D, 2005 Correlated solutions, Inc.) et Vic-3D® (version 3.1.0 Correlated

solutions, Inc.) respectivement. La figure VI montre le montage permettant la mesure de champs de déplacement 3D par stéréocorrélation d'images.

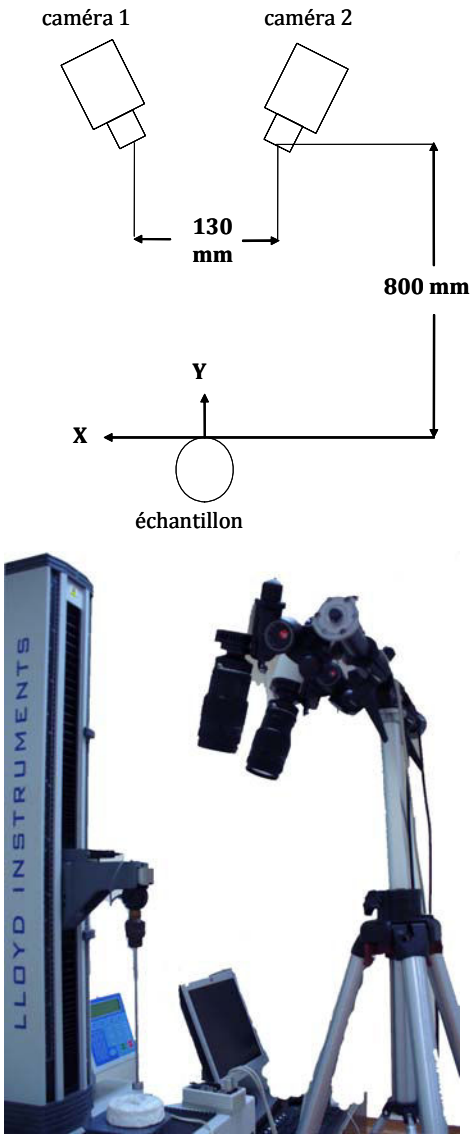

Figure VI. Montage du système de stéréocorrélation d'images

Afin de mesurer la déformation de l'échantillon, une texture aléatoire de type mouchetis est créée par projection de peinture noire à la surface (Figure VII).

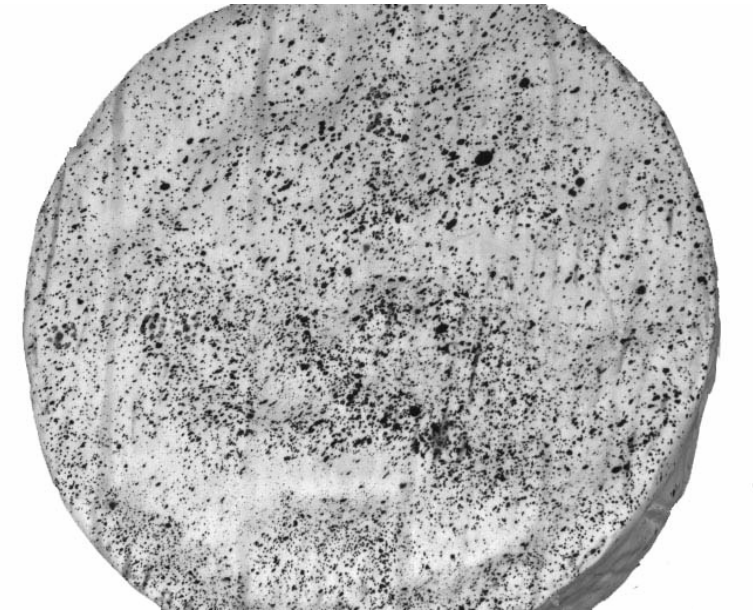

Figure VII: Image de la texture aléatoire, type mouchetis d'un Camembert avant déformation

La zone indiquée en rouge dans la figure VIII, correspond à la zone d'analyse de la déformation de l'échantillon.

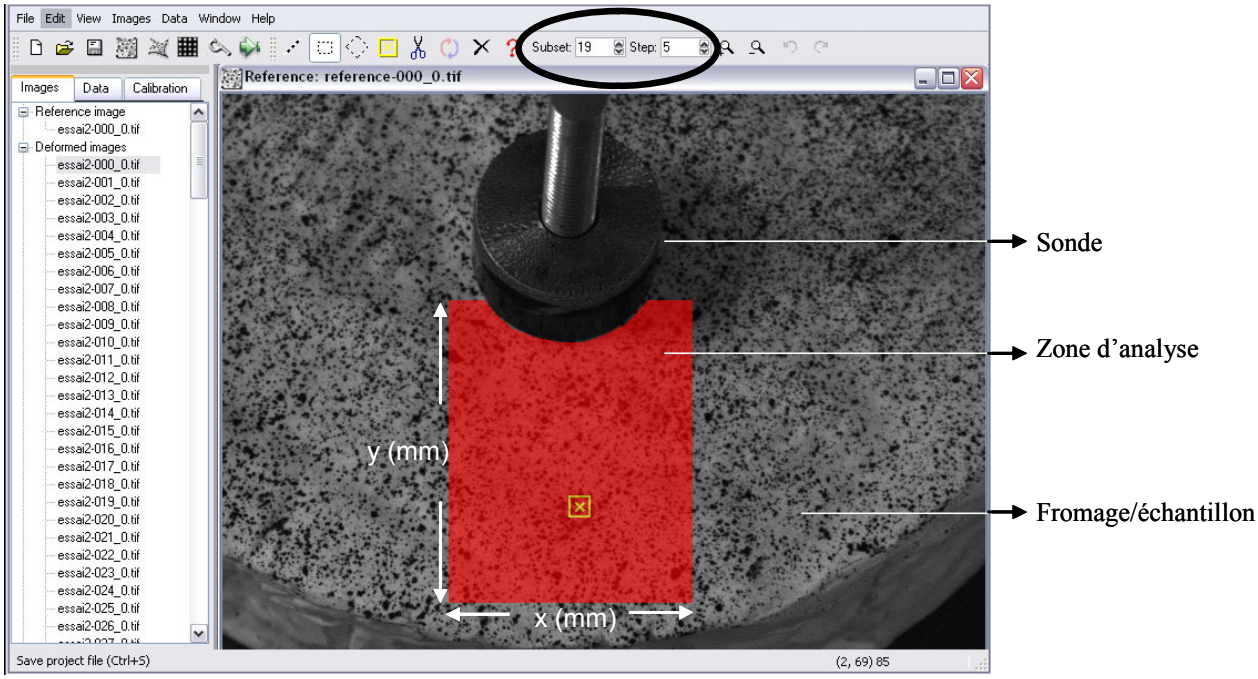

Figure VIII. Zone d'analysée par stéréocorrélation d'images

Les fromages et leurs simulants sont soumis à deux tests de pénétrométrie :

- Test à vitesse constante

Une sonde constituée par une tige métallique cylindrique d'un diamètre de 20 mm est insérée à une vitesse de 10 mm/min dans l'échantillon à 25 mm du bord de ce dernier jusqu'à une profondeur de 4 mm. Une image de l'échantillon est acquise chaque seconde.

- Test à force constante

Une force de 3N est appliquée à la surface de l'échantillon à l'aide de la sonde de 20 mm de diamètre dont la vitesse de déplacement est de 50 mm/min. Cette force est maintenue constante pendant 10 minutes, puis enlevée à une vitesse de 50 mm/min. Une image de l'échantillon est acquise chaque seconde pendant 22 minutes. Ce test est généralement réalisé afin de déterminer les paramètres viscoélastiques d'un produit.

Des expériences préliminaires ont été menées afin de choisir la force à appliquer. Une force de 3N correspond approximativement à la force qu'appliquerait une personne qui appuierait son doigt sur un Camembert en linéaire afin d'évaluer sa 'fermeté'. De plus, cette force permet de différencier les échantillons entre eux tout en évitant la rupture de la croûte du fromage. La rupture de la croûte du fromage entraîne, en effet, des erreurs dans l'analyse des images par stéréocorrélation.

La fermeté et les paramètres liés aux propriétés viscoélastiques des produits (le temps de relaxation et le module d'élasticité) sont calculés. La corrélation entre ces paramètres et ceux obtenus par le système de stéréocorrélation d'images est ensuite déterminée.

Les courbes de déplacement de surface (déplacement de surface des échantillons dans la direction de Z en fonction de la distance à partir du bord de la sonde) obtenues à partir du test de pénétrométrie à vitesse constante sont ajustées à l'équation II. Les valeurs de Z sont converties en valeurs positives pour simplifier l'équation II.

$$Z(mm) = Z_0 + a \times \exp(-bY)\,, \qquad \text{(II)}$$

Z (mm) est le déplacement de la surface de l'échantillon dans la direction de Z. Y (mm) est la distance radiale à partir du bord de la sonde. Z_0, a et b sont des coefficients.

La corrélation entre les coéfficients Z_0, *a, b* et les paramètre rhéologiques est déterminée afin de mettre en évidence une éventuelle influence des paramètres rhéologiques sur ces coefficients. Afin d'éviter une autocorrélation entre les variables (paramètres rhéologiques), seul les paramètres du premier élément de Maxwell (r_1 et E_1) sont utilisés.

2.4. Mesure topométrique tridimentionnelle de Breuckmann

Le système de mesure topométrique 3D OptoTOP-HE de Breuckmann fonctionne par triangulation optique et projection de franges, codage de lumière et analyse d'image. Son principe repose sur l'analyse par effet de Moiré de la déformation d'une lumière blanche projetée sur un objet. Une caméra capture l'image de l'objet, puis la projection d'une séquence de code de Gray et de 4 images de franges à décalage de phase connu afin de déterminer pour chaque point la différence de hauteur avec précision.
Le capteur, de type optoTOP, est constitué d'un projecteur avec un motif sinusoïdal de 128 lignes et une lampe halogène, d'une caméra haute résolution (type PixelLINK PL-A633) et de 2 pointeurs laser (Figure IX).

Figure IX. Équipement de numérisation du système de Breuckmann

Pour numériser complètement un objet, plusieurs vues sont nécessaires. Le traitement du nuage de points s'effectue sur GEOMAGIC-Studio 8. Ce logiciel permet également de faire de la reconstruction de surface à partir du nuage de points du modèle numérisé. Le nuage de points obtenu par numérisation est ensuite traité par le logiciel OptoCAT 3D-Post-Processing qui permet de fusionner les prises de vues.
Le système numérisation de Breuckmann est couplé à la machine d'essai universelle (Figure X).

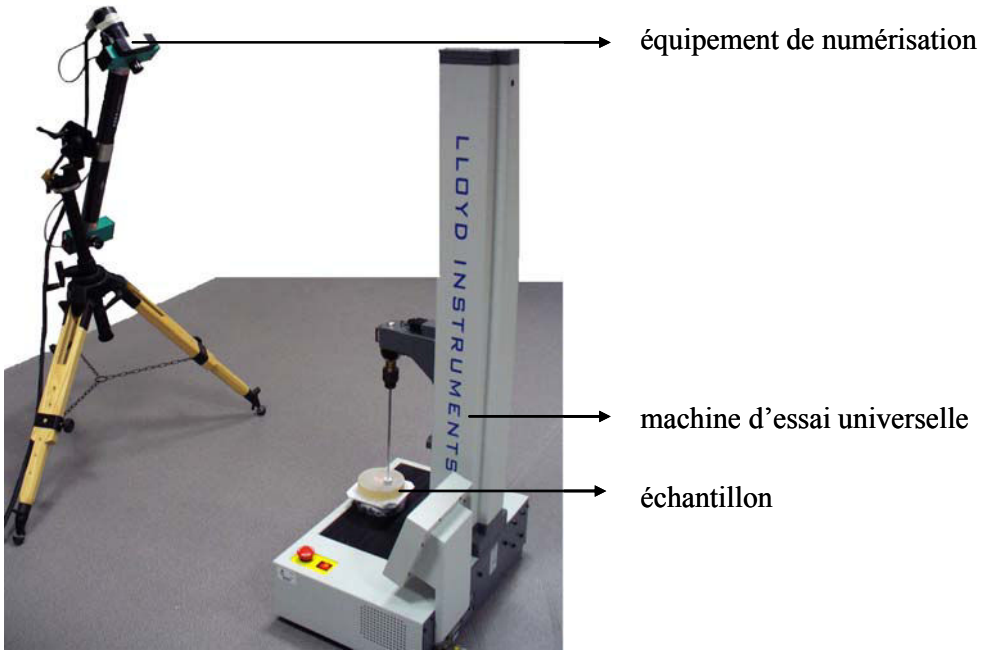

Figure X. Système de numérisation de Breuckmann Opto-TOP HE 3D

Les échantillons sont soumis au test de pénétrométrie : une sonde cylindrique d'un diamètre de 20 mm est insérée à une vitesse de 200 mm/min dans l'échantillon à 25 mm de bord de ce dernier jusqu'à une profondeur de 4 mm. La sonde est maintenue à cette profondeur pendant 30 minutes pour permettre la prise de plusieurs vues de l'échantillon pendant sa déformation.

CHAPITRE II: RÉSULTATS ET DISCUSSION

PARTIE I: FORMULATION DE GELS POLYMÉRIQUES IMITANT LA TEXTURE DES FROMAGES À PÂTE MOLLE

Quatre gels polymériques ont été formulés à partir de mélange de gélatine et de polysaccharides afin d'imiter les propriétés rhéologiques du Camembert/Coulommiers âgé de 10 jours. Une fois la composition du simulant déterminée, la concentration de ses composants est ajustée à l'aide d'un plan de mélange. L'effet de chaque composant sur les propriétés texturales du simulant est aussi étudié.

1. ÉVALUATION INSTRUMENTALE DES PROPRIÉTÉS TEXTURALES DES FROMAGES ET DES SIMULANTS

1.1. Fermeté

La fermeté est déterminée à partir de la courbe de force en fonction du déplacement de la sonde. Elle est considérée comme la force nécessaire pour insérer la sonde à une profondeur de 10 mm dans l'échantillon. La figure XI montre la fermeté des fromages et des gels formulés.

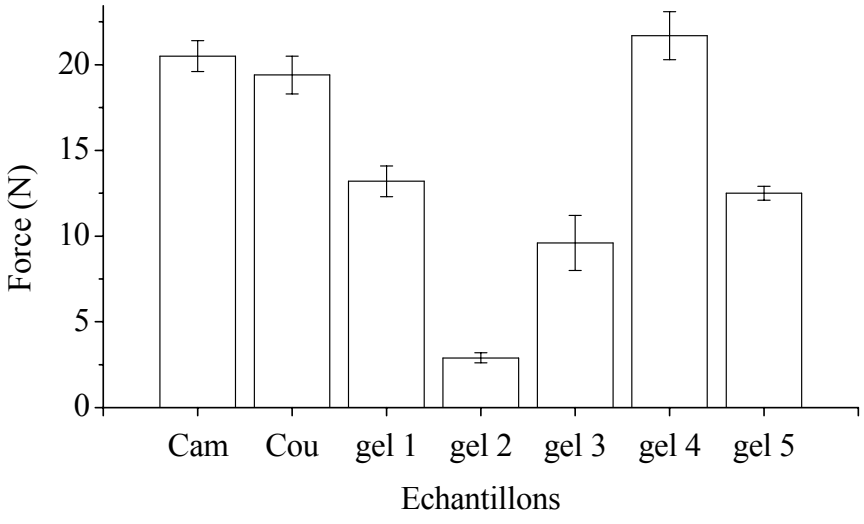

Figure XI. Fermeté du Camembert âgé de 10 jours (Cam), Coulommiers âgé de 10 jours (Cou), gel de gélatine *6%w/w* (gel 1); gel de gélatine-guar, *6/1, %w/w* (gel 2); gel de gélatine-karaya *6/3, %w/w* (gel 3), gel de gélatine-xanthane, *6/3, %w/w* (gel 4) et gel de gélatine-maltodextrine-amidon, *6/20/3, %w/w* (gel 5) déterminée à partir de la courbe de force en fonction du déplacement de la sonde. (Barre d'erreur = écart type ; nombre de répétitions : 6 pour le fromage et 3 pour les gels).

Le guar, le karaya et la xanthane modifient de manière significative la fermeté de la gélatine : le guar et le karaya induisent une diminution de la fermeté de la gélatine, alors que la xanthane entraîne une augmentation de la fermeté. Par ailleurs, la fermeté des fromages est significativement différente de celle des gels formulés, à l'exception du gel 4 (gélatine-xanthane).

1.2. Modèle de Maxwell

Les courbes de relaxation des échantillons sont ajustées à un corps de Maxwell généralisé constitué par l'association en parallèle de trois éléments de Maxwell (figure XII). L'évolution du module de relaxation, E (t), peut être alors décrite par l'équation III.

$$E(t) = E_1 \exp(-t/r_1) + E_2 \exp(-t/r_2) + E_3 \exp(-t/r_3) \qquad \text{(III)}$$

où E_1, E_2, E_3 sont respectivement le module d'élasticité du premier, deuxième et troisième élément de Maxwell et r_1, r_2 and r_3 sont respectivement le temps de relaxation du premier, deuxième et troisième élément de Maxwell. t (s) correspond à la durée d'application de la déformation.

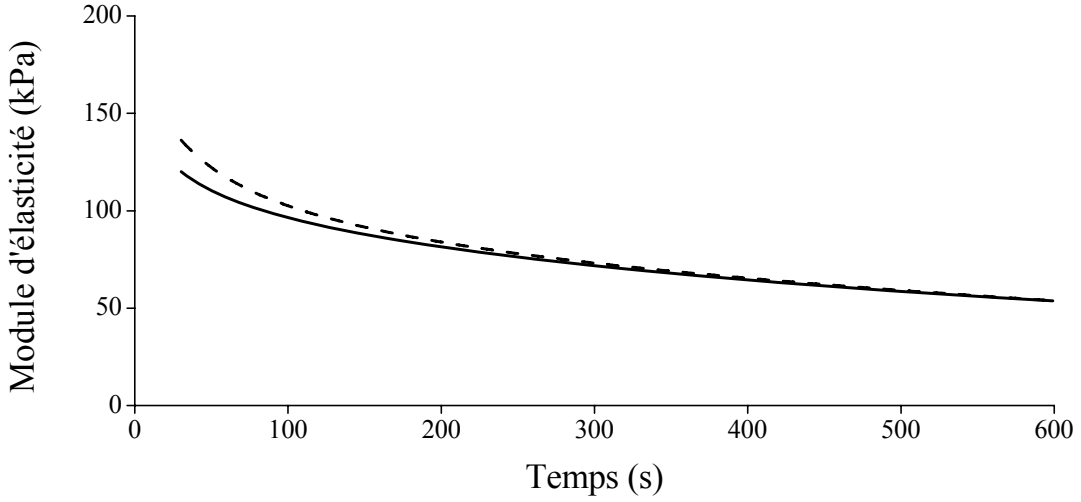

Figure XII. Courbe de relaxation expérimentale (—) ajustée au modèle de Maxwell à trois éléments (- - -) d'un Coulommiers âgé de 10 jours. La courbe du modèle de Maxwell est obtenue à partir de l'équation III. R^2 = 0.9998, Barre d'erreur = écart type ; nombre de répétitions = 6.

La figure XIII montre les valeurs du module d'élasticité des fromages et des gels formulés.

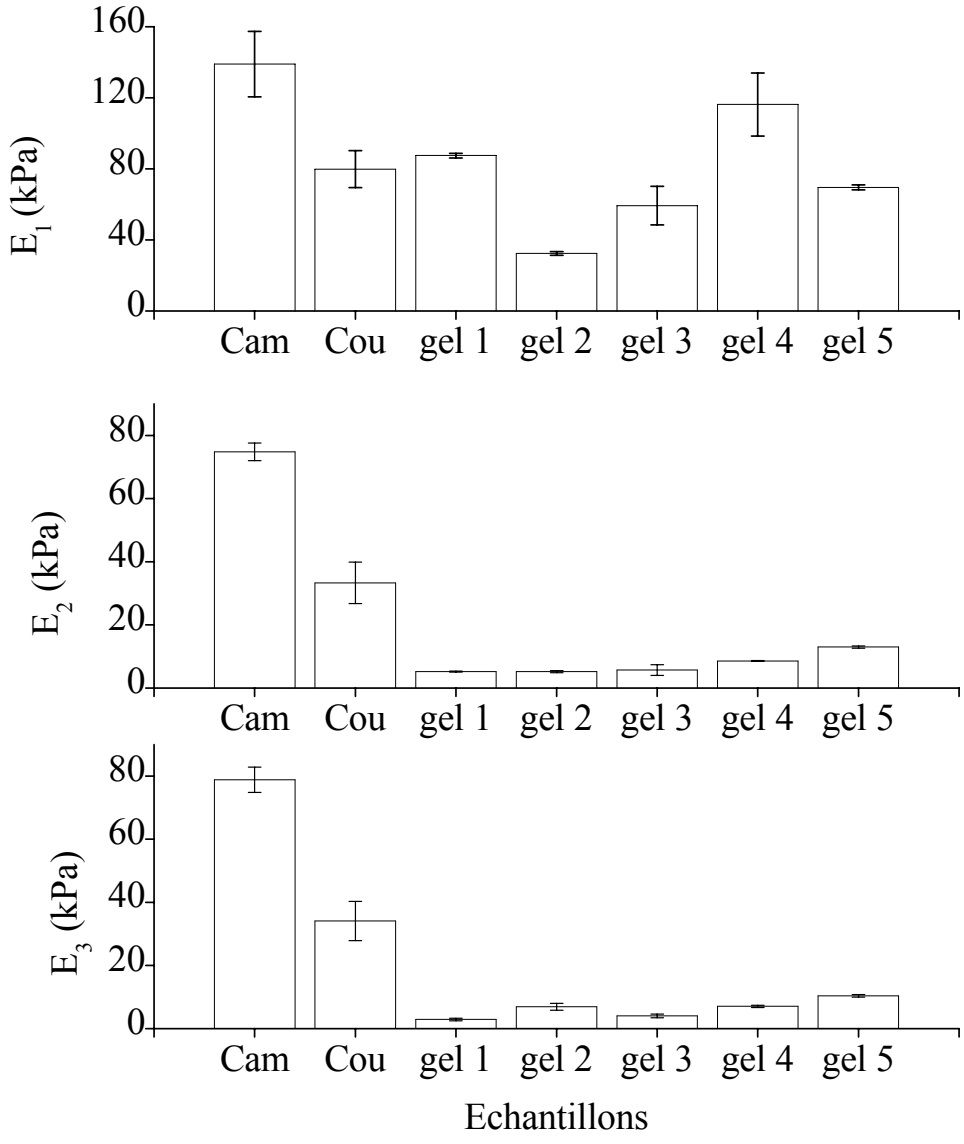

Figure XIII. Modules d'élasticité (E_1, E_2, E_3) du Camembert (Cam) et du Coulommiers (Cou) âgé de 10 jours, gel de gélatine *6/1, %w/w* (gel 1), gel de gélatine-guar gel, *6/3, %w/w* (gel 2), gel de gélatine-karaya gel *6/3, %w/w* (gel 3), gel de gélatine-xanthan gel, *6/3, %w/w* (gel 4) et gélatine-maltodextrine-amidon, *6/20/3, %w/w* (gel 5) calculés à partir des courbes de relaxation. Barre d'erreur = écart type ; nombre de répétitions : 6 pour le fromage et 3 pour les gels.

La valeur de E_1 du gel de gélatine diminue de manière significative en présence de guar et de karaya, et au contraire augmente avec l'ajout de xanthane. La xanthane, la maltodextrine et l'amidon entraînent une augmentation de la valeur de E_2 du gel de gélatine. Tous les polysaccharides ajoutés augmentent la valeur de E_2 du gel de gélatine.
Les valeurs de E_2 et E_3 des gels sont plus faibles que celles des fromages. Par ailleurs, la valeur de E_1 des fromages et des gels est supérieure à celles de E_2 et E_3. Enfin, les valeurs de E_1, E_2 and E_3 du Camembert sont supérieures à celles du Coulommiers. La teneur en matière grasse du Camembert est plus faible que celle du Coulommiers (une différence de 3%). Cette diminution de la teneur en matière grasse entraîne une augmentation du module d'élasticité du Camembert (Guinee and Law, 2002).

La figure XIV montre les valeurs du temps de relaxation des fromages et des gels formulés. La valeur de r_1 du gel de gélatine diminue de manière significative en présence de guar, maltodextrine et amidon. De plus, la valeur de r_1 des gels, sauf le gel 5 (gélatine-maltodextrine-amidon), est supérieure à celle du Camembert et du Coulommiers. En ce qui concerne les valeurs de r_2 et r_3, aucun changement significatif est noté lorsque la gélatine est mélangée avec les polysaccharides.

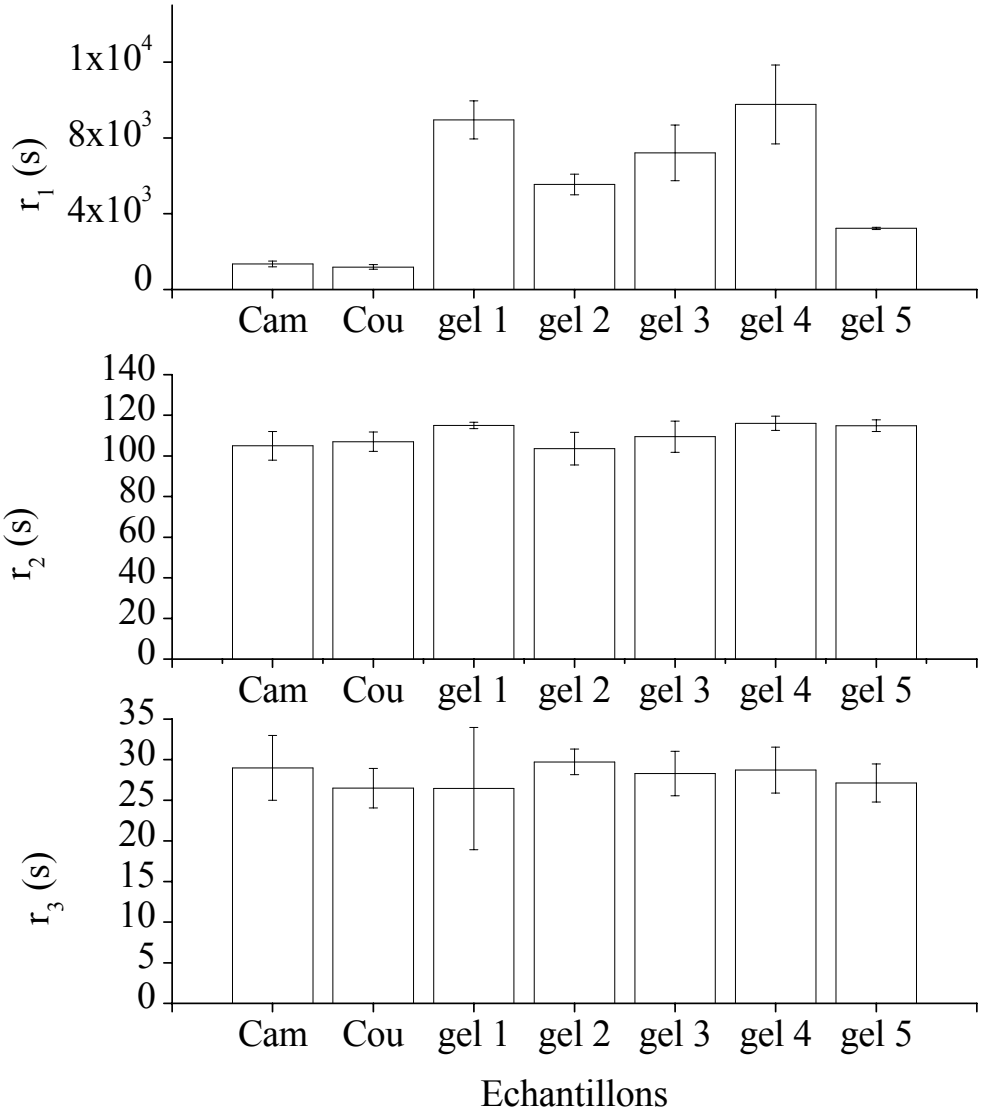

Figure XIV. Temps de relaxation (r_1, r_2, r_3) du Camembert (Cam) et du Coulommiers (Cou) âgé de 10 jours, gel de gélatine *6/1, %w/w* (gel 1), gel de gélatine-guar gel, *6/3, %w/w* (gel 2), gel de gélatine-karaya gel *6/3, %w/w* (gel 3), gel de gélatine-xanthan gel, *6/3, %w/w* (gel 4) et gélatine-maltodextrine-amidon, *6/20/3, %w/w* (gel 5) calculés à partir des courbes de relaxation. Barre d'erreur = écart type ; nombre de répétitions : 6 pour le fromage et 3 pour les gels.

Le guar et le karaya entraînent des imperfections dans le réseau de la gélatine. Cette fragilisation est probablement responsable de la diminution des valeurs de fermeté, E_1 et r_1 de la gélatine. La xanthane, au contraire, entraîne une augmentation de ces paramètres rheologiques grâce à un effet de synergie avec la gélatine.

Le gel de gélatine seule ne peut pas reproduire ces trois paramètres rhéologiques (fermeté, E_1 et r_1). L'ajout de polysaccharides a donc pour objectif de modifier ces paramètres afin de se rapprocher de ceux des fromages. Afin de déterminer lequel des gels formulés a une texture proche de celle des fromages, une classification hiérarchique est réalisée (Figure XV).

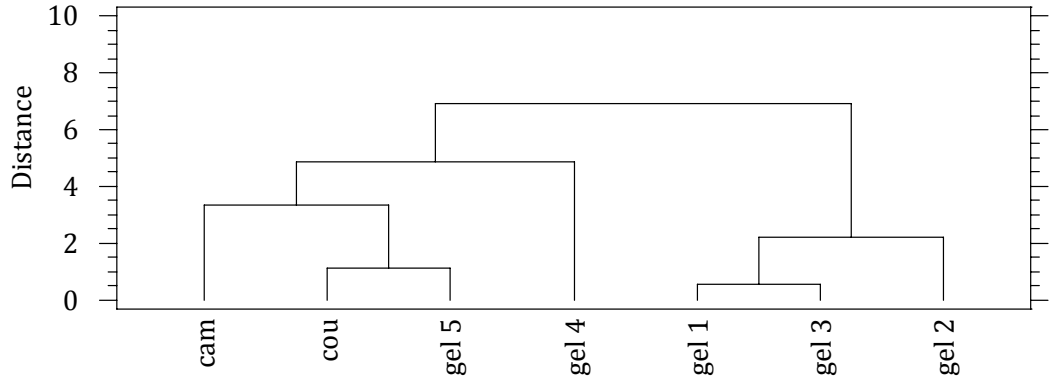

Figure XV. Classification hiérarchique réalisée à partir des valeurs de fermeté, E_1 et r_1 du Camembert (Cam) et du Coulommiers (Cou) âgé de 10 jours, gel de gélatine *6/1, %w/w* (gel 1), gel de gélatine-guar gel, *6/3, %w/w* (gel 2), gel de gélatine-karaya gel *6/3, %w/w* (gel 3), gel de gélatine-xanthan gel, *6/3, %w/w* (gel 4) et gélatine-maltodextrine-amidon, *6/20/3, %w/w* (gel 5).

D'après les résultats présentés dans la figure XV, on peut dire que le gel 5 (gélatine-maltodextrine-amidon, 6/20/3, %w/w) a une texture qui se rapproche le plus des fromages. Un plan de mélange à trois composants est ensuite utilisé afin de déterminer la concentration optimale de chaque constituant, ainsi que leur effet sur les paramètres rhéologiques des gels.

2. EFFET DES CONSTITUANTS SUR LA FERMETÉ, LE TEMPS DE RELAXATION ET LE MODULE D'ELASTICITÉ

Les résultats obtenus montrent qu'il y a une relation linéaire entre les paramètres rhéologiques des gels formulés à partir de gélatine-maltodextrine-amidon et la concentration de leurs constituants (équations IV à VIII).

$$Fermeté(N) = 4.10 \times 10^{2} X_{gélatine} - 7.57 \times 10^{1} X_{maltodextrine} + 3.89 \times 10^{1} X_{amidon} \quad \text{(IV)}$$

$$r_1(s) = 6.43 \times 10^{4} X_{gélatine} - 2.33 \times 10^{4} X_{maltodextrine} + 1.42 \times 10^{5} X_{amidon} \quad \text{(V)}$$

$$E_1(kPa) = 2.58 \times 10^{3} X_{gélatine} - 5.59 \times 10^{2} X_{maltodextrine} + 6.38 \times 10^{2} X_{amidon} \quad \text{(VI)}$$

$$E_2(kPa) = 2.62 \times 10^{2} X_{gélatine} + 2.02 \times 10^{1} X_{maltodextrine} - 2.99 \times 10^{2} X_{amidon} \quad \text{(VII)}$$

$$E_3(kPa) = 2.14 \times 10^{2} X_{gélatine} + 2.51 X_{maltodextrine} - 1.66 \times 10^{2} X_{amidon} \quad \text{(VIII)}$$

où $X_{gélatine}$, $X_{maltodextrine}$ et X_{amidon} correspondent à la concentration de gélatine, maltodextrine et amidon et qui varie respectivement de 0,05 à 0,1 ; 0,16 à 0,23 et 0,02 à 0,04. Les valeurs de r_2 et r_3 ne sont pas sensibles aux variations de concentration des constituants des gels. La valeur moyenne de r_2 et r_3 est égale à 118 et 28 s, respectivement.

Les équations IV à VIII sont validées grâce à l'analyse de quatre gels supplémentaires, avec des concentrations des constituants différentes de celles proposées par le plan de mélange (figure XVI).

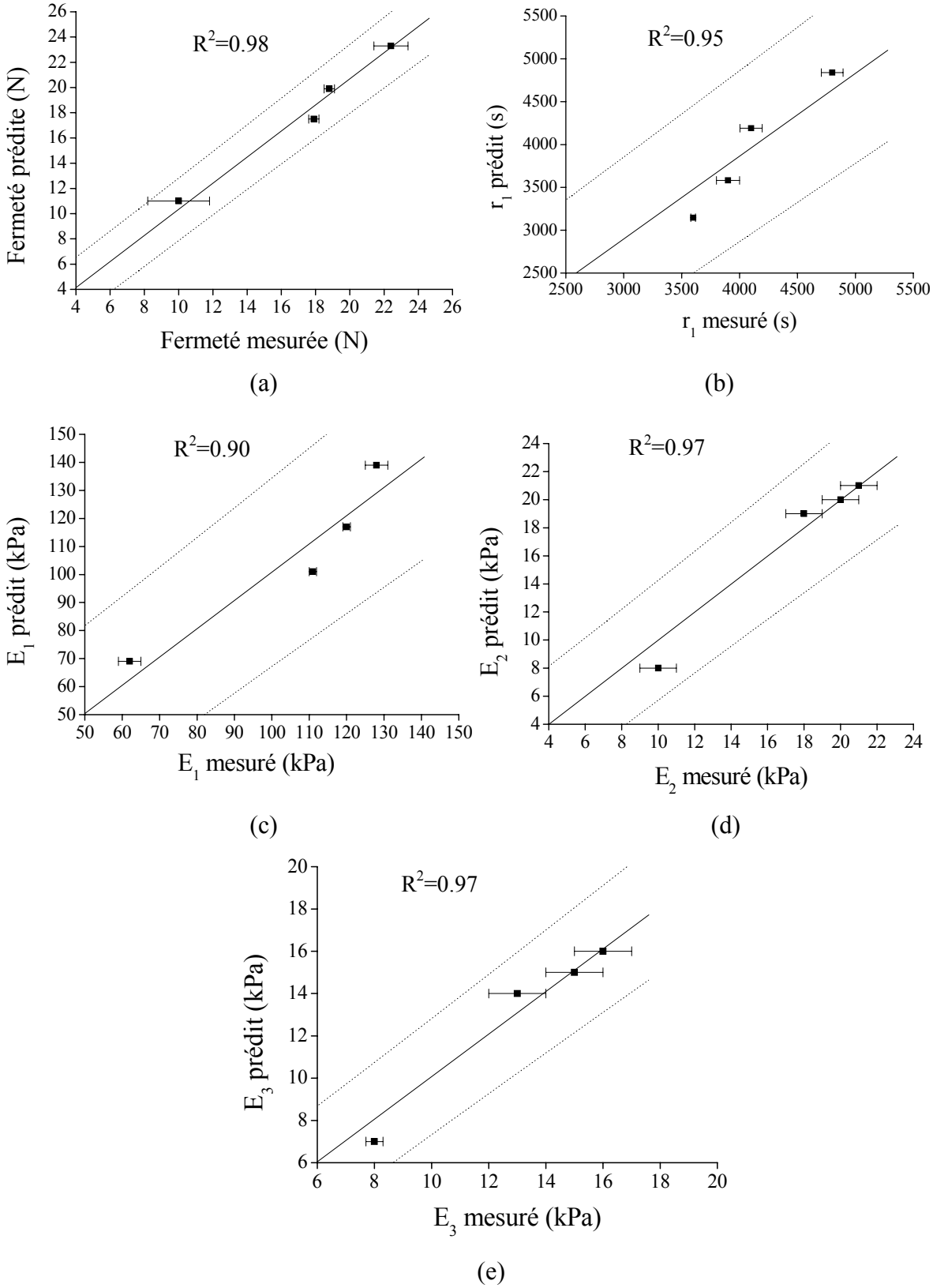

Figure XVI. Corrélation entre les valeurs prédites et mesurées de fermeté (a) r_1 (b), E_1 (c), E_2 (d) et E_3 (e). Les équations IV à VIII sont utilisées pour calculer les valeurs de fermeté, r_1, E_1, E_2 et E_3. Les courbes de tendance sont représentées par un trait continu (—) et les intervalles de confiance à 95% sont indiquées par des pointillés (·····).

Les figures XVII à XIX montrent l'influence des concentrations des constituants sur les paramètres rhéologiques (fermeté, r_1, E_1, E_2 et E_3) des gels.

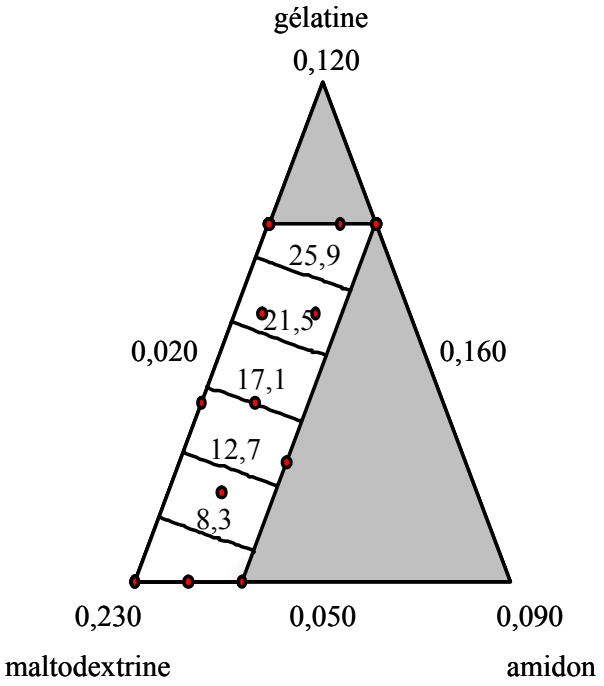

Figure XVII. Évolution de la fermeté (N) des gels en fonction de la concentration des constituants des gels du plan de mélange.

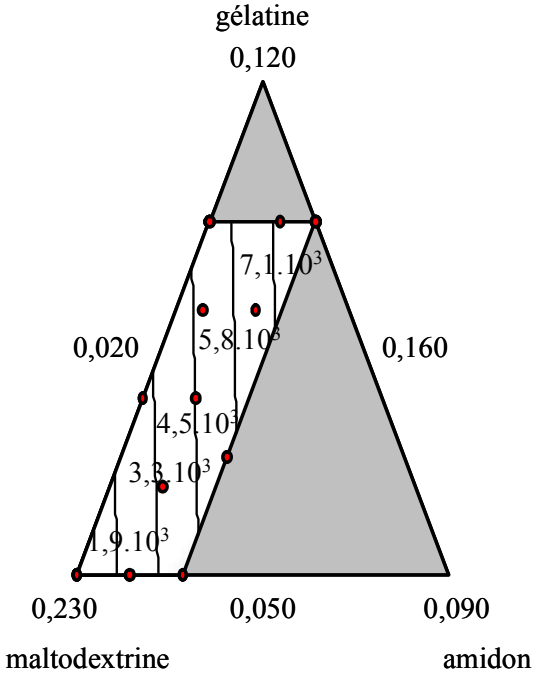

Figure XVIII. Évolution de r_1 (s) des gels en fonction de la concentration des constituants des gels du plan de mélange.

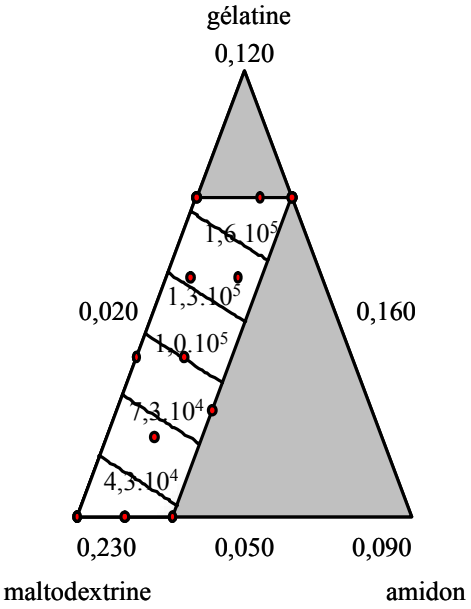

(a)

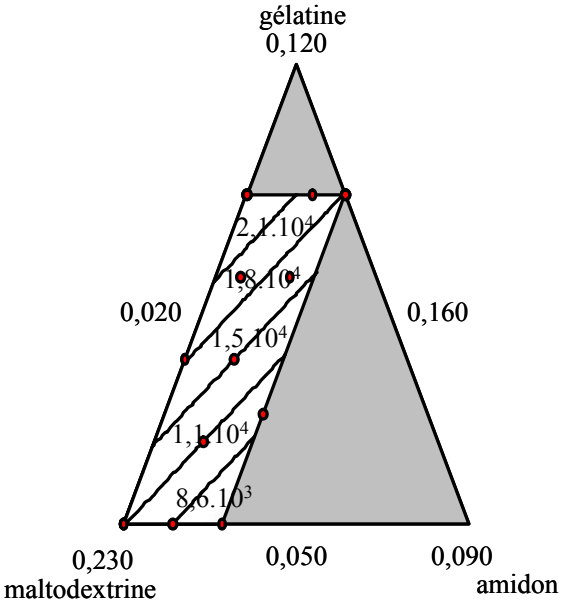

(b)

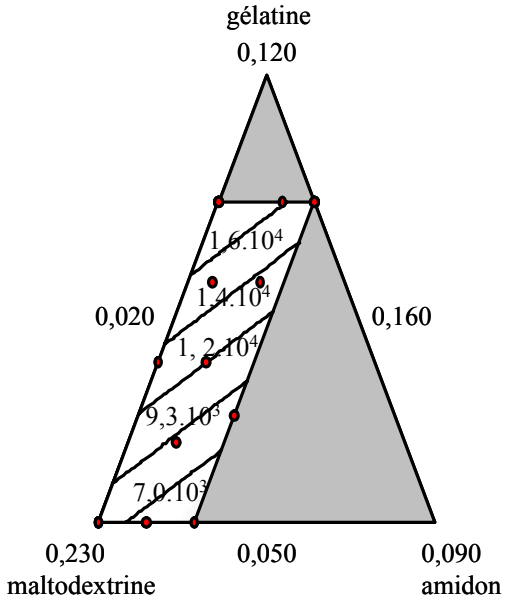

(c)

Figure XIX. Évolution de E_1, (a), E_2 (b) et E_3 (c) (kPa) des gels en fonction de la concentration des constituants des gels du plan de mélange.

L'augmentation de la concentration de gélatine, au dépend de la maltodextrine et de l'amidon, entraîne une augmentation des valeurs de fermeté, r_1, E_1, E_2 et E_3. Une augmentation de la concentration de maltodextrine, au contraire, diminue les valeurs de ces paramètres rhéologiques. La présence de maltodextrine pertube le réseau de gélatine et cette fragilisation est responsable de cette diminution. Lorsque la concentration de l'amidon est augmentée, il y a une faible variation des valeurs de fermeté et de E_1, ce qui signifie que l'amidon, par rapport à la maltodextrine et la gélatine influence moins fortement les valeurs de fermeté et de E_1 des gels. Une hausse plus marquée est observée pour les paramètres r_1, E_2 et E_3.

Par ailleurs, les lignes de niveau correspondant aux valeurs de fermeté, r_1, E_1, E_2 et E_3 sont linéaires et indiquent ainsi que les interactions entre les constituants (gélatine, maltodextrine et amidon) n'ont pas d'effet significatif sur les propriétés rhéologiques des gels formulés.

3. CONCENTRATION OPTIMALE DES CONSTITUANTS DU SIMULANT

Le module d'optimisation du logiciel Design-Expert permet de trouver les concentrations des constituants du gel avec des paramètres rhéologiques proches de ceux des fromages. Les valeurs de fermeté, modules d'élasticité et de temps de relaxation du Camembert et du Coulommiers sont rentrées dans le logiciel comme valeurs cibles. Le tableau VI montre les concentrations des constituants du simulant 'idéal' du Camembert et du Coulommiers, ainsi que les valeurs de leurs paramètres rhéologiques.

Tableau VI. Composition et valeurs de fermeté, module d'élasticité et temps de relaxation du Coulommiers et de leur simulant.

	Coulommiers	Simulant Coulommiers[a]	Camembert	Simulant Camembert[a]
gélatine (% w/w)		7,8		8,3
maltodextrine (% w/w)		20,2		19,7
amidon (% w/w)		2,0		2,0
Fermeté (N)	19 ± 1	17,9 ± 0,3	20 ± 1	18,8 ± 0,3
r_1 (s)	1200 ± 100	3600 ± 20	1300 ± 100	3900 ± 100
r_2 (s)	107 ± 5	119 ± 3	105 ± 7	117 ± 7
r_3 (s)	27 ± 2	32 ± 5	29 ± 4	29 ± 5
E_1 (kPa)	80 ± 9	111 ± 1	139 ± 10	120 ± 1
E_2 (kPa)	33 ± 4	18 ± 1	74 ± 10	20 ± 1
E_3 (kPa)	34 ± 4	14 ± 1	78 ± 7	15 ± 1

[a] composition proposée par le module d'optimisation du logiciel Design-Expert. Les paramètres rhéologiques sont obtenus à partir des tests de pénétrométrie et de relaxation.

Les données présentées dans le tableau VI montrent que les simulants ont une valeur de fermeté très proche de celle des fromages. De plus, le camembert et son simulant ont des valeurs de E_1 qui sont comparables. Par ailleurs, les simulants ont des temps de relaxation plus longs que ceux des fromages. Les simulants ont une structure plus compacte, plus homogène que les fromages. C'est pour cette raison que ces gels se relâchent moins vite que les fromages lorsqu'ils sont soumis à une déformation.

PARTIE II: GEL POLYMÉRIQUE SIMULANT LE COULOMMIERS PENDANT SA MATURATION

Des simulants du Coulommiers et du Camembert sont obtenus à partir d'un mélange de gélatine, maltodextrine et amidon. Ces simulants possèdent des propriétés texturales proches de celles des deux fromages âgés de 10 jours. Dans cette partie de l'étude, un simulant dont la texture évolue au cours du temps est formulé, le but étant d'imiter la cinétique de changement de texture du Coulommiers induits par la maturation. Pour cela, l'enzyme subtilisine carlsberg (dont le nom commercial est l'Alcalase®) est ajoutée au simulant à différentes concentrations. Les modifications des paramètres rhéologiques (fermeté, E_1 et r_1) du simulant sont ensuite suivies au cours du stockage. Des mesures sont réalisées 1, 8, 43, 50 et 120 jours après la préparation du simulant. Ces paramètres rhéologiques sont aussi déterminés pour des Coulommiers 1, 8, 15, 22, 29, 36 et 43 jours après leur emballage.

L'évolution de la fermeté, de E_1 et de r_1 du Coulommiers et des simulants est présentée dans les figures XX et XXI.

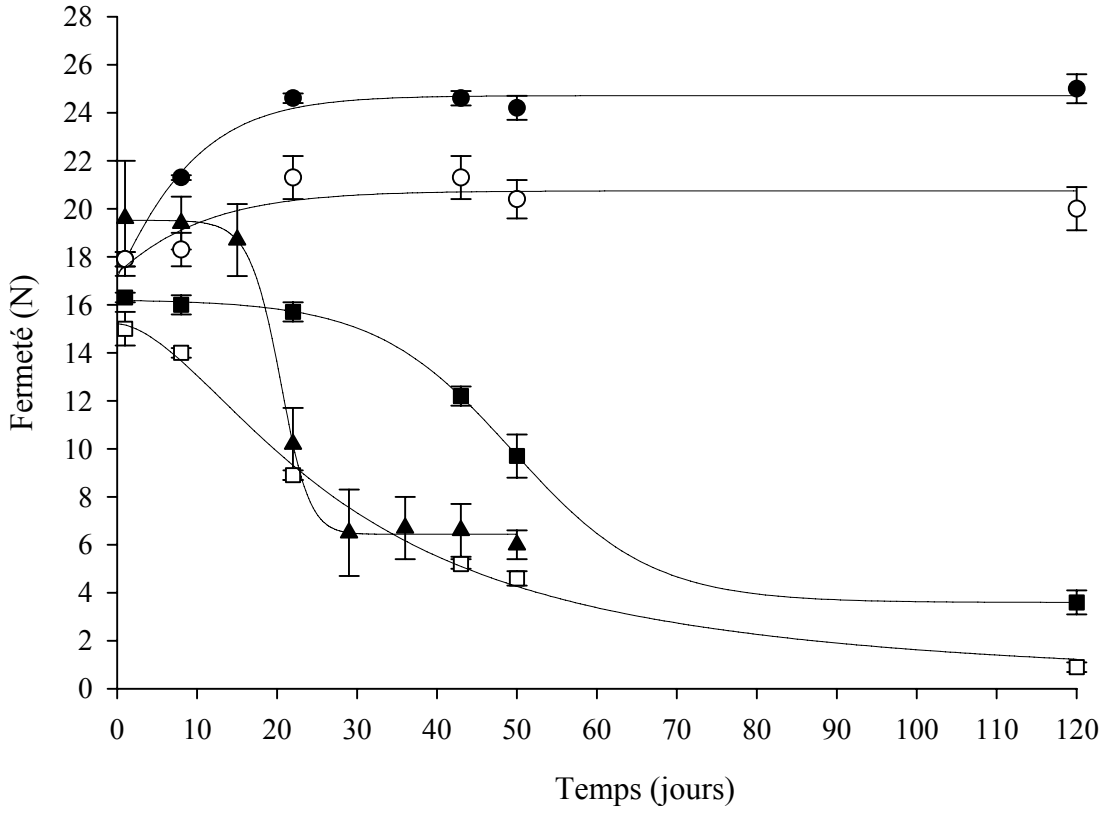

Figure XX. Evolution de la fermeté (N) du Coulommiers (▲), du simulant standard, sans Alcalase® (●), du simulant avec une activité enzymatique de l'Alcalase de 0,006 UA (○), 0,012 UA (■) et 0,030 UA (□) au cours du temps. Barre d'erreur = écart type, nombre de répétitions = 3

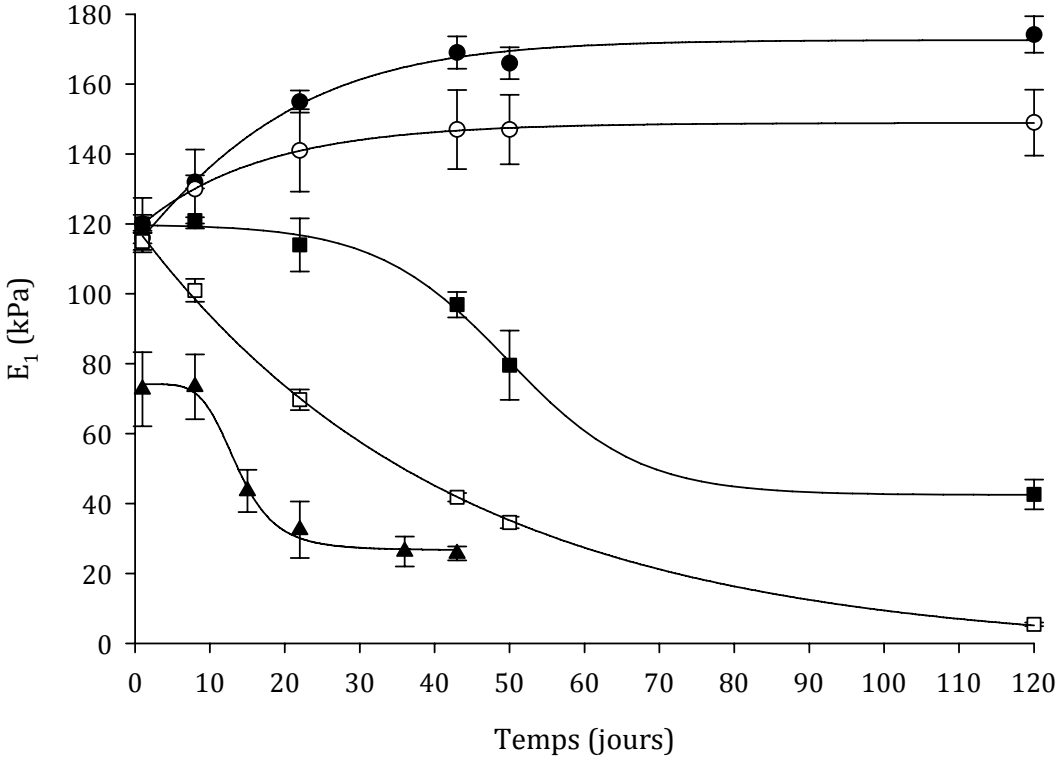

(a)

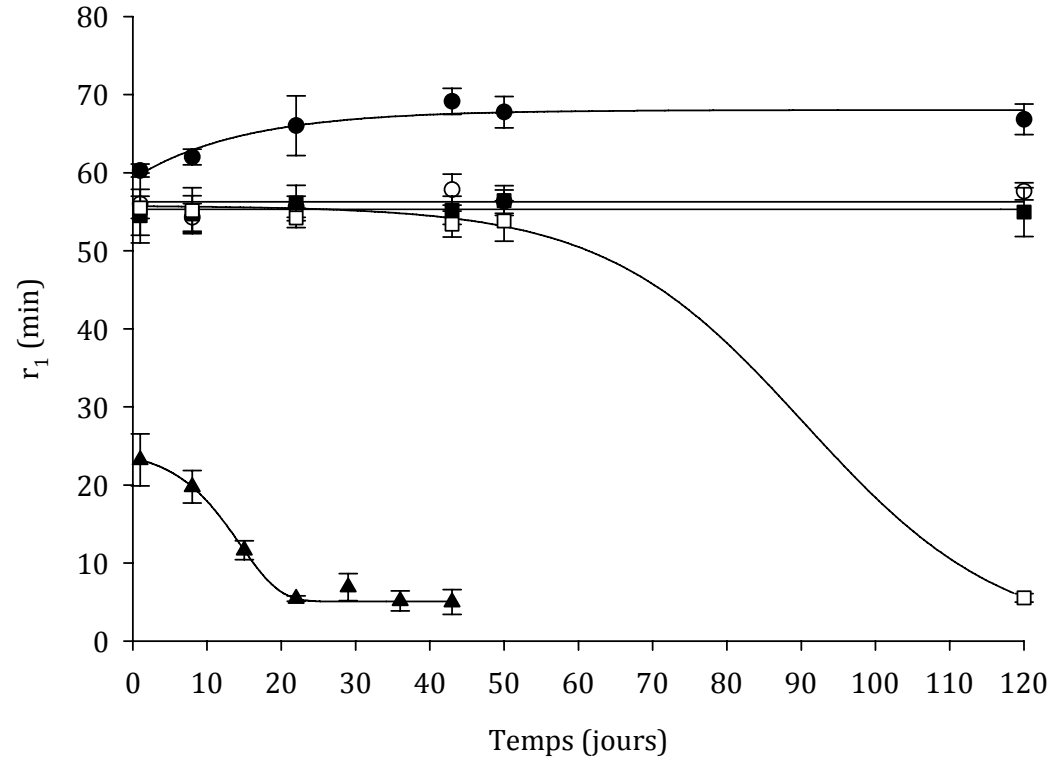

(b)

Figure XXI. Evolution de E_1 (a) et de r_1 (b) du Coulommiers (▲), du simulant standard, sans Alcalase® (●), du simulant avec une activité enzymatique de l'Alcalase de 0,006 UA (○), 0,012 UA (■) et 0,030 UA (□) au cours du temps. Barre d'erreur = écart type, nombre de répétitions = 3.

1. ÉVOLUTION DES PARAMÈTRES RHÉOLOGIQUES DU COULOMMIERS

Au cours de la maturation du Coulommiers, il y a une diminution des valeurs des trois paramètres rhéologiques étudiés. Cette baisse qui a également été observée par d'autres auteurs (Mpagana and Hardy, 1985) indique un changement dans la structure du fromage induit principalement par la protéolyse (Watase and Nishinari, 1980).
Par ailleurs une stabilisation des valeurs des paramètres rhéologiques est notée après environ 30 jours de stockage. Elle est probablement liée à l'effet de la croûte du fromage, qui offre une résistance minimale à l'insertion de la sonde.

2. ÉVOLUTION DES PARAMÈTRES RHÉOLOGIQUES DU SIMULANT STANDARD, SANS ENZYME

Les valeurs de fermeté, E_1 et r_1 du simulant standard (sans Alcalase®) augmentent au début du stockage puis se stabilisent après environ 22 jours. Cette hausse est due à l'augmentation de la taille et peut être du nombre des zones de jonctions du gel de gélatine. Par ailleurs, la croissance de la taille des zones de jonction entraîne une diminution de la mobilité des chaînes de la gélatine, ce qui se traduit par une augmentation de la valeur de r_1 du simulant standard (Comby *et al.,* 1985).

3. ÉVOLUTION DES PARAMÈTRES RHÉOLOGIQUES DU SIMULANT CONTENANT DE L'ALCALASE®

L'ajout d'Alcalase® au simulant entraîne l'hydrolyse des liaisons peptidiques de la gélatine, ce qui fragilise le réseau du gel. Ainsi, les simulants contenant de l'Alcalase® ont des valeurs de fermeté et de E_1 inférieures à celles du simulant standard (sans enzyme). Les paramètres rhéologiques évoluent en fonction de la concentration en enzyme dans le simulant. Lorsque l'activité de l'Alcalase® est égale à 0,030 UA, il y a une diminution très marquée de la fermeté et de E_1. Un changement dans la valeur de r_1 est noté après 120 jours de stockage, alors qu'il n'y avait pas d'évolution significative les 50 premiers jours de stockage. La diminution de la

valeur de r_1 est causée par la dégradation très importante que subit le simulant au bout de 150 jours conduisant à une pâte.

Lorsque l'activité de l'Alcalase® est abaissée à 0,012 UA, on remarque une diminution moins rapide des valeurs de fermeté et de E_1. La valeur de r_1 est stable au cours du stockage. La rupture des liaisons peptidiques ne semble donc pas influencer r_1.

L'ajout de 0,006 UA d'Alcalase® a aussi entraîné des ruptures de liaisons peptidiques ce qui s'est traduit par des valeurs de fermeté et de E_1 inférieures à celles du simulant standard, sans enzyme. De plus, une augmentation des valeurs de ces deux paramètres est notée au début du stockage, ce qui signifie qu'il y a une nette hausse de la taille et du nombre de zones de jonction dans le gel.

L'ajout d'Alcalase® au simulant induit bien des modifications de fermeté et de E_1. Toutefois, les valeurs des paramètres rhéologiques du Coulommiers n'évoluent pas de la même manière que celles des simulants. Il se peut que cette différence soit dû au fait que dans le fromage, il y a une synthèse continue d'enzymes, alors que dans le simulant, une quantité fixe d'Alcalase® est ajoutée au cours de sa préparation. Une façon d'améliorer le simulant, serait peut être d'assurer un relargage plus progressif de l'enzyme au cours du stockage.

PARTIE III: PROPRIÉTÉS TEXTURALES DETERMINÉES PAR NUMÉRISATION TRIDIMENSIONNELLE

La numérisation tridimensionnelle est un outil intéressant qui permet la visualisation du déplacement de surface et de la déformation des objets. Cette technique est principalement utilisée dans le domaine de la mécanique. Par exemple, elle est utilisée pour mesurer le déplacement de surface autour des points de fissure (Luo *et al.*, 1993; Luo *et al.*, 1994) ou lors des études de forage (Wu and Lu, 2000; Nelson *et al.*, 2006). Elle n'a cependant jamais été appliquée au domaine alimentaire. Ce chapitre développe ainsi l'intérêt de l'utilisation de deux techniques de numérisation tridimensionnelle, la stéréocorrélation d'image et le système de Breuckmann, pour caractériser la texture des aliments.

Les images 3D du déplacement de surface des gels de 8, 10, 15, 20 % (p/p) de gélatine, du Coulommiers âgé de 10 jours, du Camembert âgé de 30 jours, ainsi que leur simulant, sont acquises lors d'un test de pénétrométrie où la sonde est insérée à une profondeur de 4 mm dans les échantillons. Le déplacement de surface des échantillons, noté Z (mm) et mesuré par la méthode de stéréocorrélation d'images, est tracé en fonction de la distance radiale à partir du bord de la sonde (figures XXIII, XXVI, XXVII).

1. GELS DE 8, 10, 15, 20% (W/W) DE GÉLATINE

La figure XXII montre le schéma du déplacement de surface d'un gel de 8% de gélatine. La sonde est enfoncée à une profondeur de 4 mm dans le gel. Comme cela a déjà été mentionné dans la partie 'matériel et méthodes', les paramètres choisis pour l'analyse d'images par stéréocorrélation permettent de mesurer le déplacement de la surface à partir de 1 mm de la sonde. C'est pour cette raison que la partie du graphique (figure XXII) de Y=0 à 1 mm est indiquée en pointillé. Dans tous les graphiques représentant le déplacement de surface d'un échantillon (Z, mm) en fonction de la distance radiale à partir de la sonde, les courbes sont tracées à partir de Y= 1 mm.

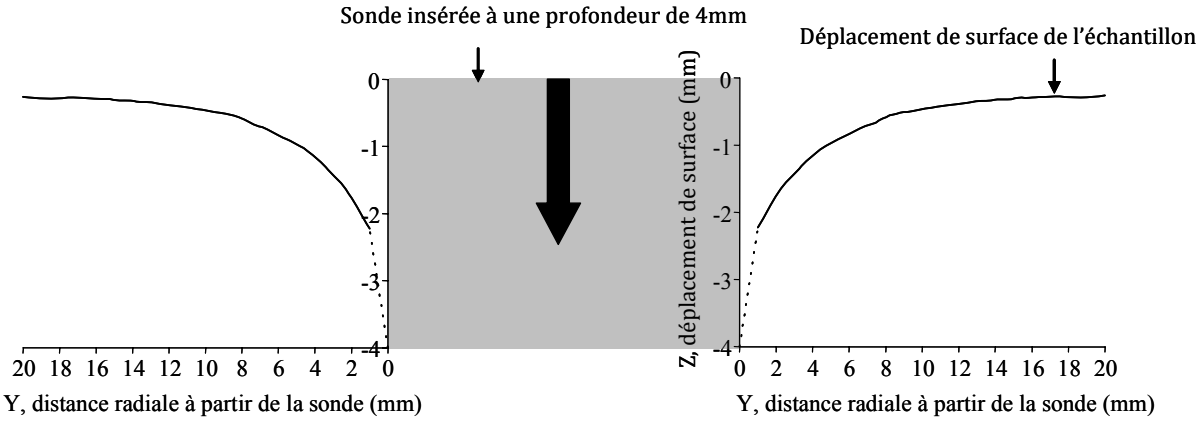

Figure XXII. Schéma du déplacement de surface d'un gel de 8% de gélatine. La sonde est enfoncée à une profondeur de 4 mm dans le gel.

La figure XXIII montre le déplacement de surface des gels de 8, 10, 15 et 20 % de gélatine lorsque la sonde de la machine d'essai universelle est insérée à une profondeur de 4 mm dans l'échantillon.

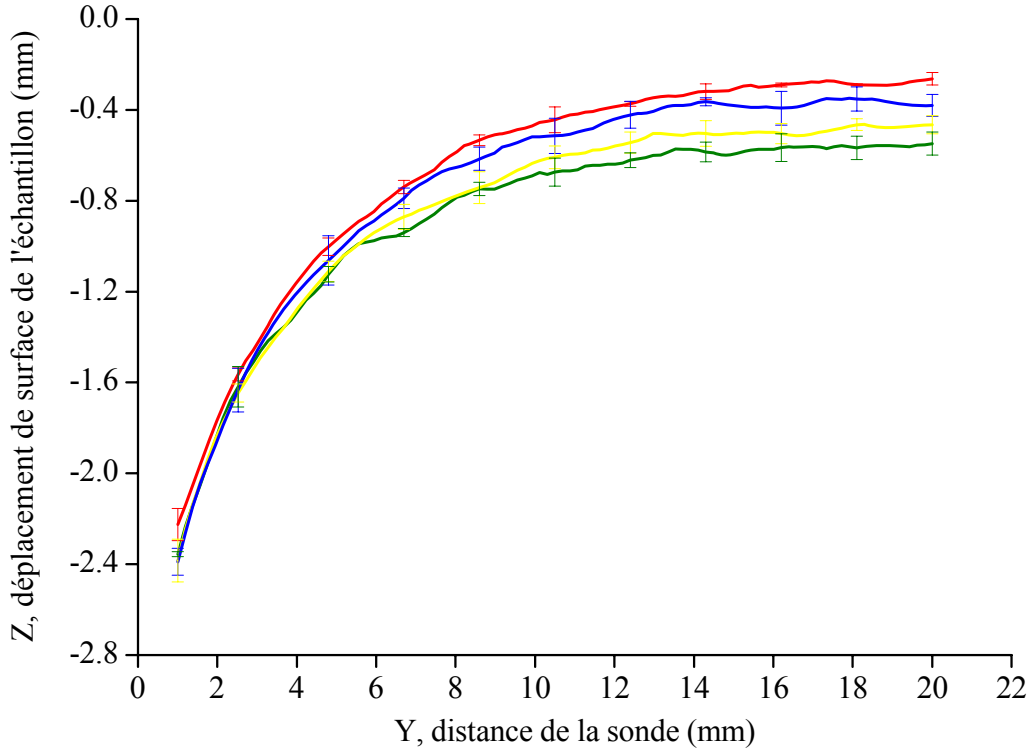

Figure XXIII. Déplacement de surface d'un gel de 8% gélatine (—), 10% gélatine (—), 15% gélatine (—), 20% gélatine (—) lorsque la sonde est insérée à une profondeur de 4 mm dans l'échantillon. Barre d'erreur = écart type, nombre de répétitions = 3.

Le déplacement de la surface des gels se situe principalement dans une zone proche de la sonde (distance radiale d'environ 6 mm) (figure XXIII). On remarque aussi qu'à une distance radiale de 20 mm de la sonde, et en augmentant la concentration en gélatine, le déplacement de surface du gel augmente. Ces observations concordent avec celles obtenues par la deuxième méthode de numérisation, le système de Breuckmann.

Les figures XXIV et XXV montrent des images tridimensionnelles d'un gel de 8% et 15% de gélatine, respectivement, lorsque la sonde est insérée à une profondeur de 4 mm. Les images sont acquises par le système de Breuckmann. Les valeurs négatives correspondent à un enfoncement de la surface du gel alors que les valeurs positives indiquent un gonflement.
La zone bleue, correspondant à un enfoncement de la surface du gel, se situe proche de la sonde pour le gel de 8% de gélatine. Cette zone s'étend plus loin lorsque la concentration en gélatine est augmentée à 15%. Par ailleurs, la zone de gonflement dans le cas du gel de 15% de gélatine se limite au niveau de sa périphérie, contrairement à ce qui est noté pour le gel de 8% de gélatine. En effet, dans le cas de ce dernier, une partie de la matière est déplacée à la surface du gel.

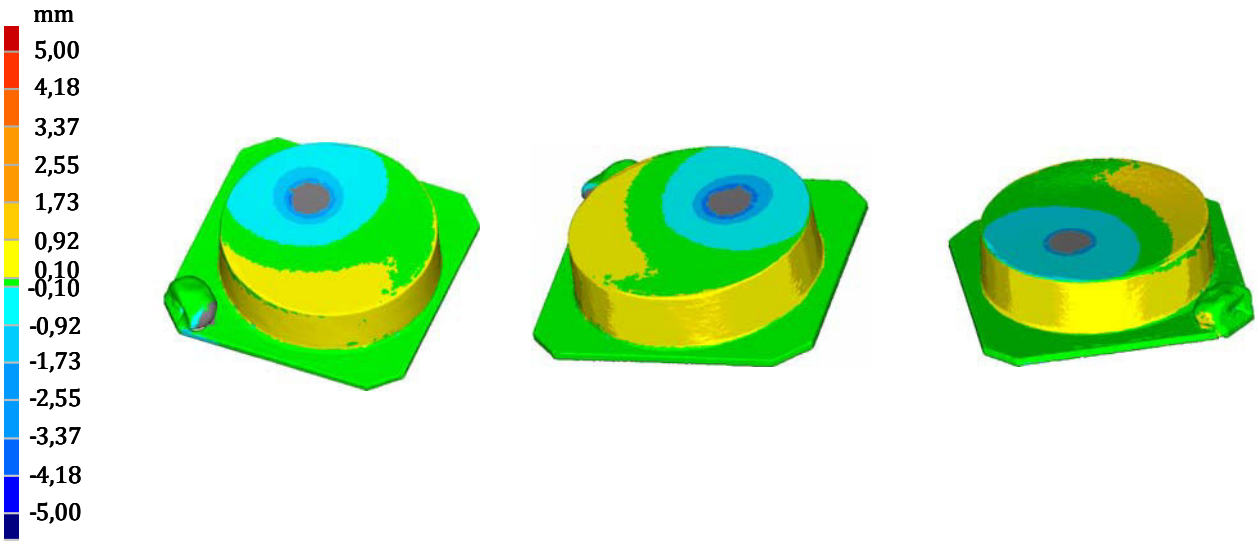

(a)

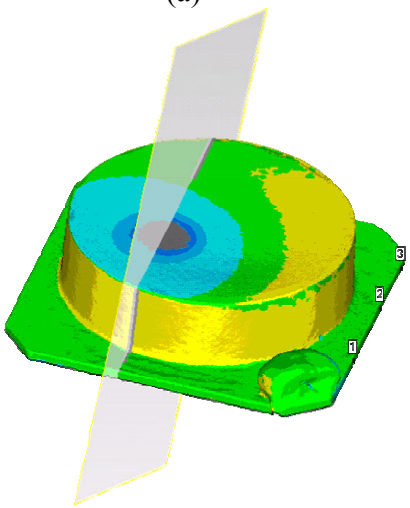

(b)

Déplacement maximale positif/négatif: 0.58/-2.28 ±0.01 mm

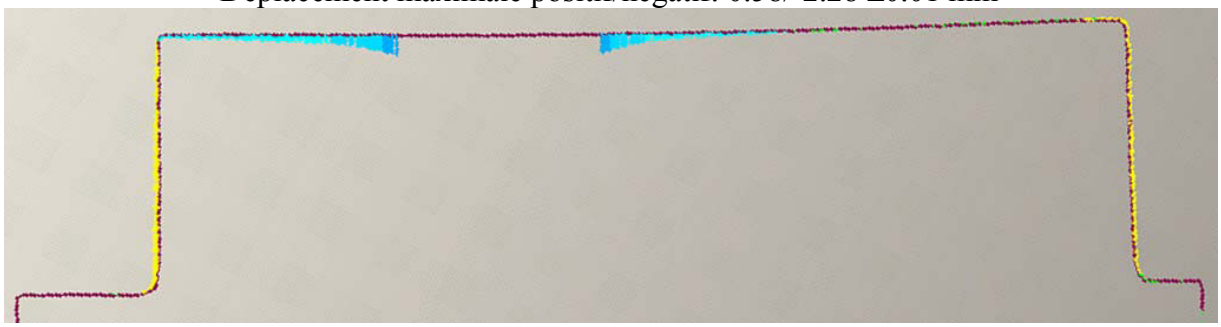

(c)

Figure XXIV. Trois vues d'un gel de 8% de gélatine. La sonde est insérée à une profondeur de 4 mm dans le gel (a), position d'une coupe transversale (b) et l'image de la coupe transversale montrant le déplacement de surface du gel (c). Les images sont acquises par le système de Breuckmann.

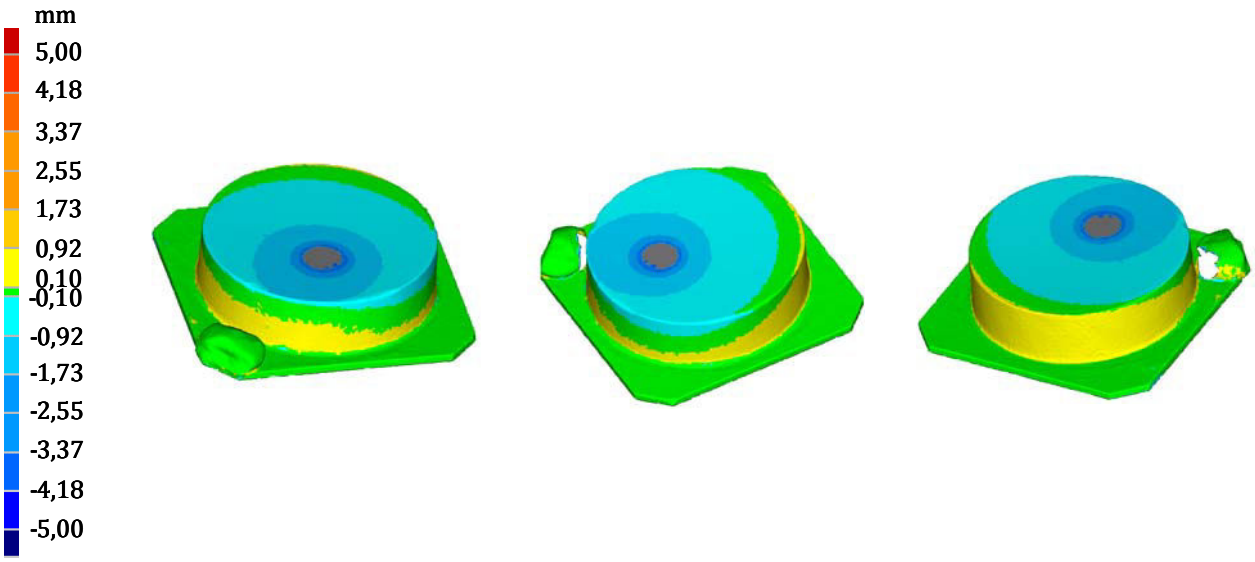

(a)

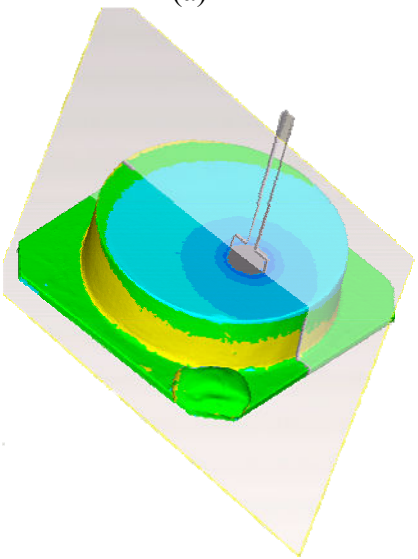

(b)

Déplacement maximale positif/négatif: 0.62/-2.32 ±0.01 mm

(c)

Figure XXV. Trois vues d'un gel de 15% de gélatine. La sonde est insérée à une profondeur de 4 mm dans le gel (a), position d'une coupe transversale (b) et l'image de la coupe transversale montrant le déplacement de surface du gel (c). Les images sont acquises par le système de Breuckmann.

2. COULOMMIERS ÂGÉ DE 10 JOURS ET DE SON SIMULANT

Des images tridimensionnelles du Coulommiers âgé de 10 jours, ainsi que de son simulant sont acquises pendant le test de pénétrométrie par la méthode de stéréocorrélation d'images. La sonde est enfoncée à une profondeur de 4 mm dans les échantillons. La figure XXVI montre le déplacement de surface du Coulommiers et de son simulant en fonction de la distance radiale à partir du bord de la sonde.

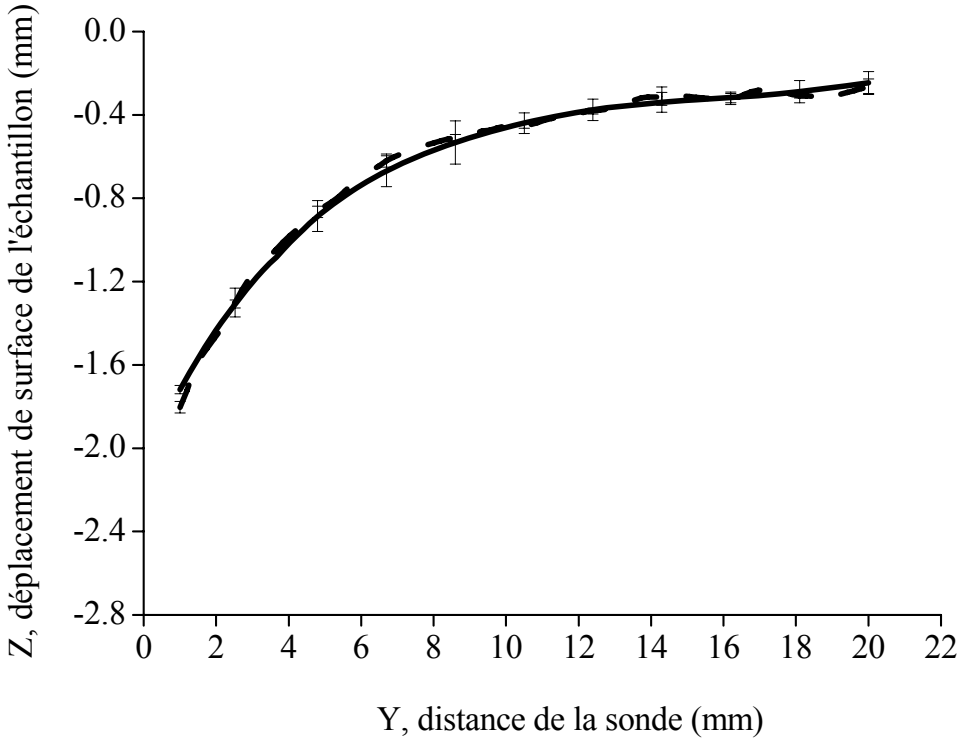

Figure XXVI. Déplacement de surface du Coulommiers âgé de 10 jours (—), et de son simulant (– – –) en fonction de la distance à partir du bord de la sonde. Barre d'erreur = écart type, nombre de répétitions = 6 pour le Coulommiers et 3 pour le gel.

Une différence significative entre le profil de déplacement de surface du Coulommiers âgé de 10 jours et de son simulant n'a pas été observée (Figure XXVI). Ce qui indique que les propriétés rhéologiques du fromage et du simulant sont très proches.

3. CAMEMBERT ÂGÉ DE 30 JOURS ET DE SON SIMULANT

La courbe de déplacement de surface du Camembert âgé de 30 jours (en fonction de la distance de la sonde) est différente de celle de son simulant. Cette différence se situe principalement dans un rayon d'environ 15 mm de la sonde (figure XXVII). Dans cette zone, la courbe du fromage est plus ou moins linéaire. Au contraire, la courbe du simulant a une forme plus convexe, plus proche des gels de gélatine présentés plus haut. Cette différence est probablement induite par le caractère plus visqueux du Camembert très affiné, par rapport au simulant qui reproduit justement moins bien cette propriété.

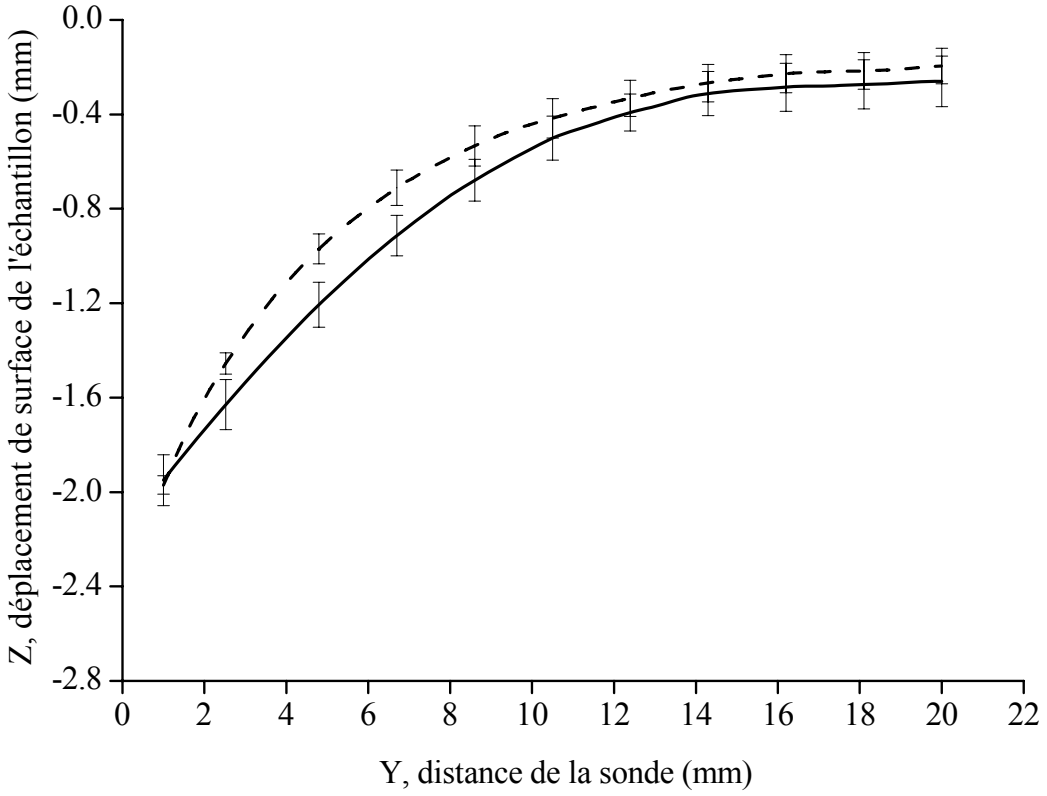

Figure XXVII. Déplacement de surface du Camembert âgé de 10 jours (—), et de son simulant (– – –) en fonction de la distance à partir du bord de la sonde. Barre d'erreur = écart type, nombre de répétitions = 6 pour le Coulommiers et 3 pour le gel.

La figure XXVIII montre les images du Camembert âgé de 30 jours (a), du simulant du Camembert (b) et d'un gel de 8% de gélatine (c). Ces images sont acquises par le système de Breuckmann lors d'un test de pénétrométrie, pendant lequel la sonde est insérée à une profondeur de 4 mm dans les échantillons.

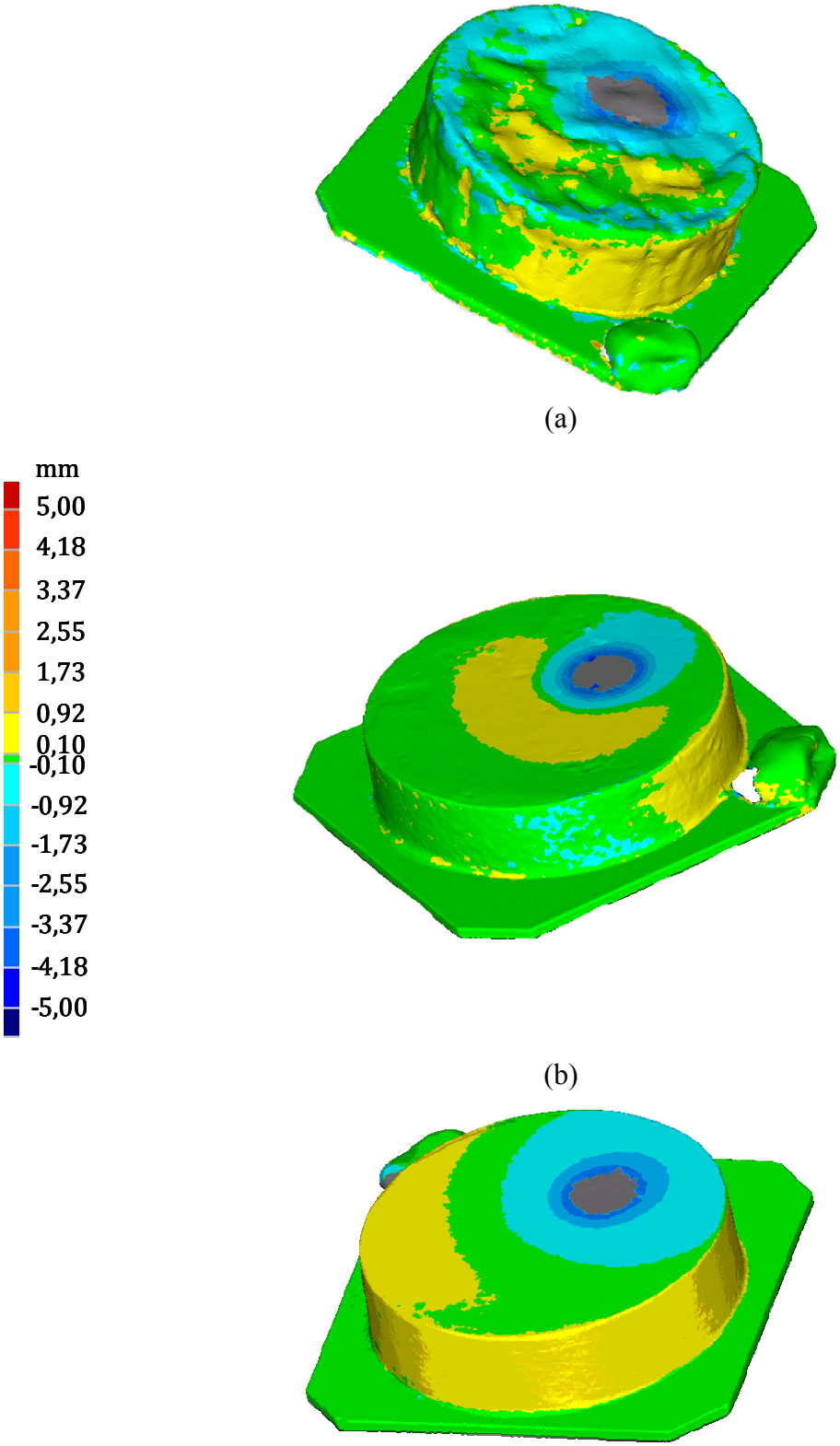

(a)

(b)

(c)

Figure XXVIII. Images du Camembert âgé de 30 jours (a), du simulant du Camembert (b) et d'un gel de 8% de gélatine (c) acquises par le système de Breuckmann. La sonde est insérée à une profondeur de 4 mm dans les échantillons.

Le système de Breuckmann, contrairement à la méthode de numérisation tridimensionnelle par stéréocorrélation d'images, permet une visualisation globale des échantillons. La zone d'enfoncement de la surface (indiquée en bleu) du Camembert âgé de 30 jours et de son simulant est très proche de la sonde (Figure XXVIII a et b). Par ailleurs, on remarque que les zones de gonflement (indiquées en jaune) apparaissent sur la partie supérieure, ainsi que sur une partie de la périphérie du fromage et de son simulant. Lorsque l'on compare ces deux échantillons à un gel de 8% de gélatine, on remarque qu'au contraire, le gonflement se situe sur toute la périphérie du gel de gélatine (Figure XXVIII c). De plus, le déplacement de la matière sur la partie supérieure du gel est différent de ce qui est observé dans le cas du camembert et du simulant. En effet, la matière est déplacée plus loin de la sonde. Le fromage et le simulant sont moins rigides et possèdent un caractère plus visqueux que le gel de 8% de gélatine. Il semblerait donc que la différence dans le déplacement de la matière notée au cours du test de pénétrométrie soit liée à une différence de viscosité des échantillons. Par ailleurs, le simulant du Camembert est préparé à partir de 6,5% (p/p) de gélatine, 21,5% (p/p) de maltodextrine et 2% (p/p) d'amidon gélatinisé. Ainsi, l'ajout de maltodextrine et d'amidon à la gélatine modifie significativement le comportement de la gélatine à la déformation, et le rapproche de celui du Camembert.

4. INFLUENCE DES PROPRIÉTÉS RHÉOLOGIQUES DES ECHANTILLONS SUR LEUR PROFIL DE DÉPLACEMENT DE SURFACE

Les résultats présentés jusqu'à présent ont montré que des échantillons qui diffèrent par leurs propriétés texturales présentent des profils de déplacement de surface différents. Afin de déterminer l'effet de ces propriétés texturales sur les profils, les courbes de déplacement de surface des échantillons en fonction de la distance de la sonde sont ajustées à l'équation II.

$$Z(mm) = Z_0 + a \times \exp(-bY) \qquad \text{(II)}$$

Les valeurs de Z_0, a et b sont obtenues à partir des profils de déplacement de surface des échantillons lors de tests de pénétrométrie avec des profondeurs d'insertion de la sonde de 2, 3 et 4 mm. Ces valeurs sont données dans le tableau VII.

Les paramètres rhéologiques notamment la fermeté, le module d'élasticité et le temps de relaxation sont présentés dans le tableau VIII.

Tableau VII. Coefficients Z_0, a et b obtenues à partir des profils de déplacement de surface des échantillons lors de tests de pénétrométrie avec des profondeurs d'insertion de la sonde de 2, 3 et 4 mm. Les valeurs indiquées correspondent à une moyenne de 3 ou 4 répétitions.

Paramètres	**gels de gélatine**				**Coulommiers**	**simulant Coulommiers**	**Camembert**	**simulant Camembert**
	8%	**10%**	**15%**	**20%**				
Z_{04mm} (mm)	0.255	0.345	0.466	0.554	0.254	0.280	0.109	0.160
a_{4mm} (mm)	2.507	2.600	2.393	2.310	1.826	1.924	2.248	2.198
b_{4mm} (mm^{-1})	0.250	0.271	0.269	0.288	0.259	0.250	0.157	0.207
R^2	0.999	0.998	0.998	0.997	0.999	0.998	0.996	0.999
Z_{03mm} (mm)	0.206	0.284	0.392	0.466	0.223	0.211	0.148	0.173
a_{3mm} (mm)	1.824	1.953	1.691	1.548	1.414	1.420	1.187	1.675
b_{3mm} (mm^{-1})	0.256	0.271	0.267	0.283	0.258	0.247	0.157	0.218
R^2	0.999	0.998	0.996	0.997	0.996	0.991	0.999	0.999
Z_{02mm} (mm)	0.152	0.203	0.266	0.348	0.194	0.131	0.136	0.106
a_{2mm} (mm)	1.120	1.162	1.063	0.930	0.748	0.946	0.670	1.040
b_{2mm} (mm^{-1})	0.258	0.271	0.268	0.281	0.250	0.251	0.154	0.217
R^2	0.996	0.997	0.993	0.996	0.984	0.993	0.999	0.999

Tableau VIII. Fermeté, temps de relaxation r_1, et module d'élasticité E_1 déterminés à partir de tests de pénétrométrie et de relaxation. Les valeurs indiquées correspondent à une moyenne de 3 ou 4 répétitions.

Paramètres	**gel de gélatine**				**Coulommiers**	**simulant Coulommiers**	**Camembert**	**simulant Camembert**
	8%	**10%**	**15%**	**20%**				
Fermeté (N)	30.0	43.4	81.2	121.6	19.0	17.9	10.7	12.2
Temps de relaxation r_1 (min)	183	180	143	138	20	60	12	57
Module d'élasticité E_1 (kPa)	200	270	600	880	80	100	33	60

La régression linéaire multiple est utilisée pour déterminer la relation entre les paramètres rhéologiques (fermeté, module d'élasticité et temps de relaxation) des échantillons et les coefficients *Zo, a et b.* Les équations IX à XI montrent qu'il y a une relation linéaire entre Z_0, *a ou b* et les paramètres rhéologiques.

$$Z_0 = k_{z1}E_1 + k_{z2}\,fermeté \qquad \text{(IX)}$$

$$b = k_{b1}E_1 + k_{b2}\,fermeté \qquad \text{(X)}$$

$$a = k_{a1}E_1 + k_{a2}\,fermeté + k_{a3}r_1 \qquad \text{(XI)}$$

k_{z1}, k_{z2}, k_{b1}, k_{b2}, k_{a1}, k_{a2}, k_{a3} sont les coefficients des équations IX à XI. Les valeurs de ces coefficients sont présentées dans le tableau IX.

Tableau IX. Coefficients des équations reliant Z_0, a et b aux paramètres rhéologiques, fermeté, module d'élasticité et temps de relaxation.

Paramètres	coefficients	Profondeur de la sonde		
		2mm	3mm	4mm
b	k_{b1}	$-3{,}9\times10^{-3}$	$-3{,}9\times10^{-3}$	$-3{,}9\times10^{-3}$
	k_{b2}	$3{,}1\times10^{-2}$	$3{,}2\times10^{-2}$	$3{,}1\times10^{-2}$
R^2		0,90	0,90	0,92
Z_0	k_{Z1}	$-2{,}2\times10^{-3}$	$-2{,}7\times10^{-3}$	$-2{,}8\times10^{-4}$
	k_{Z2}	$1{,}9\times10^{-2}$	$2{,}4\times10^{-2}$	$2{,}5\times10^{-2}$
R^2		0,98	0,97	0,96
a	k_{a1}	$-1{,}7\times10^{-2}$	$-2{,}1\times10^{-2}$	$-3{,}1\times10^{-2}$
	k_{a2}	$8{,}8\times10^{-2}$	$1{,}6\times10^{-1}$	$2{,}4\times10^{-1}$
	k_{a3}	$4{,}4\times10^{-3}$	$6{,}7\times10^{-3}$	$7{,}9\times10^{-3}$
R^2		0,92	0,93	0,93

Les coefficients k_{b1} et k_{b2} reliant le paramètre b à la fermeté et E_1 de l'échantillon sont indépendant de la profondeur d'insertion de la sonde. Le paramètre b contrôle le degré de courbure du profil de déplacement d'un échantillon. Sa valeur augmente lorsque la concentration en gélatine du gel augmente. Les autres coefficients (k_{Z1}, k_{Z2}, k_{a1}, k_{a2}, k_{a3}) des équations (X et XI) reliant a et Z_0 aux paramètres rhéologiques varient, au contraire, en fonction de la profondeur d'insertion de la sonde lors du test de pénétrométrie.

L'analyse des propriétés texturales des fromages et de leur simulant par la numérisation tridimensionnelle permet d'obtenir des nouveaux paramètres qui sont corrélés avec la fermeté, le module d'élasticité et le temps de relaxation.

CONCLUSIONS

Le but de ce travail était de créer un gel à base de gélatine pouvant simuler la texture des fromages à pâte molle tels que le Camembert et le Coulommiers. Dans un premier temps, les paramètres caractéristiques de l'appréciation instrumentale de la texture du coulommiers et du camembert ont été choisis : la fermeté, le module d'élasticité et le temps de relaxation. Ces deux derniers paramètres décrivent les propriétés viscoélastiques des produits. Un gel de gélatine ne pouvant pas reproduire la texture des fromages, l'ajout de polysaccharides est essentiel afin d'améliorer les propriétés visqueuses du gel, pour le rendre moins rigide et compact. Des mélanges de gélatine et de gomme de guar, xanthane, karaya ou maltodextrine et amidon ont été comparés aux fromages en se basant sur les trois paramètres texturaux. Le gel de gélatine, maltodextrine et d'amidon reproduisait le mieux la texture des fromages. Afin d'optimiser la concentration des constituants du gel, un plan de mélange à trois composants est utilisé. Cette approche a permis de développer des modèles mathématiques simples qui prédisent les effets de chaque composant sur les paramètres texturaux du simulant. Par ailleurs, elle a aussi mis en évidence une corrélation linéaire entre ces paramètres et la composition du gel. Une influence significative des interactions entre les constituants sur les propriétés rhéologiques n'a pas été notée.

Dans un deuxième temps, une fois la concentration des constituants du gel optimisée, ses paramètres texturaux ont été modifiés par ajout d'enzyme protéolytique - *Subtilisine Carlsberg* (Alcalase®). Le but était d'apporter des changements graduels afin d'imiter les modifications texturales des fromages à pâte molle induits par la maturation. Bien qu'une efficacité de l'Alcalase® sur la dégradation du réseau du simulant ait été notée, les trois paramètres texturaux n'évoluent pas de la même manière que ceux du fromage. Il était difficile de reproduire la cinétique des modifications dues à la protéolyse et la lipolyse qui se produisent au cours de la maturation du fromage. Une raison qui pourrait expliquer la différence entre l'évolution des changements de texture dans le simulant et le fromage est la suivante. Dans le fromage, il y a une synthèse continue d'enzymes, alors que dans le simulant, une quantité fixe d'Alcalase® est ajoutée au cours de sa préparation. Il faudrait assurer un relargage progressif de l'enzyme au cours du stockage du simulant. Pour cela, l'encapsulation de l'Alcalase® peut être envisagée.

Ce travail a aussi porté sur l'utilisation de la numérisation tridimensionnelle comme nouvelle approche pour analyser la texture des aliments. Les deux techniques utilisées sont la mesure de champs de déplacements tridimensionnels par stéréocorrélation d'image et le système de mesure topométrique tridimensionnel de Breuckmann. Contrairement à la méthode d'évaluation instrumentale de la texture à l'aide de la machine d'essai universelle, les deux techniques de numérisation utilisées donnent des informations concernant la déformation d'un échantillon autour du point d'application de la force. Une visualisation du déplacement de la matière en fonction de la viscosité du produit est aussi obtenue grâce au système de numérisation de Breuckmann. Il est aussi possible de quantifier le déplacement de la surface des produits au cours des tests instrumentaux de mesure de texture. Les résultats obtenus ont aussi montré une efficacité de ces deux systèmes de numérisation tridimensionnelle à distinguer des gels ayant des propriétés rhéologiques différentes.

De plus, le système de stéréocorrélation a permis de mettre en évidence une relation linéaire entre les paramètres texturaux et le profil du déplacement de la surface des échantillons. Ces nouveaux paramètres (Z_0, a et b) extraits du profil de déplacement de la surface des échantillons pourront être utilisés comme variables instrumentales afin de corréler les mesures instrumentales et sensorielles. Le coefficient de corrélation se situe entre 0,79 et 0,85. Dans le cas de notre étude, si on réalise une corrélation entre les données instrumentales et sensorielles, l'appréciation globale de la texture du fromage/gel par le toucher du consommateur sera fonction des paramètres rhéologiques telles que la fermeté, le module d'élasticité et le temps de relaxation. L'ajout des trois autres paramètres (Z_0, a et b) comme variables instrumentales pourrait améliorer le coefficient de corrélation. En effet, il est possible que ces nouveaux paramètres apportent des informations complémentaires (et non accessibles jusqu'à présent par la machine d'essai universelle) liées aux données visuelles du consommateur. Ainsi, ces nouveaux paramètres obtenus par la numérisation tridimensionnelle pourraient permettre d'obtenir des modèles pouvant prédire, avec précision, des mesures sensorielles hédoniques à partir de paramètres instrumentaux.

Il faut aussi souligner que trois paramètres extraits des profils de déplacement de la surface des échantillons ont été exploités. Il y a sans doute d'autres paramètres qui pourraient être utilisés tels que la quantification du déplacement de la matière lors de l'enfoncement de la sonde. En effet, le déplacement de la matière est fonction de la viscosité du produit. Il serait

aussi intéressant d'appliquer des connaissances de la mécanique du sol afin d'exploiter plus en détail les profils de déplacement de surface des échantillons.

GENERAL INTRODUCTION

Consumers' desire for greater food safety and quality urges food industries to pack products in inviolable packaging, which avoid direct consumer-product contact. Some food products namely soft cheeses like Camembert and Coulommiers, though, still remain fairly accessible to consumers. In addition, French people have a well-known habit of pressing their finger on the cheese in order to check its firmness. This action and the perceived texture of the cheese greatly influence customers' choice. However, it is very likely that they will have to give up that habit when cheeses will be sealed in inviolable packaging. Is there another means therefore for consumers and cheese manufacturers to monitor textural changes in soft cheeses during ripening?

An answer to this question was suggested and developed in this study. It consists in designing soft cheese simulants whose textural properties change in time and imitate those occurring in Camembert and Coulommiers during ripening.

Moreover, the simulant was formulated from gelatin and polysaccharides mixture, instead of cheese components (casein, lipids…). The use of cheese components in designing the simulant would most probably give a gel with textural properties close to that of soft cheeses. However, the applications of this simulant would be limited, for it would be used to imitate cheeses only. On the contrary, a polymeric gel made up of gelatin and polysaccharide broadens the range of applications of the simulant. It can be used to imitate textural properties of food products, besides that of soft cheeses.

Polymeric gels provide a good model for both natural and fabricated foodstuffs, which generally contain large quantities of water (50-90%) (van den Berg *et al.*, 2006). The wide variety of gel texture obtained by combination of native or denatured proteins with neutral or anionic polysaccharides used in foods can be regarded as highly relevant models of food structures (Tolstoguzov, 1995; de Jong and van de Velde, 2007). Multi-component gels are used in non-traditional pasta products, meat or fish analogues (Tolstoguzov, 1988) and in production of low fat spreads and fat replacers (Zasypkin *et al.*, 1996).

Because of their homogeneous composition and structure and their well-known physical and chemical properties, gelatin gels provide good food models for instrument calibration (Wilson

and Brown, 1997), in odontological research (Lassauzay *et al.*, 2000) and in the meat industry, more precisely, for meat tenderness assessment (Jones *et al.*, 2003). According to the authors, scaled firmness standards based on gelatin gels could provide a good model for meat tenderness sensory training. Indeed, despite increasing efforts made to standardize procedures to evaluate the tenderness of meat (Wheeler *et al.*, 1997), studies from different laboratories are still difficult to compare. Inaccurate texture assessment due to considerable sample variation can also be noted in cheese texture measurement.
Hence, besides the above stated purpose of formulating a polymeric gel with similar textural properties as soft cheeses, there are other applications of this simulant. It can be used, for example, as a standard rating scale to train sensory panelists in cheese texture research. Another possible use of this simulant is in the packaging process. During packaging, wrapping machines compress cheeses slightly once they have been wrapped in the plastic film to fit in the cardboard box. The force required to grip the cheeses has to be adjusted in order to avoid damage. Therefore, such gel standards, usually more stable than cheese with time, can be useful for instrument calibration.

Textural properties of cheeses are determined by sensory and instrumental/rheological measurements. It is sometimes difficult to relate rheological measurements and sensory data. Indeed, sensory texture is a complex property of foods that encompasses physical properties not detected by rheological methods (Foegeding *et al.*, 2003). Therefore, in order to improve the correlation between rheological and sensory measurements, new rheological parameters which better describe the sensory texture of food should be found. That is why, the use of optical methods (digital image correlation method and Breuckmann three-dimensional scanning system) for texture characterization have been studied in the research work. This is in fact the second objective of this study. These methods are commonly used in the field of mechanical engineering. It should however be mentioned that they have so far never been used in food science. New rheological parameters obtained from three-dimensional image analysis of cheeses/simulants under loading may improve models which predict sensory texture from to instrumental measurements.

In the literature review that follows (chapter I), the topic of rheology is taken as the central focus, and the applications of gelatin gels as model foods are examined in part I. The rheology

of gelatin gels and modifications in textural parameters induced by polysaccharides are discussed. An overview of the various efforts made in order to understand and predict the complex textural behaviors of natural foods using gelatin gels as simulant is given. Finally, the use of other polymers namely carrageenan, agar, silicon elastomers, and composite foods as food gel models are presented. Part II describes the manufacturing process of soft cheeses, the changes occurring during their ripening. The various methods used to assess textural properties of soft cheeses are presented as well.

Materials and methods used in this research are presented in chapter II.
Results and discussion follow in chapter III which is divided into three parts.
Part I details the experiments carried out in order to formulate a polymeric gel from mixtures of gelatin and polysaccharides to simulate 10-day-old Coulommiers and Camembert (soft French cheeses) texture. The objective of this section was to determine the composition and component concentration of a gel matching soft cheeses texture at a given maturation stage. The work discussed in part II describes attempts made in order to bring about gradual texture changes of the cheese simulant in order to match that of ripening Coulommiers cheese. Part III puts forward the interest in applying digital image correlation, coupled with the widely used universal testing machine, for rheological properties assessment and to improve correlation between sensory texture of food and instrumental measurements.

CHAPTER I: LITERATURE REVIEW

PART I: GELATIN AND OTHER MAIN GELS USED AS FOOD SIMULANTS IN TEXTURE STUDIES

1. PROPERTIES OF GELATIN

1.1. Source, structural and mechanical properties

Gelatin does not exist in nature but are derived from the insoluble parent protein, collagen, by processes that destroy the secondary and higher structures of the collagen and in most cases the primary structure as well (Veis, 1964). Collagen constitutes the main organic component of animal skins, bones, tendon, and loose connective tissues (Eastoe, 1955). The nature and amount of collagen vary significantly from one tissue to another and also vary with the kind of animal. Due to this heterogeneity and the kind of gelatin of interest, the preparation techniques differ in terms of the raw material and chemical reagents used, the extent of treatment and some sequential procedures in the manufacturing technology. However, the principle of gelatin preparation remains almost the same and there are two main types of gelatins. Type A, with isotonic point of 7 to 9, is derived from collagen with exclusively acid pretreatment. Type B, with isotonic point of 4.8 to 5.2, results from an alkaline pretreatment of the collagen. The clarity, transparency, and degree of purity of gelatin are of great importance for food and pharmaceutical industries. Several clarifying agents have been suggested: egg albumen and sodium carbonate neutralized with hydrogen chloride and disodium phosphate dodecahydrate. The fundamental molecular unit of collagen is the tropocollagen rod, a triple helical structure composed of three separate polypeptide chains with a total molecular weight of about 330 000 (Ross-Murphy, 1992). Gelatin is reported to contain about 18 amino acids linked in a partially ordered fashion. Three groups of amino acids are predominant: glycine, alanine and proline or hydroxyproline. Glycine or alanine accounts for about one-third to half of the total amino acid residues. In type B gelatins, glycine is the predominant N-terminal residue, while in type A gelatins, alanine tends to be larger. Proline or hydroxyproline makes up for around one-fourth of the amino-acid residues.
Reviews discussing the structure and mechanical properties of gelatin gels have been written by Clark and Ross-Murphy (1987), Ledward (2000), Djagny *et al.* (2001). Gelatin is primarily used as a gelling agent. The gel melting temperature (< 35 °C) is below body temperature, which gives gelatin products unique organoleptic properties and flavor release (Glicksman, 1985). Above 35-40 °C, gelatin in solutions behaves as flexible single coils. On cooling,

aggregation occurs and solutions having concentrations above some critical point, typically 0.4 to 1 % form clear transparent elastic thermoreversible gels. In a number of polysaccharides namely agarose and carrageenan, the coil to double helix naturation occurs very fast and resembles a true first-order phase transition. For gelatin, there is an initial phase lasting several hours, followed by a much slower process continuing probably for a very long time. This is why, it is believed that the helix nucleation step is slow and the subsequent propagation stage is even slower (Ross-Murphy, 1992).

At temperatures above 40 °C, gelatin is assumed to exist as random coils, but the high imino acid content must, to some extent, limit their flexibility. It has been suggested that even at these temperatures the chains have some structure and the actual amount depends on the imino acid content. It is now generally agreed that these pyrolidine rich regions of the chains act as potential junction zones in that, as the temperature decreases these regions, especially those with the sequence gly-prp-pro (or hypro)-gly-pro-pro (or hypro) tend to take up the poly-L-proline II helix, aggregates of three such helices, in a collagen fold formation, yielding the junction zones.
These junction zones are stabilized by interchain hydrogen bonds similar to those found in native collagen and some water molecules are also oriented and bound within the structure (Naryshkina *et al.*, 1982). It is likely that at least some of these water molecules serve to stabilize the triple helix by hydrogen bonding in a similar manner to that proposed for native collagen. Although proline is important, hydroxyproline in the third position of the triplet is believed to be the major determinant of stability due to its hydrogen bonding ability (Privalov, 1982). Although most theoretical treatments of a gelatin gel have assumed that the junction zones are individual triple helices there is evidence, from electron microscopic studies carried out on a range of mature gelatin gels, that at least some of the junctions are composed of several triple helices aggregated together. This hypothesis though is not universally accepted (Busnel *et al.*, 1989).

The strength of a gelatin gel increases as the temperature decreases due to either an increase in the number of crosslinks (Bedborough and Jackson, 1976) or the growth of existing junctions (Nijenhuis, 1981) or both. Thermal history of the gel can markedly affect its strength. Thus, holding a solution at a temperature just below that required for nucleation

gives rise to a weak gel with only a few junctions. These junctions though are very stable since the chains involved in their formation have sufficient flexibility to anneal themselves into their most stable collagen like conformation, other regions, of lower imino acid content, will not form junctions. However if this weak gel is subsequently chilled to a lower temperature, its strength will increase as these junctions grow and new ones form. A solution of the same concentration chilled directly to this lower temperature will probably have a similar number of junction zones to those formed in the gel prematured at the higher temperature. However, the gel will be weaker since the initial nucleation sites will not have been able to anneal themselves into their most stable conformation and encourage further growth of these zones on subsequent cooling (Ledward, 1986). According to Oakenfull (1984), in dilute (1-2%) gels at high temperatures, the average junction contains about 142 residues, that is 47 per chain, although at 1°C, junctions involving only 30-50 residues can be formed. Busnel *et al.* (1989) estimated that in gels matured at 10°C, about 20 residues per chain are involved in the junction zones.

An interesting outcome of the above hypothesis is that a weak gel, with a few very stable linkages, matured at a high temperature, may well have a higher melting point than a strong gel of the same solution, with numerous weaker linkages, prepared by rapid chilling to a lower temperature. The strength of a gelatin gel increases with time when held at fixed temperature, presumably due to the junction zones reorganizing themselves or to new zones forming as the gels anneal. Michon *et al.* (1997) also noted that the stability of junction zones, which is proportional to their length, depend on the aging temperature and on the time spent at that given temperature: a longer aging time and/or a higher aging temperature lead to a higher thermal stability of helical structures.

1.2. Textural behavior of gelatin gels

The development of applications dependent upon the gelling properties, for example the use of alginates to form fruit pulp to mimic the texture of original fruit (Wood and Young, 1972) has contributed to the upsurge of interest in the rheology of gels. Gels are mechanically assayed by small and large deformation (fracture). Small deformation is useful in simulating small forces acting during handling of products, and convenient when structural properties of

the intact system are studied. Large deformation can be assimilated to the action occurring during mastication or cutting.

Gel strength is therefore one of the most important attribute of gelatin. Bloom strength is essentially the rigidity of a gelatin gel formed under standard conditions, commercial value increases with increasing Bloom. The gelatin gel rigidity is measured by determining the weight (force in grams) required to depress the surface of a gelatin gel by 4 mm using a 12.7 mm diameter flat-bottomed cylindrical plunger. The gel is prepared by mixing 7.5 g of gelatin powder with 105 g of distilled water. The mixture is left to stand until the gelatin has swollen, then heated to 60 °C with gentle stirring to form a homogeneous solution. Samples are then left at room temperature for about 15 minutes prior to being cooled to 10 °C for 16-18 hours before testing.

The relationship between concentration and gel strength varies with type and origin of gelatin. For a 100-250 g Bloom gelatin, the relationship becomes (equation 1):

$$(C_1)^n \times (B_2) = (C_2)^n \times (B_1) \qquad (1)$$

Where C is gel concentration, B the bloom strength, n = 1.7 for high-Bloom gels and 1.8 to 1.9 for low-Bloom gels (150-100g). Small changes in moisture content of gelatin can appreciably affect its Bloom strength. Moisture content of commercial gelatin can range from 7-15 %. Determining the water content of gelatin samples at time of gel strength testing is therefore important.

The gel strength of all types of gelatins decrease below pH 5 and above pH 9, while in the range of pH 5 to pH 9, gel strength remains almost constant, although differences have been noted between acid and alkali processed gelatins. Bloom determination is usually carried out at the pH of the sample (4.6-7.0). It has been suggested that the control of pH is important for the comparison of protein component of gelatins. Generally, the influence of pH on gel strength is greater for dilute gels (< 2 %) (Ledward, 2000).

Gelatin gels are quite elastic: over a moderate time scale ($\approx 10^2$ s) the contribution to deformation from time dependent elements is relatively small compared to the initial

deformation. The measurement of a rigidity modulus from non-equilibrium data is therefore more meaningful than it would be for a gel that exhibits a rapid change in creep compliance with time. Thus, the dynamic rigidity modulus obtained at high frequencies is in agreement with the static modulus (Miller *et al.*, 1951).

Furthermore, the rigidity modulus does not vary linearly with strain. The increase in rigidity modulus is small at low strain and larger at higher strain. Several authors have reported that the rigidity of a given gelatin gel is closely proportional to the square of the concentration up to a certain gelatin level (Ferry, 1948; Eldridge and Ferry, 1954). For gelatin concentration less than 25 % (w/w), the low frequency elastic modulus *G* is proportional to the square of the concentration (Saunders and Ward, 1954; Saunders and Ward, 1958). Robinson *et al.* (1975) quoted values of n in the equation $G = KC^n$ (where *C* is the gelatin concentration, and *K* and *n* constants) of 1.266, 1.682, 1.985, respectively, for gels formed from acid processed gelatin, alkali processed gelatin and a 50/50 blend of the two.

Another area that has been of particular interest is the applicability of the theory of rubber elasticity to gelatin gels. The change in free energy when a rubbery network is deformed is made up of the sum of the entropy changes of the individual network chains (chains joining adjacent crosslinks). The expression for the shear modulus (*G, Pa*) obtained from this theory is (equation 2):

$$G = \frac{\rho RT}{M_c} \qquad (2)$$

where M_C is the mean molecular weight of the chains joining adjacent crosslinks, ρ is the concentration of the polymer, *R* is the gas constant and *T* is the absolute temperature. The relationship between the tensile force per unit cross-sectional area, measured in the undeformed state (*F*) and the elongation α is (equation 3):

$$F = G\left(\alpha - \frac{1}{\alpha^2}\right) \qquad (3)$$

The evidence that the theory of elasticity may be obeyed by gelatin gels have been reported by several authors (Miller *et al.*, 1951; Jopling, 1958; Saunders and Ward, 1958; Szczesniak

and MacAllister, 1964; Chasset and Thirion, 1965; Preston and Meyer, 1971; Pines and Prins, 1973) and a discussion of their works has been given by Mitchell (1976) in a review paper.

Gelatin is usually used at relatively low concentrations in water or polyhydric alcohols in the manufacture of sweets, marshmallows and a whole range of dessert products. Gelatin gives high quality gels in dilute solution with a clean 'melt in mouth' texture and at higher concentrations, it gives elastic gum-like textures which dissolve slowly in the mouth (Ledward, 2000). In spite of its wide use in the food industry, sensory texture of gelatin and gels or gel-like systems has received less attention compared to structure and texture. Henry *et al.* (1971) measured 15 sensory attributes and 15 Instron Universal testing Machine (IUTM) parameters of commercial gelatin, puddings, pie fillings and whipped toppings. They reported that gelatin gel was lowest in sensory fluffiness, oiliness, graininess and fat-like characteristics, but highest in breakability, frangibility, elasticity and springiness as compared to the other semi-solids. Gelatin gels also showed the lowest mechanical elasticity under tension and highest maximum tensile force. Munoz *et al.* (1986a) evaluated the texture of gelatin gels varying in concentration from 22 to 45 g/L in terms of firmness by manual and oral shear and compression, cohesiveness, and extent of breakdown in the mouth. These sensory data were then compared with IUTM measures of compression and shear at various deformations (40-90 %) and two crosshead speeds (50 and 200 mm/min). Sensory responses correlated most highly with the following IUTM measurements:

- Compression forces at yield and at deformations of 70 and 85 % at the higher crosshead speed;
- Compression forces below the yield point at the lower crosshead speed;
- Shear forces measured at maximum deformation (90 %) at 200 mm/min

Manual compression and biting with the front teeth discriminated well across gel concentrations. Firmness was evaluated:

- with a knife: manual evaluation of firmness as the force perceived when cutting the gel with a serrated, stainless steel kitchen knife into two equal pieces,
- through biting: oral evaluation of firmness as the force perceived when biting a cube with the front teeth,

- through manual compression: evaluation of firmness as the force perceived when compressing the cube of gelatin gels against the container with the index finger.

Cohesiveness was determined:

- manually: evaluation of the degree of compression required to rupture the cube between thumb and index finger,
- orally: evaluation of the degree of compression required to rupture the cube between tongue and palate.

Those sensory measures – firmness and cohesiveness – were found to increase with gelatin concentration.

Boyd and Sherman (1975) reported an intermediate oral hardness for gelatin gels compared to other foods as disparate as cream cheese, biscuits and glacier mints, and correlated the values with Instron Universal Texture Machine (IUTM). Compression tests with IUTM correlated satisfactorily with the panelists' oral evaluation of hardness provided that a critical percentage compression was exceeded during the instrumental tests. The critical percentage compression seemed to be lower for soft foods than for hard foods. In addition, as crosshead speed increased from 0.5 to 20.0 cm/min, the force required to achieve any percentage compression increased.

1.3. Properties of gelatin-polysaccharide mixed gels

It is the unique 'melt in mouth' property of gelatin gels during mastication and which allows flavor release that makes them so popular to the food industry. However, this characteristic also results in the unsuitability of gelatin gels for certain product applications. Thus setting and storage of gelatin-based dessert gels requires refrigeration but even more to the point, they tend to melt during handling and consumption at elevated ambient temperatures. Similarly, high sugar content confectionaries may become sticky when stored in warehouses (where temperatures can rise up to 45°C) resulting in partial structural collapse, welding and crystallization (caking) of the product. Therefore, much effort has been directed towards the development of more thermally-stable gelatin systems in a mixture with polysaccharides.

Hence, understanding the interactions between gelatin and other macromolecules is of great interest for food industries. Gels consisting of networks of proteins and polysaccharides provide functional, structural, and textural properties to formulated foods and have been the central part of many investigations. The production of caviar analogue is often cited as an example of the importance and use of filled, complex and mixed gels of gelatin with different polysaccharides. Multi-component gels are also used in non-traditional pasta products, meat or fish analogues (Tolstoguzov, 1988) and in manufacturing of low fat spreads and fat replacers (Zasypkin *et al.*, 1996).

1.3.1. Phase diagram

Mixed gels have two or more relatively independent three-dimensional networks and are formed when biopolymers concentrations in a solution exceed the critical concentration for gelation of these biopolymers. Generally, critical concentration for gelation (or gel-point) does not exceed 0.1-0.3 % for anionic polysaccharides, while for proteins this value may range from 1 % for gelatin to 13 % for the 11S broad bean globulin.
Tolstoguzov (1995) linked the structure-property relationships of mixed gels to their thermodynamic phase diagrams and explained the following (Figure 1).

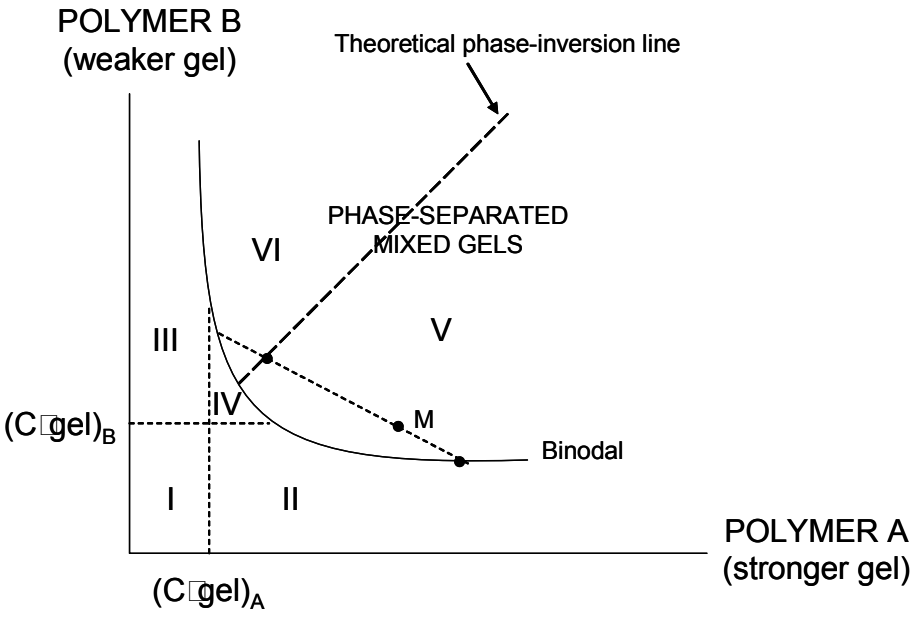

Figure 1. Phase diagram for gelation of a mixed solution of polymers (Tolstoguzov, 1995).

A mixed solution is obtained when the concentration of both polymers lies below their critical gelation concentration (Zone I). Zones II and III represent gels of a single polymer network (either A or B, respectively) in which the other polymer is present in the solution filling the pores. In these single phase regions of the phase diagram, a type of synergy due to excluded volume effects takes place. Macromolecules cannot occupy the same volume in the solution: each polymer can only use part of the volume of the mixed solution. Incompatible biopolymers mutually concentrate each other, thus each behaving as if it was more concentrated. When the overall composition of the mixture falls inside the binodal, phase separation occurs. Thus in zone IV, which is below the binodal, though the concentration of both polymers lies above the critical gelation concentration, a homogenous mixed gel is formed. Inside the binodal, phase separation involves water redistribution between the two phases. Therefore, there is a large increase in the concentration of biopolymers in one of the phases and a corresponding dilution in the other phase. Zone V represents the increase in concentration of the continuous phase containing the stronger gelling agent, leading to a synergistic effect. The other polymer is present as a gelled filler or dispersed phase. This significant increase in the concentration of the gelling agents within the continuous phase can cause a large increase in the elastic properties of the mixed gel. Indeed, several physico-chemical properties of dispersed systems are determined by those of their continuous phase. The shear modulus of a gel is proportional to the square of the hydrocolloid concentration. Mechanical properties of gels are therefore greatly affected by synergistic effect in mixed gels. When both phases of the water-in-water emulsion have the same volume, inversion of the phases can occur (zone VI). Phase inversion leads to the formation of a continuous phase consisting of the diluted, weaker-gelling agent. This antagonistic effect results in a decrease in physical and rheological properties of the mixed gel. Information from studies on gelatin-polysaccharide mixed gels is useful for formulation of gels with specific characteristics. The section below is a resume of works investigating modifications of textural behaviors of gelatin when combined with other polysaccharides.

1.3.2. Gelatin/agarose mixed gels

Through several experimental data, Tolstoguzov (1995) demonstrated the effect of changes in composition of gelatin-agarose mixed gel on its melting temperature and elasticity modulus (Figure 2).

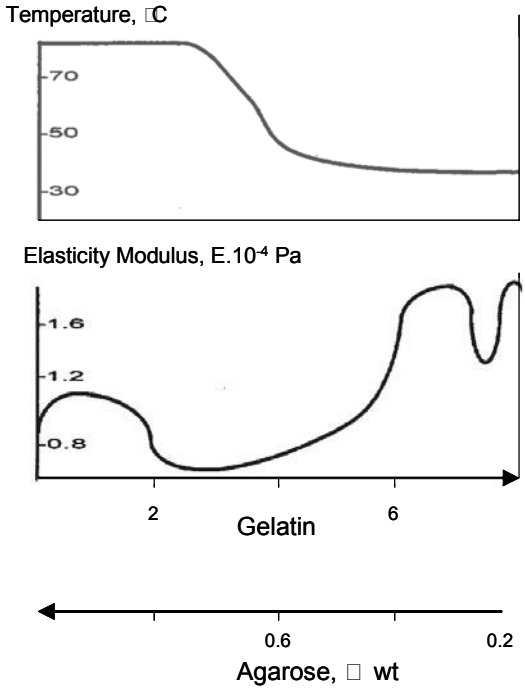

Figure 2. Composition dependence of melting point and the modulus of elasticity of mixed gelatin-agarose gels (Tolstoguzov, 1995).

Addition of small amounts of agarose increase elasticity modulus of gelatin gel due to mutual concentration effect of hydrocolloids (i.e. excluded volume effects). At higher agarose concentrations the mixed solution separates into two phases. Phase separation results in the dispersion of particles of the incompatible polymer, agarose, in the gelatin gel network thus disrupting the three dimensional gel networks. The increase in the concentration of agarose also increases the elasticity modulus of the filled gelatin gel. This is probably due to the competitive effect of gelatin phase concentration (water redistribution), the volume fraction of the dispersed agarose phase and the concentration of the continuous gelatin phase increase simultaneously. Up to a certain degree super concentration of the gelatin network can localise around the dispersed agarose particles and contribute to the elasticity modulus of the gel and compensate for the disruptive effect of the gel by the dispersed particles. However, a further

increase in volume fraction of the dispersed phase (further addition of agarose) cannot be compensated for, and gel elasticity decreases. To sum up, volume fraction, size and size distribution of dispersed phase particles as well as locally (around dispersed particles), increased concentration of the gelatin network, contribute to the mechanical properties of gels.

When the two curves in figure 2 are compared it can be noted that the gel melting point is strongly changed in the region of phase inversion composition and that a maximum gel weakening effect occurs at phase inversion, i.e. where the volume fraction of the dispersed phase is maximal. An antagonistic effect may also result from phase inversion in a water-in-water emulsion, i.e. due to a sudden strong change in the composition of the continuous phase. The continuous (or matrix) phase of a filled gel is primarily responsible for its mechanical properties. The gel melting temperature changes from one virtually constant level to another (figure 2). The gel melting temperature depends mainly on the nature of the system continuous phase and is weakly dependent on phase position and almost independent of phase volume ratio. Within the intermediate range of gel compositions the melting temperatures of gel vary proportionally with gel composition. It is also characteristic for the range of composition dependence of the elasticity modulus of multicomponent gels corresponding to a wide minimum. In both cases we are dealing with mechanical properties of gel since gel melting temperature depends not only on the thermodynamic parameter of breakdown of network crosslinks but also on temperature dependence of rheological properties of a system under given conditions. Therefore, it is also a characteristic feature of multicomponent gels that both gel melting temperature and elasticity modulus are linearly dependent on gel composition in a large intermediate area. This large intermediate area has been interpreted as corresponding to phase inversion. The composition area corresponding to phase inversion is quite extended. This relates to both range of gel melting temperature and the elasticity modulus of multicomponent gels. Within this large intermediate range of gel compositions we are presumably dealing with systems having two continuous phases which obey the additivity law for rheological and other physico-chemical properties. Such structural features, i.e. the presence of two continuous phases within quite a large range of compositions in protein-polysaccharide-water systems, seem to be typical of water-in-water emulsions because of low

interfacial tension and high viscosity of coexisting phases. This opens the way for controlling the structural functions of hydrocolloids and functional properties of food systems.

1.3.3. Gelatin/gellan mixed gels

Gellan is a bacterially derived polymer produced by a microbial fermentation process using the bacterium *Sphingomonas elodea.* The formation of gellan gels occurs in the presence of either monovalent or divalent cations by cooling hot polymer solutions. High-acyl gellan forms weak gels while low-acyl gellan forms strong gels (Sanderson, 1990). Compared to gellan gels, gelatin requires a relatively higher polymer concentration for gel formation, a longer setting time and lower setting temperature (Wolf *et al.*, 1989). Gelatin gels are quite soft and flexible, but their textural properties are generally narrow (Munoz *et al.*, 1986a; Munoz *et al.*, 1986b; Johnson-Banks, 1990). Gel strength of gelatin gels varies with gelatin concentration. Ionic strength and pH have little effect on gel strength though (Papageorgiou *et al.*, 1994). Wolf *et al*. (1989) reported that the incorporation of small amount of gellan into gelatin could greatly improve gelatin gel properties such as gelling and melting temperature, gel strength and room temperature stability. Similar results have been noted by other authors: Sanderson (1990) suggested that the addition of 0.25 % gellan to 250 Bloom type A gelatin could increase the hardness and springiness of the resulting gels. Papageorgiou *et al.* (1994) showed an increase in the gel strength of 5 % gelatin gel upon the addition of 0.5 % gellan and argued that the increased gel strength of gellan-gelatin blends was due to steric exclusion phenomena between the two polymers that promote gelation of each component independently in the mixture. Later, Papageorgiou and Kasapsi (1995) also demonstrated an increase in gel strength of gelatin/gellan mixed gels upon the addition of relatively high concentrations of co-solute (sucrose and corn syrup). Lau *et al.* (2000) noted that textural properties of gellan/gelatin mixed gels were strongly affected by calcium ion concentration as well as the gellan to gelatin ratio ($P<0.05$). According to the authors, the change in relative gellan/gelatin ratio at different calcium ion levels can provide a wide range of textural parameters for gel formulations in different foods. For example, formulation of gels for a fat replacer application might be achieved by using 0.6% gellan-1.0% gelatin with no added calcium ions, as this combination has fat-like softness. Gel hardness can be increased by the addition of suitable amounts of calcium ions to the polymer solutions and increasing the ratio

of gellan to gelatin, whereas brittleness, springiness and cohesiveness were very sensitive to low levels of added calcium (0-10mM), but less sensitive to higher calcium concentrations and gellan/gelatin ratio. In general, the addition of calcium ions caused gels to be more brittle and less cohesive and springy. The authors suggested a weak positive interaction between gellan and gelatin when no calcium was added, whereas at higher calcium levels, gellan formed a continuous network and gelatin a discontinuous phase. The combinations of gellan and gelatin may thus be useful in many food applications such as water or milk-based dessert gels, dessert syrups and toppings, fabricated fruits, vegetables, meat or fish aspics, and pet foods (Morris, 1990).

1.3.4. Gelatin/maltodextrin mixed gels

Maltodextrins are intermediate between starch and corn syrups; unlike starch, they are soluble in cold water, but unlike syrups, they are non-sweet. That is why they have found wide application in food industry as bodying agents, coatings, carrier for flavors, fragrances, and oils in cosmetics (Dokic *et al.*, 1998). In addition, the increasing trend in nutritional and health awareness triggers a strong demand from consumers for reduced or low-fat foods. Fat contributes significantly to sensory properties of food, hence the physico-chemical properties of fats are key aspects of food texture, which substitutes should mimic, if they are to be effective (Loret *et al.*, 2004). Maltodextrins are one of the most popular types of fat replacers (Roland *et al.*, 1999). The three dimensional network formed by maltodextrins when gelled is probably involved in the ability of maltodextrins to reproduce fat-like mouthfeel. The nature of this network has been studied by several authors (Reuther *et al.*, 1983; Schierbaum *et al.*, 1992). The formation of a maltodextrin network depends on the dissolution and quench-temperature, time and polymer concentration. Loret *et al.*(2004) found that a 30 % (w/w) maltodextrin, sample formed a network within 5 min at 25 °C, whereas 25% (w/w) maltodextrin gelled after about 50 min.

When maltodextrin is combined to gelatin, the gelatin/maltodextrin mixed system exhibited an initial increase in gelation time with increasing maltodextrin concentration followed by a decrease at higher concentrations due to phase inversion (Kaspasis *et al.*, 1993). Alevisopoulos and Kasapis (1999) demonstrated that the introduction of high molecular

weight fractions induced a transformation from weakened deswelled gels to reinforced composite gels. The phase inversion point from gelatin to maltodextrin continuous gels was manipulated by decreasing the length of molecular chains of the protein and/or increasing that of the polysaccharide. The formation of maltodextrin continuous structures was further assisted by quenching the binary solutions from high temperature as opposed to slow cooling. For a given concentration of gelatin, it was possible to reduce to a third the amount of maltodextrin required for phase inversion in the mixture. A special feature of maltodextrin is its ability to crystallize, in analogy with starch from which it is derived. Through confocal scanning light microscopy, Tromp *et al.* (2001) confirmed the presence of maltodextrin crystallites in a phase separated mixture of gelatin and maltodextrin.

Those crystallites appeared to be situated in the voids of the continuous gelatin matrix. The authors suggested that the formation of such a structure was because phase separation increased the local concentration of maltodextrin to above its solubility limit. Other authors also studied the physical properties and morphology of gelatin-maltodextrin gels crosslinked with non-toxic fixatives to improve biocompatibility in order to design a biopolymer composite system for novel food applications (Nickerson *et al.*, 2006). These authors suggested that phase separation can serve as a means for controlling the microstructure, and hence the swelling and mechanical properties of the gel network. They found out that the physical properties and morphology of gelatin-maltodextrin gels are affected by adjusting pH, maltodextrin levels and the type of crosslinking agent used. Based on confocal laser microscopy micrographs, phase separation was found to increase at higher pH and maltodextrin concentration. At higher pH, phase separation is induced by greater number of gelatin-gelatin chain interaction (that is higher network elasticity) and reduced entropy within the system, as gelatin is less protonated than at lower pH. Moreover, as maltodextrin concentration increased, the total polymer concentration within the sample increased which, during phase separation, effectively concentrated the gelatin chains within the continuous phase.

2. FOOD GEL MODELS

Many popular foods such as gelatin desserts, frankfurters, surimi-based shellfish analogs, and cooked egg white are gels or gel-based foods. Food gels are complex and display viscoelastic properties. As a result, part of the energy from applied force (during large deformation for example) dissipates as heat and the fracture behavior fluctuates with deformation rate, complicating interpretation of the mechanisms responsible for large deformation and fracture properties and the detailed analysis of the structural elements affecting fracture (Zhang *et al.*, 2005). Food gels also hamper their rheological analysis because of their complex composition. The crosslinks in food can be chemical and/or physical, and the network structure of the gels is quite complicated and difficult to control and quantify. Rheological properties will therefore be best understood using simple materials with well-defined chemical and physical properties (Foegeding *et al.*, 1995). Food models are therefore the first steps in developing more complex models having closer textural properties to real foods (Foegeding *et al.*, 1994). The determination of mechanical properties and application of rheological testing methods assume certain characteristics of the test specimen. It should ideally be isotropic and homogeneous (Mohsenin, 1986). Specimen geometry should preferably be simple so that the specimen can conveniently be used in apparatus. On the whole, a model food system is considered to be reasonably homogeneous and isotropic, to have a simple geometry and be free of variations in mechanical properties throughout the system. The following section highlights the interest of gelatin as model food gels in various texture studies.

2.1. Gelatin as food model

2.1.1. Sensory studies

Sensory texture is complex and both tactile (geometrical properties: mouthfeel, smoothness, grittiness, moisture properties) and kinesthetic (mechanical properties: hardness, cohesiveness, springiness) properties are evaluated in the mouth (Meilgaard *et al.*, 1999). Many of these properties can also be perceived by manipulation of cheese with the hands

(Scott Blair and Coppen, 1942). In many products, such as potato chips, visual and auditory properties of texture can be very important. With cheese, textural aspects perceived in the mouth play the most critical role, although spreadability and slicing properties can be critical texture properties perceived by the eyes and hands with some cheeses.

As mentioned already, one of the aims in this research work is to create a soft cheese simulant whose textural properties are close to that of the cheeses. The sensory texture of Camembert cheese, as perceived by a customer lightly pressing the finger against the cheese, is an important characteristic that affects the consumer's decision-making process. It is therefore worth giving some examples where in-hand sensory evaluation has been used to determine textural properties of food.

Table 1 shows some terms used in hand evaluation of textural properties. Drake *et al*. (1999) in evaluating textural properties of cheeses (Cheddar, Brie, Feta, Munster, Parmesan, Velveta) reported that both manual and oral sensory evaluation discriminated cheese texture in a similar manner. Several mouth and hand terms such as firmness, stickiness and slipperiness were directly correlated with each other. Terms like rubbery, firmness, brittleness, sticky and slipperiness appeared to discriminate the cheeses equally well. On the contrary, fracturability and rubberiness were found to be inappropriate textural attributes to discriminate between processed cheese analogues in a study carried out by Pereira and Bennett (2002). The authors argued that the type or range of factors studied was not wide enough for differences in these attributes to be detected in a significant manner.

Table 1. Hand evaluated terms

Terms	Definition	Sample/Authors
rubbery/ springy	- Press thumb onto the sample 30 to 40%. Evaluate the rate of spring or resilience once the deforming force (thumb) is removed.	cheeses (Drake *et al.*, 1999)
	- Amount of recovery to the original shape, after 2-3 s, after slightly compressing the sample to form a visible dent.	processed cheese analogues (Pereira and Bennett, 2002)
elasticity	- Manually twisting sample.	pectin, gelatin, starch gels (Kalviainen *et al.*, 2000)
firmness	- Press thumb all the way through the sample. Firmness is the force required to compress the sample completely.	cheeses (Drake *et al.*, 1999)
	- Amount of resistance to compression offered by a 1 cm thick slice of cheese, when pushed between the thumb and index finger, until fingers touch each other (force required to deform the cheese structure).	processed cheese analogues (Pereira and Bennett, 2002)
	- Force perceived when compressing the cube against the container with the index finger.	gelatin gels (Munoz *et al.*, 1986a)
hardness	- Manually pressing between thumb and forefinger.	pectin, gelatin, starch gels (Kalviainen *et al.*, 2000)
brittleness/ crumbliness	- The degree to which the samples fractures rather than deforms during the course of working the sample in the hand 3 to 6 times.	cheeses (Drake *et al.*, 1999)
cohesiveness	- Evaluation of degree of compression required to rupture sample between thumb and index finger.	gelatin gels (Munoz *et al.*, 1986a)
fracturability	- Extent to which a cheese slice (1 cm thick, 9 cm long) can be bent between the thumb and the index and the middle fingers, until the ends touch without breaking.	processed cheese analogues (Pereira and Bennett, 2002)
sticky	- The degree to which the sample sticks to the fingers during the course of working the sample 3 to 6 times in the hand.	cheeses (Drake *et al.*, 1999)
	- Extend to which the cheese sample stick to the fingers (thumb and index finger) when compressed until finger touch each other (residual on fingers).	processed cheese analogues (Pereira and Bennett, 2002)
slipperiness of film	- Take a small piece of sample and compress between thumb and forefinger. Evaluate the degree of slipperiness in the film of cheese between the fingers.	cheeses (Drake *et al.*, 1999)
curdiness	- Extend to which the original sample produces curdy lumps after being kneaded 7 times between thumb and index and middle finger	processed cheese analogues (Pereira and Bennett, 2002)

Food texture determination is complicated because it involves both sensory and instrumental measurements and their complex relationship. Numerous texture research are carried out in order to understand food structural mechanisms by fundamental rheological methods, and their corresponding sensory attributes through sensory analysis (Wium *et al.*, 1997; Drake and Gerard, 1999; Foegeding *et al.*, 2003). Those studies should allow food scientists to design products with specific textures and predicted sensory attributes.

Food biopolymer gels are good model systems to investigate the relationship between sensory perception of texture and fundamental rheological properties. Their low level of complexity compared to natural food products containing a variety of molecular interactions that contribute to overall network structure, makes those gels useful for those texture studies (Barrangou *et al.*, 2006).

One of the major steps in establishing the sensory texture profile of a food product is to create standard rating scales. The textural characteristics are divided into three classes namely:

- mechanical characteristics which are related to the reaction of food to stress,
- geometrical characteristics which refer to the physical constituents of food product namely size, shape, arrangement of particles within a food and surface roughness and,
- other characteristics which relate to the moisture and fat content of the food as perceived by the human senses (Bourne, 2002).

The standard rating scales consist of items having a particular textural property as a dominant characteristic, together with fairly uniform intervals between points in the desired characteristics. For example, the standard hardness scale is made up of nine food products ranging from low hardness (Philadelphia cream cheese) to high hardness (rock candy) (Szczesniak *et al*, 1963). The authors constructed the original scales from items available in eastern United States. Some of these items used may not be available in other places. Substitute commodities must then be selected. Furthermore, sensory scales should be flexible to adapt to changes in the food industry. Improving these scales by modifying components can generate more reliable sensory data and enhanced understanding of texture properties of food. Hence, according to Jones *et al.* (2003), the use of gelatin gels may improve these sensory scales by narrowing the scope of a particular characteristic. For example, firmness

standards made from gelatin gels may be a substitute for current scaled food items for sensory panels training.

Gelatin is an abundant constituent. Local availability of brands, sample size and temperature specifications can thus be eliminated. A potential use for gelatin gel standards exists for instrument calibration (Wilson and Brown, 1997), in odontological research (Lassauzay *et al.*, 2000) and in the meat industry, more precisely, for meat tenderness assessment. Indeed, despite increasing efforts made to standardize procedures to evaluate the tenderness of meat (Wheeler *et al.*, 1997), studies from different laboratories are still difficult to compare. This is due to a lack of uniformity in preparation, cooking and evaluation of samples. Hence, in order to provide a more standardized method of texture characterization and to decrease the variability linked to human or instrumental measurement, Jones *et al.* (2003) developed a six scaled standard for firmness (22.5, 25.0, 27.5, 30.0, 32.5 and 35.0 % w/w) to represent six distinct degrees of firmness and compared to meat tenderness categories. These authors reported that an untrained sensory panelist of 30 people were able to distinguish a difference between gels in three meat tenderness categories. A trained panel of 12 people detected significant differences between scaled standards. According to the authors, these results suggested that scaled firmness standards based on gelatin gels could provide a good model for meat tenderness sensory training.

2.1.2. Texture and flavor release

Hydrocolloids are widely used in food industry as thickeners, stabilizers and gelling agents in desserts, candies, bakery products, ice cream, beverages, jellies and sauces. In recent years, the increased health consciousness among consumers has triggered the increasing interest and use of hydrocolloids as fat substitute. Knowledge about mechanical and physical properties of hydrocolloids and the understanding of the mechanisms involved in the breakdown of food matrix and the release of flavor compounds are essential for the formulation of new food products containing hydrocolloids.

Studies have shown that thickeners such as gelatin, pectin, and kappa carrageenan produce their own characteristic texture (Daget and Collyer, 1984; Costell *et al.*, 1995). The type of thickeners affects not only texture but also taste. Kalviainen *et al.* (2000) reported that high

viscosity gels with weak and fragile texture had stronger flavor intensities and tart flavor than gels with strong and cohesive texture. Boland *et al.* (2004) investigated the influence of gelatin, starch, pectin and artificial saliva on the release of 11 flavor compounds from model gel systems. The gels were characterized by Young's modulus of elasticity. It was found that gelatin, which was the most rigid gel, had the lowest partition coefficients for six flavor compounds and the lowest maximum concentrations released for all compounds. Although starch and pectin gels had similar texture, they showed differences in flavor release attributed to matrix-flavor interactions. In the presence of saliva, because of an increase in surface area for diffusion of flavor compounds, gelatin gel showed large increase in flavor release. A reduction in flavor release probably linked to salivary proteins and the increased hydrophilic nature of the system was noted for starch and pectin gels. However, when time-intensity analysis is used instead of the traditional scaling procedures which measure flavor intensity immediately after a sample is placed in the mouth, as a single point on a scale, a more detailed account of the release of flavor from samples along time and intensity dimensions can be obtained. Using this technique, Baek *et al.* (1999) argued that studies in model systems and in people demonstrated that the different rates of flavor release observed for different gelatin concentrations (2-8 % w/w) were not due to binding of volatile to protein in the gel, nor to mucous membranes, but were due to different rates of gel breakdown in the mouth. The rates of volatile release were also different for different gels and showed a good correlation with sensory data. Previously, Guinard and Marty (1995) demonstrated, using time-intensity procedures, that hardness alone is not a good predictor of flavor release. Gelling agent (or combination), firmness of the gel and flavoring agents are involved in the rate and degree of flavor release from the gel systems. Gelatin gels have been chosen as model food in those studies because they are known to deliver flavor at different rates when the gel formulation is changed.

2.2. Non-gelatin based food gel models

Although gelatin gel was taken as central focus in this literature review section, it seems important to mention the use of other polymers as food models. This part therefore aims at giving examples of non-gelatin based systems putting to the fore the increasing interest for gels as food models.

2.2.1. Carrageenan gels

During mastication, factors like oral motion, rate of force applied, and saliva often lead to poor correlations between sensory and instrumental measurements because food texture as perceived during mastication, cannot be evaluated by conventional instruments (Rosenthal, 1999). In dental studies, electromyography is therefore used to investigate mastication process. Texture evaluation by this technique involves acquiring the electrical activity of muscles that occurs during contraction and providing a direct measure of muscle motion activity required for mastication. The electromyography signals generated by food texture in mastication are a mixture of hardness, fracturability, crispiness, cohesiveness and other texture attributes. The model food under study should therefore have a unique texture attribute that can be varied, while the other texture properties would remain unchanged, in order to identify key electromyography parameters related to the particular texture property. (Carson *et al.*, 2002) found carrageenan gels as being suitable for identifying the electromyography parameters associated with firmness attribute. Firmness of carrageenan gels can easily be manipulated without changing its cohesiveness. In this study, the concentrations in carrageenan powder were 0.8, 2.4, and 4.0 %. The firmness of these model gels correlated well to three electromyography parameters: total energy, peak energy and Fourier power, and were considered the best representation of firmness factor. When the same method was then applied to six commercial breads with different firmness, high correlation ($R > 0.82$) between bread firmness sensory measurement and electromyography parameters were found. A good correlation ($R > 0.69$) were obtained when the same method was applied to 17 commercial food products ranging from chee-tos® puffs, Club® Cracker Original, Butter cookies to Kroger® California Carrots and Corn Nuts® Original. This study clearly indicates the important part played by model systems in identifying rheological properties that correlate best with sensory perception of texture. This is often an important preliminary first step which thereafter allows comparison between real food products.

2.2.2. Agar gels

Due to its performance as stabilizing, thickening and gelling agent, agar is also of great utility as model systems. Its large temperature difference between its gelling (~30-40°C) and melting temperatures (~85-95ºC) (Armisen and Galatas, 2000) allows agar gels to be evaluated in the mouth without a temperature effect on gel structure, making it a useful food model.

Hennequin (1993) in determining the sensory textural properties of different varieties of cheeses (Munster, Brie, Carré de l'Est, Camembert, Coulommiers…) used cheese simulant made up of agar (0.5, 1, 1.5, 2 and 3%) and gelatinized starch (3%) in order to design a standard rating scale for sensory panel training. The setting up of a firmness rating scale requires equal scale interval obtained by specific agar concentration representing distinct degree of firmness. Agar was a convenient gel model since there is a linear relationship between agar concentration and firmness (measured by penetrometry test). The author however reported that elasticity, assessed by Texture Profile Analysis, shows no linear relationship with agar concentration and hence the simulant cannot be used to develop a standard rating scale to measure elasticity attribute. On the other hand, a gel made up of 3% agar was found to be useful in assessing the variability (due to the equipment or/and methods used) in instrumental characterization of rheological properties of cheeses (Hennequin, 1993).

In order to investigate the relationships between sensory perception of texture and fundamental rheological properties collected in linear, nonlinear and fracture regions, Barrangou *et al.* (2006) also used agar and agarose gels as model food systems. They found out that the sensory texture terms correlated very well with fundamental large-strain rheological properties of agar gels. First bite and chew-down sensory properties correlated well with each other and were predicted equally well with fundamental rheological parameters. Sensory properties that contribute to perception of strain-hardening were determined, and were found to behave in a similar manner as non-linear rheological behavior, which is an important first step in understanding how non-linearity influences sensory perception of texture. These findings clearly demonstrate that fundamental large-strain rheological properties give valuable information toward the understanding of sensory perception of physical properties of foods. Application of the approach used in this study to a

variety of model gel systems will lead to a broader understanding of how specific molecular interactions and network types contribute to mechanical properties, and how their corresponding sensory texture is perceived, ultimately allowing food scientists to design specific food textures from the molecular level.

A large number of foods possess a layered composite structure either naturally (fruits or vegetables) or manufactured purposely (bread, French fries and frozen desserts). In such cases, the processing operations aim at developing regions such as crust and core, which will exhibit distinct structural and mechanical differences (Pinthus *et al.*, 1995). The contrast in mechanical properties between the core and the crust can provide a pleasurable textural sensation (Brown *et al.*, 1998). Predicting the texture of composite food is important for the tailoring of the unit operation to enhance textural contrast. Scanlon and Anand (2006) thus studied the influence of food composite structure and properties, and indentation (penetrometry) testing protocols, on our ability to predict composite texture. They used model layered composite foods, prepared from a crust of dry pasta on a core of 3 % agar gel or from crust of 3 % agar gel on a core of 1 % agar gel, so that the results might be generally applicable to foodstuffs like French fries, some frozen desserts and baked goods. They found out that a model for flexure of an elastic plate on a Winkler foundation showed some promise in predicting the indentation response of "strong" food composites. Deficiencies in the model's predictive capacity arose from an interaction between the mechanical properties of the composite and the dimensions of its constituent components. For "softer" composites, a shear failure model indicates the importance of the mechanical properties of the crust in predicting the failure response of the composite.

2.2.3. Silicone elastomers

Silicone elastomers display mainly elastic properties. Their hardness can be easily controlled and are unchanged by mastication. They have thus been used for studies aiming at understanding the oral perception of hardness in viscoelastic products (Mioche *et al.*, 1991), determining the bite force and sample deformation during hardness assessment of viscoelastic models of foods (Peyron *et al.*, 1994) and studying the effects of sample hardness on chewing of human (Kohyama *et al.*, 2004). Kohyama *and al* (2004) reported that the breaking

properties of silicone samples were far from those of foods that are broken down easily by chewing. However, the chewing force was similar to the bite-off of foodstuffs between both the incisors (raw apples: about 0.2 MPa) and molars (food gels: 0.25 to 0.43 MPa, raw carrots: 0.34 MPa, crakers: 0.59 and 0.65 MPa). Those results therefore suggested that the deformability or elasticity of the rubber samples resembled that of real foods, leading the authors to conclude that the use of silicone rubber as a food model is appropriate for investigating the effects of food hardness on chewing. Furthermore, Compagnon *et al.* (1999) developed a synthetic bolus using silicone elastomers for the study of masticatory efficiency. According to these authors, the main advantage in using silicone samples, instead of natural food substances, is that the synthetic test foods have reproducible physical and rheological properties whereas natural foods show great rheological variability. It should however be noted that though the synthetic bolus produced a texture profile approaching that of natural foods, none of them reproduced all the rheological properties of natural food substances.

Silicon rubber also proved to be suitable as standard test foods for assessing individual chewing performance and efficiency, that is, to determine the particle size distribution of food particles after a given number of chewing strokes. Optosil® (Version 1980, Bayer, Germany) is a silicon rubber commonly used as a dental impression material and was chosen as the artificial test food for several masticatory studies (Edlund and Lamm, 1980; Olthoff *et al.*, 1984; Olthoff *et al.*, 1986; Slagter *et al.*, 1992; van der bilt *et al.*, 1993; Fontijn-Tekamp *et al.*, 2000). Optosil® as an artificial test food offers several advantages. Optosil® food samples can be made into any size and they undergo no change in physical properties when in contact with water or saliva, due to the hydrophobic character of Optosil®. These properties, along with the fact that the textural properties (shape, hardness, cohesiveness) of Optosil® can be reproduced, make this silicon rubber a preferred food model to natural test foods.
In addition, when the textural properties of Optosil® were compared with that of turnip, carrot, Gouda cheese and peanut, it was found that up to a compression of about 30 %, Optosil® and turnip required similar forces for deformation. Peanut, however showed a larger initial firmness, while Gouda cheese required relatively small forces for compression. Olthoff *and al.* (1984) also reported that the particle size distributions following the mastication of peanuts and Optosil® were quite similar. Moreover, no fundamental differences were noted in the shapes of the particle size distributions of Optosil®, peanuts and carrots.

However, in the case of Optosil®, a certain degree of comminution was reached with fewer chewing strokes. Since there are no fundamental differences between Optosil® and natural food as far as the intraoral process underlying the comminution of foods is concerned, this material may fulfill a need for standardization and their use deserves serious consideration in studies of mastication.

In 1992, Slagter *and al*. developed another artificial test food, Optocal®, based on Optosil® silicone rubber. It was prepared by mixing Optosil® with toothpaste, Vaseline petroleum jelly, dental plaster powder and alginate powder in the following percentages by weight: 57 %, 27 %, 3 %, 9 % and 4 % respectively. The advantage of Optocal® over Optosil® is that the former has a lower resistance to deformation and failure, which makes it more suitable than Optosil® for the quantification of masticatory performances by subjects with compromised oral conditions. Optocal® and Optosil® silicone products as artificial test foods may thus be useful, in studying the dental state or the functional effects of treatment on mastication process.

Although gels have been subjected to extensive research, they remain a challenge to food technologists. Pinpointing the exact role of gel networks in providing texture, other than maintaining general stability against syneresis and in improving mouthfeel in food products, is difficult. It is obvious that gel networks in real foods are always part of a much more complicated structure than in simplified food gel models. Food models are indeed unable to predict all the complex textural behaviors of real foods. Nevertheless, the use of a well-defined food model with known textural attribute is an approach to understanding and improving food texture. This section of the literature review has brought forward various uses of gelatin and other polymers as food simulants and their interests in texture studies.

PART II: SOFT CHEESES, MANUFACTURE AND CHANGES DURING RIPENING

Surface mould-ripened soft cheeses are characterized by the presence of white mycelia coating due to the growth of *Penicillium camemberti* on the surface. The presence of this mould gives these cheeses a characteristic appearance, as well as a typical aroma and taste. It also leads to more complex ripening patterns than in other cheese varieties with simpler microflora. A typical example of surface mould-ripened cheese is Camembert, which has a soft consistency and a flat cylindrical form, approximately 11 cm in diameter and 2.5 cm high. The other principle cheeses with a surface mould are Brie, Coulommiers and Carré de l'Est (a mild fermented cheese). In the present section, after reviewing briefly the different methods of production and technologies of soft cheeses, the various biochemical changes occurring during ripening will be considered. Finally, an overview of cheese rheology and texture will be described.

1. CHEESEMAKING

Traditional Camembert is made from raw milk with the addition of homofermentative mesophilic lactococci starter. Rennet is added to the milk when pH is about 6.4 and coagulation lasts for about 30 to 45 minutes. Coagulum is transferred to molds by means of a ladle (5 ladles/mold), either manually or using an automated system. Draining occurs at 26-28 °C spontaneously through the perforated sides of the molds during the first hours, then at gradually decreasing temperature which reaches about 20 °C at the end of draining. Intense acidification occurs during draining and a curd with a low mineral content and a pH of 4.6-4.7 is obtained at the end of draining. Cheese is then dry-salted and matured for 21 days in cellars at 11-13 °C and 90% relative humidity (Spinnler and Gripon, 2004).

Camembert, without designation of origin, is manufactured from raw or pasteurized milk. Coagulum is cut into cubes of 2-2.5 cm/side and the curds are molded 30 to 50 minutes later. Curds are salted in brine. Distribution requirements, as well as market demands, have led to modifications in existing technology and have created other types of surface mould-ripened cheeses: Pasteurized milk is renneted after a very short maturation period. Coagulum is cut into cubes, 0.7-1 cm in size, and the curds are stirred and washed. Part of the whey is drawn off before molding. The starter used consists of thermophilic streptococci or a mixture of streptococci and lactococci. The curd obtained is much less acidic than that of traditional

Camembert. These cheeses rapidly acquire a soft texture and a mature appearance. Their taste is milder than the traditional Camembert and their storage properties are improved (Spinnler and Gripon, 2004).

2. COMPOSITION AND CHANGES IN SOFT CHEESE FLORA DURING RIPENING

Composition and evolution of soft cheese flora is complex, particularly when raw milk is used. In raw milk cheese, the physico-chemical treatments select the 'technological' flora, but in pasteurized milk cheese, flora is mostly added to the milk as starters. These microorganisms (yeast, *Geotrichum candidum*, Coryneform bacteria) induce formation of different compounds responsible for change in texture, taste, flavor, color, antimicrobial activity and organoleptic qualities.

The succession of microorganisms that colonize the cheese during ripening is governed by chemical changes in their environment. Lactic acid bacteria (mainly *Lactococcus lactis* subsp. *Lastis* and *Lc. Lactis* subsp. *Cremoris*) in converting residual lactose to lactic acid lower the pH, hence stimulate the growth of acidophilic microorganisms such as yeasts and filamentous fungi. Yeast grow on the surface forming a dense layer of about 200 µm thick (Leclercq-Perlat *et al.*, 1999). These yeasts, mainly *Kluyveromyces lactis, Saccharomyces cerevisae* and *Debaryomyces hansenii*, prepare the curd and growth of *P. camemberti* is observed after 6 or 7 days of ripening. The development of this fungus is extremely fast. In 2 or 3 days, its growth is completed, bringing changes in surface pH, exhausting lactate at the surface and producing a large amount of CO_2 which may change the gaseous environment of the ripening cellar.

Fungus *G. candidum* also appears at the same time as the yeasts, but its growth is hindered by salting. It plays a major role in taste and flavor formation during cheese ripening, for its deamination activity leads to formation of ammonia, aldehydes and organic acids (Hemmes *et al.*, 1982; Lenoir *et al.*, 1983). After 15 to 20 days, when *G. candidum* and *P. camemberti* has consumed lactate for their growth and raise the pH, an aerophilic acid-sensitive bacterial flora (Staphylococcus and coryneform bacteria) establish itself on the surface of the cheese. Inside the cheese, lactococci are clearly predominant; the yeast population remains much lower than

on the surface that is about 10^6 cells/g instead of 10^8 cells/g (Hassouna *et al.*, 1996; Leclercq-Perlat *et al.*, 2004). In pasteurized milk cheese, the range of microflora is less wide, since most microorganisms present are added as starters (*Lactococcus* and *P. camemberti*). Populations of the other microorganisms are reduced and the resulting cheese has a more neutral taste than the traditional Camembert cheese.

3. PROTEOLYSIS

Proteolysis in surface mould-ripened soft cheeses is quite significant. In the outer part of a raw-milk Camembert, pH 4.6-soluble nitrogen represents about 35% of the total nitrogen, while within the cheese 25% of nitrogen is soluble at pH 4.6. The soluble nitrogen fraction contains mainly small peptides (nitrogen soluble in 12 % trichloracetic acid is about 20% of total nitrogen). Furthermore, electrophoretic studies reveal strong degradation of α_{s1}-casein in the whole cheese while β-casein undergoes greater degradation in the outer part than in the centre. This high level of proteolysis in soft cheese is due to the presence of three agents: rennet, plasmin and microbial proteinases, among which enzymes synthesized by *P. camemberti* are dominant. *P. camemberti* has a high proteolytic potential due to the production of extracellular endo and exo peptidases. The evolution of the proteolytic activity has been studied in Camembert during ripening (Lenoir and Choisy, 1970; Boutrou *et al.*, 2006) and it was noted that in the centre of the cheese, proteolytic activity is low. However, in the outer region activity increases abruptly after six to seven days of ripening, that is when *Penicillium* begins to grow.

As stated previously, *G. candidum* plays a key role in typical flavor formation of Camembert during ripening. However, its proteolytic system remains quite unknown. In addition its role in cheese proteolysis remains unclear partly because it is not the only yeast growing on the cheese. Thus, proteolysis of Camembert cheese by *G. candidum* is difficult to determine but is clearly lower than that of *P. camemberti* (Lenoir, 1984).

4. LIPOLYSIS

Intense degradation of fat is a common characteristic of mould-ripened soft cheeses. Moulds and yeasts (mainly *Geotrichum candidum* and *Penicillium camemberti*) are able to secrete a large diversity of lipases. These enzymes are active at the interface between fat globules and the continuous serum phase. Lipases hydrolyse triglycerides to form diglycerides, monoglycerides and free fatty acids. Lipolysis is not homogenous throughout the cheese and occurs mainly under the crust (Hassouna and Guizani, 1995). These authors reported that lipolysis is twice more intense just under the crust than in the interior of the cheese. The association of this phenomenon with proteolysis and particularly the relatively high pH, gives the characteristic texture of the soft part of the Camembert under the cheese crust after a long ripening time.

5. TEXTURE CHANGES IN SOFT CHEESE DURING RIPENING

The most essential characteristic of soft cheeses is the great change in consistency during ripening, resulting in cheese with a large gradient in texture from the outside to the inside: the outer part of Camembert undergoes considerable modification in texture during ripening, and the curd which is firm and brittle in the beginning of ripening, later grow softer. Softening gradually extends towards the centre of the cheese. The water content of Camembert is about 55%. Higher water content causes the outer part to flow when the ripe cheese is cut. These changes were previously attributed to the high level of proteolysis induced by *P. camemberti*. However, the diffusion of fungal proteases is limited and affects mostly the outer few millimeters. In fact, the most important change caused by *P. camemberti* and the surface flora is the establishment of a pH gradient from the surface to the centre due to the consumption of lactic acid and the production of ammonia. Increasing the pH leads to softening of the cheese. This may be explained by the fact that the increase in pH increases the net charge on caseins and hence modifies protein-protein and protein-water interactions. Casein becomes more soluble in water, resulting in modification of protein network. However, the physicochemical conditions (water content and pH) in Camembert alone cannot account for softening (Noel and Lefier, 1991). Indeed, according to Noomen (1983), rennet also causes Camembert to soften during ripening. Experimental cheeses containing no rennet and incubated in an

ammoniacal atmosphere (which allows diffusion of NH_3 into the cheese, hence increases pH) do not soften but instead, become hard and springy, while cheese with rennet activity liquefied. Furthermore, it was noted that experimental 'Camembert' cheese without surface flora did not show change in pH. The author observed no appreciable change in consistency neither in rennet-free cheese nor in rennet cheese without surface flora, although extensive proteolysis of α_{s1}-casein was found.

Therefore, it can be inferred that proteolysis alone does not induce softening, nor does pH increase in rennet free cheese. Only pH increase caused by the surface flora and the outward migration of ca^{2+} in response to the pH gradient (Spinnler and Gripon, 2004) combined with breakdown of α_{s1}-casein by rennet induces softening.

6. CHEESE RHEOLOGY AND METHODS USED TO STUDY CHEESE TEXTURE

Rheology of materials, for example cheese, may be defined as the study of their deformation and flow when subjected to a stress or strain (O'Callaghan and Guinee, 2004). The rheological properties of cheese are those that determine its response to stress or strain, as applied, for example, during compression, shearing or cutting. In practice, such stresses and strains are applied to cheese during processing (for example portioning, slicing, shredding and grating) and consumption (slicing, spreading, mastication and chewing). The rheological properties include intrinsic characteristics such as elasticity, viscosity and viscoelasticity that are related primarily to composition, structure and the strength of attractions between structural elements of the cheese. The rheological characteristics of cheese are quantified by rheological quantities that are measured in tests involving the application of stress or strain under defined experimental conditions. The output variables from these tests (for example creep, stress relaxation, compression tests), which may include change in dimensions over time, the ratio of stress to strain for certain strain levels, stress or strain required to induce fracture, enable determination of quantities such as shear modulus, fracture stress and firmness. In lay terms, the behavior of cheese when subjected to these stresses and strains is referred to by descriptive terms such as hardness, firmness, springiness, crumbliness or adhesiveness. Cheese rheology and factors that affect it have been reviewed extensively (Sherman, 1969; van Vliet, 1991b; Visser, 1991; Gunasekaran and Ak, 2003).

A wide range of instrumental techniques is used for characterizing the rheology of cheese. Instrumental methods may be arbitrarily classified as empirical or fundamental. In general, the nature of the stresses and strains in empirical methods is less well defined than in fundamental methods. Moreover, unlike fundamental methods, the measurements obtained with some empirical methods are on an arbitrary scale (for example the ball compressor).

6.1. Empirical instrumental measurements

Many textural studies have involved rheological measurements to imitate the sensory evaluation of cheese texture. The aim of the empirical test is to measure a parameter which is related to the textural characteristics of the cheese. Hence, while the test conditions are arbitrary and the stresses and strains involved may not be well defined, a value is obtained which gives some indication of the textural characteristics of the cheese and differentiates one sample from another. However, they provide only single datum values that are an overall measure of the many different facets of rheological behavior. In these tests, a sample is compressed or penetrated in one or more bites, thereby simulating the compressive and penetrative actions of the teeth on cheese during mastication.

6.1.1. Imitative tests

Imitative instruments include the bite tenderometer and the denture tenderometer which measure the forces involved in chewing using strain gauges, and typically involved compression to 60% of the original sample height. In the Volodkevich bite tenderometer, which was designed to simulate the motions of mastication, a pair of tooth-like jaws, or wedges compress a sample of about 6mm thick, imitating the squeezing and biting action of teeth. Later instruments used plungers to penetrate a sample or parallel plates to compress a sample, for example to approximately 20 to 30% of its original height (Szczesniak, 1963).
The General Food Texturometer was designed to simulate the biting of food by the jaws and teeth (Bourne, 1978). A food sample (approximately 12.6 mm high) was loaded onto a fixed plate and then subjected to a deforming force by a tooth-shaped plunger, which was mounted on a hinge and actuated to simulate the vertical action of a human jaw. The area of the

samples is at least that of the plunger base, which is available in size from 16 to 50 mm in diameter. The instrument compresses samples to a height of 3.2 mm (that is 75% compression). When the plunger deforms the sample, strain gauges detect the movement of the plunger and a force-time trace is recorded and is known as a texture profile. The sample is subjected to two successive deformations (referred to as bites). The Texturometer has been superseded by uniaxial compression instruments, such as the Instron or Llyod Universal Testing Machine, for the purpose of texture profile analysis. One distinction between the Texturometer and other instruments is that the Texturometer simulates the action of the human jaws, whereby the plunger decelerates as it reaches the end of the compression stroke, and then accelerates upwards as it withdraws. The usual practice with other instruments is compression at constant speed.

6.1.2. Cutting tests

Cutting tests measure the resistance to the passage of a knife or a wire through a cheese (for example Cherry-Burell Curd tension meter). Fracture energy during cutting is quantified by measuring the force required to push wires of different diameters at constant velocity through a cheese (Marshall, 1990). Luyten *et al.* (1991) investigated the fracture properties of Gouda cheese using wire-cutting. A typical force-time curve shows an initial rise in force, which reaches a maximum as the wire penetrates the sample surface. Once the surface has been broken, the force rapidly drops to a constant level, *F*c*,* as the wire `ploughs' through the sample. *F*c increases with cutting speed and with wire diameter. Since fracture develops around a crack, a specific fracture energy (J/m*2*), *Rf,* can be defined as the energy needed per unit area (of crack) to cause a fracture to spread. While it is not possible to determine specific fracture energy precisely, because of the inherent heterogeneity in cheese structure, its order of magnitude can be determined by measuring cutting force using wires with a series of diameters and extrapolating to a diameter of zero. The specific fracture energy is calculated as:

$$R_f = \frac{F_{c0}}{d} \qquad (4)$$

where *F*co is the cutting force, extrapolated to cutting with a wire of zero diameter, and *d* is the sample width, that is the length of wire in contact with the cheese. The fracture energy obtained with the wire-cutting method may give a more accurate prediction of the behavior of cheese during cutting (for example portioning, slicing) than that obtained using large-strain shear or compression deformation tests.

6.1.3. Penetration tests

Penetration tests involve measurement of the force required to insert a probe (cone or cylinder) a given distance into cheese, or alternatively the depth of penetration of a probe under constant load for a given time. As the probe penetrates the sample, the cheese, the cheese in its path is fractured and forced apart. The progress of the probe is retarded to an extend depending on the hardness of the cheese in its path, the adhesion of the cheese to its surface (which depends on the depth of penetration into the cheese and the thickness of the needle, or angle of the cone used). Hennequin and Hardy (1993) used a flat bottom cylindrical probe (5 mm diameter at a speed of 10 mm/min to a depeth of 10 mm) to penetrate soft cheeses (Camembert, Coulommiers, Munster) and found that the force at 10 mm penetration have a high correlation with sensory firmness (r=0.94). These authors concluded that this technique is suitable and rapid method for texture measurement of soft cheeses. Breuil and Meullenet (2001) found a significant correlation between measurements obtained using a cone penetrometer (30°C), or a 2 mm needle, and textural characteristics of a wide range of commercial cheeses (Colby, Edam, Cheddar, Mozzarella and cream cheese) as measured by a sensory panel.
The main advantage of these penetration tests is that they can be performed directly on the cheese and in its packaging.

6.2. Fundamental measurements

Large strain deformation measurements on cheese are usually undertaken using uniaxial compression, shear (or torsion), wire-cutting or bending. The methodology and

instrumentation used for these measurements, and factors affecting the measurements, are discussed below.

6.2.1. Uniaxial compression

The most common types of rheological measurement in cheese involve linear (uniaxial) displacement, for example using Instron or Llyod Universal Testing Machine (Lee *et al.*, 1978; Imoto *et al.*, 1979; Creamer and Olson, 1982; van Vliet, 1991b; Visser, 1991; Guinee *et al.*, 2001), the TA.XT2 texture analyzer or its derivatives from Stable Micro Systems (Truong, 2002; Xiong *et al.*, 2002).

Measurements are generally made in compression mode rather than in tensile mode because:

- compression behavior is relevant to sensory perception arising from chewing and mastication;
- it is difficult to grip cheese samples to carry out a tensile test and;
- hard cheese has inhomogeneities which occur in random positions and directions with respect to sample dimensions, making it difficult to obtain reproducible results for tensile fracture.

Compression measurement involves compression of a rectangular or cylindrical sample between parallel plates. Compression testing is more suited to large strain deformation than to linear viscoelastic deformation (low strain). This is because initial contact between the parallel plate and the sample usually involves some realignment of the sample surface due to imperfections in the surface smoothness, as a result of intrinsic macrostructural characteristics of the cheese (for examples cracks, failures). Moreover, the difficulty in fine precision cutting can give rise to lack of accuracy in low strain measurements (up to 0.5 mm of deformation). Ideally, the cheese sample may be conditioned by applying one or more low compression deformations (for example about 0.05) prior to testing (O'Callaghan and Guinee, 2004).
Compared to other rheological methods for evaluating cheese, large-strain deformation compression offers several advantages: the strains applied are in the range of those applied to cheese during size-reduction operations as applied commercially; it is a dynamic method for which the calculated parameters (for example strain and stress at fracture) depend on a range

of stress-strain data accumulated during the test ; sample preparation does not require specialized cutting equipment ; all cheeses, apart from soft cheeses like mature Camembert with an almost-runny consistency, can be prepared easily and tested: and the test method is simple and rapid. However, for reproducible results, sample shape and dimensions need to be precise, which can be difficult where cylindrical samples are acquired by pushing a cylindrical borer into a portion. As is common to all large strain deformation methods, a serious limitation is the difficulty in obtaining results for cheeses with eyes.

6.2.2. Large strain shear measurements

A rheometer or a viscometer may be used also, in addition to a texture analyzer, to apply large strain shear to cheese. A large shear strain may be applied with a rheometer using samples of cheese with capstan geometry (Truong and Daubert, 2001; Truong, 2002). The effect of cutting the cheese into a capstan shape is that the greatest shear stress occurs at the cross-section of minimum radius (Figure 3).

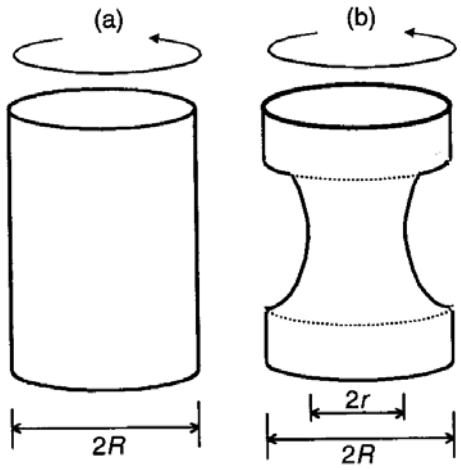

Figure 3. Illustration of sample shapes used in torsion tests, using parallel plate geometry (a), and capstan geometry (b). The capstan shape is obtained by milling a cylindrical sample using a purpose-built milling machine. R is the radius of the cylindrical sample and r is the smallest radius of the capstan shaped sample.

Bowland and Foegeding (1999) used this technique to determine the fracture properties of model processed cheese. For highly deformable cheeses, for example fresh low-moisture part-skim Mozzarella and young reduced-fat cheeses (Cheddar) which generally do not undergo elastic fracture (the sample breaks into distinct pieces), but rather plastic fracture, on compressing to strains of 0.7 to 0.8 (Fenelon and Guinee, 2000), torsion shear may be useful in determining fracture stress and fracture strain. The latter parameters may be important in some cheeses (in the formation of cheese strings containing two different-colored cheeses in a twisted helical configuration). However, preparation of capstan-shaped samples requires specialized milling equipment and is time-consuming. Vane rheometry has been used for large strain shear deformation tests in processed and natural cheeses, including Cheddar and Mozzarella.

In this method a probe, typically with four blades or vanes, is inserted into a sample and rotated slowly at a constant rate (for example 10 cycles per minute), while the torque is measured. The technique produces a shear stress against strain characteristic with a distinct peak at the point of failure. Fracture stress is shear rate-dependent in both cases, being smaller by a factor of two to three with the vane technique than with the torsion technique. Using vane rheometry and torsion, it was possible to separate different cheese types on fracture stress/fracture strain `texture maps', which were similar in both cases (Truong and Daubert, 2001). The vane method, which is rapid and does not require sample preparation, has been found to give trends comparable to those obtained using capstan geometry for processed cheese, Cheddar and Mozzarella. However, disadvantages of vane rheometry may include the difficulty of inserting the vane without cracking the cheese mass (for example hard cheeses such as Romano or Parmesan, with a low fracture strain and soft cheeses with a low fracture strain, such as Feta), and variability of results for cheeses, such as Blue or Gouda, with macrostructural heterogeneities.

A wide range of instrumental techniques is therefore available for texture assessment and as previously mentioned, some methods are more suitable than others for measuring the rheological properties of soft cheeses. The different instrumental methods that have been used to study soft cheeses are listed in table 2. Three types of tests have been used: penetrometry tests, either with needle or glass slide; compression tests either at constant speed or in

relaxation. Sensory analysis has also been used to evaluate consistency of soft cheese (Hennequin and Hardy, 1993).

The large inhomogeneity of soft cheese results in important difficulties in sampling for instrumental measurements. Various sampling procedures are used:

1. Making cylinders from young Camembert cheese with cork borer
2. Cutting off slices with a wire-cutter along a diameter axis
3. Analyzing whole Camembert cheese

Table 2: Instrumental methods used for studies on Camembert cheeses

References	Test	Experimental conditions	Test sample
Vassal *et al.*, 1986	Needle penetrometry (INSTRON with balance)	Needle: 2 mm in diameter Displacement rate:0.42cm/s Penetration depth: 5mm Temperature: 20°C Measured quantity: work done during penetration	**Camembert** Slice thickness: 2cm 9 penetrations/slice: 3 at 2mm from the crust of each side, one in the centre and the other in the middle of radius
Monnet, 1982	Slide penetrometry	Slide Thickness: 0.5mm Width: 20mm Same experimental conditions as above	**Experimental camembert** 4 penetrations/slice, respectively, at 2, 4, 10 and 15mm from one of the sides
Noel *et al.*, 1987	Needle penetrometry	Needle : 2mm Displacement rate : 0.6cm/s Measured quantity: force	**Camembert**
Mpagana and Hardy, 1985 Mpagana and Hardy, 1986	Constant compression rate Fracture test (maximum relative deformation = 80% of original height) Relaxation test (relative deformation=10 to 20% of original height)	Displacement rate: 0.02cm/s and 0.2 cm/s Temperature: 20°C Measured quantity: force	**Camembert** Cylinder diameter=14mm cylinder height=10mm

Owing to the variations in manufacturing conditions and composition, cheese exhibits a wide range of rheological behavior, ranging from the viscous behavior of soft cheese to the elastic behavior of hard cheese at low strain. The rheological properties of cheese are of considerable importance as they affect:

1. its handling, portioning and packaging characteristics;
2. its texture and eating quality, as they determine the effort required to masticate the cheese or alternatively the level of mastication achieved for a given level of chewing. The degree of chewing required may, in turn, influence the flavor/aroma properties and the suitability of the cheese for different consumer groups (children, aged persons);
3. the use of the cheese as an ingredient, as they influence its behavior when subjected to different size reduction methods (shredding, grating or shearing) and how it interacts and blends with other ingredients on foods on which cheese is an ingredient;
4. its ability to retain a given shape at a given temperature or when stacked;
5. its ability to retain gas and hence to form eyes or cracks or swell.

Hence, the rheological properties of cheese are significant quality attributes of importance to the manufacturer, pre-packer, distributor, retailer, industrial users and consumers.

The literature review gave an overview of the various efforts made in order to understand textural properties of soft cheeses. It also put forward the interest of using food simulants in texture studies. Designing a food model capable of imitating the change in rheological parameters of Camembert and Coulommiers cheeses during ripening can be of valuable interests for cheese manufacturers and consumers.

Evaluating the global textural properties of food products is not easy. Some authors reported that some instrumental rheological parameters correlate poorly with textural attributes describing sensory perception of food texture (Szczesniak, 1986; Brown *et al.*, 2003). It can be inferred that instrumental methods commonly used to characterize food texture cannot measure all the textural properties perceived through sensory evaluation. Identifying correlations between sensory and instrumental measures of texture is however necessary to increase understanding of what is actually perceived during sensory assessment of texture. Therefore, in this research work, the interest of using techniques based on optical measurements of surface displacement of food products was investigated. The three-dimensional systems studied were intended to imitate the human eyes. The digital image correlation system is, for instance, composed of two digital cameras. The action of a cheese grader or a consumer who presses the finger into the cheese was imitated by the penetrometry test performed on a universal testing machine. The fingertip was simulated by a 20 mm-diameter flat bottomed probe.

CHAPTER II: MATERIALS AND METHODS

1. MATERIALS

1.1. Soft cheeses

Camembert and Coulommiers cheeses

One-day old Coulommiers cheese was kindly supplied by La Fromagerie de Sorcy (Lactalis®) France and 10-day-old Camembert Président® (Lactalis®) cheese was bought from a local supermarket. Cheese composition, weight and size are indicated in table 3.

Table 3. Composition, weight and diameter of Coulommiers and Camembert cheeses

		Coulommiers	Camembert
Protein	g/100	20.5	22.0
Carbohydrate	g/100	_	_
Total Fat	g/100	23	20
Fat in dry matter	g/100	52	45
Calcium	g/100	0.49	0.45
Weight	g	350	250
Diameter	cm	~13	~11

1.2. Gelatin and polysaccharides gels imitating 10-day-old soft cheeses texture

In order to design a polymeric gel having textural properties close to that of soft cheeses, five types of simulants were formulated from mixtures of type A gelatin with a nominal strength of 260 Bloom (PB Gelatin France SA, Furdenheim, France) and polysaccharides (Table 4). Guar gum (Sigma Chemical Co., Mo, USA), karaya gum (Alland and Robert, Port-Mort, France), xanthan gum (Systems Bio-Industries, Boulogne, France) or maltodextrin DE 19 (Roquette Frères, France) and gelatinized wheat starch (Sigma Chemical Co., Mo, USA) were added to gelatin. Calculations were made on a dry matter basis, and all concentration values are stated in weight percent. All formulated gels also contained 0.02 % (w/w) sodium azide (Acros Organics, New Jersey, USA) to avoid microorganism development.

Table 4. Composition of the five gels studied

Gels	Composition (% w/w)
1	gelatin (6)
2	gelatin (6) - guar (1)
3	gelatin (6) - karaya gum (3)
4	gelatin (6) - xanthan gum (3)
5	gelatin (6) - maltodextrin (20) - gelatinized starch (3)

Guar gum

Guar flour is obtained from the seed endosperm of the leguminous plant *Cyamopsis tetragonoloba.* The seed is decoated and the germ is removed. In addition to the polysaccharide guar, guar flour contains 10-15 % moisture, 5-6 % protein, 2.5 % crude fiber and 0.5-0.8 % ash. Guar gum consists of a chain of β-D-manopyranosyl units joined with α (1→4) linkages. Every second residue has a side chain, a D-galactopyranosyl residue that is bound to the main chain by a β (1→6) linkage (Figure 4). It disperses and swells almost completely in hot or cold water and is insoluble in organic solvents. Guar gum forms highly viscous solutions, the viscosity of which is shear rate dependent (Belitz and Grosch, 1999).

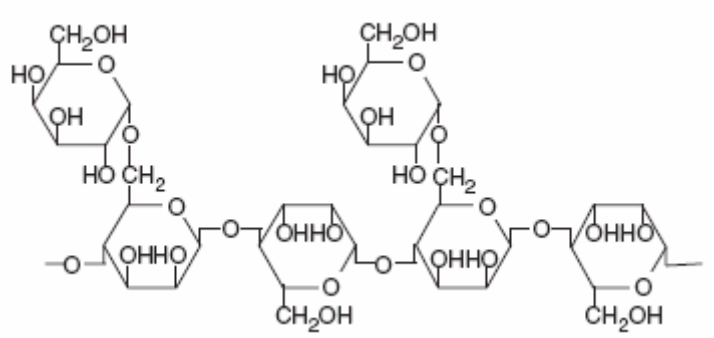

Figure 4: Guar formula (de Jong and van de Velde, 2007)

Karaya gum

Karaya gum, also called Indian tragacanth, is an exudate from an Indian tree of the *Sterculia ureus* and other *Sterculia* species. The building blocks are D-galactose, L-rhamnose, D-galacturonic acid and L-glucuronic acid (Figure 5).

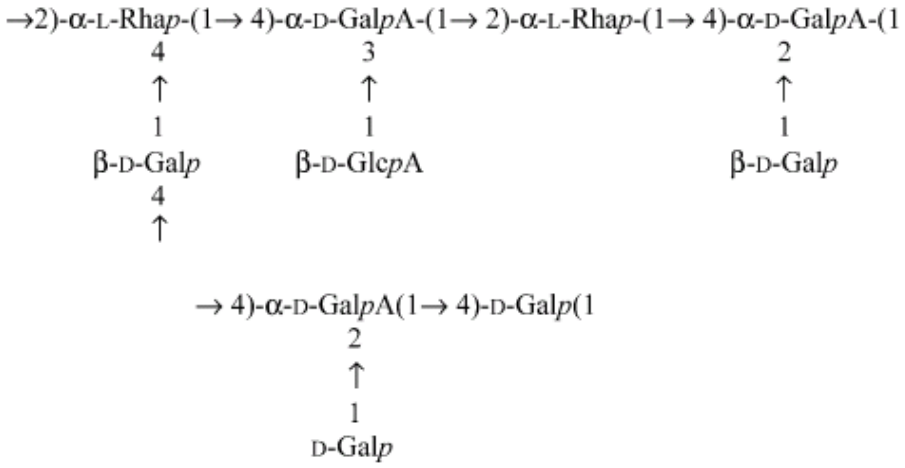

Figure 5: Structural formula of karaya gum (Silva *et al.*, 2003)

The sugars are partially acetylated (13 % acetyl groups based on dry weight). The molecule consists of three main chains which are polymers of different disaccharide units. The main chains carry side chains and are also covalently linked via the side chain (Belitz and Grosch, 1999). Due to the acetyl group on the gum structure, this polysaccharide does not fully dissolve in water to give a clear solution; instead it absorbs water rapidly and forms a viscous colloidal dispersion at low concentration. The fine mesh gum hydrates much more rapidly than coarser gum, and gives a smooth, homogenous solution, whereas coarse granules yield a grainy dispersion. Up to 4 % of gum may be hydrated in cold water to give a viscous gel-like paste of uniform smoothness and texture: the gum concentration in gelatin-karaya mixture in our study was thus limited to 3 %. Moreover, karaya will form viscous solutions in 60 % alcohol, but is insoluble at higher concentrations. Deacetylation by using alkali in solution can modify the gum's characteristics from water swellable to water soluble (Weiping, 2000). The viscosity of Karaya dispersions ranges from about 120 to 400 cps for 0.5 % dispersions to about 10000 cps for 3 % dispersions. The gum is compatible with most gums as well as with proteins and carbohydrates. Blending karaya with other gums, such as alginate, can modify the solution characteristics (Le Cerf and Muller, 1994), while the addition of 0.1 M NaCl to karaya gum causes a decrease in its gel strength (Brito *et al.*, 2005)

Xanthan gum

Xanthan gum is an anionic polysaccharide produced by the bacterium *Xanthomonas campestris*, which is found on cruciferous vegetables such as cabbage and cauliflower. This

polysaccharide can be regarded as a cellulose derivative. The main chain consists of 1,4 linked β-glucopyranose residues. On an average, every second glucose residue bears in the 3-position a trisaccharide of the structure β-D-Manρ-(1→4)- β-D-GlcρA(1→2)-α-D-Manρ as the side chain. The mannose bound to the main chain is acetylated in position 6 and approximately 50 % of the terminal mannose residues occur ketalized with pyruvate as 4,6-O-(1-carboxyethylidene)-D-mannopyrannose (Figure 6).

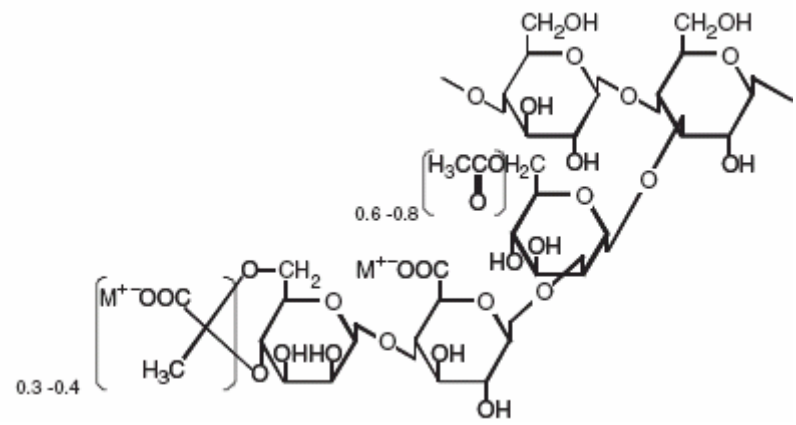

Figure 6: Xanthan gum formula (de Jong and van de Velde, 2007)

Xanthan gum has high low-shear viscosity and strong shear-thinning character. The relatively low viscosity at high shear rate makes it easy to mix, pour, and swallow; its high viscosity at low shear rate gives it good suspension properties and lends stability to colloidal suspensions (Sun *et al.*, 2007).

Starch

Starch is the major form of stored carbohydrate in plants. Starch is composed of a mixture of amylose and amylopectin. Amylose is an essentially linear polysaccharide, while amylopectin is a highly branched polysaccharide (Figure 7).

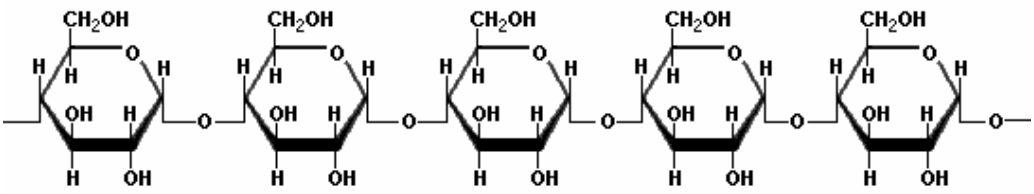

(a)

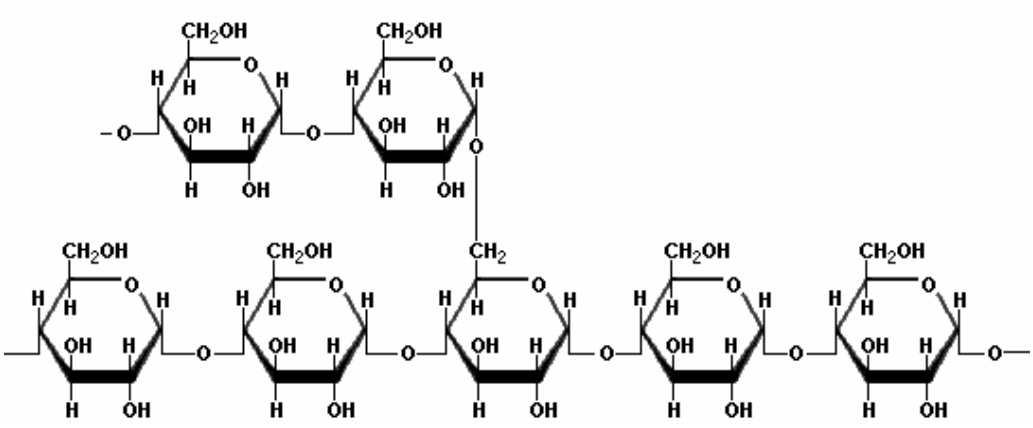

(b)

Figure 7. Structural formula of amylose (a) and amylopectin (b)

Natural starches contain 10-20% amylose and 80-90% amylopectin. Amylose forms a colloidal dispersion in hot water, while amylopectin is completely insoluble. Amylose typically consists of 200 to 20 000 glucose units, which form a helix as a result of the bond angles between the glucose units. Amylopectin may contain up to two million glucose units.

Maltodextrin

Maltodextrin is a neutral dextrin, enzymatically derived from starch with dextrose equivalent values (DE) lower than 20, consisting of (1→4 and 1→6)-*α*-D-glucopyranose-linked residues. DE is defined as the total number of reducing sugars relative to a glucose baseline 100 and is expressed on a dry-weight basis. Hydrolysis products with a DE above 20 are generally referred to as ‘glucose syrups’, which as the name implies are liquids supplied in the form of

aqueous solutions. It is, in part, the solubility of the hydrolysis product that distinguishes the two classes of material, that is above a DE of 20, the product is made of short oligomers that are freely soluble in water, whereas below 20, there is a sufficient proportion of long polymeric chains to inhibit solubility and promote gelation (Loret *et al.*, 2004). Formation of a maltodextrin network depends on the dissolution and quenching temperature, time and polymer concentration. Loret *et al.* (2004) found that an approximately 30 % (w/w) maltodextrin sample formed a network within 5 min at 25 °C, whereas 25 % (w/w) maltodextrin gelled after about 50 min.

1.2.1. Gelatin gel

Gelatin powder was dispersed in distilled water at a temperature of 22±2 °C. The suspension was stirred quickly with a glass rod and left undisturbed for approximately 30 minutes. Then, the suspension was heated at 60 °C for 30 minutes and gently stirred. The latter was then poured into plastic containers, 11 cm in diameter and 3.5 cm high. Each container held 300 g of suspension so that the height of gel obtained was around 3 cm, similar to most Camembert/Coulommiers cheeses. Gels were kept at 7±1 °C for 12 hours before analysis.

1.2.2. Gelatin-guar gum gel

Guar suspension was prepared by dispersing the gum in distilled water and heated at 90 °C for 30 minutes. Gelatin suspension was separately prepared according to procedures mentioned above (gelatin gel). It was then added to the guar suspension, and the mixture was stirred during 30 minutes. The latter was then poured into containers, covered with a paraffin film and kept at 7±1 °C for 12 hours before analysis.

1.2.3. Gelatin-Karaya gum gel and gelatin-xanthan gum gel

Gelatin-karaya and gelatin-xanthan gels were prepared in the same way. Karaya (or xanthan) powder was dispersed in distilled water and kept at 7±1 °C for 12 hours for particle hydration.

Gelatin suspension was separately prepared according to procedures mentioned above (gelatin gel). It was then added to karaya (or xanthan) suspension and the mixture was heated at 60 °C for 15 minutes, gently stirred and then poured into containers and covered with a paraffin film. Gels were kept at 7±1 °C for 12 hours before analysis.

1.2.4. Gelatin-maltodextrin-starch gel

Maltodextrin powder was dispersed in distilled water and heated to 90 °C for 30 minutes under magnetic stirring at 300 rpm. Starch powder was added to distilled water and the suspension was heated at 90 °C, until a completely gelatinized solution was obtained. Full gelatinization was confirmed by polarized light microscopy. Maltodextrin and gelatinized starch solutions were then added to gelatin suspension and poured into containers, and covered with a paraffin film before storage at 7±1 °C for 12 hours before analysis.

1.3. Coulommiers cheese simulant imitating 10-day-old Coulommiers cheese

When the textural properties of the various gels above have been compared to those of Coulommiers cheese (Results and discussion section, Part I), gel containing 7.8% (w/w) gelatin (PB Gelatin France SA, Furdenheim, France), 20.2% (w/w) maltodextrin DE 19 (Roquette Frères, France) and 2% (w/w) gelatinized starch (Sigma Chemical Co., Mo, USA) was found to imitate best Coulommiers cheese texture. This simulant component was previously determined through a mixture design experiment. Details are given in the 'Results and discussion section, part I'.

The simulant was prepared by dispersing maltodextrin powder in distilled water and heated to 90 °C for 30 minutes under magnetic stirring at 300 rpm. Starch powder was added to distilled water and the suspension was heated at 90 °C, until a completely gelatinized solution was obtained. Maltodextrin and gelatinized starch solutions were then added to gelatin suspension and poured into containers, and covered with a paraffin film before storage at 7±1 °C for 12 hours before analysis.

This gel was subjected to:
- penetrometry and stress relaxation tests to study change in textural properties during ripening (Results and discussion section: Part II-Polymeric gel simulating cheese during ripening) and;
- to digital image correlation analysis (Results and discussion section: Part III-Rheological properties determined by digital image correlation).

1.4. Coulommiers simulant with Subtilisin Carlsberg (Alcalase®) imitating ripening cheese texture

Benchmark enzyme, Alcalase®, type FG (protease Subtilisin Carlsberg, Novo Nordisk, Denmark) was added in varying amount to the Coulommiers simulant-7.8% (w/w) gelatin, 20.2% (w/w) maltodextrin DE 19 and 2% (w/w) gelatinized starch-to bring about textural changes in the gels. The Alcalase activity is 2.4 Anson units/g (AU/g). One Anson unit is defined as the amount of enzyme which, under specified conditions, digests urea-denatured hemoglobin at an initial rate such that there is liberated an amount of trichloroacetic acid (TCA)-soluble product per minute which gives the same color with Folin-Ciocalteu Phenol reagent as one milliequivalent of tyrosine at 25 °C at pH 7.50. The liquid density of Alcalase® is 1.25 g/mL.

Since the required volume of Alcalase® was small (less than 10µL), a diluted solution was prepared by adding 1mL of the enzyme to 10mL of distilled water to allow more accurate uptake measurement. However, thereafter in the text, when the quantity of enzyme in the simulant is given, it refers to the amount of enzyme actually present in the gel (that is dilution has been accounted for).

Four types of Coulommiers simulants were prepared: One gel without enzyme, which will be referred to as the standard gel and three gels containing 2, 4 and 10 µL of Alcalase®; that is 0.006, 0.012 and 0.03 AU respectively (which also corresponds to an enzyme/gelatin ratio of 0.06, 0.12 and 0.30 µL/g respectively).

The enzyme containing Coulommiers simulant was prepared according to the following procedures. Maltodextrin powder was dispersed in distilled water and heated to 90 °C for 30 minutes under magnetic stirring at 300 rpm. Starch powder was added to distilled water and the suspension was heated at 90 °C, until a gelatinized solution was obtained. Alcalase® was added to maltodextrin suspension previously cooled to 30 °C.
Maltodextrin and gelatinized starch solutions were then added to gelatin suspension and poured into containers, and covered with a paraffin film before storage at 7±1 °C for 12 hours before analysis. All gels samples also contained 0.02 % (w/w) sodium azide (Acros Organics, New Jersey, USA) to prevent microorganism growth.

These gels were subjected to penetrometry and stress relaxation tests 1, 8, 43, 50 and 120 days after preparation.

1.5. Camembert cheese simulant imitating 30-day-old Camembert cheese

In order to design the simulant which would imitate textural properties of 30 days old Camembert cheese, the optimization module in Design-Expert software was used to generate the composition of the gel. Detailed account of the use of this software in setting up a mixture design experiment is given in the 'materials and methods' section of this chapter.

Camembert simulant imitating textural properties of 30 days old Camembert cheese was made from 6.5% (w/w) gelatin (PB Gelatin France SA, Furdenheim, France), 21.5% (w/w) maltodextrin DE 19 (Roquette Frères, France) and 2% (w/w) gelatinized starch (Sigma Chemical Co., Mo, USA). The gel was prepared following same procedures as that of Coulommiers simulant (materials and methods section, paragraph 1.3)

The gel was subjected to digital image correlation analysis (Results and discussion section: Part III-Textural properties determined by digital image correlation).

2. METHODS

2.1. Instrumental characterization of textural properties

Textural properties of both cheeses and their simulants were determined from instrumental tests performed on Lloyd universal testing machine (Llyod Instruments LRX) integrated with Nexygen Series 4.5 materials testing software (Lloyd Instruments Ltd., Hants, UK). All samples were evaluated instrumentally at 7±1 °C. Cheeses were removed from their wrapping material and cardboard box before analysis. Six and three replicates of cheese and simulant respectively, were subjected to penetrometry and stress relaxation tests.

2.1.1. Penetrometry test

2.1.1.1. Principle

Penetrometry or puncture test is one of the simplest and most widely used methods for measurement of textural characteristics (van Vliet, 1991a; Anand and Scanlon, 2002). The test measures the force required to push an indenter into a food (Bourne, 2002). Use of penetrometry tests for evaluation of mechanical properties of foods has been commonly cited (deMan, 1969; Gregson *et al.*, 1999; Ross and Scanlon, 1999). In this test, a rigid indenter (usually made of high carbon steel and also known as probe, punch or die) is pressed against the surface of the test specimen. The data thus obtained are used to generate a force-deformation curve which is analyzed to obtain various mechanical properties (Mohsenin, 1986). Advantages of the indentation test include its simplicity, rapidity, and lesser dependence on the geometry of the specimen. It is an ideal test for texture evaluation in localized regions of foods. The test has been the subject of much research in the areas of food science and engineering, materials science, civil, geotechnical and mechanical engineering, and biomechanics.

2.1.1.2. Procedure

During penetrometry test, a 20 mm-diameter flat-bottomed cylindrical probe was forced into samples, 25 mm from sample border, at crosshead speed of 10 mm/min to a depth of 10 mm. Load cell of 500 N was used and data were recorded at a sampling rate of 80 HZ.

2.1.1.3. Data processing

Firmness is defined as the stress (force) necessary to attain a given deformation or stress (force) required to compress between the molar teeth (for solids) or between tongue and the palate (for semi-solids) to a given deformation or penetration (van Vliet, 1991b). It was considered as the force, in Newton, necessary to insert the cylindrical probe to a depth of 10 mm into the sample (Figure 8).

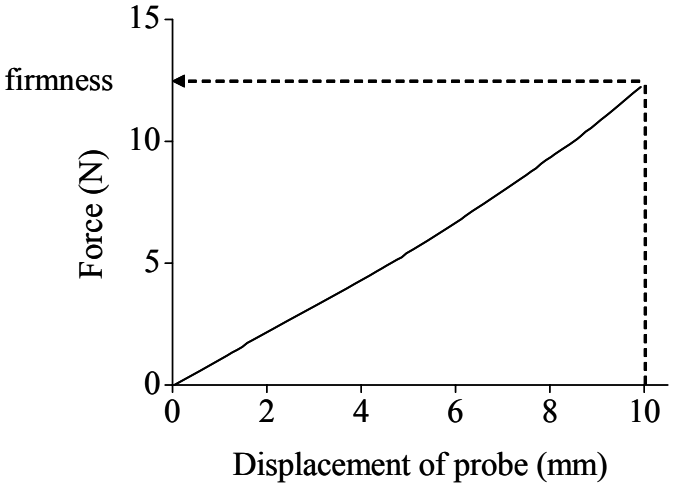

Figure 8. Typical force-displacement curve obtained from penetrometry test of Coulommiers cheese and firmness is considered as the force (N) required to insert probe to a depth of 10 mm into sample

2.1.2. Stress relaxation test

2.1.2.1. Principle

Cheese may be considered as a composite material. The presence of fat particles (the filler), brine, holes and cracks and boundaries between curd granules changes the properties of casein matrix. During manufacture, treatment of curd may modify the system structure. Rheological properties of fat are added to those of the casein matrix so that the cheese as a whole is viscoelastic (Prentice et al., 1993). This implies that supplied mechanical energy is partly stored in the material (elastic deformation) and partly dissipated (viscous flow). Stress relaxation tests have widely been used to determine viscoelastic behavior of cheeses (Mpagana and Hardy, 1985; Mpagana, 1986; Kfoury *et al.*, 1988; Hennequin and Hardy, 1993; Hort and Le Grys, 2001). In stress relaxation, the test specimen is suddenly brought to a given deformation (strain) and the stress required to hold the deformation constant, is measured as a function of time. The results are expressed in terms of time-dependent modulus *E(t)* in tension or compression, *G(t)* in shear, or *K(t)* in bulk compression. The rheological model commonly used to represent stress relaxation is the generalized Maxwell model given in figure 9. The model is composed of *n* Maxwell elements with a spring in parallel with the *n*th element.

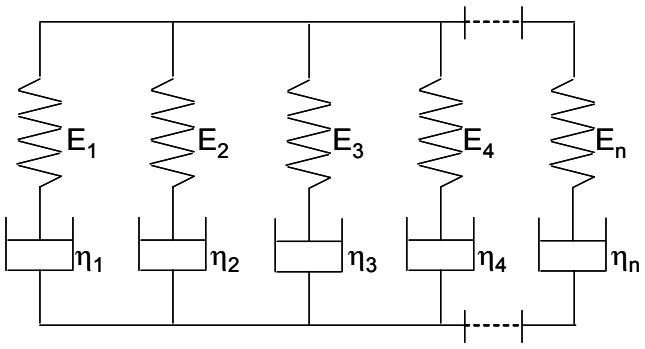

Figure 9. Generalized Maxwell model

E_n stands for the modulus of elasticity (kPa) of the *n*th element and η_n is its coefficient of viscosity (kPas). One of the most important viscoelastic parameters which can be obtained from a stress relaxation test is the time of relaxation. It is a measure of the rate at which a material dissipates stress after receiving a sudden force (Mohsenin, 1986).

2.1.2.2. Procedure

Relaxation test was performed by applying a constant deformation of 10% of sample height for 10 minutes, with a 20 mm-diameter flat-bottomed cylindrical probe, traveling at a crosshead speed of 200 mm/min. Deformation was applied at 25 mm from sample border. Load cell of 10 N was used and data were recorded at a sampling rate of 80 Hz.

2.1.2.3. Data processing

Relaxation times and elastic modulus of sample were calculated using OriginPro 7.5 software (OriginLab Corporation, Northampton, MA, USA) by fitting a three-parameter Maxwell model to stress relaxation curves obtained (Figure 20). The Maxwell model parameters were determined by successive residuals method (Mohsenin, 1986).

2.2. Mixture design

In order to determine gelatin, maltodextrin and gelatinized starch concentrations resulting in simulants approaching the soft cheeses textural parameters, a three-component mixture design was used.

2.2.1. What is a mixture design?

In a mixture experiment, the independent factors are proportions of different components of a blend. For example, to optimize the firmness of the simulant, the factors of interest are the proportions of gelatin, maltodextrin and starch in the gel. In a mixture design, the proportions of the different factors must sum to 100 %. When the mixture components are subject to the constraint that they must sum to one, there are standard mixture designs for fitting standard models, such as *Simplex-Lattice* designs and *Simplex-Centroid* designs. When mixture components are subject to additional constraints, such as a maximum and/or minimum value for each component (which is the case in this study), designs other than the standard mixture

designs, referred to as constrained mixture designs or *Extreme-Vertices* designs, are appropriate.

In mixture experiments, the measured response is assumed to depend only on the relative proportions of the ingredients or components in the mixture and not on the amount of the mixture. The amount of the mixture could also be studied as an additional factor in the experiment; however, this would be an example of mixture and process variables being treated together. In mixture problems, the purpose of the experiment is to model the blending surface with some form of mathematical equation so that:

1. Predictions of the response for any mixture or combination of the ingredients can be made empirically, or
2. Some measure of the influence on the response of each component singly and in combination with other components can be obtained.

2.2.2. Models

The difference between the models of the experimental designs for independent variables and the models of a mixture design is that in a mixture design, there is no constant term.

The canonical forms of the mixture models are as follows:

Linear $$E(Y) = \sum_{i=1}^{q} \beta_i x_i$$

Quadratic $$E(Y) = \sum_{i=1}^{q} \beta_i x_i + \sum_{i=1}^{q} \sum_{i<j}^{q} \beta_{ij} x_i x_j$$

Cubic $$E(Y) = \sum_{i=1}^{q} \beta_i x_i + \sum_{i=1}^{q} \sum_{i<j}^{q} \beta_{ij} x_i x_j + \sum_{j=1}^{q} \sum_{i<j}^{q} \delta_{ij} x_i x_j (x_i - x_j) + \sum_{k=1}^{q} \sum_{j<k}^{q} \sum_{i<j}^{q} \beta_{ijk} x_i x_j x_k$$

Special cubic $$E(Y) = \sum_{i=1}^{q} \beta_i x_i + \sum_{i=1}^{q} \sum_{i<j}^{q} \beta_{ij} x_i x_j + \sum_{k=1}^{q} \sum_{j<k}^{q} \sum_{i<j}^{q} \beta_{ijk} x_i x_j x_k$$

The terms in the canonical mixture polynomials have simple interpretations. Geometrically, the parameter β_i in the above equations represents the expected response to the pure mixture x_i=1, x_j=0, $i \neq j$, and is the height of the mixture surface at the vertex x_i=1. The portion of each of the above polynomials given by

$$\sum_{i=1}^{q} \beta_i x_i ,$$

is called the linear blending portion. When blending is strictly additive, then the linear model form above is an appropriate model.

2.2.3. Experimental set up

Experimental domain was chosen according to preliminary experiments; gelatin gels below 5 % (w/w) were too soft and gels above 10 % (w/w) were too firm and rigid compared to cheeses (Table 5).

Table 5. Lower and upper limits of the component range with a constant water content of 70 % (w/w)

Components	lower limit, % (w/w)	upper limit, (% w/w)
Gelatin	5	10
Maltodextrin	16	23
Starch	2	4

Starch and maltodextrin were added to gelatin in order to adjust gelatin textural properties to that of cheeses, thus their minimum and maximum concentrations were chosen accordingly. Although distilled water was a constituent of the simulants, it was not included, as a component, in the mixture design. Gels had a constant water content of 70 % (w/w). In order to estimate the coefficients of a cubic Scheffe polynomial, a D-optimal mixture design was constructed with Expert-Design 6.0.6 trial software (Stat-Ease Inc., Minneapolis, MN, USA). The D-optimal criteria select design points in a way that minimizes the variance associated with the estimates of specified model coefficients. The steps to set up the D-optimal design are given below.

1. The number of factors and their constraints are selected (table 5).
2. A cubic model is chosen.
3. The software creates overall candidate point set depending on the model chosen.
4. The software chooses the design points, including replicates.

The number of candidate points generated by the software depends on the model. In our case, as already mentioned, a cubic model was chosen. Ten 'model' points determined by the D-optimal criteria was selected. Two 'lack of fit' points and three 'replicate' points were also added. Compositions of gels for the experimental runs are given in table 6.

Table 6. Experimental runs of the mixture design

Run	Gelatin (%w/w)	Maltodextrin (%w/w)	Starch (%w/w)
1	7.5	20.5	2.0
2	8.8	18.8	2.5
3	7.5	19.5	3.0
4	10.0	16.0	4.0
5	5.0	23.0	2.0
6	10.0	16.0	4.0
7	10.0	18.0	2.0
8	10.0	18.0	2.0
9	8.8	17.7	3.5
10	5.0	22.0	3.0
11	5.0	21.0	4.0
12	6.3	20.7	3.0
13	10.0	16.7	3.3
14	5.0	23.0	2.0
15	6.7	19.3	4.0

Furthermore, four gels with composition different from those used in building up the mixture design were formulated in order to check the validity of mathematical models found (Table 7).

Table 7. Composition of four additional gels used to validate mathematical models

Run	Gelatin (%w/w)	Maltodextrin (%w/w)	Starch (%w/w)
16	6.0	20.0	4.0
17	9.0	19.0	2.0
18	8.3	19.7	2.0
19	7.8	20.2	2.0

The gels were prepared and their firmness, elasticity modulus (E_1, E_2, E_3) and relaxation time constants (r_1, r_2, r_3) measured. These rheological parameters were inserted as responses in the mixture design.

2.2.4. Optimization of components concentration of simulant

In order to determine the component concentration of the simulant which imitate best the textural properties of the soft cheeses, the optimization module in Design-Expert was used. The latter searches for a combination of factor levels that simultaneously satisfy the requirements placed on each of the responses and factors. Optimization of one response or the simultaneous optimization of multiple responses can be performed graphically or numerically.

The desired goal for each factor and response must be chosen. The possible goals are: maximize, minimize, target, within range, none (for responses only) and set to an exact value (factors only). A minimum and a maximum level must be provided for each parameter included. A weight can be assigned to each goal to adjust the shape of its particular desirability function. The "importance" of each goal can be changed in relation to the other goals. The default is for all goals to be equally important at a setting of 3 pluses (+++). If one goal is more important, it can be changed to 5 pluses (+++++).
The goal for firmness, r_1, E_1, E_2 and E_3 was set to 5, 4, 4, 3 and 3 pulses respectively. Firmness is the parameter which generally correlates best with its sensory descriptor. E_2 and E_3 values show greater lack of fit to the Maxwell model compared to E_1 value. Therefore their ‘importance’ was set to 3.

The goals are combined into an overall desirability function. The program seeks to maximize this function. The goal seeking begins at a random starting point and proceeds up the steepest

slope to a maximum. There may be two or more maximums because of curvature in the response surfaces and their combination into the desirability function. By starting from several points in the design space chances improve for finding the "best" local maximum. The default is 10 starting points.

2.3. Digital image correlation

2.3.1. Principle of digital image correlation

Digital image correlation method is a technique used for measuring surface displacements and strains based on the matching pixel gray level values between two digital images taken at different times in a deformation process. Two digitized images of a random speckle pattern representing the undeformed and deformed states were captured. According to the statistical principle of the correlation, deformation measurement of each pixel location on the surface can be accomplished by determining the movement of the central point of subset (small local neighborhoods are commonly referred to as subsets). The gray level of each pixel location among the subset can be read from the saved image. The measured displacement of a subset is accomplished mathematically through maximization of a normalized cross-correlation coefficient. By overlapping pixel subsets the full-field displacement information is obtained.
According to the statistical concept, the correlation coefficient is shown as follows (equation 5):

$$C = \frac{\sum f(x,y)g(x^*,y^*)}{\sqrt{\sum f^2(x,y)\sum g^2(x^*,y^*)}} \quad (5)$$

When C is equal to 1, the two subsets are fully correlative, and when C=0, the two subsets are not correlative. It can also be expressed in another formulation, which treats the unknown variables as independent parameters. The correlation factor S can be defined as (equation 6)

$$S\left(u,\frac{\partial u}{\partial x},\Lambda,\frac{\partial^2 u}{\partial x\partial y};v,\frac{\partial v}{\partial x},\Lambda,\frac{\partial^2 v}{\partial x\partial y}\right)=1-C=1-\frac{\sum f(x,y)g(x^*,y^*)}{\sqrt{\sum f^2(x,y)\sum g^2(x^*,y^*)}} \quad (6)$$

where S=0 represents a best match, and S=1 is no match.

In general, there are two methods to gain the displacement and the gradient. One is the simple searching method, which makes use of equation 5 to search for the best correlation position and calculate the corresponding displacement between the undeformed image and deformed image. By suitable post processing, the displacement fields are converted to strain fields. The other is the iterative correlation method, which is making use of equation 6 to determine not only the subset center displacements, but also rotations and strains (Chen *et al.*, 2005).

2.3.2. Optical measurements

In the system, 2 cameras (QICAM Fast 1394 CCD camera, equipped with Nikon 35-70 mm f/2.8 AF-D lenses) with aperture and exposure time set to f/5.6 and 47 ms respectively (most effective parameters chosen from preliminary experiments) and a computer were used to acquire digitized images of sample surface before, during and after deformation. Vic Snap® (version 3.0D, 2005 Correlated solutions, Inc.) software was used to capture images processed by Vic-3D® (version 3.1.0 Correlated solutions, Inc.) software. The 3D image correlation setup is indicated in figure 10.

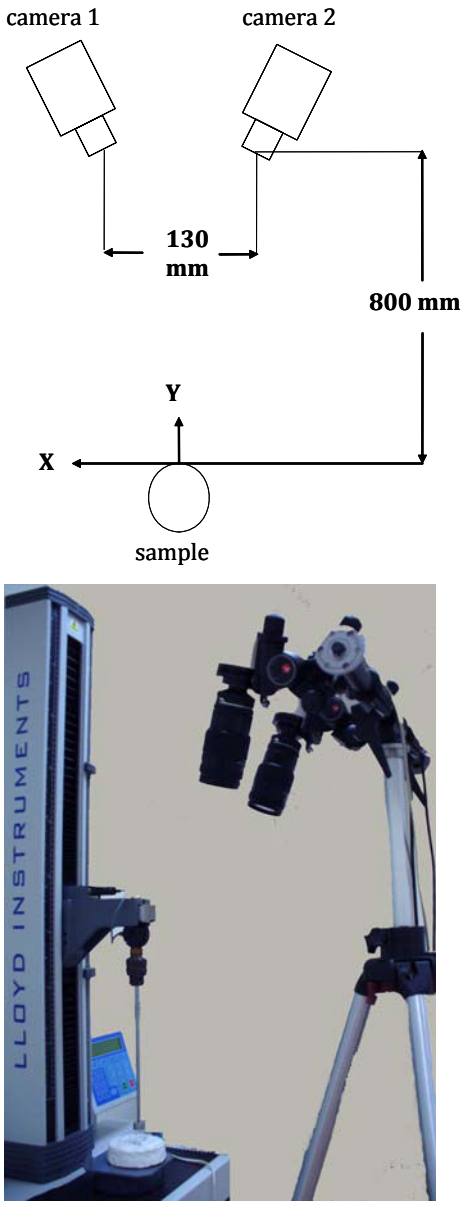

Figure 10. 3D image correlation setup

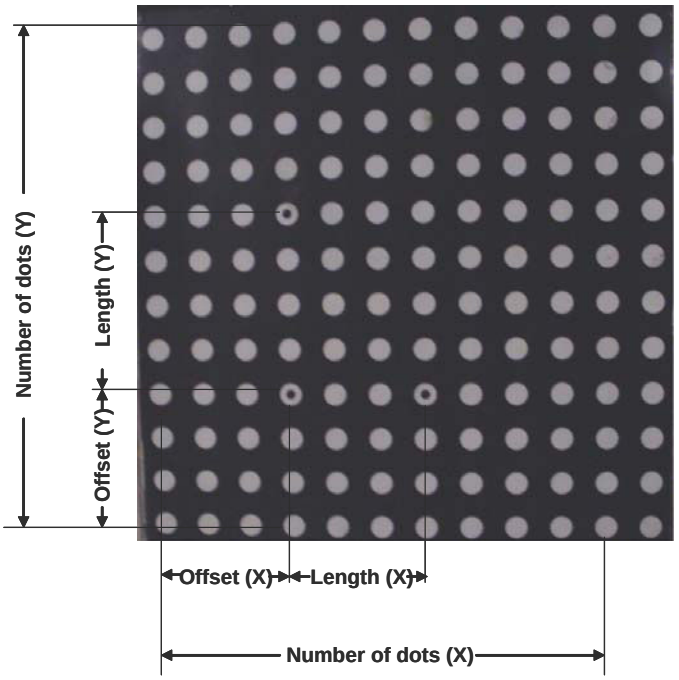

number of dots in X	12
number of dots in Y	12
offset in X	4
offset in Y	4
length in X	3
length in Y	4
grid spacing	10 mm

Figure 11: Custom calibration target

An important task in three-dimensional computer vision is camera calibration, especially when metric information is required for applications involving accurate dimensional measurements. The technique used only requires the camera to observe a (quasi planar) pattern shown at a few different orientations. The motion of the pattern need not be known and lens distortion is taken into account. The calibration of the stereo system was performed using the custom calibration target 12x12-10.0 mm (Figure 11). Ten to fifteen image positions of dots were captured and extracted from the calibration images. Once calibration was completed, a calibration report was displayed (Figure 12). The calibration report provides useful information as to the quality of the calibration. The overall standard deviation, as well as standard deviations for each grid configuration, is shown in the report.

Sample was pretreated for optical measurements by spraying a random paint (dot) pattern to its surface (Figure 13). An image was acquired of the "speckled" sample before loading. This image was regarded as the reference image. The sample was then subjected to surface deformation as load was applied. A series of images were captured during this loading. These other images showed a deformed random dot pattern relative to the initial, undeformed random dot pattern of the reference image. From the difference in the deformed images and

the reference image, a deformation plot can be calculated for each image. These deformation plots can be superimposed over the original image successively showing a deformation "movie." The correlation results are precise to ±0.02 pixels.

Camera parameters after camera calibration

Parameter	Camera 1	Camera 2
center (x)	354.253	254.676
center (y)	-121.497	-288.665
Focal length (x)	6922.75	7076.63
Focal length (y)	6782.55	6921.04

Starting global optimization... Calibration done after 0.078 seconds.

Camera parameters after global optimization:

Parameter	Camera 1	Camera 2
center (x)	382.878	343.652
center (y)	277.155	240.949
Focal length (x)	6818.18	6809.51
Focal length (y)	6818.18	6809.51
Skew	0	0
kappa 1	0.129024	0.140767

Standard deviation of residuals for all views: 0.0172366

Standard deviations for individual views:

Image File	Camera 1 (pixels)	Camera 2 (pixels)
calibration-000_0.tif	0.0168421	0.0145124
calibration-001_0.tif	0.0150400	0.0133253
calibration-002_0.tif	0.0148065	0.0123231
calibration-003_0.tif	0.0186287	0.0167001
calibration-004_0.tif	0.0181806	0.0175873
calibration-005_0.tif	0.0175187	0.0136993
calibration-006_0.tif	0.0145109	0.0129074
calibration-007_0.tif	0.0161506	0.0129573
calibration-008_0.tif	0.0249744	0.0292059
calibration-010_0.tif	0.0209835	0.0165838
calibration-011_0.tif	0.0151077	0.0162585
calibration-012_0.tif	0.0178037	0.0175832

Figure 12. Typical calibration results

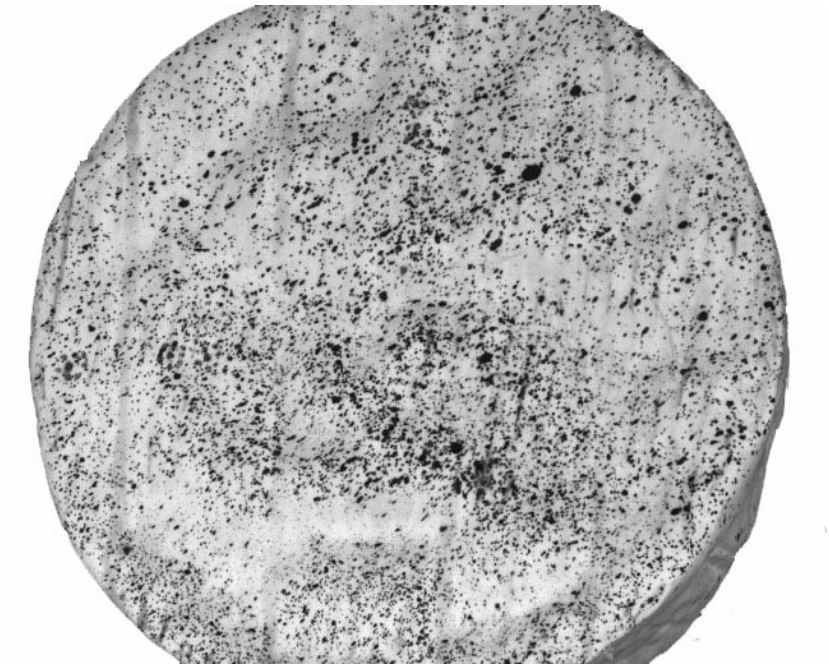

Figure 13: Image of "speckled" Camembert cheese before loading

In order to carry out the correlation, an area of interest of the undeformed image should be chosen. This area, relative to the probe position is indicated in figure 14. In order to ensure that the same area was selected (especially the radial distance from probe, Y) from one sample to another, 'reference dots' which could be identified were marked on the sample. It is also worth pointing out that the area of interest should not contain any of the probe image itself because the probe is not continuous with the speckled pattern and surface of interest and it may corrupt the results in unexpected ways.

Moreover, before selecting an area of the reference image for correlation, subset and step size should be selected (Figure 14). The subset size controls the area of the image that is used to track the displacement between images (The method of digital image correlation can directly measure the transformation by tracking the gray value pattern inside the subsets). The subset size has to be large enough to ensure that there is a sufficiently distinctive pattern contained in the area used for correlation. In general, when the number of the pixels in the subset is increased, the random error of each correlation function will be decreased. However, it is not true that the larger the subset is, the better the measurement precision is. If the subset size is too large, the calculating speed will be very slow, and the cutting error of the correlation

function will be increased (Chen *et al.*, 2005). In our case, a subset size of 19 pixels was selected. This subset size allowed image analysis as close as about 1 mm from the edge of the probe. Reducing the subset size enables image analysis closer to the probe edge. However, using a smaller subset size does have the effect of increasing noise and in some cases even corrupted our results.

The step size controls the spacing of the points that are analyzed during correlation. If a step size of 1 pixel is chosen, a correlation analysis is performed at every pixel inside the area of interest. A step size of 5 pixels was chosen in our case, which means that a correlation was carried out at every 5 other pixels in both the horizontal and vertical direction. Reducing the step size increased calculating speed and did not improve accuracy.

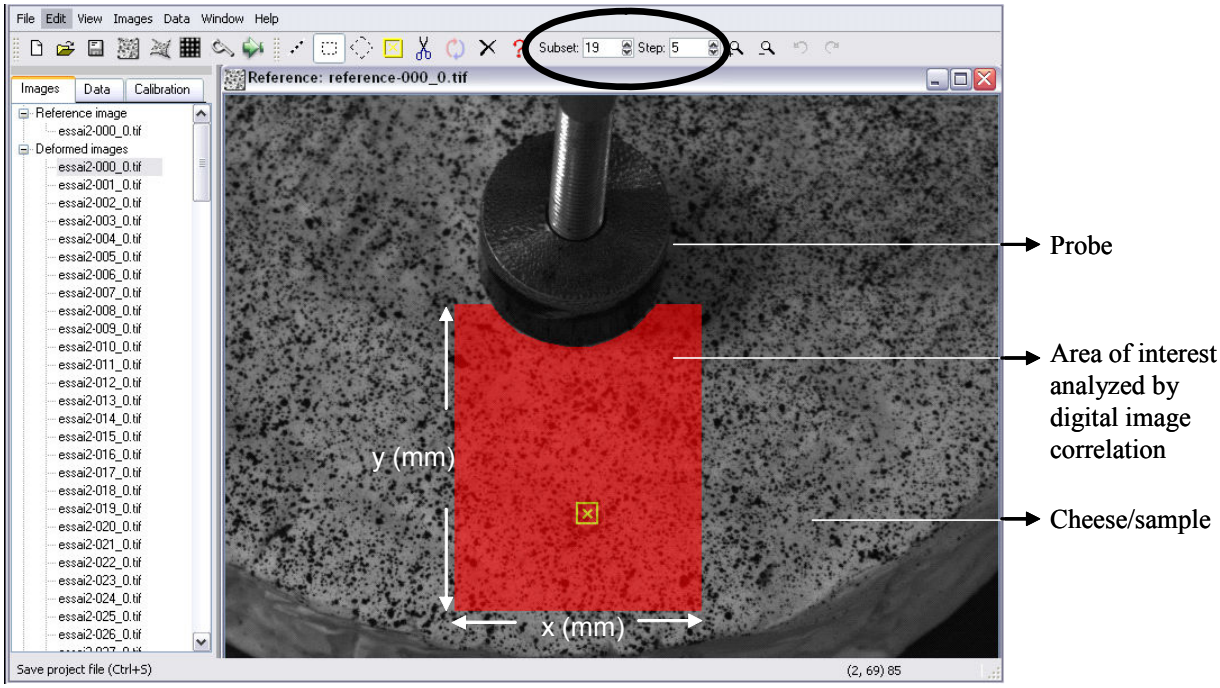

Figure 14. Area of interest analyzed by DIC relative to probe position

Six and three replicates of each cheese and simulants respectively were subjected to two different penetrometry tests. The first one consisted in studying the surface displacement profile of sample when a 20 mm-diameter flat-bottomed cylindrical probe was inserted into

samples, 25 mm from sample border, at crosshead speed of 10 mm/min to a depth of 4 mm. One image was taken every second during 30 seconds.

The other test was carried out in order to determine time-dependant parameters relating to the viscoelastic behavior of sample when the latter was subjected to constant loading for a given period of time. This test will be referred to as 'stress-controlled test'. A load of 3 N was applied to the sample, with a 20 mm-diameter flat-bottomed cylindrical probe at a crosshead speed of 50 mm/min and held constant. The load was removed at a rate of 50 mm/min. One image was acquired every second during 22 minutes. Preliminary experiments were carried out in order to choose the applied load. Ten persons were asked one by one to deform a Coulommiers cheese, placed on a weighing balance, with their index finger, just as they would if they wanted to evaluate its 'firmness'. The weight applied was noted for each person and was found to range from 200 to 1000g (2 to 10N). 3N was found suitable in order to avoid rupture of cheese crust during the time dependant test and sufficient to distinguish between samples texture. Indeed from the point of view of the image correlation process, a local failure produced a new feature not present in the reference image. If enough feature remained near the local failure, then the image correlation continued. If not, the analysis began to fail. Visible crust rupture corrupted results analysis.

Firmness, as well as viscoelastic parameters such as relaxation time constants and elastic modulus of the three-parameter Maxwell model, was also determined. Details of tests procedures are given in 'Materials and methods' section, paragraph entitled 'Instrumental characterization of textural properties'. These rheological parameters were assayed in an attempt to determine possible correlation between these data and parameters obtained by the digital image correlation method.

2.3.3. Data analysis and construction of mathematical models

The surface displacement curves (displacement of samples in Z direction under load as a function of radial distance from probe edge), obtained from penetrometry test were fitted to equation 7 using non linear regression analysis (SigmaPlot for Windows version 6.10, 2000).

Z values were however converted into positive values before fitting was done in order to simplify the fitting equation 7.

$$Z(mm) = Z_0 + a \times \exp(-bY)\,, \qquad (7)$$

where *Z* (*mm*) is the sample displacement in *Z* direction. *Z* will also be referred to as 'surface depression' in following discussions. *Y* (*mm*) is the radial distance from probe. Z_0, *a* and *b* are fitting parameters. Z_0 is the value to which the surface displacement will tend to when *Y* value is very large. Strictly speaking, Z_0 should actually be equal to zero when *Y* tends to infinity. In other words, Z_0 should be removed from equation 7. However, in our case, measurements were done up to only 20 mm from the probe. Therefore, the equation used to predict surface depression profile of sample should contain Z_0 in order to reduce variability between predicted and actual *Z* values.

In order to determine whether any of the fitting parameters Z_0, *a* or *b* of equation 7 could be affected by changes in rheological parameters of the samples, correlation between firmness, relaxation time constant and elastic modulus of the first term of the Maxwell model and these fitting parameters was done. The relaxation time constants of the first, second and third elements (r_1, r_2, r_3) of the three-parameter Maxwell model are interdependent. The same remark applies for the elasticity modulus of the three elements (E_1, E_2, E_3). Inserting the relaxation time constants and elasticity modulus of the three elements into the mathematical models relating rheological parameters and fitting parameters Z_0, *a* or *b* would lead to serious autocorrelation between variables. Therefore, only the first element of the Maxwell model (hence r_1 and E_1) were used as viscoelastic variables.

Mathematical models of the surface displacements of sample according to its textural properties were constructed using multiple regression analysis (Statgraphics Plus for Windows 2.1-trial version). A backward stepwise regression was chosen as mathematical model for deciding which variables were to be included in the regression equations. Initially, development of the mathematical models relied on data (firmness, relaxation time constants, elastic modulus and Z_0, *a* and *b* fitting parameters) obtained from 4 mm depth penetrometry test. These models were then checked on data from 2 and 3 mm depth penetrometry tests.

2.4. Topometric three-dimensional (3D) scanning system

2.4.1. Principle of topometric 3D scanning system

The topometric Breuckmann Opto-TOP HE digitization system is a rapid 3D white light scanning method that uses fringe projection technology to provide a fast and extensive capture of complex surfaces. This approach allows the simultaneous measurement of a large portion of the object in a single view. Over a million points are acquired in less than one second. Table 8 shows some measurement specifications of the Breuckmann scanning system.

Table 8. Measurement specifications of the Breuckmann scanning system

light source	***100 W halogen lamp***
number of projected fringes	128
min. measuring time	980 ms
sensor weight	2 - 3 kg
digitization (x,y)	1380 x 1036 pixel
size of measuring range	about 0.8 x 0.6 of image diagonal
depth of measuring volume	typically 1 / 2 of image diagonal
X,Y resolution	typically 1 / 1.500 of image diagonal
feature accuracy	typically 1 / 15.000 of image diagonal
noise (Z)	typically 1 / 20.000 of image diagonal

specifications of typical fields of view						
image diagonal*	[mm]	50	100	200	400	800
X,Y resolution*	[µm]	30	60	120	240	480
resolution limit (Z)*	[µm]	1	2	4	8	16
noise (Z)*	[µm]	± 5	± 7	± 10	± 20	± 40
feature accuracy*	[µm]	± 7	± 10	± 15	± 30	± 60

Patterns of well defined periodic fringes are projected onto the sample in rapid sequence (Figure 15). The digital camera records these patterns. At first, images of gray code, phase shift and contrast are generated. Secondly, 3D point clouds or polygon meshes are derived from these to describe the surface geometry.

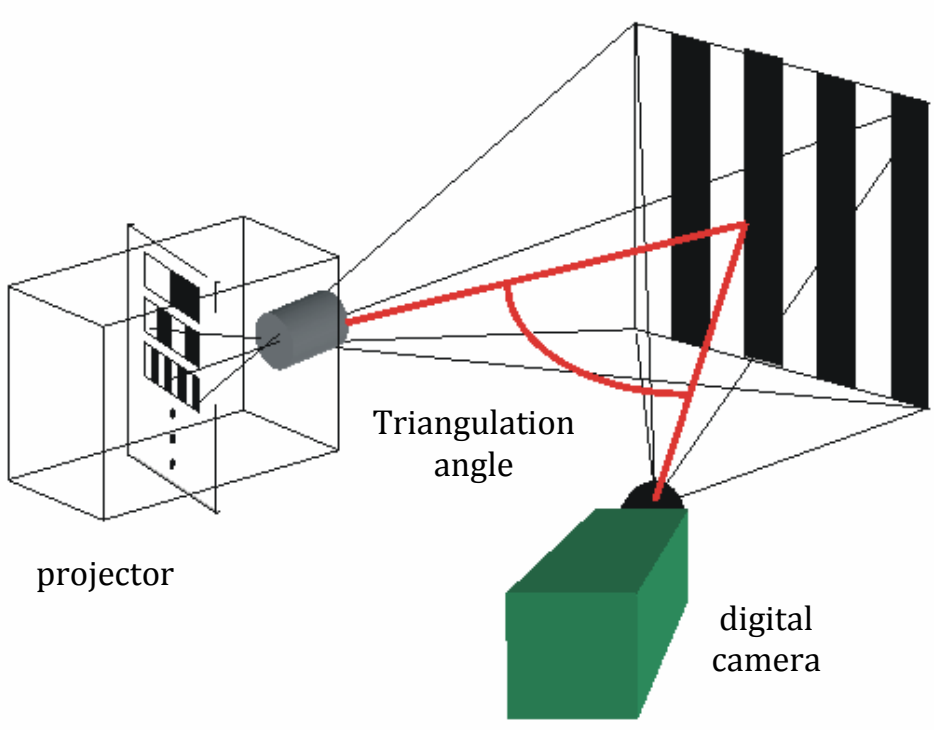

Figure 15. Measuring principle of the Breuckamnn Opto-TOP HE digitization system

2.4.2. Optical measurements

In the system, the digitizing unit comprises a high resolution digital camera (PixelLINK PL-A633) and a projection unit of 128 fringes and a 100W halogen lamp. These units are mounted on either end of a carbon fiber sensor bar (Figure 16).

Figure 16. Digitizing unit of Breuckmann Opto-TOP HE

The sensor bar also contains a laser positioning guide to define the center of the optimal measuring depth of field. The system is configured with a computer and the OPTOCAT software acquired images while controlling the aperture and exposure time of the camera.

Calibration of the system was performed using a calibration plate (Figure 17). The idea of the calibration process is to create a calculation path that allows one to determine real (*x,y,z*) Cartesian coordinates. The calibration process creates a matrix on the basis of measurement of the known geometrical model (calibration plate). Then the 3D coordinates can be easily calculated from the real object measurement using the calibration matrix (Sitnik *et al.*, 2002). About 10 images of the calibration plate were captured at varying distances from the sensor.

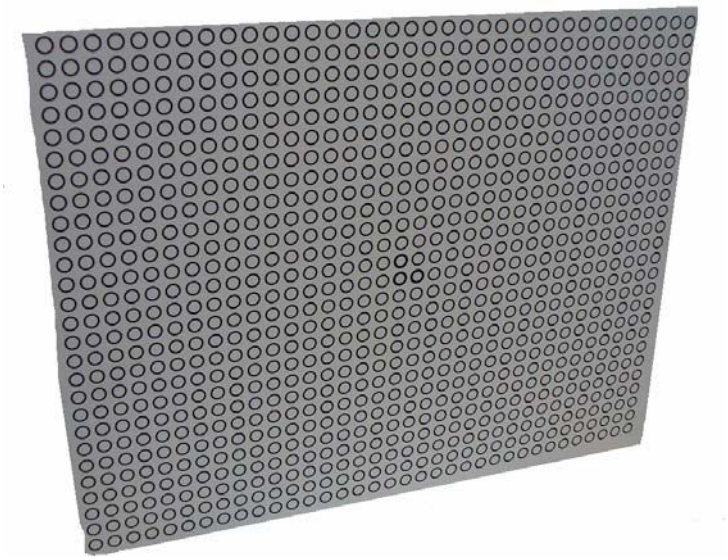

Figure 17. Breuckmann Opto-TOP HE calibration plate

In order to digitize a whole sample, multiple views are captured. The cloud of points is analyzed and processed by GEOMAGIC-Studio 8 software. Post processing of the cloud of points is then carried out using OptoCAT 3D-Post-Processing software, to merge different views of the sample. The Breuckmann Opto-TOP HE 3D digitization system was coupled with the Llyod universal testing machine and the system setup is indicated in figure 18. Samples were subjected to penetrometry test, where a 20 mm-diameter flat-bottomed cylindrical probe was inserted into samples; 25 mm from sample border, at crosshead speed of 200 mm/min to a depth of 4 mm. Constant deformation was maintained during 30 minutes in order to allow views of sample before and during loading to be captured. The surface displacement of the deformed sample was determined by aligning the undeformed (reference) 3D image of the sample with the deformed one. The images were aligned with an accuracy of about 0.03 mm (sample holder)

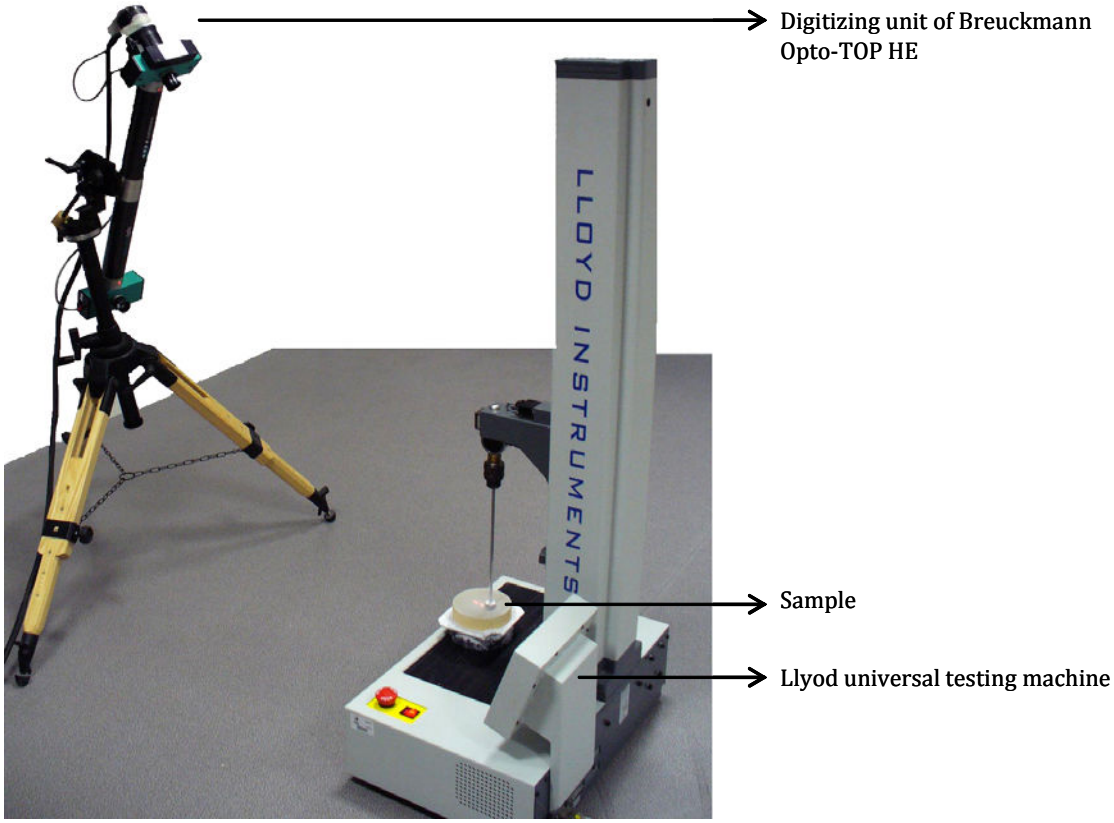

Figure 18. Breuckmann Opto-TOP HE 3D digitization system setup

CHAPTER III: RESULTS AND DISCUSSION

PART I: FORMULATING POLYMERIC GELS SIMULATING SOFT CHEESE TEXTURE

Four polymeric gels were formulated from gelatin and polysaccharides which were added to the protein to modify its rheological parameters so as to approach that of 10-day-old Camembert and Coulommiers cheese.

Components concentration of the gel imitating best the texture of the soft cheeses was then adjusted through a mixture design experiment. Effect of matrix composition on gel model texture was also investigated.

1. INSTRUMENTAL CHARACTERIZATION OF TEXTURAL PROPERTIES

1.1. Firmness

Firmness was determined from force-displacement curve of penetrometry test (Figure 8) and was considered as the force required to insert probe to a depth of 10 mm into samples. Figure 19 shows firmness of cheeses and gel models.

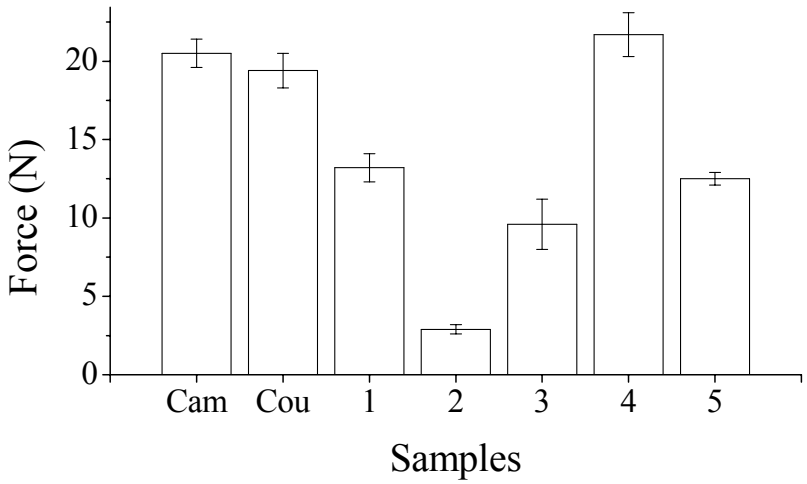

Figure 19. Firmness of 10-day-old Camembert (Cam); 10-day-old-Coulommiers (Cou); *6%w/w* gelatin gel (1); gelatin-guar gel, *6/1, %w/w* (2); gelatin-karaya gel, *6/3, %w/w* (3), gelatin-xanthan gel, *6/3, %w/w* (4) and gelatin-maltodextrin-starch gel, *6/20/3, %w/w* (5) determined from force displacement curves. Error bars indicate standard deviation calculated from 6 and 3 repetitions for cheeses and gels, respectively.

The firmness of gelatin gels changed ($P < 0.05$) when guar, karaya or xanthan gum was added to the protein. Guar and karaya induced a decrease in gelatin firmness and xanthan increased gelatin firmness. The firmness of Camembert and Coulommiers was different ($P < 0.05$) from that of the gel models, except for gel 4 (gelatin-xanthan) which was not significantly different from Coulommiers cheese firmness.

1.2. Three-parameter Maxwell model

Stress relaxation test is most commonly used to study the viscoelastic behavior of cheese (Gunasekaran and Ak, 2003; Subramanian *et al.*, 2006) and gels (Fiszman *et al.*, 1998). Elastic components, E_1, E_2, E_3 (kPa) and relaxation time, r_1, r_2, r_3 (s) were determined by fitting stress relaxation curves to a three-parameter Maxwell model (Figure 20) represented by equation 8.

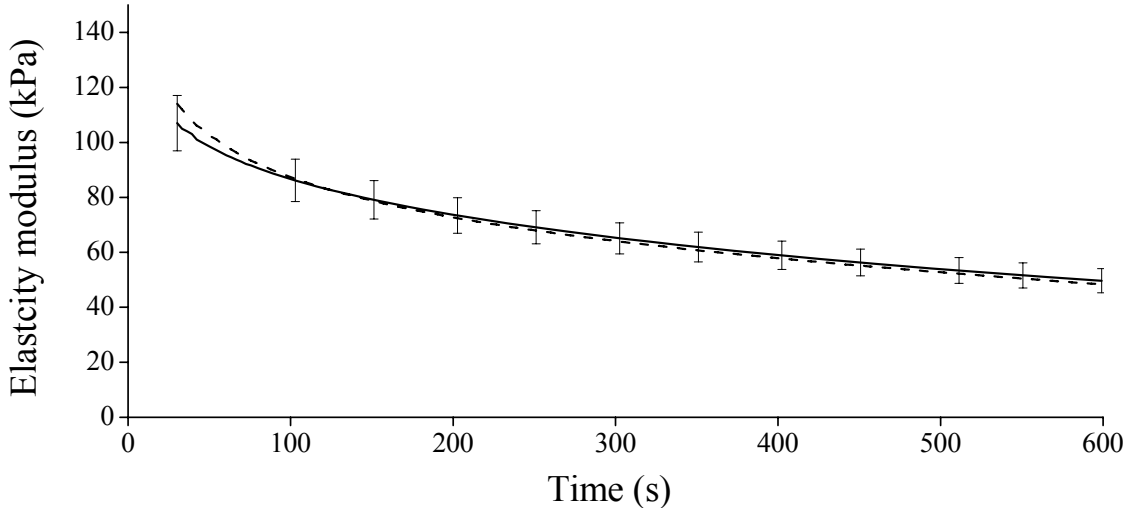

Figure 20. Experimental data (—) and three-parameter Maxwell fitted curve (- - -) for stress relaxation of 10-day-old Coulommiers. R^2 is equal to 0.9998. Maxwell model curve was plotted using equation 8. Error bars indicate standard deviation calculated from 6 repetitions of Coulommiers cheese.

$$\sigma/\varepsilon = E_1 \exp(-t/r_1) + E_2 \exp(-t/r_2) + E_3 \exp(-t/r_3), \qquad (8)$$

where σ (kPa) is the stress, ε is the natural strain, t (s) is the time of applied deformation, E_1, E_2, E_3 are, respectively, the elasticity modulus of the first, second and third element of Maxwell model and r_1, r_2 and r_3 are, respectively, the relaxation time constant of the first, second and third element of Maxwell model. The results obtained showed more than 99 % correlation between experimental and theoretical stress relaxation curves of cheeses and gels models. When the stress relaxation curve was fitted to a two or one-parameter Maxwell model, respectively, 99 and 95 % correlation were obtained between experimental and theoretical values. Maxwell model has previously been found to be successful at modeling the stress relaxation behavior of Camembert (Mpagana and Hardy, 1985), Cheddar cheese (Hort and Le Grys, 2001), and Reggianito Argentino (Bertola *et al.*, 1995). Although other mathematical models namely the Nussinovich and Peleg models have been used to describe the viscoelastic properties of biological materials, they were found to be less accurate in predicting experimental data, compared to the Maxwell model (Hassan *et al.*, 2005).

Figure 21 shows the elastic modulus of samples. Addition of guar and karaya to gelatin decreased ($P < 0.05$) the E_1 value, while xanthan increased ($P < 0.05$) the E_1 value of gelatin. Xanthan, maltodextrin and starch increased ($P < 0.05$) the E_2 value of gelatin. All polysaccharides increased the E_3 value of gelatin. Moreover, E_2 and E_3 values of simulants were smaller ($P < 0.05$) than that of the cheeses. The E_1 value of cheeses and simulants was higher than that of E_2 and E_3, reflecting greater elasticity associated with the first element of the Maxwell model. It can also be noted that E_1, E_2 and E_3 values of Camembert were greater ($P < 0.05$) than that of Coulommiers. This is because fat content in Camembert is lower than in Coulommiers cheese (3%) and a reduction in fat content is generally paralleled by an increase in elasticity modulus (Guinee and Law, 2002).

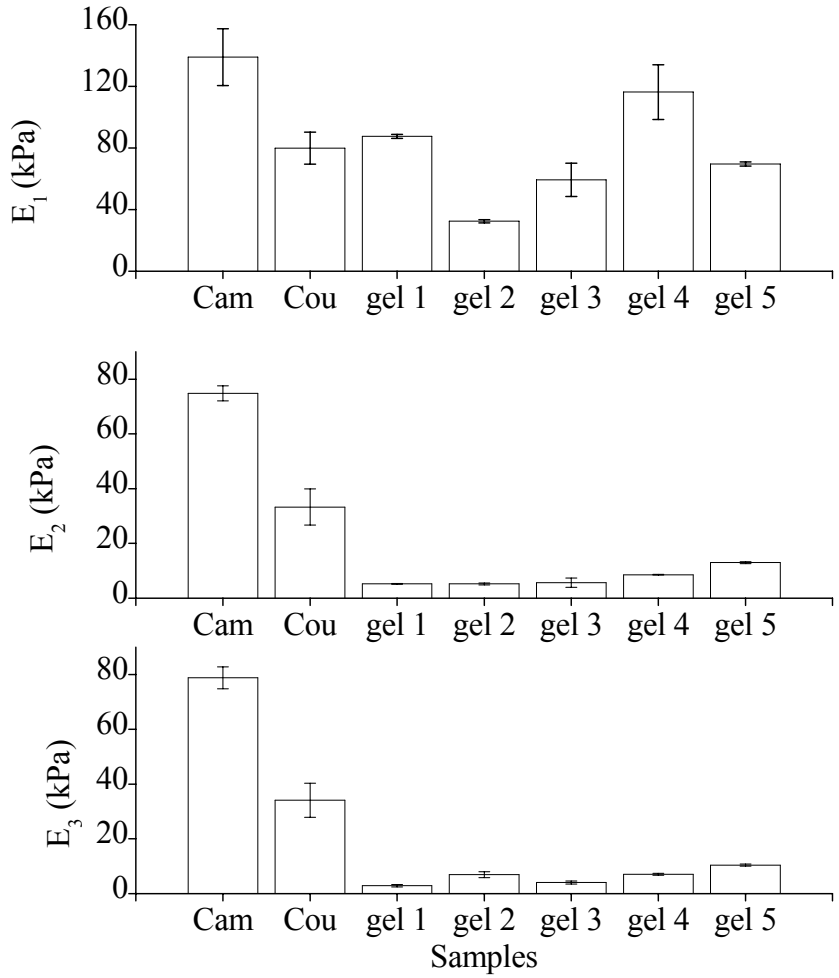

Figure 21. Elastic modulus (E_1, E_2, E_3) of 10-day-old Camembert (Cam), 10-day-old Coulommiers (Cou), gelatin gel, *6/1, %w/w* (1), gelatin-guar gel, *6/3, %w/w* (2), gelatin-karaya gel, *6/3, %w/w* (3), gelatin-xanthan gel, *6/3, %w/w* (4) and gelatin-maltodextrin-starch gel, *6/20/3, %w/w* (5) determined by fitting stress relaxation curves to a three-parameter Maxwell model. Error bars indicate standard deviation calculated from 6 and 3 repetitions for cheeses and gels, respectively.

Figure 22 shows the relaxation time values of samples. Guar, maltodextrin and starch decreased ($P < 0.05$) the r_1 value of gelatin. Moreover, the r_1 value of all simulants was greater ($P < 0.05$) than that of Camembert and Coulommiers, except for gel 5, whose r_1 was not significantly different from that of Camembert. It was also noted that r_2 and r_3 value of gelatin did not vary significantly upon addition of the polysaccharides and that r_2 and r_3 values of both cheeses were not significantly different from that of the simulants. It is worth pointing out that r_1 accounted for nearly 90 and 98 % of overall relaxation time of the three-parameter Maxwell model for cheeses and gels, respectively.

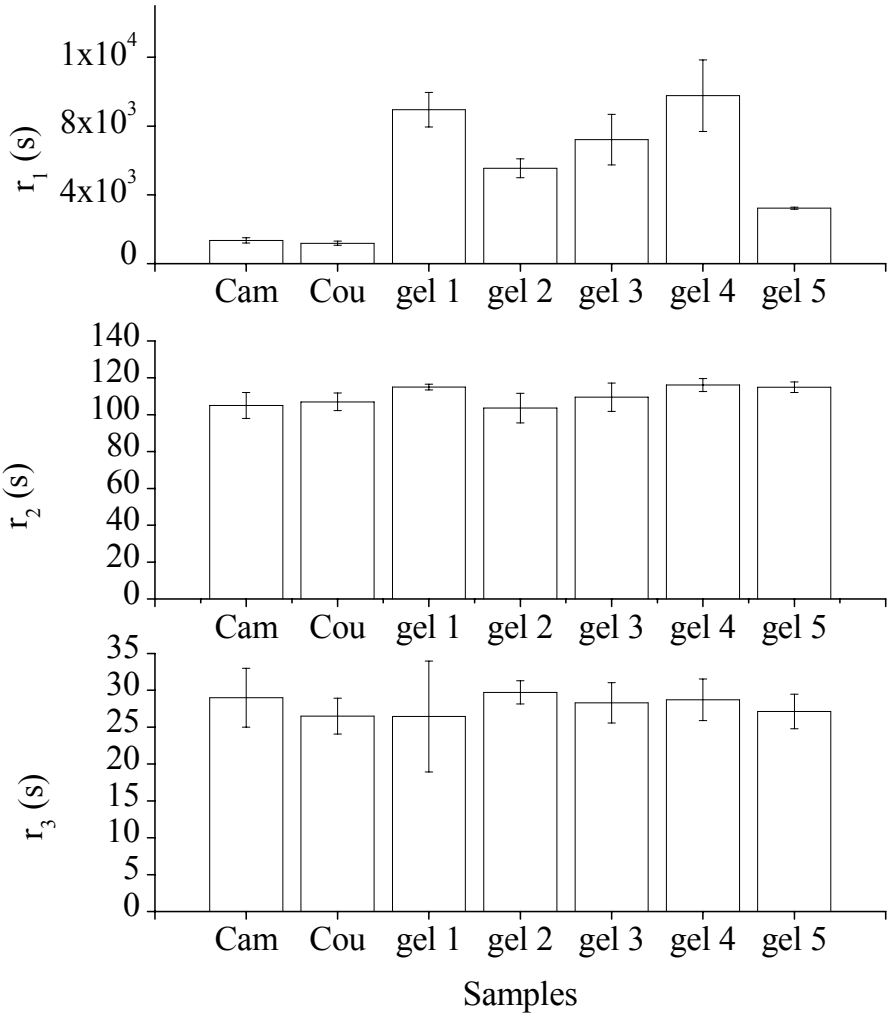

Figure 22. Relaxation time (r_1, r_2, r_3) 10-day-old Camembert (Cam), 10-day-old Coulommiers (Cou), gelatin gel, *6/1, %w/w* (1), gelatin-guar gel, *6/3, %w/w* (2), gelatin-karaya gel, *6/3, %w/w* (3), gelatin-xanthan gel, *6/3, %w/w* (4) and gelatin-maltodextrin-starch gel, *6/20/3, %w/w* (5) determined by fitting stress relaxation curves to a three-parameter Maxwell model. Error bars indicate standard deviation calculated from 6 and 3 repetitions for cheeses and gels, respectively.

The decrease in firmness, E_1 and r_1 of gelatin induced by guar and karaya could be related to imperfections in the gelatin gel network caused by the two polysaccharides. The presence of guar and karaya might have rendered gelatin gels weaker, with fewer interconnections in the structure. On the contrary, when xanthan was combined with gelatin, firmness, E_1 and r_1 increased, probably due to a synergic effect between gelatin and xanthan. Another example of such effect can be obtained when locust bean gum is added to xanthan. Long galactomannan molecules attached to xanthan actually link and reinforce the xanthan gel network (Urlacher and Dalbe, 1992).

Basically, gels made up of gelatin only could not imitate textural properties of Camembert and Coulommiers. Although its concentration can be varied in order to adjust gel firmness and elastic modulus to match more or less those of cheeses, its relaxation time constant r_1 remained significantly greater than that of cheeses. Among the polysaccharides studied, it was found that maltodextrin significantly decreased the r_1 value of gelatin, while firmness and E_1 remained unchanged. Gels made up of gelatin, maltodextrin, and starch imitated best the 'global textural properties' (relaxation time, elastic modulus and firmness) of cheese.

Figure 23 shows a vertical hierarchical tree plot, where distance linkage was calculated using the Ward's method, that is a hierarchical cluster procedure that calculates the distance between two clusters as the sum of squares between the two clusters summed over all the variables (Ward, 1963). Distances between the samples are expressed as Euclidean distances. This option uses the square root of the sum of the squared distances between observations. Euclidean distance measures the length of a straight line drawn between two objects; it is the most commonly used distance measurement.

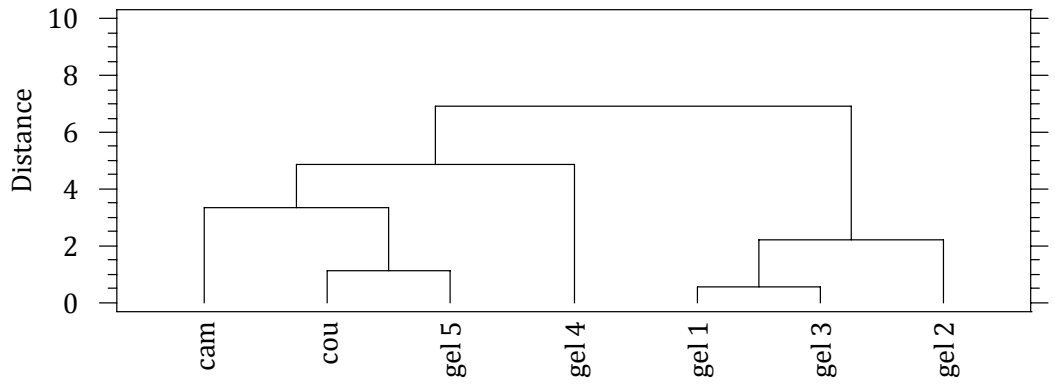

Figure 23. Vertical hierarchical tree plot where distance linkage was calculated using Ward's method. The tree was constructed from r_1 relaxation time, elastic modulus and firmness data 10-day-old Camembert (Cam), 10-day-old Coulommiers (Cou), gelatin gel, *6/1, %w/w* (gel 1), gelatin-guar gel, *6/3, %w/w* (gel 2), gelatin-karaya gel, *6/3, %w/w* (gel 3), gelatin-xanthan gel, *6/3, %w/w* (gel 4) and gelatin-maltodextrin-starch gel, *6/20/3, %w/w* (gel 5) simulants.

The tree was constructed from relaxation time, elastic modulus, and firmness data of simulants and cheeses. It can be inferred that among the five gels studied, the one made from

gelatin, maltodextrin, and starch had the closest value of firmness, relaxation time, and elastic modulus to 10-day-old Coulommiers. From those results, it was concluded that a synthetic cheese could be formulated from gelatin, maltodextrin and starch. A mixture design was then used to determine the effect of each component on relaxation time, elastic modulus and firmness of gel 5 (gelatin, maltodextrin and starch, *6/20/3, %w/w*) and also to find the optimum component concentration of that gel, so that it would match more closely Coulommiers and Camembert textural properties.

2. EFFECT OF EACH COMPONENT ON FIRMNESS, RELAXATION TIMES AND ELASTIC MODULUS

The results obtained from the mixture design indicated that the effect of each component on firmness, r_1, E_1, E_2 and E_3 could be explained by linear equations 9 to 13, respectively:

$$Firmness(N) = 4.10\times10^{2} X_{gelatin} - 7.57\times10^{1} X_{maltodextrin} + 3.89\times10^{1} X_{starch} \quad (9)$$

$$r_1(s) = 6.43\times10^{4} X_{gelatin} - 2.33\times10^{4} X_{maltodextrin} + 1.42\times10^{5} X_{starch} \quad (10)$$

$$E_1(kPa) = 2.58\times10^{3} X_{gelatin} - 5.59\times10^{2} X_{maltodextrin} + 6.38\times10^{2} X_{starch} \quad (11)$$

$$E_2(kPa) = 2.62\times10^{2} X_{gelatin} + 2.02\times10^{1} X_{maltodextrin} - 2.99\times10^{2} X_{starch} \quad (12)$$

$$E_3(kPa) = 2.14\times10^{2} X_{gelatin} + 2.51 X_{maltodextrin} - 1.66\times10^{2} X_{starch} \quad (13)$$

where $X_{gelatin}$, $X_{maltodextrin}$ and X_{starch} is the actual gelatin, maltodextrin and starch concentrations varying from 0.05 to 0.1, 0.16 to 0.23 and 0.02 to 0.04, respectively. Stanley (1999) reported that when mathematical models are developed to predict properties for any change in structure (for example those induced by a change in formulation), a linear dependence of a property on composition is to be expected in the case of mixed gels or alloys. Non-linearity in structure-property relationships of gels arise largely because of the architecture at the microstructural level (for example, composites or cellular gels).

r_2 and r_3 were regarded as slack variables, which implies that there was no significant change in r_2 and r_3 values when component concentrations varied, and it was already mentioned above that r_2 and r_3 did not change significantly upon the addition of different gelling agents

to gelatin. The mean values of r_2 and r_3 were equal to 118 and 28 s, respectively. Relaxation time, r_1, of the first element of the three-parameter Maxwell model contributed to more than 90 % of the total relaxation time. The validity of the mathematical models suggested by the mixture design to predict firmness, r_1, E_1, E_2 and E_3 of polymer gels studied was checked by four additional gels (with composition different from that of gels used in the mixture design). The R^2 statistic obtained indicated that the mathematical models explained respectively, 98%, 95%, 90%, 97% and 97 % of the variability in firmness, r_1, E_1, E_2 and E_3 (Figure 24).

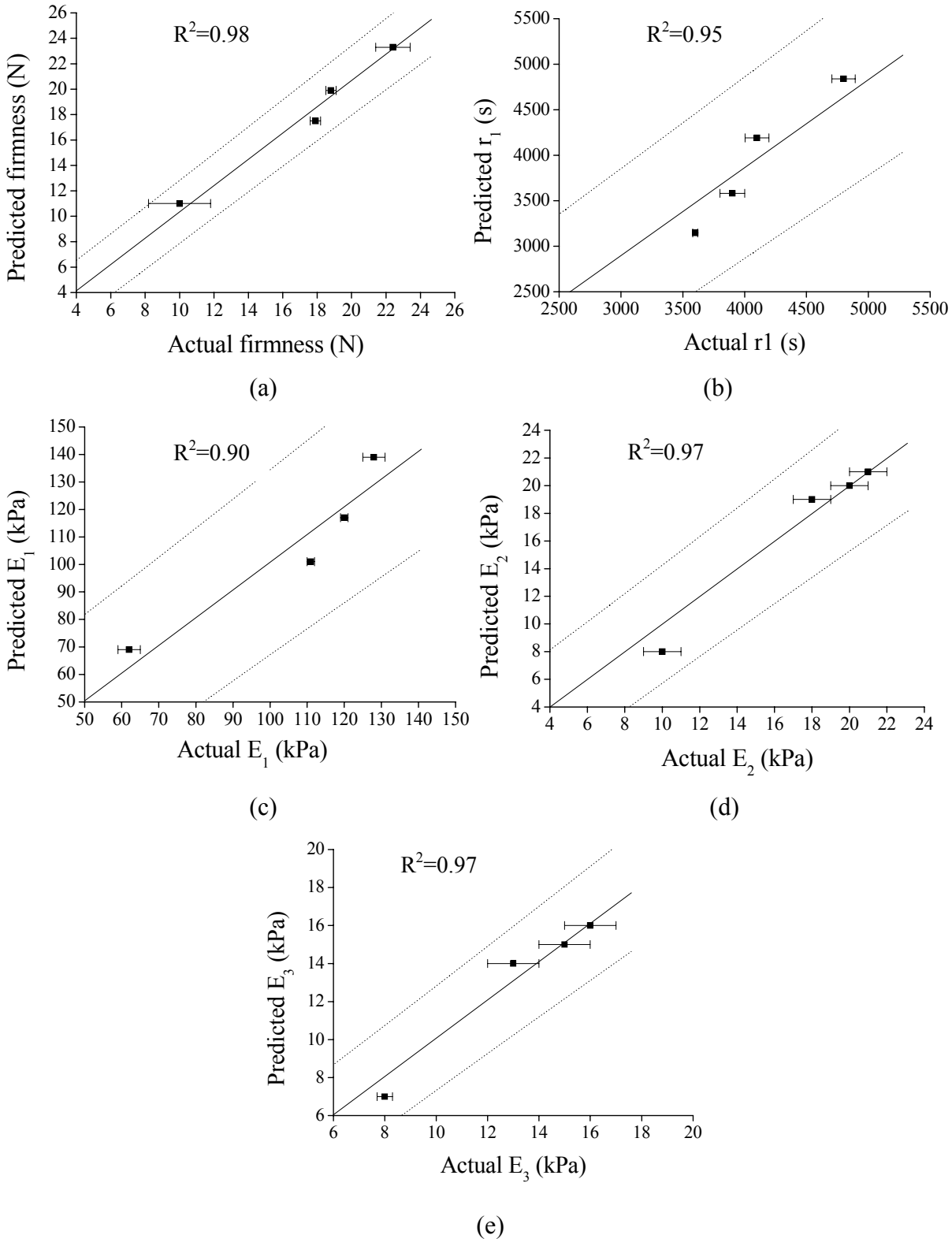

Figure 24. Correlation between actual and predicted data for firmness (a), r_1 (b), E_1 (c), E_2 (d) and E_3 (e). Predicted data for firmness, r_1, E_1, E_2 and E_3 were calculated from equation 9, 10, 11, 12 and 13, respectively. Linear fit is represented by solid line (—) and the upper and lower 95% confidence limits are shown by dotted lines (·····).

Figures 25 to 27 show, respectively, trace plots for firmness, r_1, E_1, E_2 and E_3 of gels.

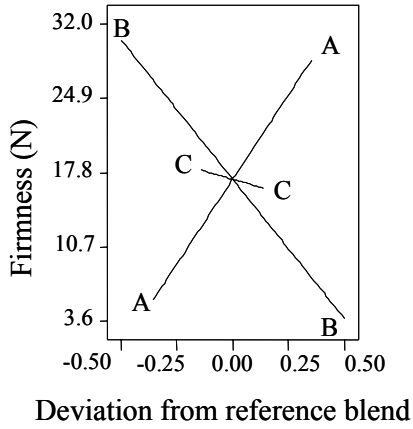

Figure 25. Trace plot for firmness (N) of gels obtained in the centre of the experimental design (A=gelatin, B=maltodextrin, C=starch).

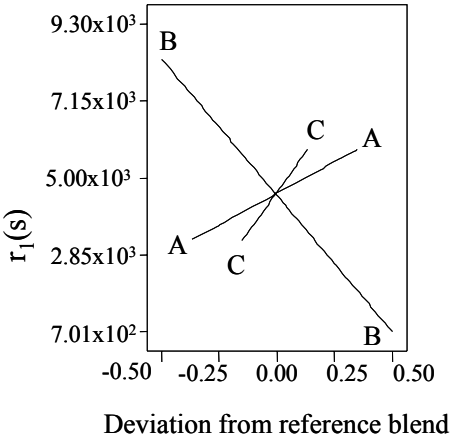

Figure 26. Trace plot for r_1 (s) of gels obtained in the centre of the experimental design (A=gelatin, B=maltodextrin, C=starch). r_2 and r_3 are slack variables and they cannot be represented by means of trace plots.

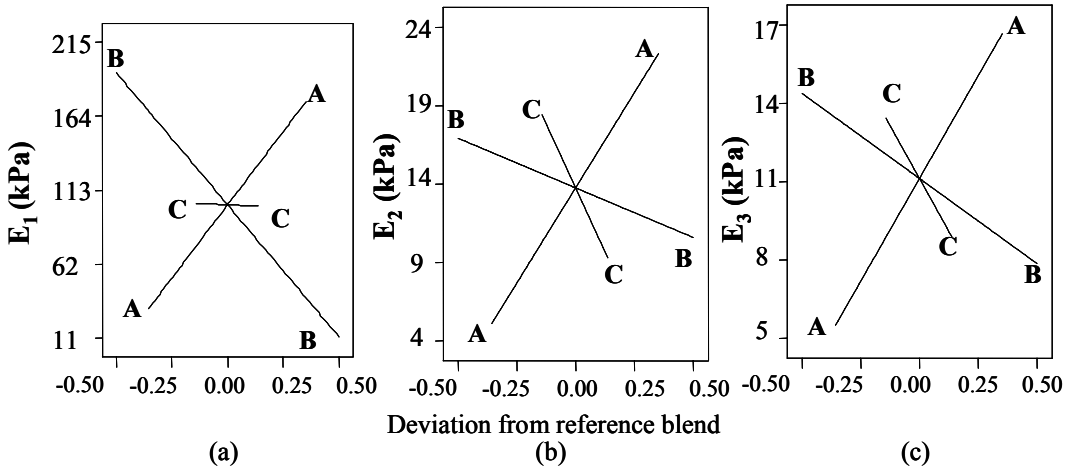

Figure 27. Trace plot for E_1 (a), E_2 (b) and E_3 (c) of gels obtained in the centre of the experimental design (A=gelatin, B=maltodextrin, C=starch).

Since r_2 and r_3 are slack variables, they cannot be represented by means of trace plots. The effects of the three components in the design space can be compared by means of these trace plots. They illustrate the impact of changing each mixture component while holding the two other constituents in a constant ratio. The response is drawn while moving along an imaginary line from a reference blend to the vertex of the component that is being increased. The reference blend is the centroid of the design, that is gelatin, maltodextrin and starch have pseudo values of 0.357, 0.5 and 0.143 respectively. As the amount of one component increases, the amount of the two other components decreases, but their ratio to one another remains constant. The trace plots have been constructed using Piepel's direction, that is, the scales are given in pseudo units (the actual values of the components which represent the weight percentage of the different constituents are normalized so that the components vary between 0 and 1 (Depypere *et al.*, 2003). Figures 28 to 30 show respectively the change in firmness, r_1, E_1, E_2 and E_3 when maltodextrin was gradually replaced by starch in gels with constant gelatin content. The values for firmness, r_1, E_1, E_2 and E_3 were calculated using the linear model equations.

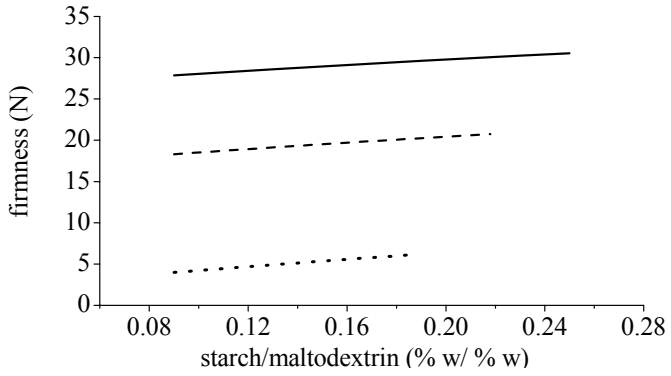

Figure 28. Modelization of change in gel firmness (N) as a function of starch/maltodextrin ratio (% w/%w) at 5 (···), 8 (– – –), 10 (—) % w of gelatin. Values of firmness are calculated from equation 9.

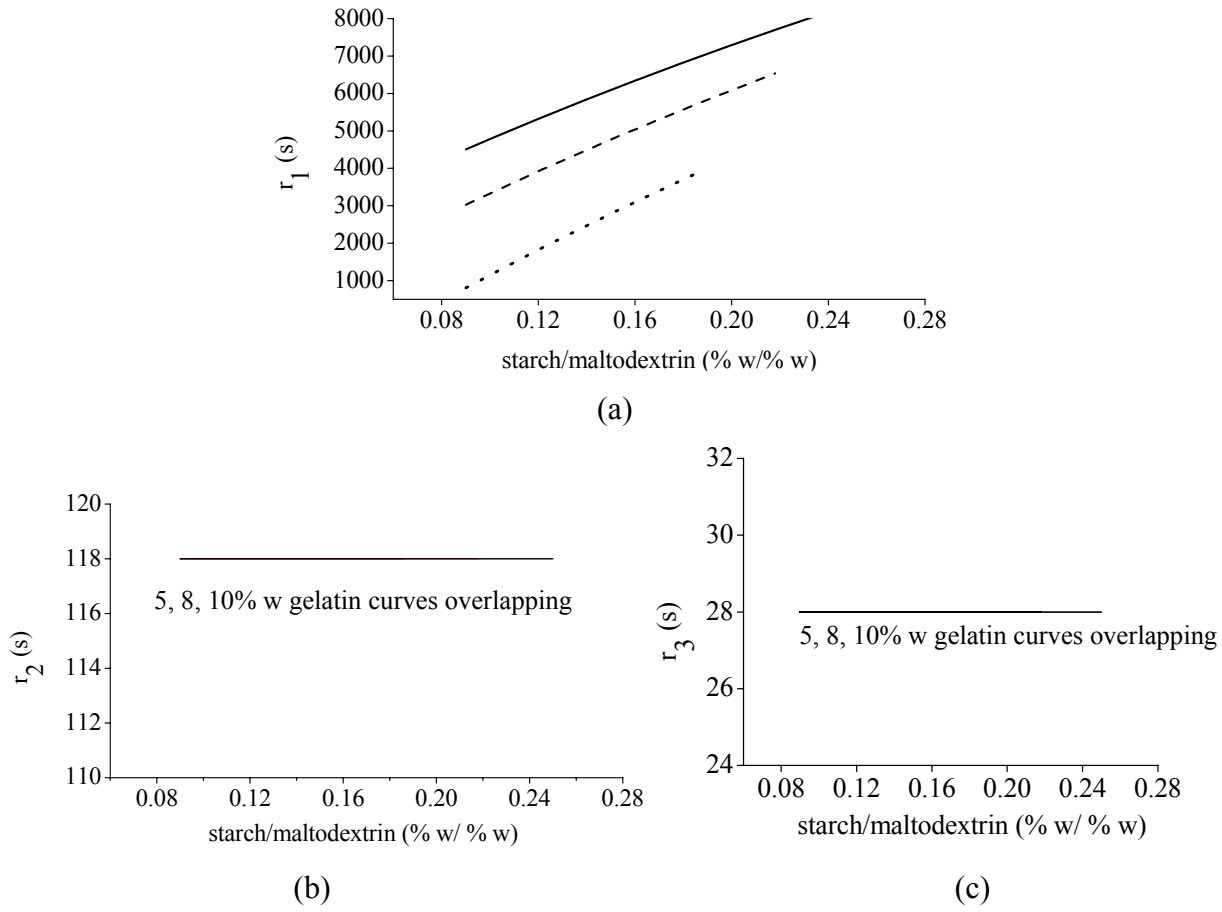

Figure 29. Modelization of change in gel r_1 (a), r_2 (b), r_3 (c) values as a function of starch/maltodextrin ratio (% w/%w) at 5 (···), 8 (– – –), 10 (—) % w of gelatin. Values of r_1 are calculated from equation 10. r_2 and r_3 are slack variables and do not vary with gelatin, maltodextrin or starch content.

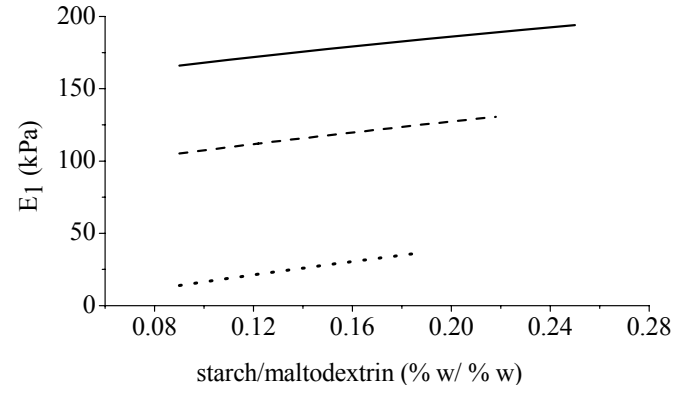

(a)

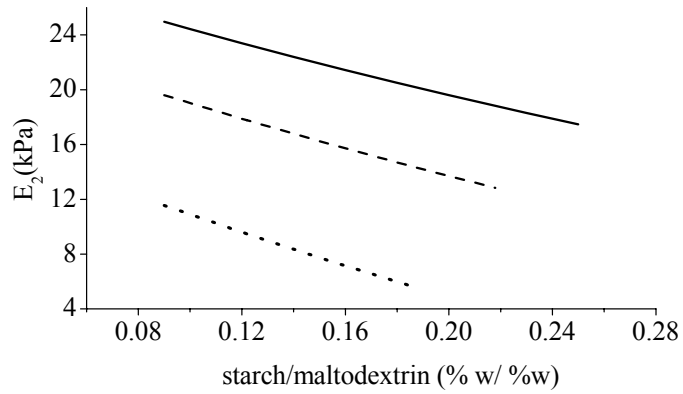

(b)

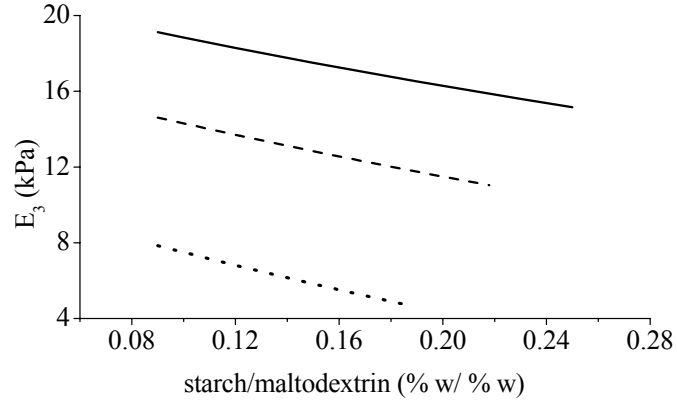

(c)

Figure 30. Modelization of change in gel E_1 (a), E_2 (b) and E_3 (c) values as a function of starch/maltodextrin ratio (% w/%w) at 5 (···), 8 (– – –), 10 (—) % w of gelatin. Values of E_1, E_2 and E_3 are respectively calculated from equation 11, 12 and 13.

According to figures 25 to 27 the addition of gelatin, at the expense of maltodextrin and starch, always resulted in an increase in gel firmness, r_1, E_1, E_2 and E_3 and on the contrary, the value of these rheological parameters always decreased when maltodextrin is increased in the mixture. It can also been noted from figure 25 that the trace plot of maltodextrin is steeper than that of starch. This means that when gelatin and starch are simultaneously substituted by maltodextrin in the mixture, a larger decrease in firmness occurs compared to when gelatin and maltodextrin are replaced by starch. The same response was noted for E_1 (Figure 27a). It should also be mentioned here that the trace plots of starch for firmness and E_1 are rather flat lines, suggesting that firmness and E_1 are quite insensitive to changes in starch content in the mixture. This argument can further be supported by figures 28 and 30a. It can be seen that the addition of starch in a mixture with constant gelatin concentration, which implies a decrease in maltodextrin content, resulted in an increase in firmness and E_1. This increase is mainly due to the decrease in maltodextrin content rather than the direct effect of increasing content of starch. Elastic modulus of filled gelatin gels increased with the filler concentration in the single phase region but decreased in the two-phase region because of the increasing imperfection of the gel network (Kasapis *et al.*, 1993; Al-Ruqaie *et al.*, 1997). In our study, a gel rather than a liquid was obtained macroscopically. It can therefore be assumed that the morphology was a continuous gelatin-rich phase interspersed by a liquid maltodextrin-starch-rich phase. The addition of maltodextrin and starch to the gelatin network leads to the disruption of the three-dimensional gel networks. If a small amount of filler particles are added (maltodextrin and starch) to the filled gelatin gel, the gelatin network can still localize around the dispersed particles and compensate for the disruptive effect of the gelatin gel by the dispersed particles. However, due to the large amount of filler particles actually added, the dispersed phase could not be compensated for. Hence, increasing the maltodextrin content weakened the gelatin gel network and therefore decreased the gel firmness and elastic modulus E_1 of the first element of the three-parameter Maxwell model.

On the contrary, trace plots of starch for E_2 and E_3 (Figure 27b and c) are steeper than that of maltodextrin, indicating that when both gelatin and maltodextrin are replaced by starch in the mixture, there is a larger decrease in E_2 and E_3 than when gelatin and starch are substituted by maltodextrin. Figure 30b and c show that when starch is increased, implying a decrease in maltodextrin, while gelatin content is kept constant, E_2 and E_3 decreased as expected. Starch

had therefore a greater influence on E_2 and E_3 than maltodextrin. It is however important to note that E_1 is more suitable to compare the gels rheological parameters, since E_1 accounted for most of the change in component concentrations. For instance, the highest E_1 value (in the mixture design) is 15 folds greater than that of the smallest E_1 value, while E_2 and E_3 values showed only 4 folds difference between the highest and the lowest value.

Figure 26 indicates a different effect of starch on r_1. Indeed, it can be seen that when starch is added, at the expense of gelatin and maltodextrin, there is an increase in r_1 and the trace plot of starch is steeper than that of gelatin. In addition, when starch content was increased (and maltodextrin decreased and gelatin kept constant) there is a sharp increase in r_1 (Figure 29a), due to the change in content of both starch and maltodextrin. Figure 29b and c show that r_2 and r_3 did not vary when gelatin, maltodextrin or starch content was changed. Moreover, all the trace plots are linear, which indicates that the impact of interactions between constituents of the gels on firmness, relaxation times and elastic components are not significant.

3. OPTIMUM COMPONENT CONCENTRATION OF GEL

The optimization module in Design-Expert looks for a combination of factor levels that simultaneously satisfies the requirements of responses (firmness, relaxation time constants and elastic modulus). When firmness, relaxation time constants and elastic modulus values of Camembert and Coulommiers cheeses were set as target values, the optimization module generated the composition of gels that imitated best the textural properties of the cheeses (Table 9). Coulommiers and Camembert simulants were then prepared and penetrometry and relaxation tests were carried out on these gels.

From table 9, it can be seen that these simulants successfully imitated the firmness of the two cheeses. In addition, E_1 of Camembert simulant closely matched that of Camembert cheese, however, that of Coulommiers simulant was higher than that of Coulommiers cheese. Moreover, both simulants had a lengthier relaxation and lower E_2 and E_3 compared to Coulommiers and Camembert cheeses.

Table 9. Composition and actual values of relaxation time constants and elastic modulus of cheeses and gels regarded as imitating best textural properties of Coulommiers and Camembert cheeses

	Coulommiers	Simulant Coulommiers[a]	Camembert	Simulant Camembert[a]
gelatin (% w/w)		7.8		8.3
maltodextrin (% w/w)		20.2		19.7
starch (% w/w)		2.0		2.0
Firmness (N)	19 ± 1	17.9 ± 0.3	20 ± 1	18.8 ± 0.3
r_1 (s)	1200 ± 100	3600 ± 20	1300 ± 100	3900 ± 100
r_2 (s)	107 ± 5	119 ± 3	105 ± 7	117 ± 7
r_3 (s)	27 ± 2	32 ± 5	29 ± 4	29 ± 5
E_1 (kPa)	80 ± 9	111 ± 1	139 ± 10	120 ± 1
E_2 (kPa)	33 ± 4	18 ± 1	74 ± 10	20 ± 1
E_3 (kPa)	34 ± 4	14 ± 1	78 ± 7	15 ± 1

[a] composition generated by optimization module in Design-Expert. Rheological data indicated were obtained from penetrometry and relaxation tests carried out on Coulommiers and Camembert simulants.

Although both simulants closely imitate the texture of Camembert and Coulommiers cheeses, simulating their global textural properties (firmness, relaxation time constant and elastic modulus) is not easy. This can be explained by the fact that cheeses are non-homogeneous. Within an individual cheese, there may be considerable variation in rheological properties, depending on how it is turned during ripening, moisture distribution and content and proteolytic activity within the cheese. Cheeses with crust may lose water more rapidly from their surface so that the composition of the core will be quite different from the outer regions. Moreover, turning of cheeses subjects the top and bottom regions to alternating high and low compressive stresses under their own weight, while the central core is subject to much less variation. Therefore, firmness also varies with distance from the surface (Prentice *et al.*, 1993). Food simulants designed in this study, on the contrary, are more homogeneous and have a more compact protein matrix. Consequently, the simulants are less porous with a more compact solid behaviour compared to cheeses. Del Nobile, Chillo, Mentana and Baiano (2007) reported that relaxation times strongly depends on food structure. These authors also noted that for spongy food such as mozarella cheese and white pan bread, the relaxation time distribution curve vanishes to zero at relaxation times ranging between 600 and 1000 s, whereas for bulky food matrices, such as meat, ripened cheese and agar gels, the relaxation time distribution curves vanishes to zero at lengthier relaxation times ranging between 2000

and 5000 s. Nonetheless, simulants designed in this study can be regarded as good simulants of the textural properties of soft cheeses. They are stable and display reproducible textural properties. They can be used as standard scale in sensory measurements of cheese texture or as soft cheese model in designing packaging.

4. CONCLUSION

Gels made up of gelatin only cannot imitate the textural properties of Camembert and Coulommiers. Gelatin concentration can be varied to adjust gel firmness and elastic modulus to match that of cheeses. However, relaxation time constant remains significantly higher than that of cheeses. Maltodextrin and starch, compared to guar, karaya and xanthan, were found to be most suitable in lowering relaxation time constant of the first element of a three-parameter Maxwell model of gelatin so that the gel model could match more closely the textural properties of 10-day-old Camembert and Coulommiers cheeses. Moreover, the use of a mixture design approach is shown to be useful in investigating systems consisting of multiple ingredients for which proportions in the mixture are dependent on each other. The mathematical model developed in this study successfully explained the effect of each component on the textural properties of gelatin-maltodextrin-starch simulants. A linear dependence of firmness, relaxation time and elastic modulus of the first element of the Maxwell model on composition of simulants was noted. Increasing gelatin content resulted in an increase in rheological parameters, while the opposite effect was obtained when maltodextrin content was raised. Firmness and elastic modulus of the first term of the Maxwell model were found to be insentitive to changes in starch content (varying from 1 to 2%). Moreover, no significant effect of interactions between gelatin, maltodextrin, and starch were noted on the rheological parameters studied.

PART II: POLYMERIC GEL SIMULATING COULOMMIERS CHEESE DURING RIPENING

As described in part I of the results and discussion chapter, a gel simulant imitating firmness and viscoelastic properties of soft cheese has been formulated from gelatin, maltodextrin and starch and its component concentration adjusted through the use of a mixture design experiment. Gel simulants were designed to match the rheological parameters of 10 days old Coulommiers and Camembert cheeses. The objective of the work described in this section was to bring about gradual textural changes in the cheese simulant so that it would match those occurring in Coulommiers cheese during ripening. Attention was focused only on Coulommiers cheese this time, owing to availability. One-day old Coulommiers cheese was easily obtained from a nearby cheese manufacturer whereas Camembert cheese was available as from 10 days old from a local supermarket.

To achieve this, protease enzyme, Subtilisin Carlsberg (which will be referred to by its commercial name, Alcalase®) was added to the simulants during preparation and their effects on gel network were studied by assessing the rheological parameters of the simulants during ripening.

Figures 31 and 32 show the change in rheological parameters (firmness, elasticity modulus and relaxation time constants) during the ripening of Coulommiers cheese and simulants. Alcalase® with varying enzyme activity was added to the gels in order to reproduce the textural changes occurring during ripening of the soft cheese. Firmness, elasticity modulus and relaxation time constants of gels were measured 1, 8, 43, 50 and 120 days after preparation. Rheological parameters of Coulommiers cheese were monitored through ripening the day after packaging and thereafter each week during six weeks (that is after 8, 15, 22, 29, 36 and 43 days).

Change in firmness of Coulommiers cheese and simulants is presented in figure 31.

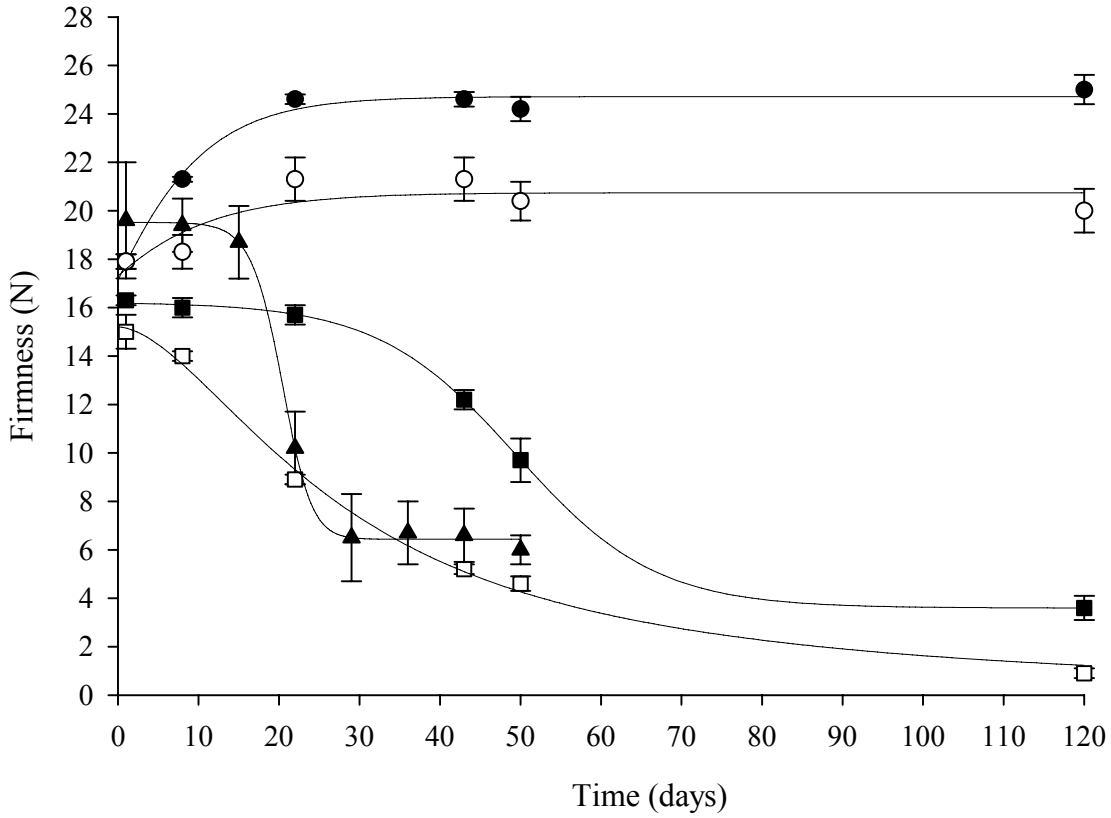

Figure 31. Change in firmness (N) of Coulommiers cheese (▲), standard simulant without Alcalase® (●), simulant with an Alcalase activity of 0.006 AU (○), 0.012 AU (■) and 0.030 AU (□) with time. Error bars indicate standard deviation calculated from 3 repetitions for cheeses and gels.

Firmness of the cheese decreased during ripening, with a marked fall after 15 days, which then leveled off to about 6 N after 30 days. Expectedly, firmness of standard simulant (without Alcalase®) was higher than that of enzyme containing simulants. The standard simulant and simulant with an Alcalase activity of 0.006 AU showed an increase in firmness (during early stage of ripening) which then remained fairly constant after 22 days. Increasing Alcalase activity increased the rate of change of firmness: for instance, the initial hydrolysis rate was slower at an Alcalase activity of 0.012 AU than at 0.030 AU.

The changes in elasticity modulus (E_1) and relaxation time constant (r_1) of the first element of the three-parameter Maxwell model of Coulommiers cheese and simulants are presented in figure 32.

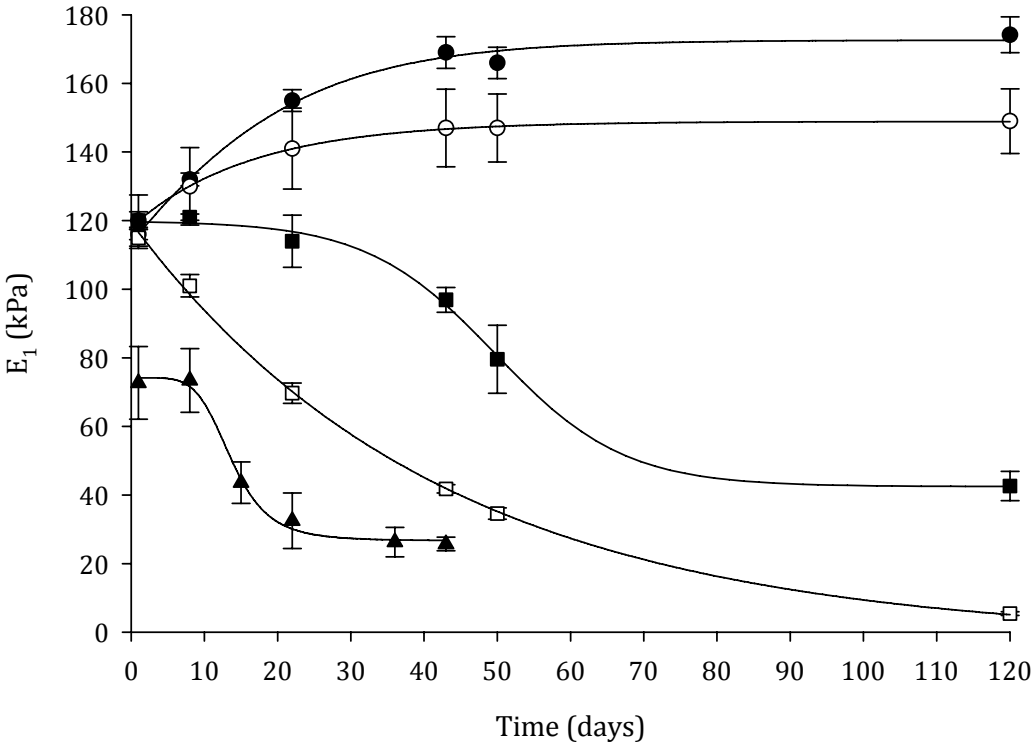

(a)

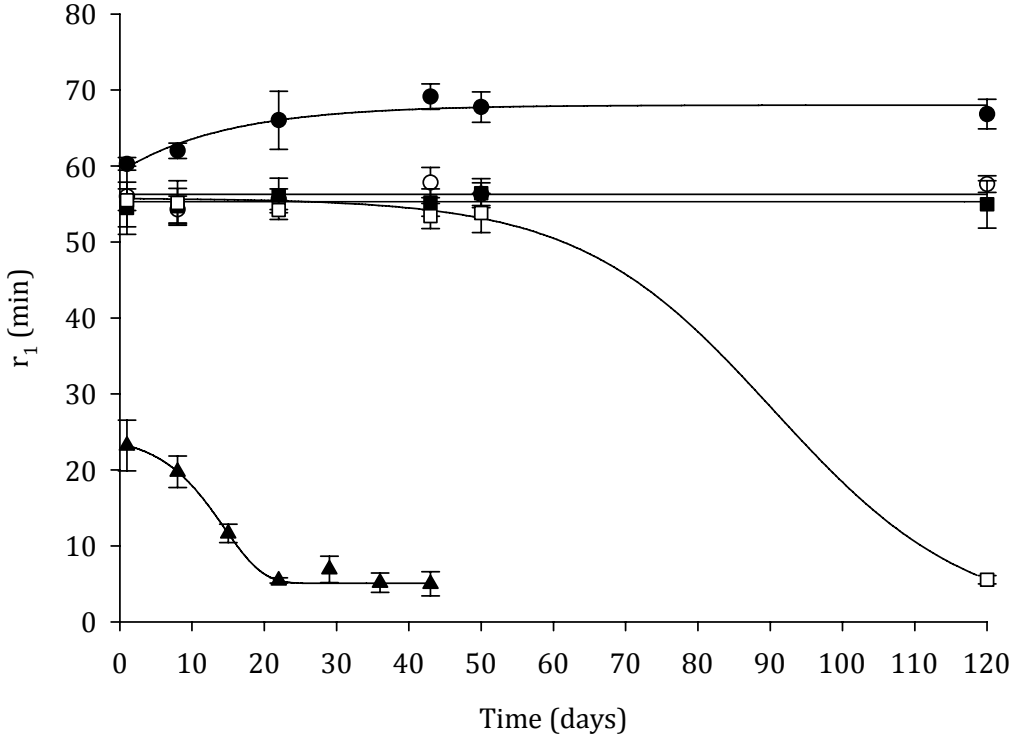

(b)

Figure 32. Changes in elasticity modulus E_1 (a) and relaxation time constant, r_1 (b) of Coulommiers cheese (▲), standard simulant without Alcalase® (●), simulant with an Alcalase activity of 0.006 AU (○), 0.012 AU (■) and 0.030 AU (□) with time. Error bars indicate standard deviation calculated from 3 repetitions for cheeses and gels.

The changes in E_1 values during ripening of Coulommiers cheese and simulants showed similar trend to that of firmness. The r_1 value of Coulommiers cheese saw a decrease during ripening, while a slight increase in r_1 was noted during the first 22 days for standard simulant. Moreover, r_1 of simulants with Alcalase activity of 0.006 and 0.012 AU showed no significant change during aging, while increasing the enzyme activity to 0.030 AU did cause a fall in r_1 value which was noted on day 120. During the first 50 days of aging, r_1 value remained fairly constant.

In this section, attention has been focused upon the first element of the Maxwell model (r_1 and E_1), since the second and third elements (r_2, r_3, E_2 and E_3) were to a much lesser extent influenced by changes in component concentrations or structure of gels (as already pointed out and based upon previous results obtained in this study). First element of the three-parameter Maxwell model indeed accounted for most of the modifications undergone by the samples during aging.

1. CHANGES IN RHEOLOGICAL PARAMETERS OF COULOMMIERS CHEESE

Ripening of Coulommiers cheese was associated with a decrease in firmness and first elements of the three-parameter Maxwell model: elastic modulus (E_1) and relaxation time constant (r_1). This reflected a change in time of the cheese basic structure (Watase and Nishinari, 1980). Mpagana and Hardy (1985) also reported a decrease in E_1 and r_1 values during ripening of Camembert cheese. These authors attributed this observation to a gradual damage of Camembert structure during ripening. Stress relaxed faster, r_1 values thus decreased. Multiple linear regression analysis was used in order to determine factors which influenced most of the changes in r_1 value. Proteolysis was the primary factor causing the fall in r_1 value, while dehydration occurring during ripening (which actually caused r_1 value to increase) influenced to a lesser extent r_1 value. Other authors argued that the softening of cheeses during proteolysis is caused by the weakening, loss in structure and an increase in mobility of microstructure in the cheeses (Green *et al.*, 1981).
Moreover, the leveling off in rheological parameters values of Coulommiers cheese noted after a ripening period of 30 days was probably due to crust effect rather than the texture of

the core matter itself. In fact, the rheological parameters should actually go on decreasing due to continued softening of the core matter. However, this was not the case because the crust ensured a minimum constant resistance to the push of the probe of the testing machine.

2. CHANGES IN RHEOLOGICAL PARAMETERS OF STANDARD SIMULANT

The firmness and the first element of the three-parameter Maxwell model, elasticity modulus (E_1) and relaxation time (r_1) increased during aging of standard simulant (without Alcalase®) and leveled off after about 22 days. During an aging period of about 22 days, the increase in number of crosslinks or/and the growth of existing junctions caused firmness and rigidity of the standard simulant (without Alcalase®) to increase. Hence E_1 increased.
Its r_1 value also increased slightly during aging which indicated a simultaneous increase in compactness of the gel. Comby *et al*. (1985) also suggested that a decrease of chain mobility, associated to the increase in crosslinks number, can be reflected by an increase in the r_1 value.

3. CHANGES IN RHEOLOGICAL PARAMETERS OF SIMULANTS WITH ALCALASE®

Addition of Alcalase® to simulant caused bonds cleavage during hydrolysis, which was reflected by simulants having lower firmness and rigidity (smaller E_1 value) than standard simulant (with no enzyme). The changes in rheological parameters during aging varied according to Alcalase activity. When Alcalase activity was equal to 0.006 AU, the firmness and the E_1 values increased during aging (increase in crosslinks, reinforcing the gel network during aging). These values then leveled off after about 22 days, but were lower than that of standard simulant, which indicated bond cleavage. However, the number of bonds formed was greater than that cleaved during hydrolysis.
Interestingly, when Alcalase activity was raised to 0.012 and 0.030 AU, not only did firmness and elasticity modulus have lower values than standard simulant, but they also decreased during aging. Higher enzyme content led to greater bond breaking than bond formation and

caused hydrolysis to last longer. Therefore, firmness and rigidity of simulant decreased gradually during 150 days.

In addition, according to Surowka (1997), the presence of protein hydrolysate can further weaken gelatin network. This author examined the texture of gels containing 2 to 8% of gelatin and 1 to 10% of Alcalase® protein hydrolysate and reported that the peptides molecules (hydrolysate) being relatively small and mobile, partly block those fragments of gelatin which are capable of forming junction zones. The resulting lattice was not sufficiently dense and hence was weaker. Moreover, the products of protein hydrolysis are significantly hydrophilic and presumably act by preventing to some extent hydrogen bond formation in junction sites and/or modifying the structure of the liquid water in the vicinity of these sites. This disturbs the hydration equilibrium in the gel and, in consequence, leads to deterioration of gel characteristics.

The relaxation time constants remained fairly constant during aging of simulant with an Alcalase activity of 0.006 AU. Therefore, compactness of gel remained constant. It is likely that the increase in crosslinks, which is in this case lower than that noted for standard simulant, did not give rise to a more compact gel structure (decreasing chains mobility), as opposed to the standard simulant where r_1 slightly increased during aging.

Increasing ratio of Alcalase activity to 0.012 AU did not cause relaxation time values to change with time. Compactness of the gel therefore remained more or less constant, although crosslinks decreased and rigidity lowered during hydrolysis. Comby *et al*. (1985) in studying the stress relaxation of high-methoxyl pectin gels also noted that the elasticity modulus and the relaxation time constant evolved in different ways. These authors suggested that the changes in elasticity modulus and relaxation are not governed by the same mechanism at a molecular level. However, the simulant with the highest Alcalase activity (0.030 AU) saw significant decrease in relaxation time constants on day 120. The high proteolysis extent probably caused dramatic damage in the gel network, resulting in the sticky paste-like gel observed after 120 days.

4. CONCLUSION

The firmness and the rigidity of enzyme containing simulants changed gradually during aging at, as can be expected, faster hydrolysis speed when Alcalase activity was increased from 0.012 to 0.030 AU. The textural changes induced by ripening of Coulommiers cheese occurred in a different way. Indeed, after a rather slow decrease in firmness and rigidity, a marked fall in firmness and rigidity was noted after 15 and 8 days, respectively. Afterwards, those rheological parameters remained almost constant during ripening. Cheese can be considered in most cases as a system constituted of a network of paracasein, in which fat globules and bacterial colonies are dispersed, and an aqueous phase. The composition of the aqueous phase changes continuously during ripening due to the activity of the numerous enzymes involved: the endogenous milk enzymes, the rennet enzymes, the extracellular enzymes of bacteria and fungi and the intracellular enzymes resulting from the lysis of lactic acid bacteria. The composition of cheese matrix and the aqueous phase differs according to the stage of ripening (Boutron *et al.*, 1999). Those proteolytic and physico-chemical changes responsible for the textural evolution occurring in Coulommiers cheese during ripening could not easily be reproduced by the action of one enzyme. Although Alcalase® was successful in bringing gradual textural variation in the Coulommiers simulant, the rate of change in the gel differed from that of the cheese. Production and growth of endogenous enzymes in Coulommiers cheese most probably occurred in the early ripening stage (first 8/15 days) during which rheological parameters of the cheese remained constant. After this phase, the action of these enzymes on the breakdown of the cheese network was greatest, hence the marked fall in the rheological parameters values noted. As opposed to the enzymes action in Coulommiers cheese, Alcalase® caused gradual damage to the gel network of the simulant through aging. The rate of change in rheological parameters in the gel may perhaps approach that of the Coulommiers cheese if the action of Alcalase® in the simulant could be controlled, through timed release for example.

PART III: TEXTURAL PROPERTIES DETERMINED BY DIGITAL IMAGE CORRELATION

Digital image correlation is an interesting optical method to measure deformation on an object surface based on the modern digital image processing technology and optical measurement. Optical measurements like moiré, holography, and speckle interferometry require pretreatment of the surface of object with spraying paint, coating or reproducing grid to give full-field information of object deformation from the interferometric fringe. The texture or the random artificial speckle on the object surface is the carrier of deformed information. Digital image correlation method allows surface displacements and strains measurement. Three dimensional displacement measurements has been an area of interest in many engineering problems. For example, the study of displacements in the vicinity of the crack tip within a deformed body is an area of active research (Luo *et al.*, 1993; Luo *et al.*, 1994). 3D image correlation approach is also used to measure micron-sized surface displacements caused by localized stress relief associated with hole drilling (Wu and Lu, 2000; Nelson *et al.*, 2006). Although image analysis is gaining increasing interest in food industries to study surface of products, digital image correlation method has so far never been used for food texture assessment (Davies, 2000). Therefore, in this chapter, the application of digital image correlation and topometric 3D scanning system as tools for cheese texture analysis has been studied. These three-dimensional systems were intended to imitate the human eyes and give additional information (not available by the universal testing machine) to describe better the texture of the cheese/gel as perceived by a person. Both visual and tactile properties of the food come into play during sensory evaluation of texture. Therefore, in imitating the fingertip with the probe of the universal testing machine and the eyes with the digital cameras, models which are able to predict accurately the sensory texture of food from instrumental measurements may be developed.

1. SURFACE DISPLACEMENT OF SAMPLES DURING PENETROMETRY TEST

Surface displacement images of 8, 10, 15, 20% (w/w) gelatin gels, 10-day-old Coulommiers cheese and 30-day-old Camembert cheese and their gel simulants were captured during 4 mm penetrometry test. Surface displacement profiles were obtained from digital image correlation method. *Z* displacement (or surface depression) of each sample was plotted as a function of the radial distance from probe edge (Figures 34, 38, 40 and 41).

1.1. Gelatin gels: 8, 10, 15, 20% (w/w)

Figure 33 shows the schematic view of surface displacement of 8% gelatin gel under loading and with the probe inserted to a distance of 4 mm into the gel. As already stated in the 'Materials and methods' section, the system setup allowed image analysis as close as 1 mm from the edge of the probe. This is why the section of the graph in figure 33 from Y=0 to 1 mm is indicated as dotted line. In the figures that follow (figure 34, 38, 40 and 41), surface displacement profiles are shown as from 1 mm distance from the probe.

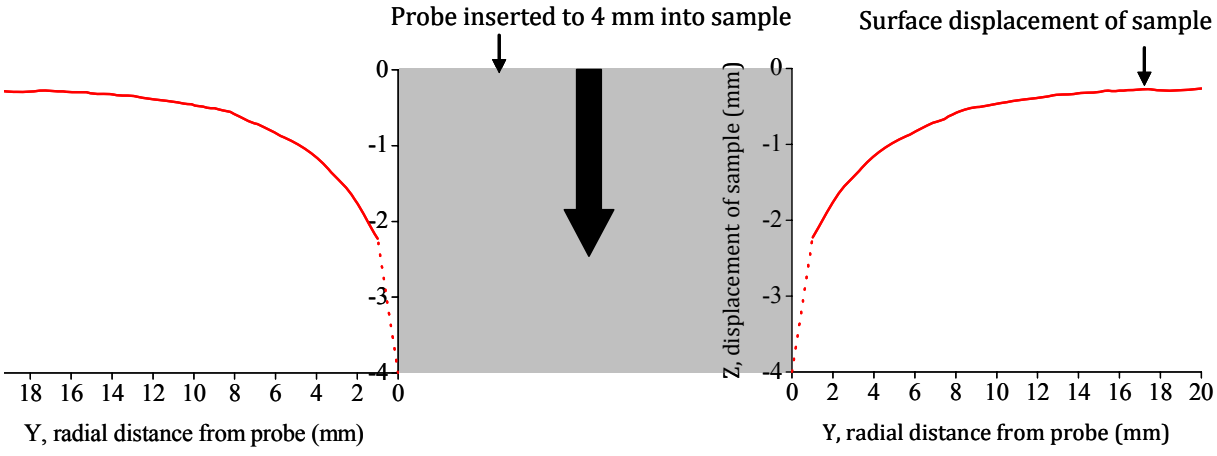

Figure 33. Schematic view of surface displacement of 8% gelatin gel under loading and with the probe inserted to a distance of 4 mm into the gel.

Figure 34 shows the surface displacement profile of 8, 10, 15 and 20 % gelatin gels with probe inserted to a depth of 4 mm into sample.

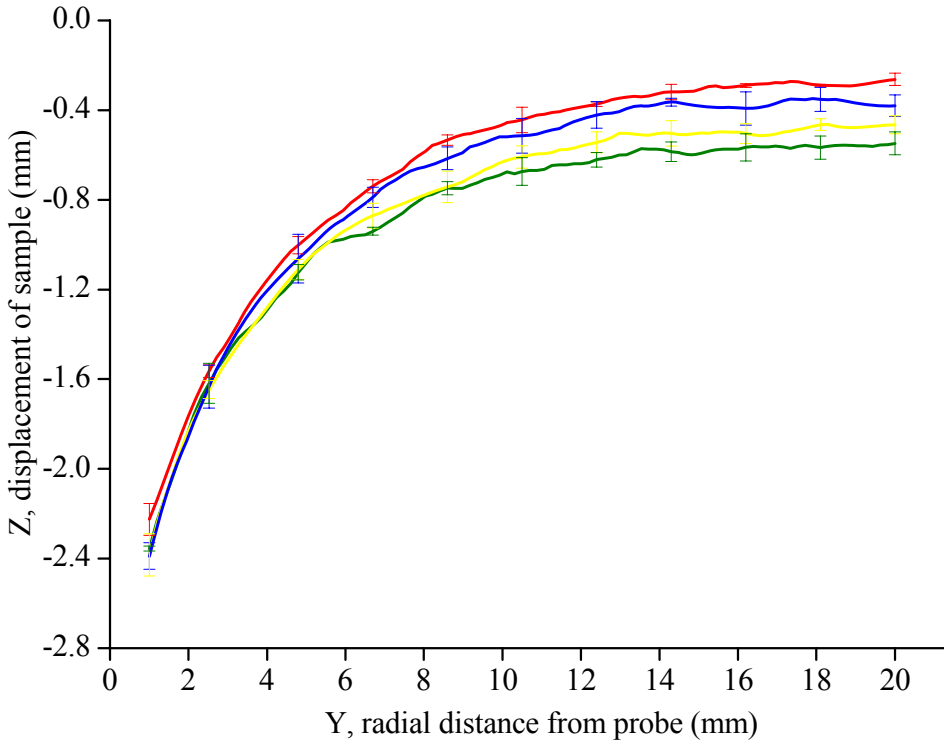

Figure 34. Surface displacement profile of 8% gelatin gel (—), 10% gelatin gel (—), 15% gelatin gel (—), 20% gelatin gel (—) with probe inserted to a depth of 4 mm into sample. Error bars indicate standard deviation calculated from 3 repetitions. Closest radial distance from probe was equal to 1 mm.

It can be noted (Figure 34) that depression induced by loading was mainly located close to the probe edge (about 6 mm radial distance). The distance (from probe edge) to which surface depression spread around from the probe varied with gelatin concentration of gels: increasing gelatin concentration increased surface depression (away from probe edge). Similar observations were made when sample analysis was carried out with the Breuckmann 3D scanning system.

Figure 35 shows the images acquired when 8% gelatin gel was scanned by the Breuckmann 3D system. These images were obtained from comparison between the deformed gel (20 mm diameter flat-bottomed probe inserted to 4 mm inside gel) and the reference undeformed gel. The colors indicate the surface displacement (in mm) of deformed sample (relative to the undeformed one) under loading; negative values reflect surface depression, while positive values indicate bulging. Figure 35a shows three views of 8% gelatin gel with probe inserted to a depth of 4 mm into sample. Figure 35b indicates the position of the cross sectional cut giving rise to the two dimensional view below it (Figure 35c).

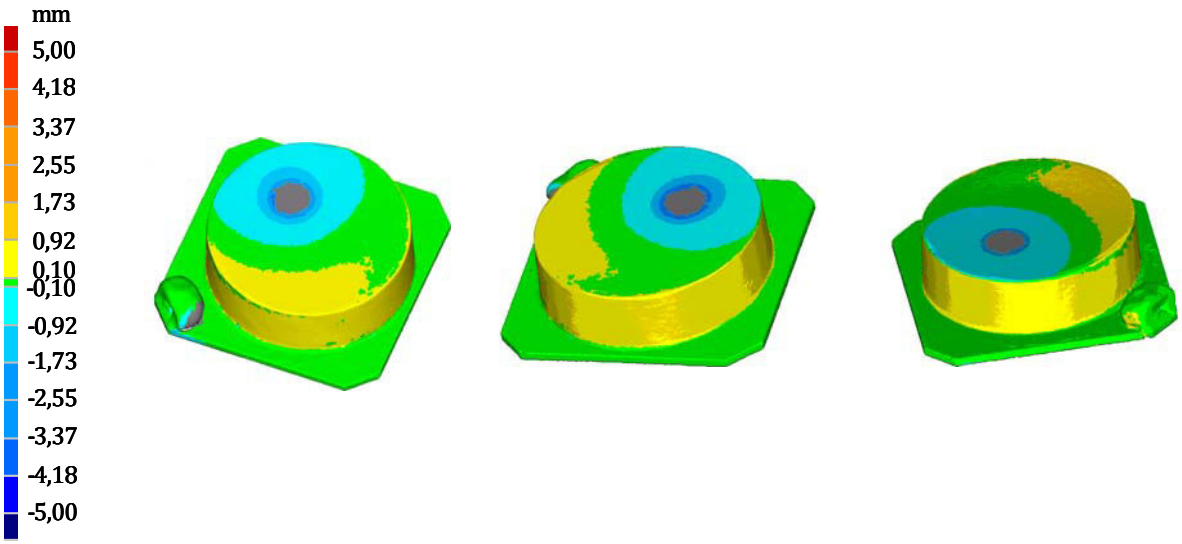

(a)

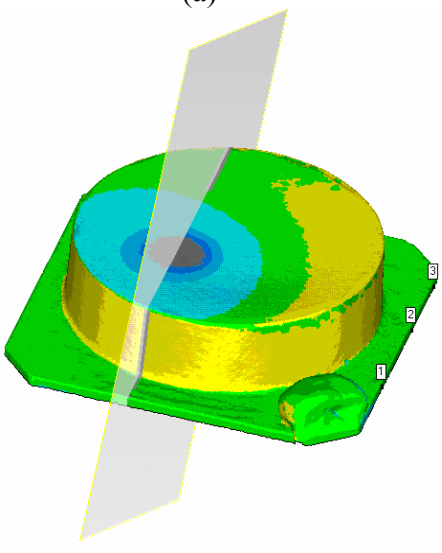

(b)

Maximum positive/negative displacement: 0.58/-2.28 ±0.01 mm

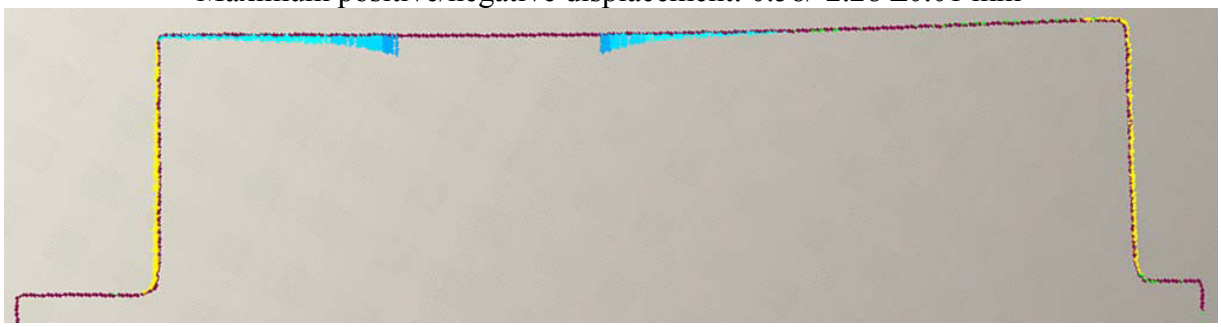

(c)

Figure 35. Three views of 8% gelatin gel with probe inserted to a depth of 4 mm into sample (a), position of the cross sectional cut (b), view of cross sectional cut (c). Images were acquired by Breuckmann 3D scanning system.

According to figure 35, surface depression of 8% gelatin gel was located close to the probe edge. Surface displacement of 15% gelatin gel (figure 36) differed from that of 8% gelatin gel. Surface depression was indeed more spread out. It can be noticed that the blue colored zone (figure 36) extended further away from the probe edge. This result was consistent with that noted by the digital image correlation method.

Comparison between the gels can also be based upon bulging. This matter will be discussed later in this section.

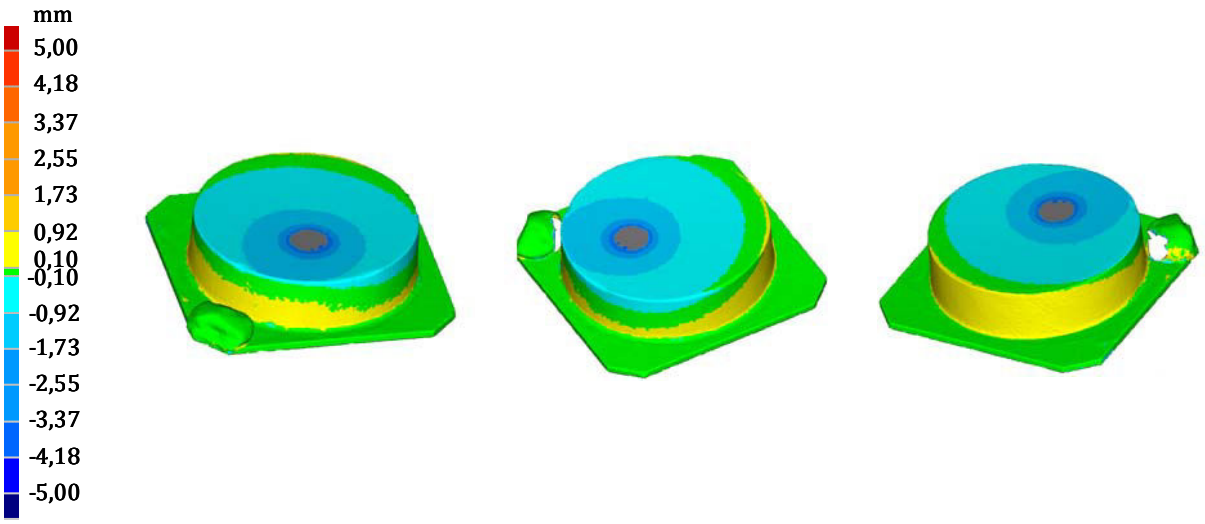

(a)

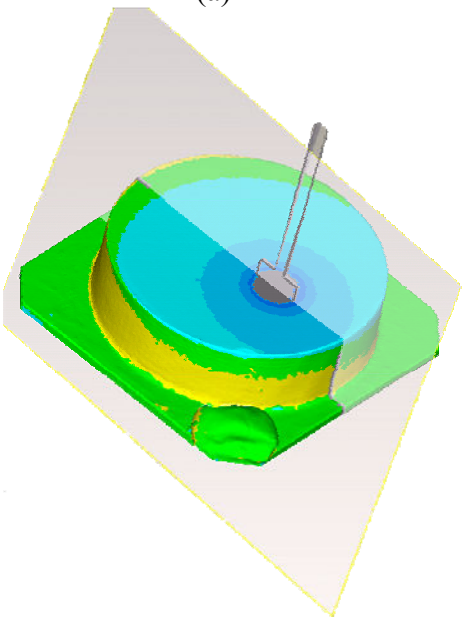

(b)

Maximum positive/negative displacement: 0.62/-2.32 ±0.01 mm

(c)

Figure 36. Three views of 15% gelatin gel with probe inserted to a depth of 4 mm into sample (a), position of the cross sectional cut (b), view of cross sectional cut (c). Images were acquired by Breuckmann 3D scanning system.

These gels differed in gelatin concentration and in rheological parameters (firmness, elasticity and relaxation time constant) which most probably accounted for the difference in gelatin gels surface displacement profiles.

Contour figures, indicating the *Z* displacement (mm) of gelatin gels surrounding the probe, were plotted from data obtained by digital image correlation method (Figure 37).

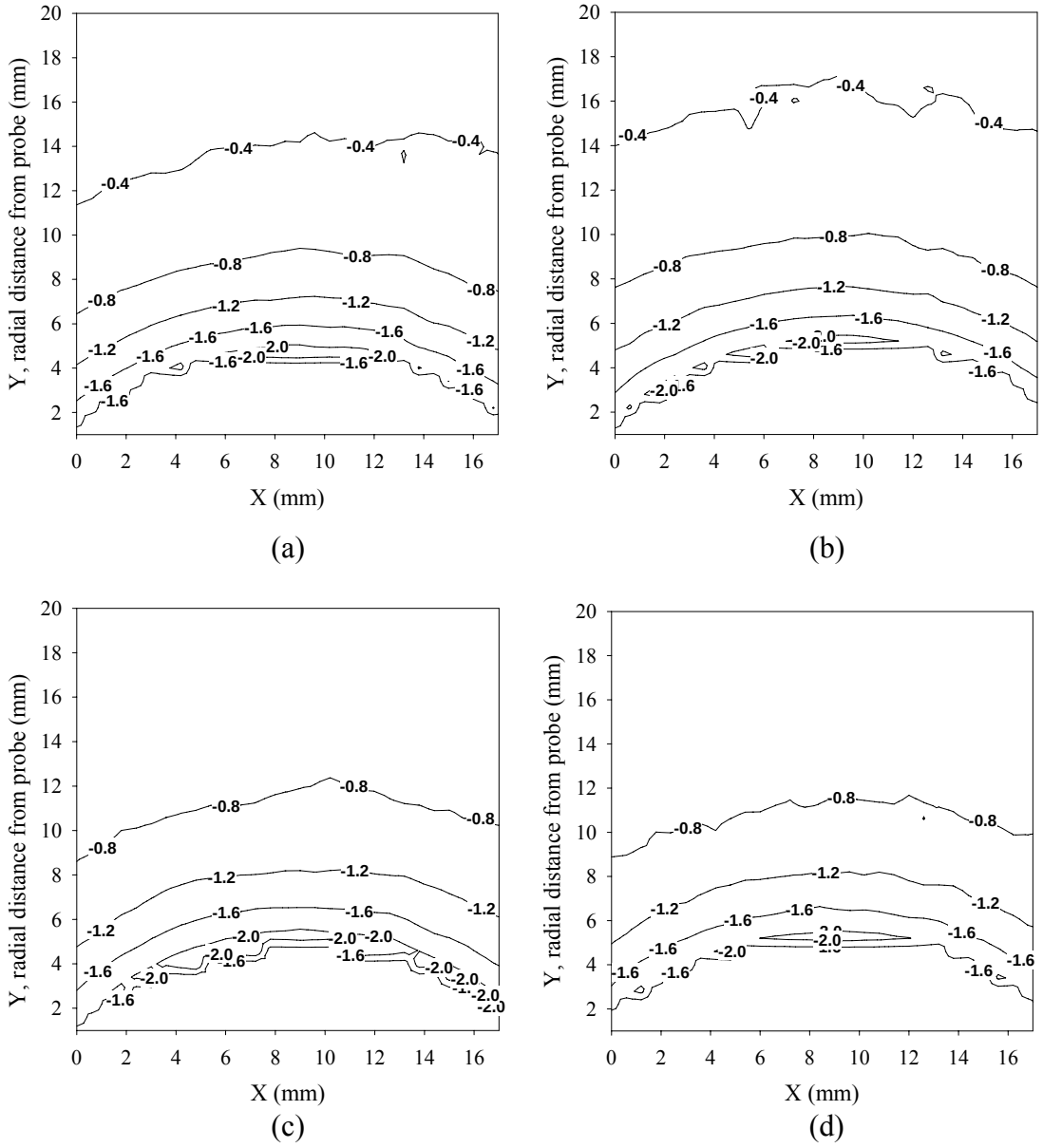

Figure 37. Contour plot for displacement component *Z* (mm) of 8 % gelatin gel (a), 10 % gelatin gel (b), 15 % gelatin gel (c), 20 % gelatin gel (d) with probe inserted to a depth of 4 mm into sample. The contour line interval was set to 0.4 mm. The closest radial distance from probe edge was 1 mm. Data were acquired by digital image correlation method.

When moving closer to the probe, the distance between contour lines decreased; a large part of the depression induced by the load was indeed located close to the probe edge (about 6 mm radial distance). In addition, the distance (from probe edge) to which surface depression spread around from the probe varied with gelatin concentration of gels.

1.2. Ten-day-old Coulommiers cheese and its simulant

Ten-day-old Coulommiers cheese and its simulant were captured during 4 mm penetrometry test and their surface displacement profiles were obtained from digital image correlation method. Figure 38 shows the surface displacement profile of 10-day-old Coulommiers cheese and its gel simulant.

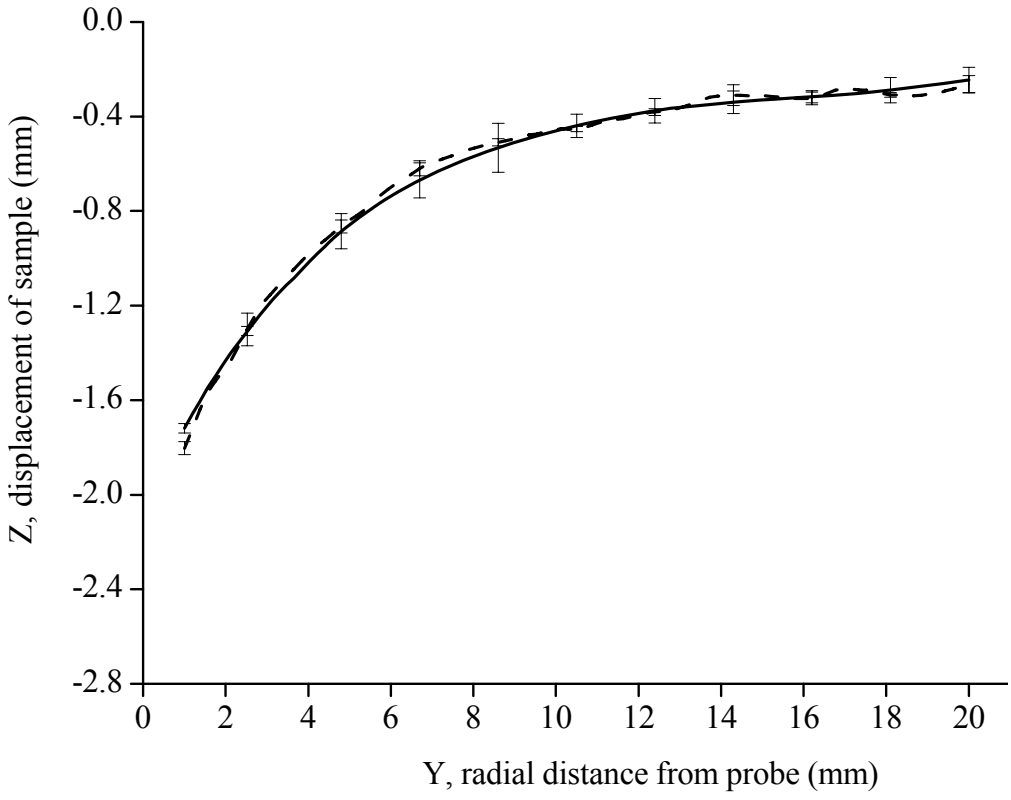

Figure 38. Surface displacement profile of 10-day-old Coulommiers cheese (—), Coulommiers simulant (– – –). Error bars indicate standard deviation calculated from 6 and 3 repetitions for cheeses and gel, respectively. Closest radial distance from probe was equal to 1 mm.

The surface displacement profile of 10-day-old Coulommiers cheese and its simulant was not significantly different which suggested close rheological parameters between the cheese and the gel.

Contour figures, indicating *Z* displacement (mm) of 10-day-old Coulommiers cheese and its gel simulant surrounding the probe are shown in figure 39.

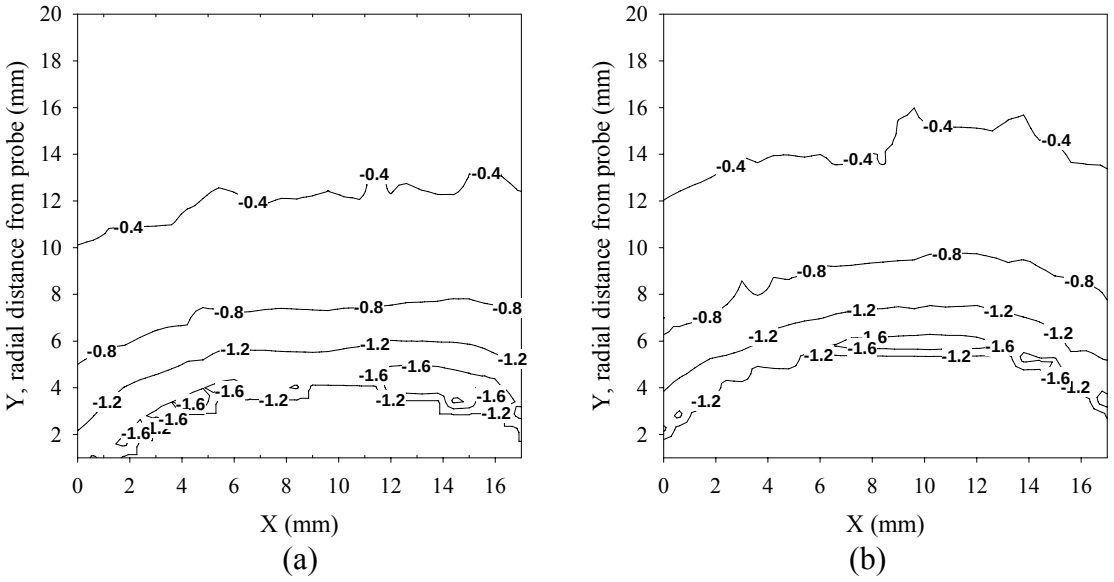

Figure 39. Contour plot for displacement component *Z* (mm) of 10-day-old Coulommiers cheese (a) and Coulommiers simulant (b) with probe inserted to a depth of 4 mm into sample. The contour line interval was set to 0.4 mm. The closest radial distance from probe edge was 1 mm. Data were acquired by digital image correlation method.

The interval between the contour lines of 10-day-old Coulommiers and its simulant was rather similar, which explains why their surface displacement profiles were not significantly different (Figure 38). These contour plots provided additional information regarding the surface depression of the sample. The contour lines of the 10-day-old Coulommiers cheese were rather flat, in the zone illustrated in figure 39, compared to that of the gel which had a more rounded shape.

1.3. Thirty-day-old Camembert cheese and its simulant

The surface displacement profile of 30-day-old Camembert cheese differed from that of its gel model, especially in the 15 mm radius zone surrounding probe edge (Figure 40).

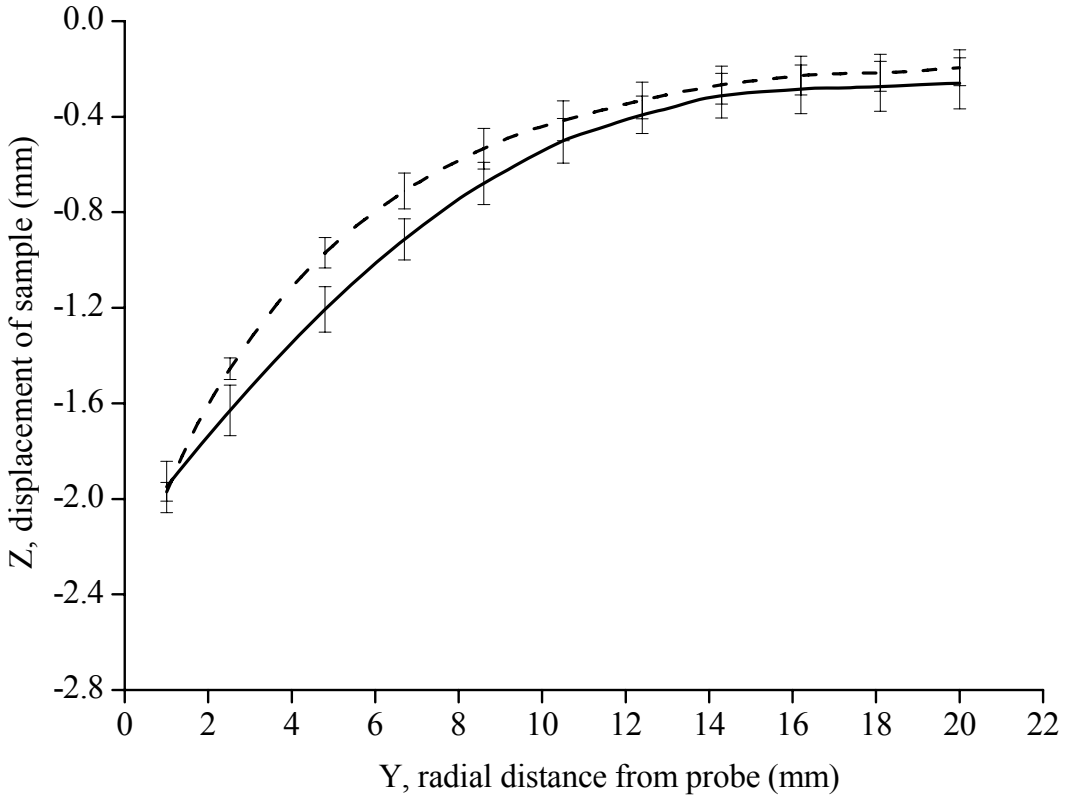

Figure 40. Surface displacement profile of 30-day-old Camembert cheese (—), Camembert cheese simulant (– – –). Error bars indicate standard deviation calculated from 6 and 3 repetitions for cheese and simulant respectively. Closest radial distance from probe was equal to 1 mm.

The shape of the surface displacement profile of the 30-day-old Camembert cheese was rather linear like in that zone, while the camembert simulant profile resembled that of the other gel samples in having a more convex shape. Similar profiles to that obtained for the 30-day-old Camembert cheese were noted for aging Coulommiers cheese (Figure 41).

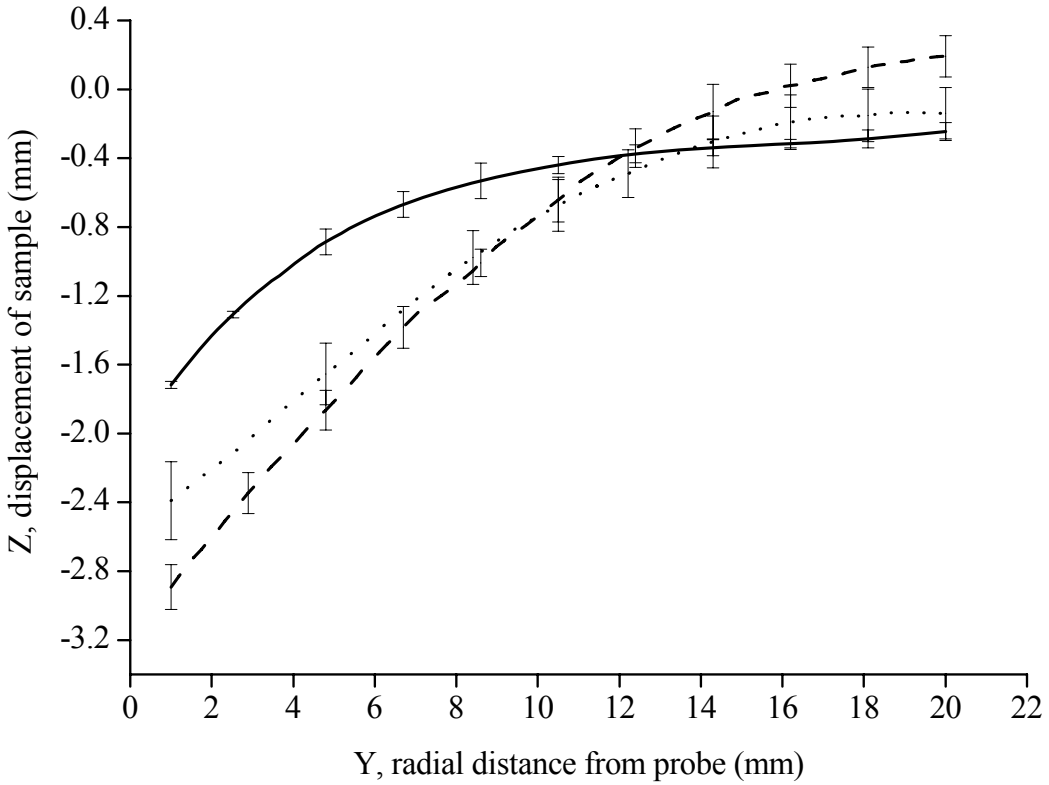

Figure 41. Surface displacement profile of 10 (—), 28 (• • • •) and 40 (– – –) days old Coulommiers cheese. Error bars indicate standard deviation calculated from 6 repetitions. Closest radial distance from probe was equal to 1 mm.

Indeed, the convex shape of the surface displacement profile gave way to a more linear graph in the 15 mm radius zone surrounding the probe edge. A significant increase in thickness of cheese crust (and therefore an increase in rigidity and a decrease in flexibility) might have accounted for the linear shape of the surface depression profiles noted during ripening of the cheese. However, this was not the case, for contrary to what could be expected, no significant difference in crust thickness was noted for 10, 30 and 40 days old Camembert and Coulommiers cheeses. Therefore, a more plausible explanation could be related to the fact that in soft aged cheese, lipolysis is twice more intense just under the crust than in the interior of the cheese (Hassouna and Guizani, 1995). The association of lipolysis and proteolysis probably gives the paste-like material under the cheese crust. Therefore, under loading, the crust would slide readily over the inner material and slant, thus showing deeper surface depression around the probe edge.

Those observations were also noted when Camembert cheese and its simulant were analyzed by the Breuckmann 3D scanning system. Figures 42 and 43 show the surface displacement of 30-day-old Camembert cheese and its simulant, respectively, with probe inserted to a depth of 4 mm into the sample. Surface depression was located, for both samples, near the probe. Moreover, two dimensional figures of cross sectional cut indicated deeper surface depression for the cheese compared to its simulant around the probe, although the radial distance to which surface depression spread around the probe did not seem to differ. This result was in agreement with that obtained by the digital image correlation method.

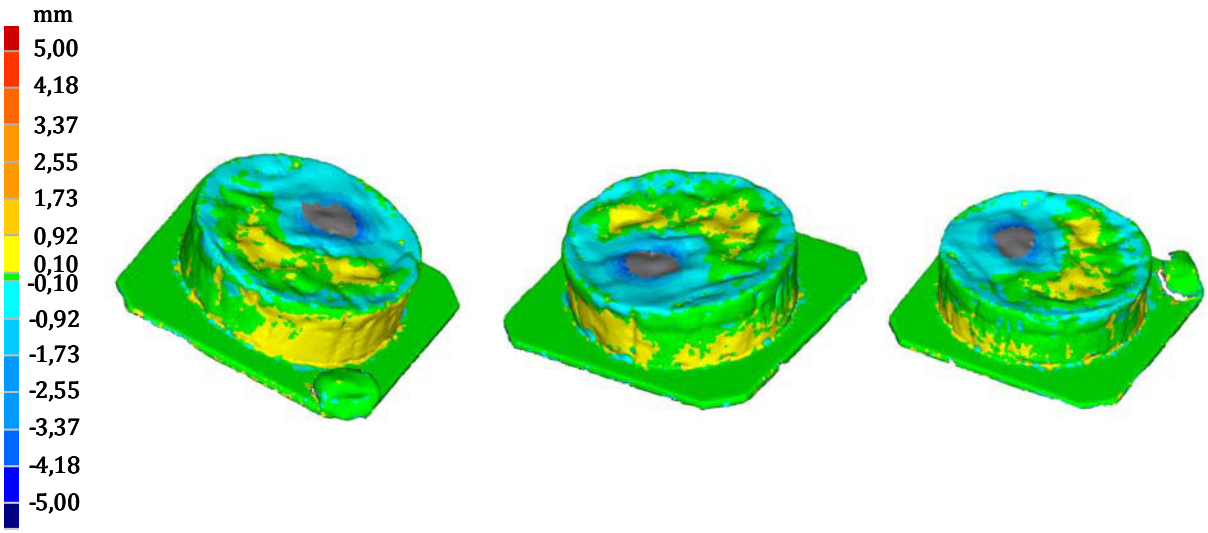

(a)

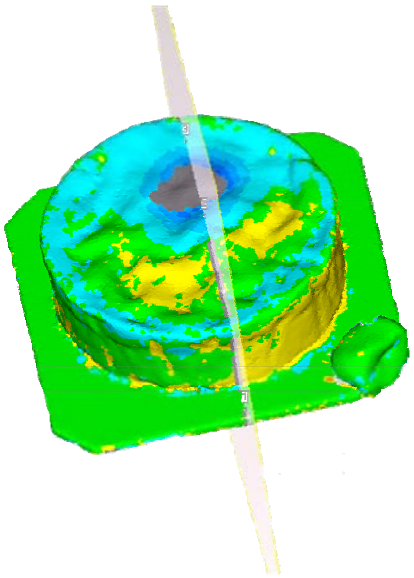

(b)

Maximum positive/negative displacement: 0.54/-2.61 ±0.01 mm

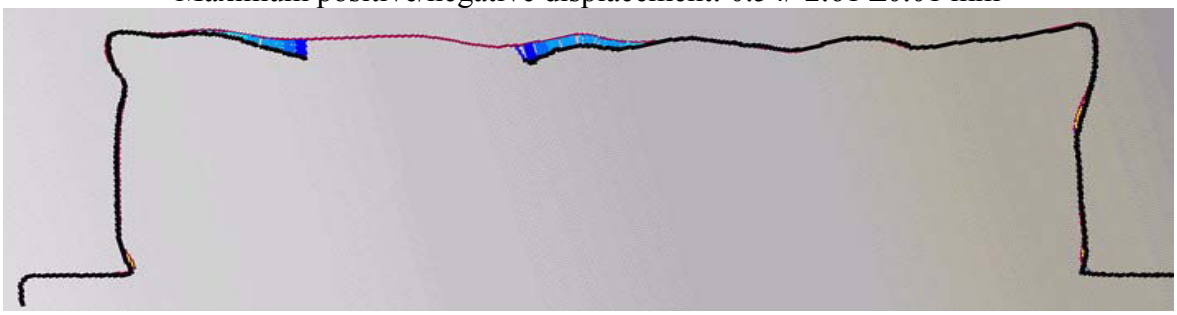

(c)

Figure 42. Three views of 30-day-old Camembert cheese with probe inserted to a depth of 4 mm into sample (a), position of the cross sectional cut (b), view of cross sectional cut (c). Images have been acquired by Breuckmann 3D scanning system

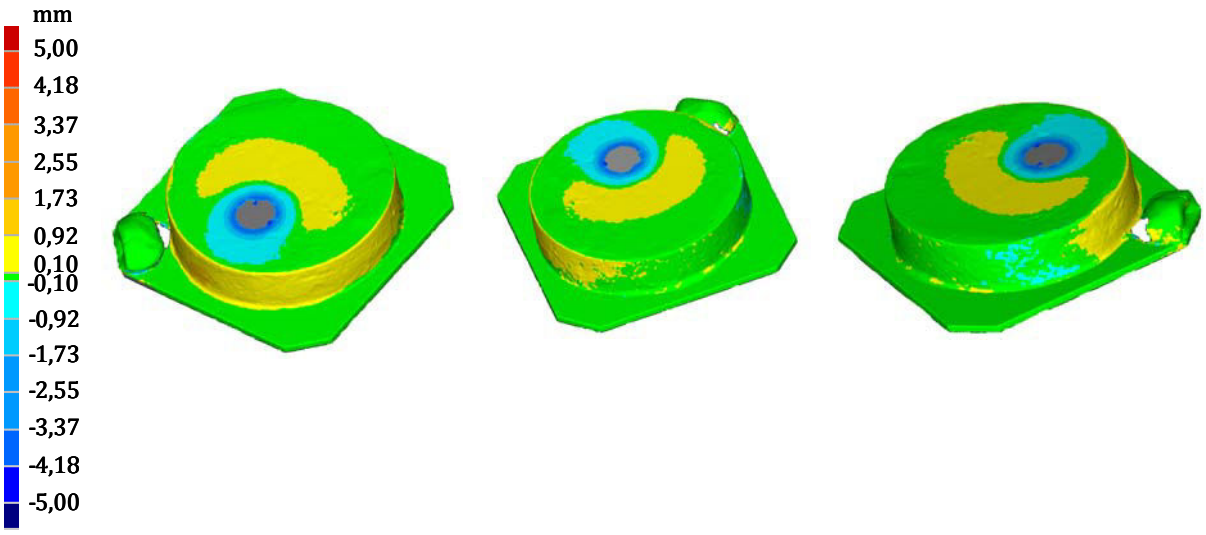

(a)

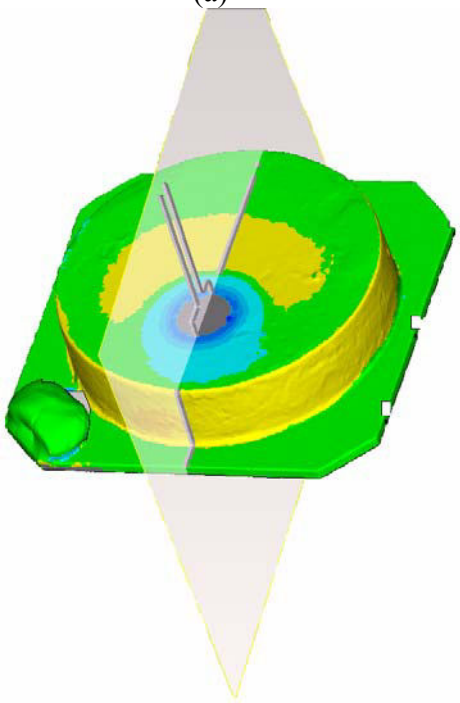

(b)

Maximum positive/negative displacement: 0.75/-2.23 ±0.01 mm

(c)

Figure 43. Three views of Camembert simulant with probe inserted to a depth of 4 mm into sample (a), position of the cross sectional cut (b), view of cross sectional cut (c). Images have been acquired by Breuckmann 3D scanning system

Contour figures, indicating *Z* displacement (mm) of 30-day-old Camembert cheese and its gel simulant around the probe are shown in figure 44.

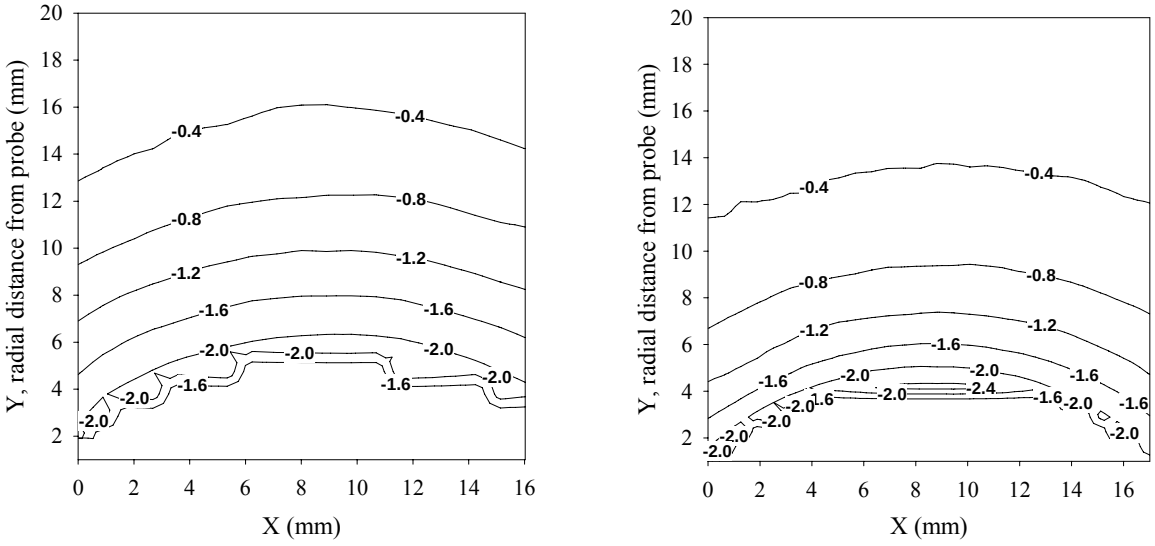

(a) (b)

Figure 44. Contour plot for displacement component Z (mm) of 30-day-old Camembert cheese (a) and Camembert simulant (b) with probe inserted to a depth of 4 mm into sample. The contour line interval was set to 0.4 mm. The closest radial distance from probe edge was 1 mm. Data were acquired by digital image correlation method.

Camembert cheese contour plot showed quite different pattern from contour plots of previous samples. Clearly, the distance between the contour lines was wider and more evenly spread out, instead of being closely packed near the probe edge as was the case for its gel simulant. This pattern further confirmed the fact that surface depression grew deeper during ripening of cheese.

1.4. Bulging (Breuckmann 3D scanning system)

As stated already, positive values of surface displacement indicate bulging (yellow colored areas). Comparison between 8% and 10% gelatin gels, 30-day-old Camembert cheese and cheese simulant can be done based upon the way the samples bulged under loading. According to figure 35, it can be seen that for 8% gelatin gel, bulging (~ 0.1-0.9 mm) appeared on the side and on top, more precisely away from the probe edge. It seemed that

when the probe was inserted into the 8% gelatin gel, matter was pushed away from the probe and also, the gel being compressed (downward) matter moved to the side of the cylindrical gel.

When gelatin concentration was raised to 15%, bulging did not appear on the top of the gel, but on the side (figure 36). In addition it can be seen that when the gel was compressed, matter moved away from the probe, hence bulging appeared on the side opposite to the one where probe was inserted. Also, on this side (where load was applied), bulging was located on the lower part of the gel, instead of being along the full height of the sample (as was the case for 8% gelatin gel)

The increase in rigidity and compactness of the gel probably induced a different behavior under loading. This might explain why bulging appeared further away from the probe. It seemed that the portion of the gel above the red line (imaginary boundary) behaved like a rigid plank and under loading, moved as a solid block and, in turn, compressed the part below the red line which therefore bulged (Figure 45). The incline angle of the red line most probably depends on the position/distance from edge where loading is applied. This assumption may be checked by recording several measures where probe position is varied.

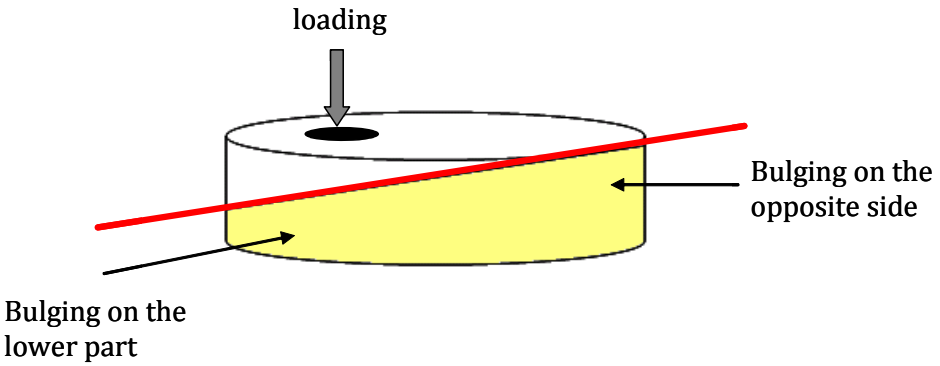

Figure 45. Schematic view of 15% gelatin gel under loading

Figures 42 and 43 indicate a non homogenous, less well defined bulging phenomenon. Put in more simply, the yellow and green colored zones did not show clear cut separation (contrary to what was noted for 8% and 10% gelatin gels). Bulging appeared closer to the probe (compared to 8% gelatin gel), on the top and also on the side of the sample. The displacement of matter (induced by probe) seems therefore to be closely related to the viscoelastic properties of the samples. The 30-day-old Camembert cheese and its simulant show greater

viscous flow under loading compared to the 8% gelatin gel. Since the Camembert simulant is made up of 6.5% (w/w) gelatin, 21.5% (w/w) maltodextrin DE 19 and 2% (w/w) gelatinized starch, it can be inferred that the addition of maltodextrin and starch successfully modified the textural properties of the gelatin gel and allowed it to imitate more closely those of the Camembert cheese.

1.5. Correlation between surface depression profile (from penetrometry test) and rheological parameters

In order to investigate the effect of rheological parameters on the surface depression profiles, the curves shown in figures 34, 38, and 40 were fitted to equation 9.

$$Z(mm) = Z_0 + a \times \exp(-bY) \qquad (9)$$

Values of Z_0, a and b obtained for surface displacement profiles of samples at 2, 3 and 4 mm deformation are presented in table 10. Other parameters such as firmness, first term relaxation time constant and first term elasticity modulus are shown in table 11.

Table 10. Fitting parameters (Z_0, a and b) obtained from samples surface displacement profiles after 2, 3 and 4 mm depth penetrometry tests. Values indicated are means of 3 or 4 repetitions.

Parameters	**Gelatin gels**				**Coulommiers**	**Coulommiers simulant**	**Camembert**	**Camembert simulant**
	8%	**10%**	**15%**	**20%**				
Z_{04mm} (mm)	0.255	0.345	0.466	0.554	0.254	0.280	0.109	0.160
a_{4mm} (mm)	2.507	2.600	2.393	2.310	1.826	1.924	2.248	2.198
b_{4mm} (mm^{-1})	0.250	0.271	0.269	0.288	0.259	0.250	0.157	0.207
Adjusted R^2	0.999	0.998	0.998	0.997	0.999	0.998	0.996	0.999
Z_{03mm} (mm)	0.206	0.284	0.392	0.466	0.223	0.211	0.148	0.173
a_{3mm} (mm)	1.824	1.953	1.691	1.548	1.414	1.420	1.187	1.675
b_{3mm} (mm^{-1})	0.256	0.271	0.267	0.283	0.258	0.247	0.157	0.218
Adjusted R^2	0.999	0.998	0.996	0.997	0.996	0.991	0.999	0.999
Z_{02mm} (mm)	0.152	0.203	0.266	0.348	0.194	0.131	0.136	0.106
a_{2mm} (mm)	1.120	1.162	1.063	0.930	0.748	0.946	0.670	1.040
b_{2mm} (mm^{-1})	0.258	0.271	0.268	0.281	0.250	0.251	0.154	0.217
Adjusted R^2	0.996	0.997	0.993	0.996	0.984	0.993	0.999	0.999

Table 11. Firmness, relaxation time constant, $r_{1,}$ and elasticity modulus, E_1 determined from 10 mm depth penetrometry test and stress relaxation tests. Values indicated are means of 3 or 4 repetitions.

Parameters	**Gelatin gels**				**Coulommiers**	**Coulommiers simulant**	**Camembert**	**Camembert simulant**
	8%	**10%**	**15%**	**20%**				
Firmness (N)	30.0	43.4	81.2	121.6	19.0	17.9	10.7	12.2
Relaxation time constant r_1 (min)	183	180	143	138	20	60	12	57
Elasticity modulus E_1 (kPa)	200	270	600	880	80	100	33	60
Firmness/rigidity ratio ($NkPa^{-1}$)	0.150	0.161	0.135	0.138	0.237	0.179	0.324	0.203

In order to model the relationship between rheological parameters (obtained from penetrometry and stress relaxation tests) such as firmness, relaxation time constant and elasticity modulus (explanatory variables) and *Zo, a or b* (response variables), multiple linear regression analysis was used and the mathematical models are given by equations 14 to 16.

$$Z_0 = k_{z1}E_1 + k_{z2}firmness \quad (14)$$

$$b = k_{b1}E_1 + k_{b2}firmness \quad (15)$$

$$a = k_{a1}E_1 + k_{a2}firmness + k_{a3}r_1 \quad (16)$$

$k_{z1,}\ k_{z2,}\ k_{b1,}\ k_{b2,}\ k_{a1,}\ k_{a2,}\ k_{a3}$ are coefficient of the mathematical models.

Coefficients of mathematical models relating $Z_{0,}$ a and b parameters to firmness, elasticity modulus and relaxation time constant for 2, 3 and 4 mm depth penetrometry test are shown in table 12. Adjusted R^2 statistic explained more than 96, 92 and 90% of the variability in $Z_{0,}$ a and $b,$ respectively.

Table 12. Coefficients of mathematical models relating Z_0, a and b parameters to firmness, elasticity modulus and relaxation time constant for 2, 3 and 4 mm depth penetrometry test

Fitting parameters	coefficients	Depth		
		2mm	3mm	4mm
b	k_{b1}	-3.9×10^{-3}	-3.9×10^{-3}	-3.9×10^{-3}
	k_{b2}	3.1×10^{-2}	3.2×10^{-2}	3.1×10^{-2}
Adjusted R^2		0.90	0.90	0.92
Z_0	k_{Z1}	-2.2×10^{-3}	-2.7×10^{-3}	-2.8×10^{-4}
	k_{Z2}	1.9×10^{-2}	2.4×10^{-2}	2.5×10^{-2}
Adjusted R^2		0.98	0.97	0.96
a	k_{a1}	-1.7×10^{-2}	-2.1×10^{-2}	-3.1×10^{-2}
	k_{a2}	8.8×10^{-2}	1.6×10^{-1}	2.4×10^{-1}
	k_{a3}	4.4×10^{-3}	6.7×10^{-3}	7.9×10^{-3}
Adjusted R^2		0.92	0.93	0.93

According to table 12, coefficients ($k_{b1,}$ k_{b2}) of the mathematical model relating b value to sample rheological parameters were independent of the depth to which the probe was inserted. This equation suggests that the slope of the surface depression of sample under load was mainly affected by the firmness and the elasticity modulus of the sample. It has been explained previously (chapter III, part II) that E_1 value can be regarded as the rigidity of the sample, while r_1 is associated to sample density and compactness of structure. Hence, firmness and rigidity influenced b values in different ways. Increasing firmness increased the convex shape, while increasing rigidity of the sample led to the inverse effect.
It has also been noted that when the ratio of firmness to elasticity decreased (which is the case when gelatin concentration increased), b value increased; the surface depression profile became more convex in shape.

Parameters a and Z_0 relate to the surface depression of the sample under loading. Therefore, quite expectedly, coefficients ($k_{a1,}$ $k_{a2,}$ $k_{a3,}$ $k_{z1,}$ k_{z2}) of the models relating a and Z_0 to the rheological parameters varied with the depth to which the probe was inserted. Although the mathematical models given by equations 14 and 16 depend on the depth to which the probe was inserted, they still provide useful information regarding the influence of rheological parameters on surface displacement profile. For instance, Z_0 indicates the surface displacement of the sample at about 20 mm away from probe edge. From the mathematical

model, it can be said that firmness and elasticity modulus has a significant effect on the depth to which the surface (approximately 20 mm away from load) is pulled down when probe was inserted to 4 mm.

2. SURFACE DISPLACEMENT PROFILES OF SAMPLES DURING STRESS-CONTROLLED TEST

As mentioned earlier, a material, such as cheese, is considered viscoelastic if during (and after) deformation, part of the mechanical energy supplied to it is stored in the material (elastic part) and part is dissipated (viscous part). The ratio of dissipated to stored energy depends on the time scale of the deformation and the consequence is that the material response is time-dependent. Moreover, energy dissipation may cause (part of) the deformation to be long lasting or permanent (Lucey *et al.*, 2003).

According to van Vliet (1999), the origin of the time-dependent behavior of foods lies in their structure. The structure of most food materials is not static; the majority of bonds between structural elements are not permanent. These bonds will occasionally break and reform due to Brownian motion. The rate by which these processes proceed may vary greatly and is accelerated by the application of a stress, which is the introduction of mechanical energy. For ideal elastic materials this rate is effectively zero. In a liquid, bonds are also present between structural elements, but they break and reform much faster than the timescale of the experiment, and all energy supplied will be immediately dissipated as heat. In viscoelastic materials, to which a stress is applied, an intermediate behavior occurs because bond lifetime is of the same order of magnitude as the duration of the experiment.

Therefore, in order to assess the viscoelastic properties of samples, their response to a time dependant test, during which they were subjected to 3N load for 10 minutes was studied. The load was then removed and images were captured for another 12 minutes. Surface depression of sample (mm) at 1 mm from probe edge was plotted against time (seconds) (Figures 46 to 49).

2.1. Elastic and viscous behavior

From figure 46a, it can be seen that the surface displacement of samples at 1 mm from probe edge increased with time (0 < time < 600 seconds). The slope of the curve for this time interval varied with the sample. In increasing gelatin concentration, from 8 to 20%, the slope decreased from $1.5x10^{-4}$ to $5.7x10^{-5}$ mm/s. In other words, increasing gelatin concentration increased elastic behavior and decreased fluidity (viscous behavior) of gel.

The slope of the curve (0 < time < 600 seconds) of Coulommiers and its model was more than four times greater than that of 8% gelatin gel, thus reflecting greater fluidity of 10-day-old Coulommiers and cheese model compared to the gelatin gel (Figure 47a). Analysis of 30 days old Camembert cheese showed that its surface depression increased gradually with time when the constant 3N load was applied during 10 minutes (although the increase was less obvious at 20 mm distance from probe)(Figure 48). The slope of the Camembert curve was also about five times greater than that of 10 days old Coulommiers cheese. That is because ripening brought about greater fluidity in the sample: the breakdown of the camembert structure during proteolysis caused the cheese to flow readily under constant loading. This argument can further be supported by results presented in figure 49. As the Coulommiers cheese aged, magnitude of surface displacement of cheese at 1 mm distance from probe edge increased.

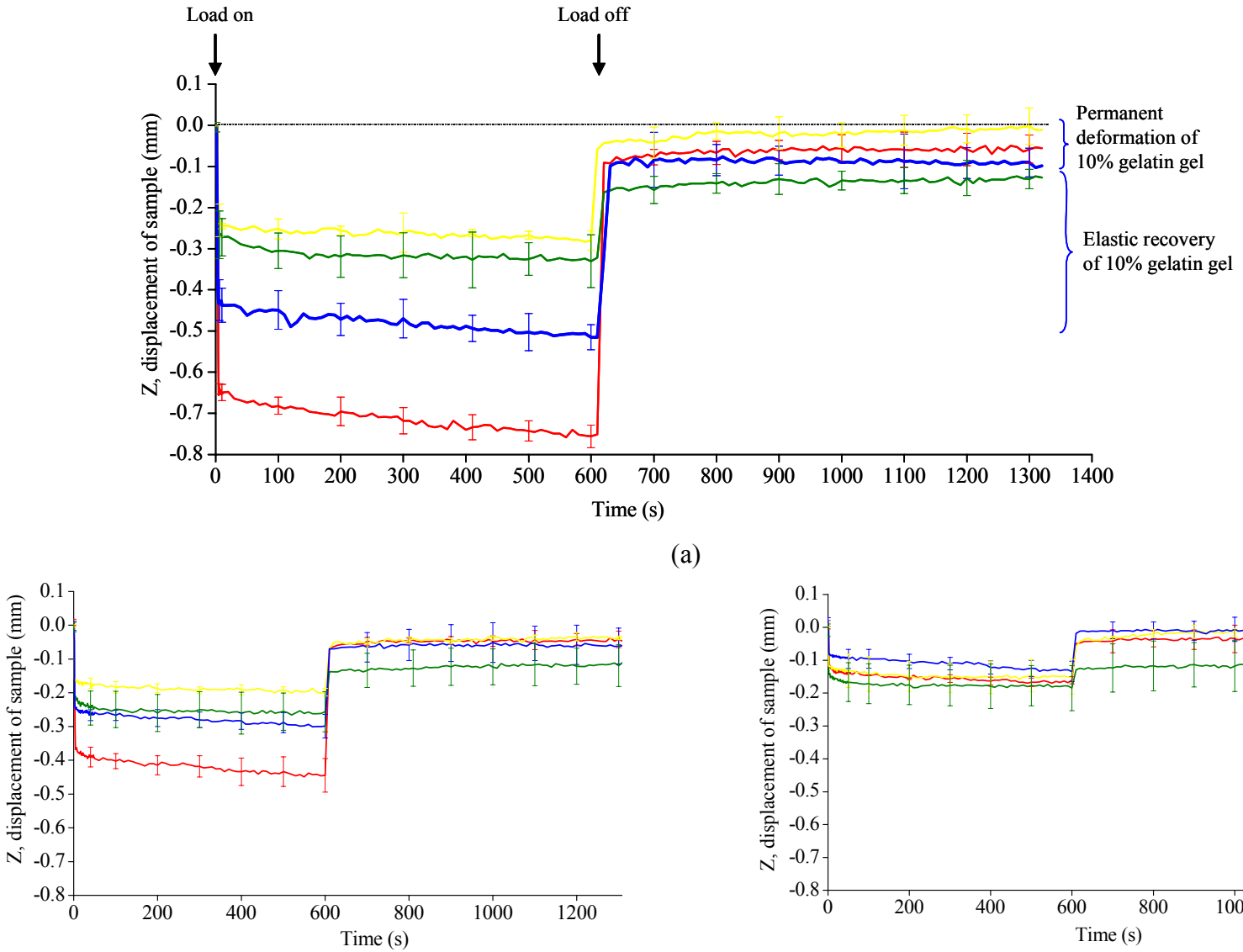

Figure 46. Surface displacement profile of 8% gelatin gel (—), 10% gelatin gel (—), 15% gelatin gel (—), 20% gelatin gel (—) at 1mm (a), 5 mm (b) and 20mm (c) from probe edge and with 3N load applied for first 600 seconds and then removed, while sample images were still recorded for the next 700 seconds. Error bars indicate standard deviation calculated from 3 repetitions.

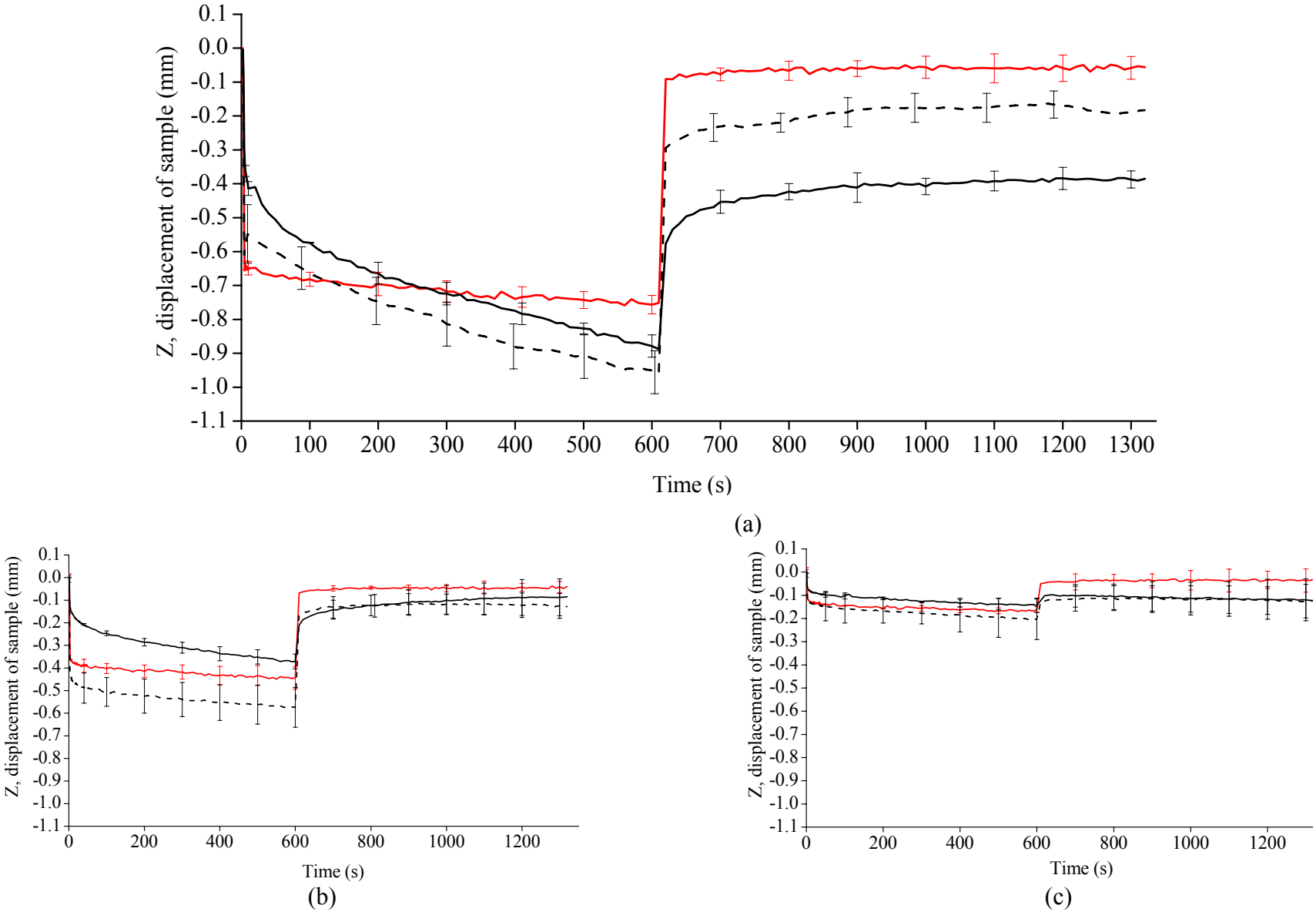

Figure 47. Surface displacement profile of 8% gelatin gel (—), 10-day-old Coulommiers cheese (—), Coulommiers simulant (– – –) at 1mm (a), 5 mm (b) and 20mm (c) from probe edge and with 3N load applied for first 600 seconds and then removed, while sample images were still recorded for the next 700 seconds. Error bars indicate standard deviation calculated from 6 and 3 repetitions for cheeses and gels respectively.

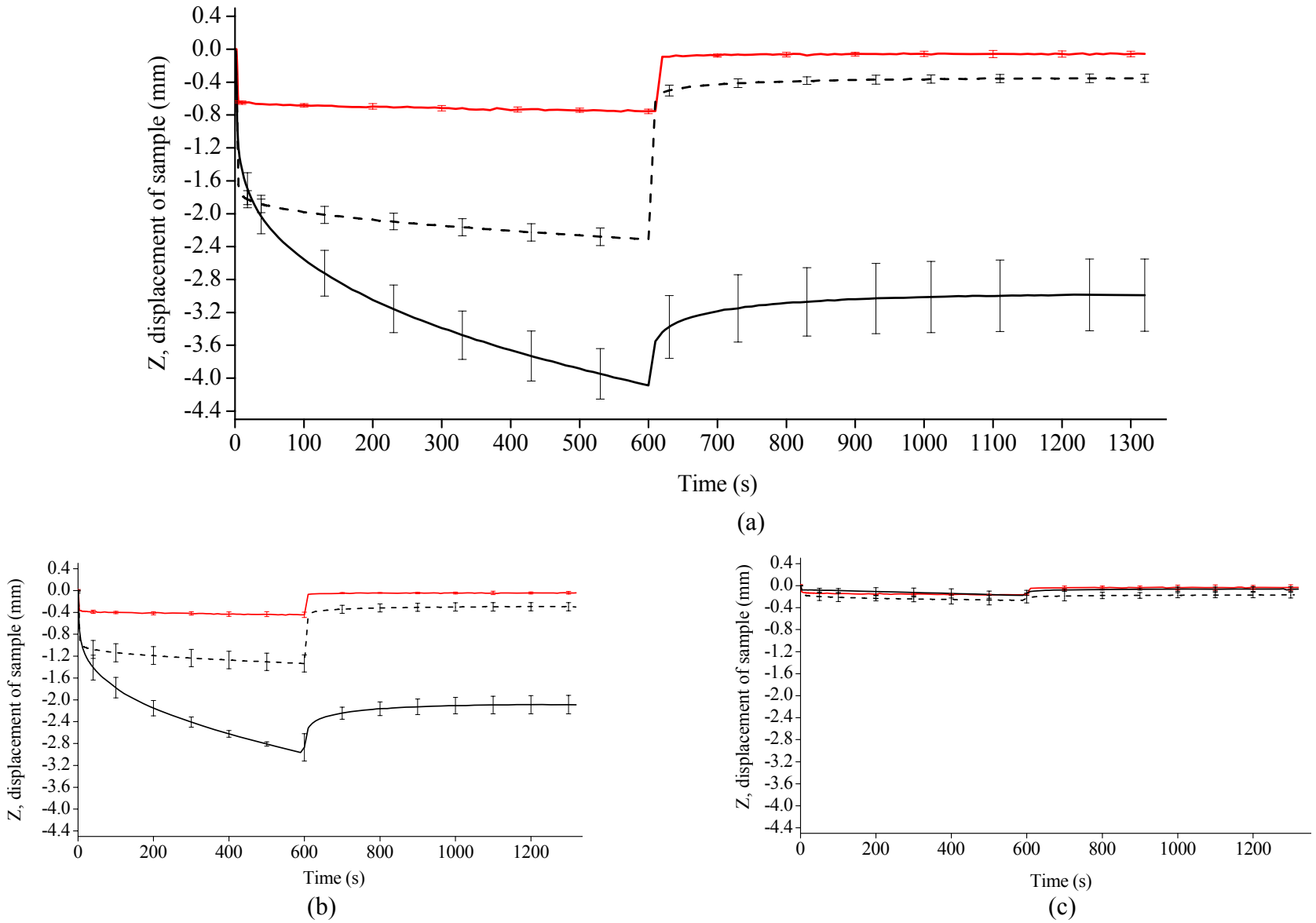

Figure 48. Surface displacement profile of 8% gelatin gel (—), 30-day-old Camembert cheese (—), Camembert simulant (– – –) at 1mm (a), 5 mm (b) and 20mm (c) from probe edge and with 3N load applied for first 600 seconds and then removed, while sample images were still recorded for the next 700 seconds. Error bars indicate standard deviation calculated from 6 and 3 repetitions for cheeses and gels respectively.

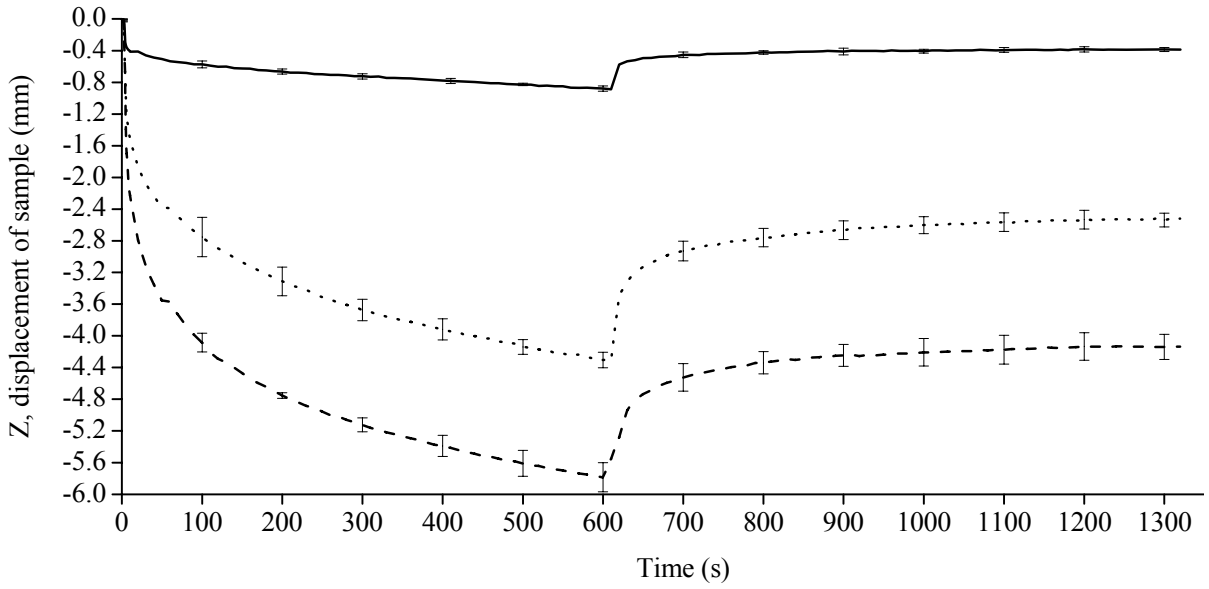

Figure 49. Surface displacement profile of 10 (—), 28 (• • • •) and 40 (– – –) days old Coulommiers cheese at 1mm from probe edge and with 3N load applied for first 600 seconds and then removed, while sample images were still recorded for the next 700 seconds. Error bars indicate standard deviation calculated from 6 repetitions.

2.2. Lasting or permanent deformation

The second part of figures 46 to 48, that is after 600 seconds and after load removal from sample surface, was a good indicator of the delay recovery (or elastic after effect) and the lasting/permanent deformation in samples. Delay recovery is basically the time taken for the curve to reach the flat portion once load is removed from sample. In an ideal elastic solid, the deformation (strain) occurs instantaneously when the stress is applied, and it disappears instantaneously when stress is removed and the original shape is regained (Borwankar, 1992). The delay recovery of gelatin gels was almost instantaneous. On removal of load, surface displacement of sample returned more or less to its initial position (Z<0.15 mm). This was not the case for the cheeses and their simulant. Indeed, according to figure 47, when load was removed, there was a recovery delay of about 200 seconds before for the curve reached the flat portion. Moreover, permanent deformation could be noted for Coulommiers cheese: at 1 mm from probe edge, surface depression remained at about 0.5 mm from initial position (0 mm). Permanent deformation of Coulommiers model was less obvious. Surface depression was found to be less than 0.2 mm, that is, twice less than that of Coulommiers cheese. This

vertical distance from the flat portion of the recovery curve to the time axis is the non-recoverable strain, which is related to the amount of structural damage undergone by the sample during the test. As the cheese is deformed under the dead load, there is rearrangement of components, the breakage and reformation of bonds within the cheese matrix.

During ripening and proteolysis, and hence weakening of the matrix, failure of the structure may occur (Prentice *et al.*, 1993). Brown *et al.* (2003) also reported that as cheese networks break down and the firmness and elastic element decrease, the viscoelastic response becomes more viscous, and the recovery become less. Therefore, as expected, greater permanent deformation was noted for the 30-day-old Camembert cheese (surface depression of about 3 mm) in our case (figure 48). The weaker cheese matrix (compared to that of the younger 10-day-old Coulommiers cheese), thus showed lesser resistance to the 3N load and readily flow under the probe.

In the elastic region of the creep curve, the cheese/gel matrix absorbs and stores the stress energy, which is instantly released on removal of stress, enabling the sample to regain its original dimensions. The extent and duration of the elastic region depend on the magnitude of stress and the structural and compositional characteristics of sample (Prentice *et al.*, 1993). When strain is greater than critical strain (beyond elastic limit), the structure of the cheese/gel is altered via the breaking of bonds between structural elements, which are stressed beyond their elastic limit. Eventually, when the stress-bearing structural matrix has fractured, the cheese/gel is said to flow. Failure to appreciate this characteristic can often lead to loss of shape (for example, manifested by bulging, inclined surface) during storage, distribution and retailing, especially if cheeses of different consistencies are laid haphazardly upon each other.

In addition, it can be seen from figure 46 that gelatin gels also underwent permanent/lasting deformation. The vertical distance from the flat portion of the recovery curve to the time axis was however less than that noted for the cheese and its simulant, thus suggesting a lesser degree of structural damage in the gelatin gels.
The amount of structural damage undergone by 8 and 10% gelatin gels was not significantly different (vertical distance from flat portion of recovery curve to the time axis). When gelatin content was raised to 15%, the number of crosslinks being higher (gel was more rigid), it can

be assumed that a larger number of bonds remained unbroken during loading, hence the 15% gelatin gel readily regain more or less its original shape when load was removed. However, 20% gelatin gel behaved in a different way. Indeed, structural damage was greater than that of the gels with lower gelatin content. This can be explained by the fact that at this high gelatin concentration, air bubbles could not be removed (despite vacuum degassing at about 60°C) and they remained inside the gel matrix. Those bubbles favored cracks formation during loading (Tang *et al.*, 1998) and hence resulted in the gel having greater permanent damage. And obviously, the gel less readily regained its original shape when the load was removed.

3. CONCLUSION

Digital image correlation is an interesting technique to measure surface displacement of food products. This method was successful in distinguishing between gels and cheeses, varying in firmness and viscoelastic properties, according to their surface displacement profiles. For instance, firmness and elasticity modulus were found to have significant effect on the shape of the surface depression surrounding a probe inserted to 4 mm distance into the sample. Moreover, surface displacement profile resulting from stress-controlled test clearly put forward the difference in viscoelastic properties between samples. The results obtained by digital image correlation method were checked by another optical technique, the Breuckmann 3D scanning system. The results obtained by both methods were consistent. The main difference between them lies in the fact that digital image correlation method is able to track changes in surface displacement and deformation of sample in course of time, while Breuckmann 3D scanning system is more convenient for image acquisition at a given moment. This is because the latter requires several minutes for various views of the sample to be captured and merged in order to obtain a 3D image of the whole sample.

CONCLUSIONS

The aim of this research work was to design a gel simulant whose textural properties match that of soft cheeses-Camembert and Coulommiers cheeses. To achieve this, textural properties of cheeses were first expressed in term of three rheological parameters namely firmness, elasticity modulus and relaxation time constants. Firmness was determined by penetrometry test, while elasticity modulus and relaxation time constants were obtained by stress relaxation test which is commonly used to describe viscoelastic behavior of food products.

Comparison between 10-day-old Camembert and Coulommiers cheeses and four polymeric gels elaborated to simulate cheese texture were based on these rheological parameters. The gels were formulated from gelatin and polysaccharides. Gelatin was chosen as solid protein matrix. However, although its concentration can be varied in order to adjust gel firmness and elasticity modulus to match that of the cheeses, relaxation time constants remained significantly greater than that of the cheeses. Hence, in order to make the gel relax faster when deformed (under loading), that is in other word, decrease its degree of compactness, guar, karaya, xanthan or maltodextrin and gelatinized starch was added to the protein. Among those polysaccharides, maltodextrin combined with starch were found to be most efficient in lowering the relaxation time constants, their values were significantly higher than that of the cheeses though.
Furthermore, a three-component mixture design allowed the determination of gelatin, maltodextrin and starch concentration resulting in the simulant imitating closely the rheological parameters of the soft cheeses. The mixture design approach was useful in developing mathematical model which explained the effect of each component of the simulant on its textural properties. A linear dependence of firmness, first-term relaxation time constant and elasticity modulus on composition of simulant was noted. In addition, no significant effect of interactions between gelatin, maltodextrin and starch was noted on the rheological parameters.

Once the optimum component concentration was found, the simulant was further modified by the addition of protease enzyme Subtilisin Calsberg (Alcalase®) in order to bring about gradual (time dependent) textural changes in the gel, so as to imitate those occurring in

Coulommiers cheese during ripening. The enzyme brought textural changes in the simulant. However, the rate of change of the rheological parameters was different from that taking place in soft cheeses during ripening. The fact that in the cheeses, enzymes are constantly being synthesized while in the simulants a given amount of enzyme was added during preparation may account for this difference in rate of change of rheological parameters. A slower and prolonged hydrolysis may improve the properties of the simulant. This can be obtained by encapsulating Alcalase® which will ensure a more gradual release of the enzyme in the gel during storage.

This study also focused upon the use of optical techniques coupled with the widely used universal testing machine for texture assessment. Digital image correlation and Breuckmann three-dimensional scanning system provided interesting and additional information regarding the textural behaviors of samples under loading.. These techniques also allow measurement of deformation around the probe. When using the universal testing machine, measurements under the probe only are available. Bulging or depression can also be observed with the Breuckmann scanning system. Displacement of matter during loading was found to vary according the viscosity of the sample. Food products varying in rheological parameters can be distinguished based upon the analysis of their surface displacement profile obtained by the digital image correlation system.

The new parameters (Z_0, a and b) obtained by the system can be used as additional variables when correlating instrumental and sensory measurements. For example, instead of correlating the global textural properties of cheese/gel with firmness, elasticity modulus and relaxation time constants only, these three new parameters can also be used. The addition of Z_0, a and b as variables may increase the correlation coefficient between instrumental and sensory measurements. Indeed, maybe these parameters can bring additional information (not available by the universal testing machine) and therefore describe better the texture of the cheese/gel as perceived by a person. Indeed, both the visual and tactile properties of the food are perceived through sensory evaluation of texture. Therefore, in imitating the fingertip with the probe of the universal testing machine and the eyes with the digital cameras, models which are able to predict accurately the sensory texture of food from instrumental measurements may be developed.

It should also be mentioned that in this study, only three parameters have been derived from surface displacement profiles of the samples. There are, most probably, other parameters which could be used. For example, the displacement of matter during bulging could be determined. This would give an indication about the viscosity of the product. The principles of soil mechanics can also be applied to further analyze the surface displacement of sample under loading.

REFERENCES

Al-Ruqaie, I., Kasapis, S. and Abeysekera, R. (1997). Structural properties of pectin-gelatin gels. Part II: effect of sucrose/glucose syrup *Carbohydrate polymers*, 34, 309-321.

Alevisopoulos, S. and Kasapis, S. (1999). Molecular weight effects on the gelatin/maltodextrin gel. *Carbohydrate polymers*, 40, 83-87.

Anand, A. and Scanlon, M.G. (2002). Dimensional effects on the prediction of texture-related mechanical properties of foods by indentation. *Transactions of the ASAE*, 45, 1045-1050.

Armisen, R. and Galatas, F. (2000). Agar. In G.O. Phillips and P.A. Williams, *Handbook of hydrocolloids* (21-40). Boca Raton: CRC.

Baek, I., Linforth, R.S.T., Blake, A. and Taylor, A.J. (1999). Sensory perception is related to the rate of change of volatile concentration in-nose during eating of model gels. *Chemical senses*, 24, 155-160.

Barrangou, L.M., Drake, M.A., Daubert, C.R. and Foegeding, E.A. (2006). Textural properties of agarose gels. II. Relationships between rheological properties and sensory texture. *Food hydrocolloids*, 20, 196-203.

Bedborough, D.S. and Jackson, D.A. (1976). Brillouin scattering study of gelatin gel using a double passed Fabry-Perot spectrometer *Polymer*, 17, 573-584.

Belitz, H.D. and Grosch, W. (1999). *Food chemistry*. Verlag-Berlin-Heidelbeig-New York: Springer.

Bertola, N.C., Bevilacqua, A.E. and Zatritzky, N.E. (1995). Rheological behaviour of reggianito Argentino cheese packaged in plastic film during ripening. *Food science and technology*, 28, 610-615.

Boland, A.B., Buhr, K., Giannouli, P. and Van Ruth, S.M. (2004). Influence of gelatin, starch, pectin and artificial saliva on the release of 11 flavour compounds from model gel systems. *Food chemistry*, 86, 401-411.

Borwankar, R.P. (1992). Food texture and rheology: A tutorial review. *Journal of food engineering*, 16, 1-16.

Bourne, M. (1978). Texture profile analysis. *Food technology*, 32, 62-72.

Bourne, M. (2002). *Food texture and viscosity: Concept and measurement*. San Diego, California: Academic Press.

Boutron, R., Gaucheron, F., Piot, M., Michel, F., Maubois, J.L. and Leonil, J. (1999). Changes in the composition of juice expressed from camembert cheese during ripening. *Le lait*, 79, 503-513.

Boutrou, R., Kerriou, L. and Gassi, J.-Y. (2006). Contribution of Geotrichum candidum to the proteolysis of soft cheese. *International dairy journal*, 16, 775-783.

Bowland, E.L. and Foegeding, E.A. (1999). Factors determining large-strain (fracture) rheological properties of model processes cheese. *Journal of dairy science*, 82, 1851-1859.

Boyd, J.U. and Sherman, P. (1975). A study of force-compression associated with hardness evaluation in several foods. *Journal of texture studies*, 6, 507-522.

Breuil, P. and Meullenet, J.F. (2001). A comparison of three instrumental tests for predicting sensory texture profiles of cheese. *Journal of texture studies*, 32, 41-45.

Brito, A.C.F., Sierakowski, M.R., Reicher, F., Feitosa, J.P.A. and de Paula, R.C.M. (2005). Dynamic rheological study of *Sterculia striata* and karaya polysaccharides in aqueous solution. *Food hydrocolloids*, 19, 861-867.

Brown, J.A., Foegeding, E.A., Daubert, C.R., Drake, M.A. and Gumpertz, M. (2003). Relationships among rheological and sensorial properties of young cheeses. *Journal of dairy science association*, 86, 3054-3067.

Brown, W.E., Eves, D., Ellison, M. and Braxton, D. (1998). Use of combined electromyography and kinesthesiology during mastication to chart the oral breakdown of foodstuffs: relevance to measurement of texture. *Journal of texture studies*, 29, 145-167.

Busnel, J.P., Morris, E.R. and Ross-Murphy, S.B. (1989). Interpretation of the renaturation kinetics of gelatin solutions. *International journal of biological macromolecules*, 11, 119-125.

Carson, L., Sun, X., Setser, C. and Peng, Y. (2002). Assessing food firmness using an electronic sensing system with a model food system. *Journal of texture studies*, 33, 389-399.

Chasset, R. and Thirion, P. (1965). *Physics of non-crystalline solids*. Amsterdam: North-Holland publishing company.

Chen, J., Xia, G., Zhou, K., Xia, G. and Qin, Y. (2005). Two-step digital image correlation for micro-region measurement. *Optics and Lasers in Engineering*, 43, 836-846.

Clark, A.H. and Ross-Murphy, S.B. (1987). Structural and mechanical properties of bioplymer gels. *Advances in polymer science*, 83, 57-192.

Comby, S., Doublier, J.L. and Lefebvre, J., 1985. *Stress-relaxation study of high-methoxyl pectin gels*, Proceedings of the 3rd international conference, Wrexham, Clwyd, Wales, Gums and stabilisers for the food industry, Elsevier applied science publishers, David J. Wedlock Glyn O. Phillips, and Peter A. Williams, 203-212.

Compagnon, D., Veyrune, J.L., Morenas, M. and Faulks, D. (1999). Development of a synthetic bolus using silicone elastomer for the study of masticatory efficiency. *Journal of prosthetic and dentistry*, 81, 704-709.

Costell, E., Trujillo, C., Damasio, M.H. and Duran, L. (1995). Texture of sweet orange gels by free-choice profiling. *Journal of sensory studies*, 10, 163-179.

Creamer, L.K. and Olson, N.F. (1982). Rheological evaluation of maturing Cheddar cheese. *Journal of food science*, 47, 631-646.

Daget, N. and Collyer, S. (1984). Comparison between quantitative descriptive analysis and physical measurements of gel systems and evaluation of sensorial method. *Journal of texture studies*, 15, 227-245.

Davies, E.R. (2000). *Image processing for the food industry*. Singapore, NJ, London: World scientific publishing

de Jong, S. and van de Velde, F. (2007). Charge density of polysaccharide controls microstructure and large deformation properties of mixed gels. *Food hydrocolloids*, 21, 1172-1187.

Del Nobile, M.A., Chillo, S., Mentana, A. and Baiano, A. (2007). Use of the generalized Maxwell model for describing the stress relaxation behavior of solid-like foods. *Journal of food engineering*, 78, 978-983.

deMan, J.M. (1969). Food texture measurements with penetration method. *Journal of texture studies*, 1, 19-37.

Depypere, F., Verbeken, D., Thas, O. and Dewettinck, K. (2003). Mixture design approach on the dynamic rheological and uniaxial compression behaviour of milk desserts. *Food hydrocolloids*, 17, 311-320.

Djagny, K.B., Wang, Z. and Xu, S. (2001). Gelatin: A valuable protein for food and pharmaceutical industries: review. *Critical reviews in food science and nutrition*, 41, 481-492.

Dokic, P., Jakovljevic, J. and Dokic-Baucal, L. (1998). Molecular characteristics of maltodextrins and rheological behaviour of diluted and concentrated solutions. *Colloid and surfaces. A: Physicochemical and engineering aspects*, 141, 435-440.

Drake, M.A. and Gerard, P.D. (1999). Relationship between instrumental and sensory measurements of cheese texture. *Journal of texture studies*, 30, 451-476.

Drake, M.A., Gerard, P.D. and Civille, G.V. (1999). Ability of hand evaluation versus mouth evaluation to differentiate texture of cheese. *Journal of sensory studies*, 14, 425-441.

Eastoe, J.E. (1955). The amino acid composition of mammalian collagen and gelatin. *Biochemical journal*, 1955, 589-600.

Edlund, J. and Lamm, C.J. (1980). Masticatory efficiency. *Journal of oral rehabilitation*, 1980, 123-130.

Eldridge, J.E. and Ferry, J.D. (1954). Studies of the cross-linking process in gelatin gels. III. Dependence of melting point on concentration and molecular weight. *Journal of physical chemistry*, 58, 992-995.

Fenelon, M.A. and Guinee, T.P. (2000). Primary proteolysis and textural changes during ripening in Cheddar cheeses manufactured to different fat contents. *International dairy journal*, 10, 277-288.

Ferry, J.D. (1948). Mechanical properties of substances of high molecular weight. IV. Rigidities of gelatin gels, dependence on concentration, temperature and molecular weight. *Journal of the american chemical society*, 70, 2244-2249.

Fiszman, S.M., Pons, M. and Damasio, M.H. (1998). New parameters for instrumental texture profile analysis: instantaneous and retarded recoverable springiness. *Journal of texture studies*, 29, 499-508.

Foegeding, E.A., Bowland, E.L. and Hardin, C.C. (1995). Factors that determine the fracture properties and microstructure of globular protein gels. *Food hydrocolloids*, 9, 237-249.

Foegeding, E.A., Brown, J., Drake, M. and Daubert, C.R. (2003). Sensory and mechanical aspects of cheese texture. *International dairy journal*, 13, 585-591.

Foegeding, E.A., Gonzalez, C., Hamann, D.D. and Case, S. (1994). Polyacrylamide gels as elastic models for food gels. *Food hydrocolloids*, 8, 125-134.

Fontijn-Tekamp, F.A., Slagter, A.P., Van der bilt, A., Van 'T hof, M.A., Witter, D.J., Kalk, W. and Jansen, J.A. (2000). Biting and chewing in overdentures, full dentures, and natural dentitions. *Journal of dental research*, 79, 1519-1524.

Glicksman, M. (1985). Hydrocolloids in fabricated foods. *Food technology in New Zealand*, 20, 75-85.

Green, M.L., Turvey, A. and Hobbs, D.G. (1981). Development of the structure and texture in cheddar cheese. *Journal of dairy research*, 48, 343-355.

Gregson, C.M., Hill, S.E., Mitchell, J.R. and Smewing, J. (1999). Measurement of the rheology of polysaccharide gels by penetration. *Carbohydrate polymers*, 38, 255-259.

Guinard, J.X. and Marty, C. (1995). Time-intensity measurement of flavor release from a model gel system: Effect of gelling agent and concentration. *Journal of food science*, 60, 727-730.

Guinee, T.P., Feeney, E.P. and Fox, P.F. (2001). Effect of ripening temperature on low moisture Mozzarella cheese: 2. Texture and functionality. *Le lait*, 81, 475-485.

Guinee, T.P. and Law, B.A. (2002). Role of milk fat in hard and semi-hard cheeses. In K.R. Kanes, *Fats in food technology* (275-331). Sheffield, England: Sheffield academic press.

Gunasekaran, S. and Ak, M.M. (2003). *Cheese rheology and texture*. Boca Raton, London, New York: CRC Press.

Hassan, B.H., Alhamdan, A.M. and Elansari, A.M. (2005). Sress relaxation of dates at khalal and rutab stages of maturity. *Journal of food engineering*, 66, 439-445.

Hassouna, M. and Guizani, N. (1995). Evolution de la flore microbienne et des characteristiques physico-chimiques au cours de la maturation du fromage Tunisien de type Camembert fabriqué avec du lait pasteurisé. *Microbiol. Hyg. Alim.*, 18, 14-23.

Hassouna, M., Nafti, A. and Ghrir, R. (1996). L'affinage d'un fromage à pâte molle et à croute fleurie de type camembert au lait cru de brebis: aspect microbiologiques et physico-chimiques. *Sciences des aliments*, 16, 187-203.

Hemmes, D., Bouillanne, C., Metro, F. and Desmazeaud, M. (1982). Microbial catabolism of amino acids during cheese ripening. *Science des aliments*, 2, 113-123.

Hennequin, D., (1993). *Composition, structure et texture des fromage à pâte molle: une analyse multidimensionnelle pour une approche scientifique de l'innovation.*, ENSAIA, PhD

Hennequin, D. and Hardy, J. (1993). Evaluation instrumentale et sensorielle de certaines propriétés texturales de fromages à pâte molle. *International dairy journal*, 3, 635-647.

Henry, W.F., Katz, M.H., Pilgrim, F.J. and May, A.J. (1971). Texture of semi-solid foods: Sensory and physical correlates. *Journal of food science*, 36, 155-161.

Hort, J. and Le Grys, G. (2001). Developments in the textural and rheological properties of UK Cheddar cheese durimg ripening. *International dairy journal*, 11, 475-481.

Imoto, E.M., Lee, C.H. and Rha, C. (1979). Effect of compression ratio on the mechanical properties of cheese. *Journal of food science*, 44, 343-345.

Johnson-Banks, F.A. (1990). Gelatin. In P. Harris, *Food gels* (233-289). New York: Elsevier science publishing Co., Inc.

Jones, R.R., Steffe, J.F. and Harte, J.B. (2003). Sensory firmness scale based on gelatin gels. *Journal of texture studies*, 33, 543-558.

Jopling, D.W. (1958). A note on the rubber-like properties of gelatin. *rheologica acta*, 1, 133.

Kalviainen, N., Roinnen, K. and Tuorila, H. (2000). Sensory characterization of texture and flavor of high viscosity gels made with different thickners. *Journal of texture studies*, 31, 407-420.

Kasapis, S., Morris, E.R., Norton, I.T. and Clark, A.H. (1993). Phase equilibria and gelation in gelatin/maltodextrin systems. Part IV: composition-dependence of mixed-gel moduli. *Carbohydrate polymers*, 21, 269-276.

Kaspasis, S., Morris, E.R., Norton, I.T. and Clark, A.H. (1993). Phase equilibria and gelation in gelatin/maltodextrin systems. Part IV: composition-dependence of mixed-gel moduli. *Carbohydrate polymers*, 21, 269-276.

Kfoury, M., Mpagana, M. and Hardy, J. (1988). Influence de l'affinage sur les propriétés rhéologiques du camembert et du saint-paulin. *Le lait*, 69, 137-149.

Kohyama, K., Hatakeyama, E., Sasaki, T., Dan, H., Azuma, T. and Karita, K. (2004). Effects of sample hardness on human chewing force: a model study using silicone rubber. *Archives of oral biology*, 49, 805-816.

Lassauzay, C., Peyron, M.A., Albuisson, E., Dransfield, E. and Woda, A. (2000). Variability of the masticatory process during chewing elastic food models. *European journal of oral sciences*, 108, 484-492.

Lau, M.H., Tang, J. and Paulson, A.T. (2000). Texture profile and turbidity of gellan/gelatin mixed gels. *Food research international*, 33, 665-671.

Le Cerf, D. and Muller, G. (1994). Mechanical spectroscopy of karaya gum--alginate mixed dispersions. *Carbohydrate polymers*, 23, 241-246.

Leclercq-Perlat, M.N., Buono, F., Lambert, D., Latrille, E., Spinnler, H.E. and Corrieu, G. (2004). Controlled production of Camembert-type cheeses. Part I: Microbilogical and physicochemical evolutions. *Journal of dairy research*, 71, 346-354

Leclercq-Perlat, M.N., Oumer, A., Bergère, J.L., Spinnler, H.E. and Corrieu, G. (1999). Growth of *Debaryomyces hansenii* on a bacterial surface-ripened cheese. *Journal of dairy research*, 66, 271-281.

Ledward, D.A. (1986). *Functional properties of food macromelecules*. London: Elsevier applied science.

Ledward, D.A. (2000). Gelatin. In G.O. Phillips and P.A Williams, *Food hydrocolloids* (67-86). Boca Raton: CRC.

Lee, C.H., Imoto, E.M. and Rha, C. (1978). Evaluation of cheese texture. *Journal of food science*, 43, 1600-1605.

Lenoir, J. (1984). The surface flora and its role in the ripening of cheese. *International dairy federation, Brussels*, Bulletin 171, 3-20.

Lenoir, J. and Choisy, C. (1970). Aptitude de l'espèce Penicillium caseicolum à la production d'enzymes protéolytiques. *Lait*, 51, 138-157.

Lenoir, J., Lamberet, G. and Schmidt, J.L. (1983). L'élaboration d'un fromage: l'exemple du Camembert. *Pour la science*, 8, 30-42.

Loret, C., Meunier, V., Frith, W.J. and Fryer, P.J. (2004). Rheological characterisation of the gelation behaviour of maltodextrin aqueous solutions. *Carbohydrate polymers*, 57, 153-163.

Lucey, J.A., Johnson, M.E. and Horne, D.S. (2003). Invited Review: Perspectives on the Basis of the Rheology and Texture Properties of Cheese. *American dairy science association*, 86, 2725-2743.

Luo, P.F., Chao, Y.J. and Sutton, M.A. (1994). Application of stereo vision to the three-dimensional defromation analyses in francture experiments. *Optical engineering*, 33, 981-990.

Luo, P.F., Chao, Y.J., Sutton, M.A. and Peters, W.H. (1993). Accurate measurement of three dimensional deformations in deformable and rigid bodies using computer vision. *Experimental mechanics*, 33, 123-132.

Luyten, H., Van Vliet, T. and Walstra, P. (1991). Characterization of the consistency of Gouda cheese: Rheological properties. *Neth. milk dairy journal*, 45, 33-53.

Marshall (1990). Composition, structure, rheological properties, and sensory texture of processes cheese analogues. *Journal of science and food agriculture*, 50, 237-252.

Meilgaard, M.M., Civille, G.V. and Carr, Y. (1999). Descriptive analysis techniques. In *Sensory evaluation techniques* New York: CRC Press.

Michon, C., Cuvelier, G., Relkin, P. and Launay, B. (1997). Influence of thermal history on the stability of gelatin gels. *International journal of biological macromolecules*, 20, 259-264.

Miller, M., Ferry, J.D., Schremp, F.W. and Eldridge, J.E. (1951). Studies of the cross-linking process in gelatin gels. *Journal of physical and colloidal chemistry*, 55, 1387.

Mioche, L., Auroy, P., Lepetit, J. and Compagnon, D. (1991). Oral perception of hardness in viscoelastic products. *Journal of texture studies*, 22, 333-347.

Mitchell, J.R. (1976). Rheology of gels. *Journal of texture studies*, 7, 313-339.

Mohsenin, N.N. (1986). Some basic concepts of rheology. In *Physical properties of plants and animal materials* (129-221). New York: Gordon and Breach Science Publishers.

Monnet, V., (1982). *Etude de l'influence du pH sur la texture et la protéolyse des fromages du type Camembert*, DEA de Sciences alimentaires

Morris, E.R. (1990). Mixed polymer gels In P. Harris, *Food gels* (291-359). New York: Elsevier Science Publishing Co., Inc.

Mpagana, M., (1986). *Propriétés rhéologiques des fromages à pâte molle, influence du salage et de l'affinage*, ENSAIA, PhD

Mpagana, M. and Hardy, J. (1985). Propriétés de compression et de relaxation des fromages à pâtes molle. Influence de l'affinage. *Sciences des Aliments*, 5, 91-96.

Mpagana, M. and Hardy, J. (1986). Effect of salting on some rheological and properties of fresh Camembert cheese as measured by uniaxial compression. *Milchwissenschaft*, 41, 210-213.

Munoz, A.M., Pangborn, R.M. and Noble, A.C. (1986a). Sensory and mechanical attributes of gel texture. I. Effect of gelatin concentration. *Journal of texture studies*, 17, 1-16.

Munoz, A.M., Pangborn, R.M. and Noble, A.C. (1986b). Sensory and mechanical attributes of gel texture. II. Gelatin, sodium alginate and kappa-carrageenan gels. *Journal of texture studies*, 17, 17-35.

Naryshkina, E.P., Volkov, V., Dulinnyi, I. and Izmailova, V.N. (1982). *Kolloidn. Zh.*, 44, 356-362.

Nelson, D.V., Makino, A. and Schmidt, T. (2006). Residual Stress Determination Using Hole Drilling and 3D Image Correlation. *Experimental mechanics*, 46, 31-38.

Nickerson, M.T., Paulson, A.T., Wagar, E., Farnworth, R., Hodge, S.M. and Rousseau, D. (2006). Some physical properties of crosslinked gelatin-maltodextrin hydrogels. *Food hydrocolloids*, 20, 1072-1079.

Nijenhuis, K. (1981). Investigation into the ageing process in gels of gelatin/water systems by the measurement of their dynamic moduli *Colloid and polymer science*, 257, 1017-1026.

Noel, Y. and Lefier, D. (1991). Factors affecting the consistency of ripened soft and semi-soft cheese. *Bulletin of the international dairy federation*, N° 268, 44-47.

Noel, Y., Pain, J.P., Francois, O. and Antonini, G.A., 1987. *A penetrometer for grading cheese maturity*, Meeting on measurement of rheological properties of dairy products, Wageningen (The Netherlands), ICDRL, 22-23.

Noomen, A. (1983). The role of the surface flora in the softening of cheeses with low initial pH. *Netherland milk dairy journal*, 37, 229-232.

O'Callaghan, D.J. and Guinee, T.P. (2004). Rheology and texture of cheese. In P.F. Fox, P.L.H. McSweeney, T. Cogan and T.P. Guinee, *Cheese: Chemistry, physics and microbiology* (511-540). London, California: Elsevier Applied Science.

Oakenfull, D. (1984). A Method for using Measurements of Shear Modulus to Estimate the Size and Thermodynamic Stability of Junction Zones in Noncovalently Cross-Linked Gels. *Journal of food science*, 49, 1103-1104, 1110.

Olthoff, L.O., Van der bilt, A., De Boer, A. and Bosman, F. (1986). Comparison of force-deformation characteristics of artificial and several natural foods for chewing experiments. *Journal of texture studies*, 17, 275-289.

Olthoff, L.W., Van der bilt, A., Bosman, F. and Kleizen, H.H. (1984). Distribution of particle sizes in food comminuted by human mastication. *Archives of oral biology*, 29, 899-903.

Papageorgiou, M. and Kasapsi, S. (1995). The effect of added sucrose and corn syrup on the physical properties of gellan-gelatin mixed gels. *Food hydrocolloids*, 9, 211-220.

Papageorgiou, M., Kasapsi, S. and Richardson, R.K. (1994). Steric exclusion phenomena in gellan/gelatin systems I. Physical properties of single and binary gels. *Food hydrocolloids*, 8, 97-112.

Pereira, R.B. and Bennett, R.J. (2002). In-hand sensory evaluation of textural charachetristics in model processed cheese analogues. *Journal of texture studies*, 33, 255-268.

Peyron, M.A., Mioche, L. and Culioli, J. (1994). Bite force and sample deformation during hardness assessment of viscoelastic models of foods. *Journal of texture studies*, 24, 59-76.

Pines, E. and Prins, J.A. (1973). Structural-Property relations of thermoreversible macromolecular hydrogels. *Macromolecules*, 6, 888.

Pinthus, E.J., Weinberg, P. and Saguy, I.S. (1995). Deep fried potato product oil uptake as affected by crust physical properties. *Journal of food science*, 60, 770-772.

Prentice, J.H., Langley, K.R. and Marshall, R.J. (1993). Cheese rheology. In P.F. Fox, *Cheese: chemistry, physics and microbiology* (303-340). London, Glasgow, New York, Tokyo, Melbourne, Madras: Chapman and Hall.

Preston, B.N. and Meyer, F.A. (1971). Physical behaviour of gelatin gels. A simple model for connective tissue. *Biopolymers*, 10, 35-46.

Privalov, P.L. (1982). Stability of proteins: Proteins which do not present a single cooperative system. *Advances in protein chemistry*, 35, 1-104.

Reuther, F., Plietz, P., Damaschun, G., Purschel, H.V., Krober, R. and Schierbaum, F.R. (1983). Structure of maltodextrin gels-a small angle x-ray scattering study. *Colloid and polymer science*, 261, 271-276.

Robinson, J.A., (1975). *A study of some physical properties of gelatin*, University of Nottingham, Ph.D. Thesis

Roland, A.M., Phillips, L.G. and Boor, K.J. (1999). Effects of fat replacers on the sensory properties, color, melting, and hardness of ice cream. *Journal of dairy science*, 82, 2094-2100.

Rosenthal, A.J. (1999). Relation between instrumental and sensory measures of food. In A.J. Rosenthal, *Food texture measurement and perception* (1-17). Gaithersburg, Maryland: Aspen Publishers.

Ross-Murphy, S.B. (1992). Structure and rheology of gelatin gels: recent progress. *Polymer*, 33, 2622-2627.

Ross, K.A. and Scanlon, M.G. (1999). Analysis of the elastic modulus of agar gel by indentation. *Journal of texture studies*, 30, 17-27.

Sanderson, G.R. (1990). Gellan gum. In P. Harris, *Food gels* (201-232). New York: Elsevier science publishing Co., Inc.

Saunders, P.R. and Ward, A.G., 1954. *An absolute method for the rigidity modulus of gelatin gels*, Proceedings of the Second International Congress on Rheology, Oxford, 284.

Saunders, P.R. and Ward, A.G. (1958). A note on the elasticity of gelatin gels. In I. Mason and N. Wookey, *The rheology of elastomers* (45). London: Pergamon press.

Scanlon, M.G. and Anand, A., Texture modelling of composite foods, *Industries alimentaires et agricoles*, 2006; 123: 14-17.

Schierbaum, F.R., Radosta, S., Vorwerg, W., Yuriev, V.P., Braudo, E.E. and German, M.L. (1992). Formation of thermally reversible maltodextrin gels as revealed by low resolution h-nmr. *Carbohydrate polymers*, 18, 155-163.

Scott Blair, G.W. and Coppen, F.M.V. (1942). The subjective conception of the firmness of soft materials *The american journal of psychology*, 55, 215-229.

Sherman, P. (1969). A texture profile of foodstuffs based upon well-defined rheological properties. *Journal of food science*, 34, 458-462.

Silva, D.A., Brito, A.C.F., de Paula, R.C.M., Feitosa, J.P.A. and Paula, H.C.B. (2003). Effect of mono and divalent salts on gelation of native, Na and deacetylated Sterculia striata and Sterculia urens polysaccharide gels. *Carbohydrate polymers*, 54, 229-236.

Sitnik, R., Kujawinska, M. and Woznicki, J. (2002). Digital fringe projection system for large-volume 360-deg shape measurement. *Optical engineering*, 41, 443-449.

Slagter, A.P., Van der glas, H., Bosman, F. and Olthoff, L.O. (1992). Force-deformation properties of artificial and natural foods for testing chewing efficiency. *Journal of prosthetic and dentistry*, 68, 790-799.

Spinnler, H.E. and Gripon, J.C. (2004). Surface mould-ripened cheeses. In P.F. Fox, P.L.H. McSweeney, T. Cogan and T.P. Guinee, *Cheese: chemistry, physics and microbiology* (157-174). London, California: Elsevier Applied Science.

Stanley, D.W. (1999). Food structuring. In G.V Barbosa-Canovas, *Microstructural principles of food processing and engineering* (211-245). Gaithersburg: Aspen publication.

Subramanian, R., Muthukumarappan, K. and Gunasekaran, S. (2006). Linear Viscoelastic Properties of Regular- and Reduced-Fat Pasteurized Process Cheese During Heating and Cooling. *International Journal of Food Properties*, 9, 377 - 393.

Sun, C., Gunasekaran, S. and Richards, M.P. (2007). Effect of xanthan gum on physicochemical properties of whey protein isolate stabilized oil-in-water emulsions. *Food hydrocolloids*, 21, 555-564.

Surowka, K. (1997). Effect of protein hydrolysate on the instrumental texture profile of gelatine gels. *Journal of texture studies*, 28, 289-303.

Szczesniak, A.S. (1963). Objective measurements of food texture. *Journal of food science*, 28, 410-420.

Szczesniak, A.S. (1986). Correlating sensory with instrumental texture measurements - An overview of recent developments. *Journal of texture studies*, 18, 1-15.

Szczesniak, A.S. and MacAllister, R.V. (1964). Study of gelatin gels and the effect of urea on their formation. *Journal of applied polymer science*, 8, 1391-1401.

Tang, J., Tung, M.A. and Zeng, Y. (1998). Characterization of gellan gels using stress relaxation. *Journal of food engineering*, 38, 279-295.

Tolstoguzov, V.B. (1988). Some physico-chemical aspects of protein processing into foodstuffs. *Food hydrocolloids*, 2, 339-370.

Tolstoguzov, V.B. (1995). Some physico-chemical aspects of protein processing in foods. Multicomponent gels. *Food hydrocolloids*, 9, 317-332.

Tromp, R.H., Van der velde, F., Van Riela, J. and Paques, M. (2001). Confocal scanning light microscopy (CSLM) on mixtures of gelatine and polysaccharides. *Food research international*, 34, 931-938.

Truong, V.D. (2002). Vane rheometry for textural characterization of Cheddar cheeses: correlation with other instrumental and sensory measurements. *Lebensmittel-Wissenschaft und-Technologie*, 35, 305-314.

Truong, V.D. and Daubert, C.R. (2001). Textural characterization of cheeses using vane rheometry and torsion analysis. *Journal of food science*, 66, 716-721.

Urlacher, B. and Dalbe, B. (1992). Xanthan gum. In A. Imerson, *Thickening and gelling agents for food* (202-226). London: Blackie academic and professional.

van den Berg, L., van Vliet, T., van der Linden, E., van Boekel, M.A.J.S. and van de Velde, F. (2006). Breakdown properties and sensory perception of whey proteins/polysaccharide mixed gels as a function of microstructure. *Food hydrocolloids*, doi: 10.1016/j.foodhyd.2006.08.017,

van der bilt, A., Othoff, L.W., Bosman, F. and Oosterhaven, S.P. (1993). The effect of missing postcanine teeth on chewing performance in man. *Archives of oral biology*, 38, 423-429.

van Vliet, T. (1991a). Inventory of test methods. *Bulletin of the international dairy federation*, N° 268, 16-29.

van Vliet, T., Terminology to be used in cheese rheology, Bulletin of the International dairy federation n°268, *Rheological and fracture properties of cheese*, 1991b; 5-15.

van Vliet, T. (1999). Factors determining small-deformation behaviour of gels. In *Food Emulsions and Foams; Interfaces, Interactions and Stability* (307-317). E. Dickinson and J. M. Rodriguez Patino.

Vassal, L., Monnet, V., Le Bars, D., Roux, C. and Gripon, J.C. (1986). Relation entre le pH, la composition chimique et la texture des fromages de type Camembert. *Lait*, 66, 341-351.

Veis, A. (1964). *The macromolecular chemistry of gelatin*. New York and London: Academic press.

Visser, J., Factors affecting the rheological and fracture properties of hard and semi-hard cheese, Bulletin of the International dairy federation n°268, *Rheological and fracture properties of cheese*, 1991; 49-61.

Ward, J.H. (1963). Hierachical grouping to optimize an objective function. *Journal of the American Statistical Association*, 58, 236-244.

Watase, M. and Nishinari, K. (1980). Rheological properties of agarose-gelatin gels. *rheologica acta*, 19, 220-225.

Weiping, W. (2000). Tragacanth and karaya. In Glyn O. Phillips and Peter A Williams, *Handbook of hydrocolloids* (231-245). Woodhead publishing limited.

Wheeler, T.L., Shackelford, S.D., Johnson, L.P., Miller, M.F., Miller, R.K. and Koohmaraie, M. (1997). A comparison of Warner-Bratzler shear force assessment within and among institutions. *Journal of animal science*, 75, 2423-2432.

Wilson, C.E. and Brown, W.E. (1997). Influence of food matrix structure and oral breakdown during mastication on temporal perception of flavour. *Journal of sensory studies*, 21, 69-86.

Wium, H., Gross, M. and Qvist, K.B. (1997). Uniaxial compression of UF-Feta cheese related to sensory texture analysis. *Journal of texture studies*, 28, 455-476.

Wolf, C.L., Beach, S., La Velle, W.M. and Clark, R.C., Gellan gum/gelatin blends, *United States Patent*, 4876105, 1989.

Wood, F.W. and Young, R., Foods with textures, *German Patent*, 2,156,067, 1972.

Wu, Z. and Lu, J. (2000). Study of surface residual stress by three-dimensional displacement data at a single point in hole drilling method. *Journal of engineering materials and technology*, 122, 215-220.

Xiong, R., Meullenet, J.F., Hankins, J.A. and Chung, W.K. (2002). Relationship between sensory and instrumental hardness of commercial cheeses. *Journal of food science*, 67, 877-883.

Zasypkin, D., Dumay, E. and Cheftel, J.C. (1996). Pressure- and heat-induced gelation of mixed beta-lactoglobulin/ xanthan solutions. *Food hydrocolloids*, 10, 203-211.

Zhang, J., Daubert, C.R. and Foegeding, E. (2005). Characterization of polyacrylamide gels as an elastic model for food gels. *rheologica acta*, 44, 622-630.

INSTITUT NATIONAL
POLYTECHNIQUE
DE LORRAINE

AUTORISATION DE SOUTENANCE DE THESE
DU DOCTORAT DE L'INSTITUT NATIONAL
POLYTECHNIQUE DE LORRAINE

o0o

VU **LES RAPPORTS ETABLIS PAR :**
Madame Catherine DACREMONT, Professeur, ENSBANA, Dijon

Madame Laurence MIOCHE, Professeur, INRA, Saint-Genès Champanelle

Le Président de l'Institut National Polytechnique de Lorraine, autorise :

Madame LI YUET HEE Mary Lynn

NANCY BRABOIS
2, AVENUE DE LA
FORET-DE-HAYE
BOITE POSTALE 3
F – 5 4 5 0 1
VANDŒUVRE CEDEX

à soutenir devant un jury de l'INSTITUT NATIONAL POLYTECHNIQUE DE LORRAINE, une thèse intitulée :

"Caractérisation texturale et analyse par stéréocorrélation d'images de la déformation des fromages à pâte molle et de leurs simulants formulés"

en vue de l'obtention du titre de :

DOCTEUR DE L'INSTITUT NATIONAL POLYTECHNIQUE DE LORRAINE

Spécialité : **« Procédés biotechnologiques et alimentaires** »

Fait à Vandoeuvre, le 01 octobre 2007"
Le Président de l'I.N.P.L.,
F. LAURENT

TEL. 33/03.83.59.59.59
FAX. 33/03.83.59.59.55